



# Synthesis and homogeneous catalytic applications of nickel(II)-N-heterocyclic carbene complexes

Mickaël Henrion

## ► To cite this version:

Mickaël Henrion. Synthesis and homogeneous catalytic applications of nickel(II)-N-heterocyclic carbene complexes. Catalysis. Université de Strasbourg, 2014. English. NNT : 2014STRAF057 . tel-01130979

**HAL Id: tel-01130979**

**<https://theses.hal.science/tel-01130979>**

Submitted on 12 Mar 2015

**HAL** is a multi-disciplinary open access archive for the deposit and dissemination of scientific research documents, whether they are published or not. The documents may come from teaching and research institutions in France or abroad, or from public or private research centers.

L'archive ouverte pluridisciplinaire **HAL**, est destinée au dépôt et à la diffusion de documents scientifiques de niveau recherche, publiés ou non, émanant des établissements d'enseignement et de recherche français ou étrangers, des laboratoires publics ou privés.

**ÉCOLE DOCTORALE DES SCIENCES CHIMIQUES**

**Laboratoire de Chimie Moléculaire — UMR 7509**

# THÈSE

présentée par

**Mickaël HENRION**

soutenue le **16 juin 2014**

pour obtenir le grade de

**Docteur de l'université de Strasbourg**

Discipline/ Spécialité : Sciences Chimiques

## **Synthèses et applications en catalyse homogène de complexes nickel(II)–carbène *N*-hétérocyclique**

**THÈSE dirigée par :**

**M. CHETCUTI Michael J.**

**M. RITLENG Vincent**

Professeur, Université de Strasbourg

Maître de Conférences, Université de Strasbourg

**RAPPORTEURS :**

**M. FORT Yves**

**M. DE VRIES Johannes G.**

Professeur, Université de Lorraine

Professeur, Rijksuniversiteit Groningen

---

**AUTRES MEMBRES DU JURY :**

**M. PFEFFER Michel**

**M. DARCEL Christophe**

Directeur de Recherche émérite, CNRS, Strasbourg

Professeur, Université de Rennes I

*A mes parents, Annick et Yves*



*"Simplicity is the ultimate sophistication"*

**Leonard de Vinci (1452 - 1519)**



# Remerciements





## Remerciements

---

Cette thèse a été réalisée au sein de l'Equipe de Chimie Organométallique Appliquée appartenant au Laboratoire de Chimie Moléculaire (UMR 7509 du CNRS) de l'Université de Strasbourg, sous la direction de Michael J. Chetcuti, Professeur à l'Université de Strasbourg, et de Vincent Ritleng, Maître de Conférences à l'Université de Strasbourg.

J'aimerais avant tout remercier mes deux chefs, Michael et Vincent, pour m'avoir donné la possibilité de rejoindre ce groupe, et sans qui cette thèse n'aurait été possible. Je vous suis infiniment reconnaissant pour la confiance et la liberté que vous m'avez accordées, et espère que ces trois ans de plaisir ne sont que le début d'une longue collaboration/amitié.

Je tiens également à exprimer ma profonde gratitude à l'Agence Nationale de la Recherche et au CNRS, dont l'appui financier a permis la réalisation de cette thèse.

Je suis profondément reconnaissant aux Professeurs Yves Fort, Johannes G. de Vries et Christophe Darcel ainsi qu' au Docteur Michel Pfeffer qui ont bien voulu me faire l'honneur de faire partie de mon jury de thèse.

Les résultats obtenus durant cette thèse n'auraient été rien sans l'aide du Docteur Michel Schmitt du service RMN, des Docteurs Corinne Bailly et Lydia Brelot du service de radiocristallographie, sans oublier les membres des services communs de microanalyses et de spectrométrie de masse de l'Institut de Chimie de l'Université de Strasbourg. Qu'ils trouvent ici l'expression de ma profonde gratitude.

J'aimerais tout particulièrement remercier Professeur Christophe Darcel et Docteur Jean-Baptiste Sortais de l'Université de Rennes I, ainsi que Docteurs Vincent César, Guy Lavigne et Noël Lugan de l'Université de Toulouse, pour m'avoir offert la possibilité de collaborer avec eux, et m'avoir permis de m'ouvrir à d'autres thématiques de recherche.

Je ne saurais oublier tous les membres, passagers ou permanents, de l'équipe pour la bonne ambiance, mais surtout, pour m'avoir supporté dans les moments difficiles ! Merci à vous donc, Anaïs, Mansuy, Haithem, Saurabh, Thanh, Alexis et Lobna, et à ceux que j'ai oubliés. Je remercie également les nombreux membres de l'UMR que j'ai côtoyés, pour les bons moments passés ensemble, leur soutien et leurs conseils. Une pensée toute particulière

pour Mathieu et Karima, dont les pots et BBQ organisés entre collègues de l'UMR ont été de sérieux coups de boost !

J'aimerais aussi remercier le "labo DM", et tout particulièrement Eric, Rafa et Mathieu, qui ont été de véritables modèles lors de mes deux stages Master, et avec qui j'ai appris énormément.

Impossible aussi d'oublier ma famille et en particulier mes parents, dont les sacrifices ont été indispensables dans la réalisation de ce projet. Je ne vous remercierai jamais assez pour votre soutien sans faille et la confiance que vous me portez.

Enfin, merci à toi, Marie, non seulement pour avoir été à mes côtés depuis plus de quatre ans, même dans les moments difficiles, mais aussi pour avoir supporté mon fantôme lors de ces derniers mois de rédaction, ce qui n'a pas du être évident !

Merci aussi à vous tous, ceux que j'ai oubliés mais que je ne considère pas moins, qui avez de près ou de loin contribué au bon déroulement de cette thèse !

## **Abbreviations**



## Abbreviations

---

Å	Ångström
Ar	aryl
CAAC	cyclic (alkyl)(amino) carbene
COD	cycloocta-1,5-diene
Cp	cyclopentadienyl
Cp*	pentamethylcyclopentadienyl
CPME	cyclopentyl methyl ether
$\delta$	chemical shift (ppm)
DFT	density functional theory
Dipp	diisopropylphenyl
DMC	dimethyl carbonate
DME	dimethoxyethane
DMF	dimethylformamide
<i>ee</i>	enantiomeric excess
equiv.	equivalent
ESI	electro-spray ionization
FT-IR	Fourier-Transformed Infra Red
GC	gas chromatography
HMDS	Hexamethyldisilazane
Mes	mesityl
MS	mass spectroscopy
NHC	<i>N</i> -heterocyclic carbene
NPs	nanoparticles
PMHS	polymethylhydrosiloxane
ppm	parts per million
THF	tetrahydrofuran
TM	transition metal
TMDS	tetramethyldisiloxane
VT NMR	Variable Temperature Nuclear Magnetic Resonance



## Résumé





Chaque jour, les exigences économiques et environnementales évoluent et mènent à des changements fondamentaux au niveau de l'optimisation des procédés dans l'industrie chimique. A cet égard, la catalyse, qui est utilisée dans près de 75% de ces procédés, joue un rôle central, contribuant de manière remarquable à la diminution des coûts de production des produits chimiques et à celle de leur impact environnemental. Bien qu'un travail considérable ait été effectué dans ce domaine depuis de nombreuses années, le manque de catalyseurs qui soient à la fois efficaces et bon marché rend crucial le travail de recherche afin de toujours mieux répondre à ces exigences.

Dans cette optique, le projet de thèse a été dirigé vers l'élaboration de catalyseurs de nickel associés à des ligands carbènes *N*-hétérocyclique (NHCs), en vue de potentielles applications dans des réactions chimiques éco-compatibles. Le choix de cette thématique a été guidé par trois principales motivations : (i) l'utilisation du nickel, un métal abondant et peu onéreux, (ii) l'association de ce métal avec des ligands NHCs, qui se révèle souvent bénéfique en catalyse, et (iii) la recherche de réactions chimiques produisant le moins de déchets possible.

L'utilisation de catalyseurs à base de nickel a pendant longtemps été éclipsée par le succès connu par les métaux nobles tels que le ruthénium pour la métathèse des oléfines, ou encore le palladium pour les réactions de couplages croisés impliquant la formation de liaisons Carbone–Carbone. Cependant, leur faible abondance, corrélée à un prix très élevée, incite au développement d'alternatives plus viables à long terme. A cet égard, le nickel représente une option économiquement attractive, comme en témoignent les prix actuels des métaux (**Figure 1**).

26 55,85 <b>Fe</b> fer 0,007 \$	27 58,93 <b>Co</b> cobalt 2 \$	28 58,70 <b>Ni</b> nickel 1 \$	29 63,55 <b>Cu</b> cuivre 0,4 \$
44 101,07 <b>Ru</b> ruthénium 230 \$	45 102,91 <b>Rh</b> rhodium 3700 \$	46 106,40 <b>Pd</b> palladium 2900 \$	47 107,87 <b>Ag</b> argent 70 \$
76 190,20 <b>Os</b> osmium 2500 \$	77 192,22 <b>Ir</b> iridium 3700 \$	78 195,08 <b>Pt</b> platine 9000 \$	79 196,97 <b>Au</b> or 8000 \$

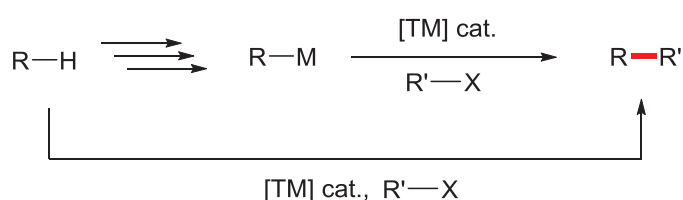
**Figure 1.** Prix des métaux exprimés en \$/mol en juin 2014 (source : [www.infomine.com](http://www.infomine.com))

Par ailleurs, l'association de ligands aux métaux de transition permet d'accorder les propriétés électroniques et stériques de ces derniers afin d'aboutir à des réactivités et des efficacités accrues en catalyse. Dans cette perspective, l'utilisation de NHCs a fortement contribué à l'amélioration des performances de la plupart des catalyseurs organométalliques. En effet, ces ligands fortement  $\sigma$ -donneurs ont tendance à amoindrir la rétrodonation  $\pi$  du métal vers le carbène, les rendant plus riches en électrons qu'avec les trialkylphosphines. En outre, la dissociation de la liaison métal–NHC est défavorable, ce qui permet d'aboutir à des systèmes catalytiques plus stables, et parfois plus actifs. Ces espèces, initialement considérées comme "simples curiosités de laboratoire", sont ainsi rapidement devenues des ligands incontournables en catalyse homogène. Comme il a été observé pour la plupart des métaux de transition, l'emploi de NHCs a permis la diversification, et dans certains cas l'amélioration des performances des catalyseurs à base de nickel. Le **Chapitre I** de ce manuscrit présente l'état de l'art des applications catalytiques des systèmes Ni–NHC depuis leur première application en 1999. De façon impressionnante, ces systèmes sont efficaces dans des réactions aussi variées que la formation de liaisons Carbone–Carbone et Carbone–Hétéroatome par couplage croisé, impliquant dans la plupart des cas la fonctionnalisation de liaisons Carbone–Hydrogène, et les réactions d'oxydation et de réduction. Ils sont également actifs en couplage réductif à trois composants, ou encore en oligomérisation et polymérisation d'oléfines, mais ces thématiques ne seront pas traitées dans le premier chapitre.

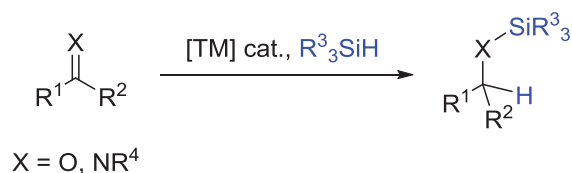
Enfin, notre motivation est centrée sur l'application de ces catalyseurs Ni–NHC dans des réactions éco-compatibles. Parmi ces transformations, la fonctionnalisation directe de liaisons Carbone–Hydrogène, principalement pour la formation de liaisons Carbone–Carbone et Carbone–Hétéroatome, a considérablement attiré l'attention des chercheurs. En effet, en comparaison, par exemple, avec les couplages croisés classiques qui nécessitent l'utilisation de réactifs organométalliques coûteux et/ou non-commerciaux, cette méthodologie plus directe est d'un intérêt économique et environnemental certain (**Schéma 1**).

D'autre part, la réduction de composés (pseudo)carbonylés est une réaction fondamentale en chimie organique. La réduction de ces fonctionnalités par hydrogénation catalytique est considérée comme la voie idéale, car simple et économe en atome. Cependant, les conditions très contraignantes requises (pressions et températures élevées) ont poussé les chercheurs à développer des alternatives moins coûteuses en énergie et moins dangereuses. A cet égard, l'hydrosilylation de fonctions (pseudo)carbonylées catalysée par les métaux de

transition constitue une option prometteuse permettant de travailler dans des conditions douces, et permettant de réaliser une séquence de réduction/protection en une seule étape, ce qui peut s'avérer fort intéressant dans l'optique de fonctionnalisations ultérieures (**Schéma 2**). Cependant, cette méthodologie nécessite souvent l'emploi de métaux nobles, peu abondants et coûteux. Appliquer des systèmes Ni–NHC dans ces transformations représentait ainsi un défi de grand intérêt.

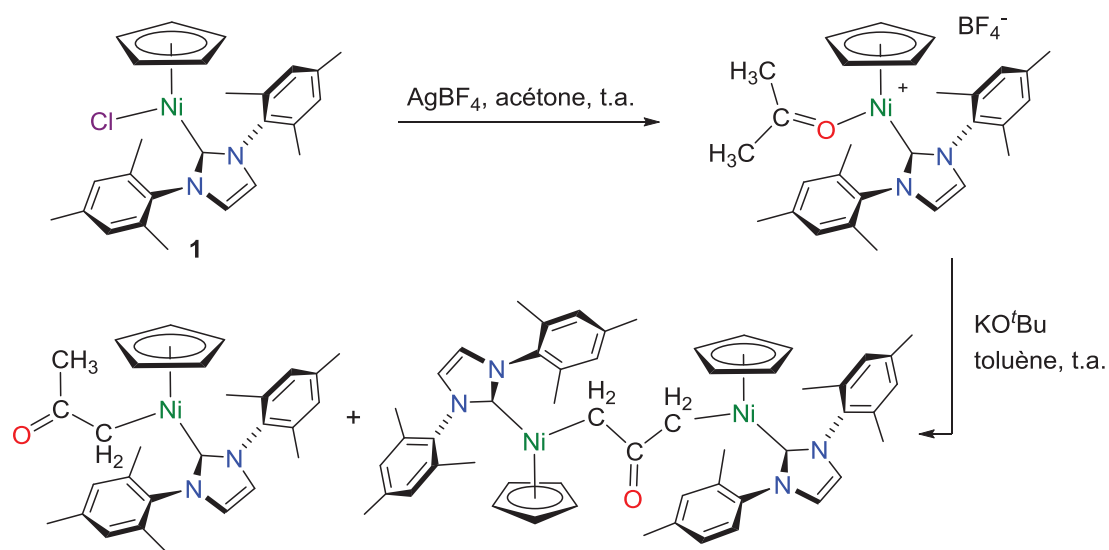


**Schéma 1.** Comparaison entre couplage croisé classique et fonctionnalisation directe d'une liaison Carbone–Hydrogène



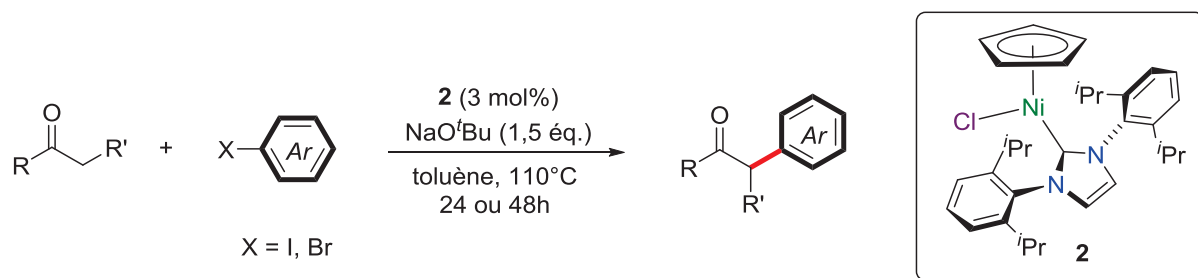
**Schéma 2.** Hydrosilylation de composés (pseudo)carbonylés catalytique

Dans ce contexte, notre laboratoire a récemment montré que des complexes demi-sandwich du type [Ni(NHC)XCp], qui sont stables à l'air et synthétisés de manière très aisée par réaction du nickelocène avec le sel d'imidazolium correspondant, sont capables d'activer des liaisons Carbone–Hydrogène de l'acétonitrile et de l'acétone en présence de quantités stoechiométriques d'une base forte. De façon surprenante, l'activation de l'acétone par le complexe [Ni(IMes)ClCp] **1** a abouti à la formation d'un rare exemple de complexe nickel–acétonyle, et à l'unique formation d'un complexe dinickel–oxyallyle, provenant respectivement de la simple et de la double activation de l'acétone (**Schéma 3**).



**Schéma 3.** Nickelation de l'acétone en présence d'une base forte

L'isolement de telles espèces nickel-énolate C-liées, qui sont d'importants intermédiaires en  $\alpha$ -arylation de composés carbonylés, nous a incité à tester les complexes de type  $[\text{Ni}(\text{NHC})\text{XCp}]$  en  $\alpha$ -arylation de cétones acycliques. Cette transformation fait intervenir la fonctionnalisation d'une liaison Carbone-Hydrogène en  $\alpha$  d'une cétone énoisable acyclique avec un halogénure d'aryle en milieu basique. Il est important de noter que dans la grande majorité des cas, des catalyseurs à base de palladium sont utilisés en réaction d' $\alpha$ -arylation de dérivés carbonylés. De plus, les quelques exemples où des catalyseurs de nickel ont été employés sont limités à l'emploi de cétones cycliques, avec des charges importantes en  $\text{Ni}(\text{COD})_2$ , qui est pyrophorique et sensible à l'air. A notre connaissance, seul un exemple d'un complexe bien défini nickel(II)-NHC a permis l'emploi de cétones acycliques, toujours avec d'importantes charges catalytiques, et avec un champ réactionnel relativement limité. Ces complexes demi-sandwich se sont effectivement montrés actifs dans cette transformation, et cette étude est détaillée dans le **Chapitre II** de cette thèse. Les meilleurs résultats ont été obtenus en faisant réagir les cétones acycliques avec des iodures/bromures d'aryles et 1,5 équiv. de  $\text{NaO}^t\text{Bu}$  comme base, dans le toluène à  $110^\circ\text{C}$  pendant 24 à 48 h en présence de 3 mol% du complexe  $[\text{Ni}(\text{IPr})\text{ClCp}]$  **2** (**Schéma 4**). De façon satisfaisante, la charge en pré-catalyseur a même pu, dans certains cas, être abaissée à 1 mol%, et les résultats obtenus après 48 h de réaction soulignent la longue durée de vie de l'espèce active.



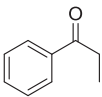
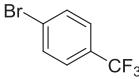
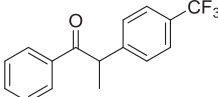
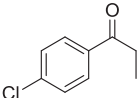
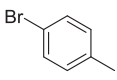
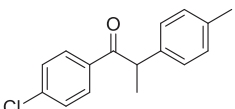

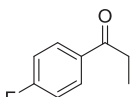
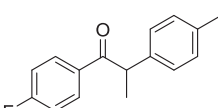
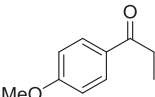
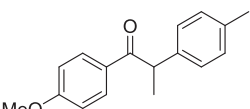
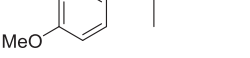
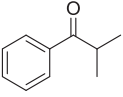
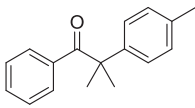

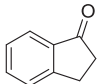
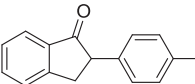
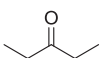
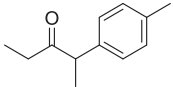
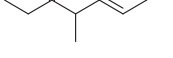
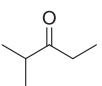
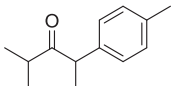
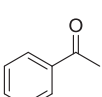
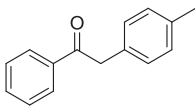
**Schéma 4.**  $\alpha$ -Arylation de cétones acycliques catalysée par [Ni(IPr)ClCp] **2**

Le **Tableau 1** montre qu'une large gamme d'iodures et de bromures d'aryles peut être employée, qu'ils soient riches ou pauvres en électrons (entrées 1-4 et 7-11).

**Tableau 1.**  $\alpha$ -Arylation de cétones avec des halogénures d'aryles catalysée par **2**<sup>a</sup>

Entrée	Cétone	Halogénure d'aryle	Produit de couplage	Temps (h)	Rendement (%) <sup>b</sup>
1				24	73
2				24	< 1 <sup>c</sup>
3				24	92
4				24	65
5				24	10
6				48	17
7				24	89
8				24	53
9				48	93
10				24	52
11				48	85

Tableau 1. (suite)

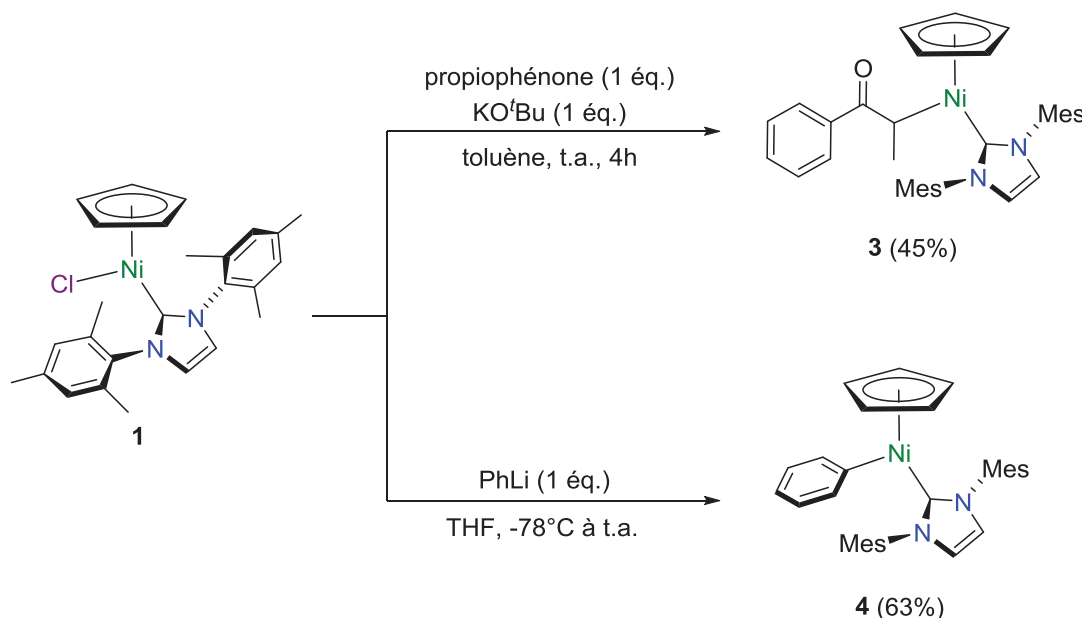
Entrée	Cétone	Halogénure d'aryle	Produit de couplage	Temps (h)	Rendement (%) <sup>b</sup>
12				24	42
13				24	66
14				48	89
15				24	71
16				24	84
17				48	92
18				24	13
19				48	21
20				24	< 1
21				24	68
22				48	79
23				24	55 <sup>d</sup>
24				24	< 1 <sup>e</sup>

<sup>a</sup> Conditions réactionnelles: cétone (1,2 mmol), halogénure d'aryle (1 mmol), NaO<sup>t</sup>Bu (1,5 mmol), **2** (3 mol%) dans le toluène (3 mL) à 110°C pendant 24 ou 48 h. <sup>b</sup> Rendements isolés ; valeur moyenne de deux expériences. <sup>c</sup> Rendement déterminé par CPG ; valeur moyenne de deux expériences. <sup>d</sup> Un mélange 2:1 de 2-(*p*-tolyl)-4-méthylpentan-3-one et 2-(*p*-tolyl)-2-méthylpentan-3-one est obtenu. <sup>e</sup> Des produits de condensation aldoliques ont été observés.

La propiophénone et ses dérivés, ainsi que quelques cétones aliphatiques se sont également montrées être des substrats totalement compatibles avec cette méthodologie (entrées 1, 12-19 et 21-23). Cependant, une limitation majeure de ce système concerne l'emploi de substrats

encombrés pour lesquels une nette chute d'activité a été observée (entrées 5, 6, 18 et 19), et de cétones méthyléniques avec lesquelles la réaction d'aldolisation prend le pas sur la réaction d' $\alpha$ -arylation (entrée 24). Enfin, en présence d'un chlorure d'aryle (entrée 2) ou d'une cétone cyclique (entrée 20), aucune activité catalytique n'a été observée.

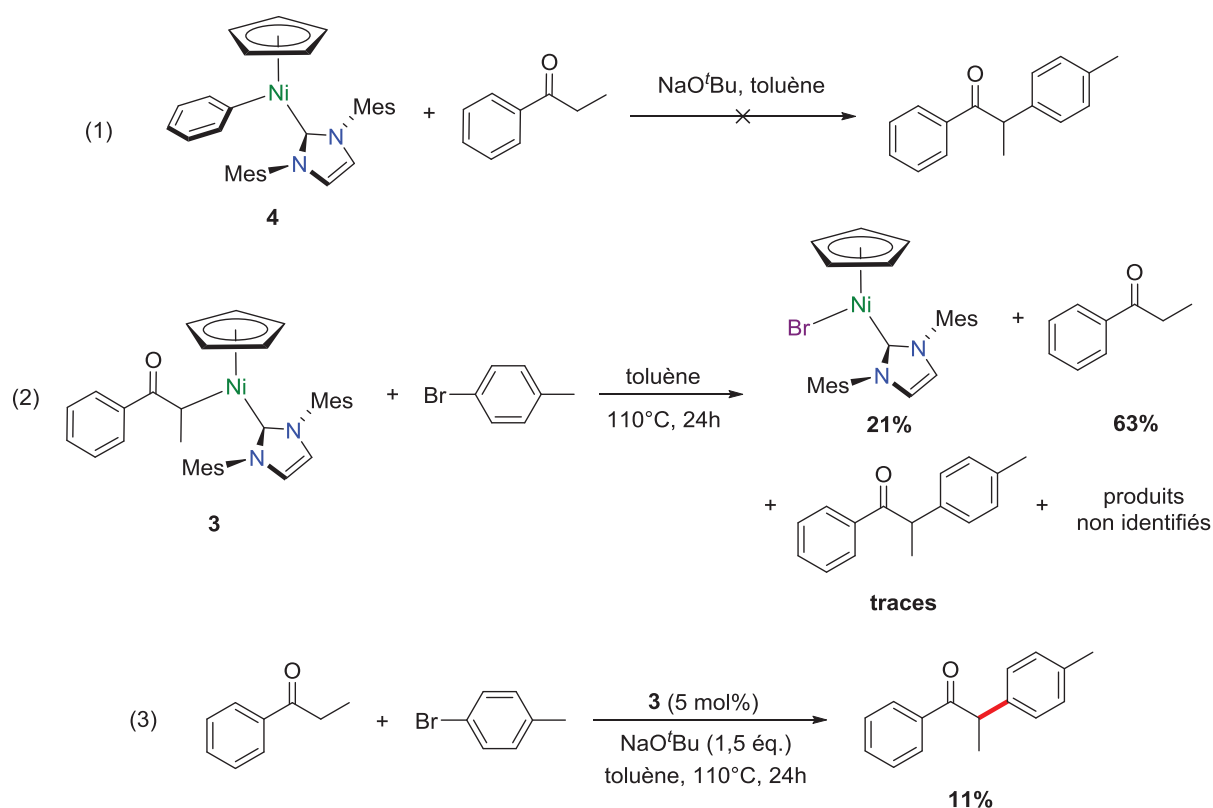
Une étude du mécanisme réactionnel d' $\alpha$ -arylation catalysée par ces complexes demi-sandwich Ni–NHC a également été réalisée. En premier lieu, un test au mercure a permis de montrer que la réaction était très probablement le résultat d'une véritable catalyse homogène. Des potentiels intermédiaires Ni–énolate et Ni–aryl dérivés du complexe [Ni(IMes)ClCp] **1**, lui aussi actif en  $\alpha$ -arylation de cétones acycliques, ont alors été synthétisés (**Schéma 5**). Le dérivé Ni–énolate **3** C-lié a été obtenu avec un rendement de 45% par réaction de **1** avec 1 équiv. de KO<sup>t</sup>Bu et de propiophénone dans le toluène à température ambiante en 4 h. D'autre part, la substitution du ligand chlorure de **1** par un groupement phényle, par réaction avec 1 équiv. de phényllithium à froid, a mené à la formation du composé Ni–aryle **4** qui a été isolé avec 63% de rendement après purification. Ce dernier a par ailleurs été caractérisé par diffraction de rayons X sur monocristal.



**Schéma 5.** Synthèse des complexes Ni–énolate **3** et Ni–aryle **4** dérivés de **1**

Les complexes **3** et **4** ont ensuite été évalués comme potentiels intermédiaires réactionnels par une série d'expériences en conditions stoechiométriques et/ou catalytiques (**Schéma 6**). La réaction entre le complexe Ni–aryle **4** et la propiophénone en milieu basique

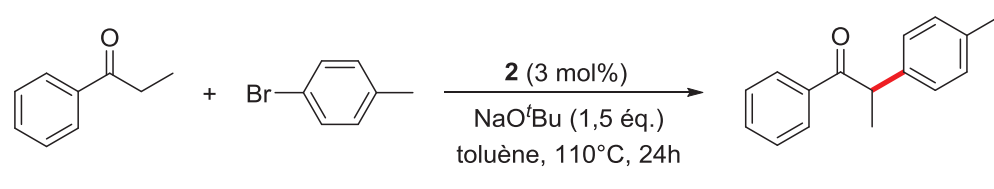
n'a rien donné (**Schéma 6**, éqn. 1), ce qui exclut sa participation au mécanisme. Par contre, la réaction entre le complexe Ni-énolate **3** et le 4-bromotoluène dans le toluène à reflux a majoritairement résulté en la formation de propiophénone (63%) avec une quantité non négligeable du complexe [Ni(IMes)BrCp], ainsi qu'à celles de traces du produit de couplage (**Schéma 6**, éqn. 2). Ce résultat suggère que le complexe [Ni(IMes)BrCp] proviendrait majoritairement de la réaction de déhalogénéation du 4-bromotoluène étant donné la formation majoritaire de propiophénone, mais pourrait également partiellement provenir du couplage de **3** avec le 4-bromotoluène, étant donné la formation de traces du produit de couplage. Pour vérifier cette hypothèse, l' $\alpha$ -arylation de la propiophénone avec le 4-bromotoluène a été réalisée avec le complexe Ni-énolate **3** en conditions catalytiques (**Schéma 6**, éqn. 3), et un rendement de 11% en 1-phényl-2-(*p*-tolyl)-propan-1-one a été mesuré par GC. Le complexe **3** est donc un intermédiaire possible de la réaction d' $\alpha$ -arylation, mais la chute d'activité observée, en comparaison avec le complexe [Ni(IMes)ClCp] **1** qui donne 25% de rendement dans les mêmes conditions, suggère qu'au moins une partie du produit est vraisemblablement obtenu *via* un autre mécanisme.



**Schéma 6.** Evaluation des complexes **3** et **4** comme intermédiaires d' $\alpha$ -arylation de cétones



Dans cette perspective, de récents travaux sur l'emploi de catalyseurs de nickel nous ont conduit à considérer un mécanisme de type radicalaire. La réaction entre propiophénone et 4-bromotoluène catalysée par **2** a alors été réalisée en présence d'inhibiteurs et d'initiateurs de radicaux (**Schéma 7**). Une inhibition totale de la réaction a alors été observée en présence d'1 équiv. d'inhibiteur radicalaire tel que le TEMPO ou le galvinoxyle. De plus, en présence de 20 mol% d'AIBN comme initiateur radicalaire, sans base ni catalyseur, une légère activité a été détectée. En conséquence, nous pensons que le mécanisme principal impliqué dans ce processus d' $\alpha$ -arylation est de nature radicalaire, et que si un dérivé énolate C-lié de **2** est effectivement impliqué, il n'a qu'un rôle mineur.



**Conditions classiques : 78% (GC)**

**TEMPO (1 éq.) : < 1% (GC)**

**galvinoxyl (1 éq.) : < 1% (GC)**

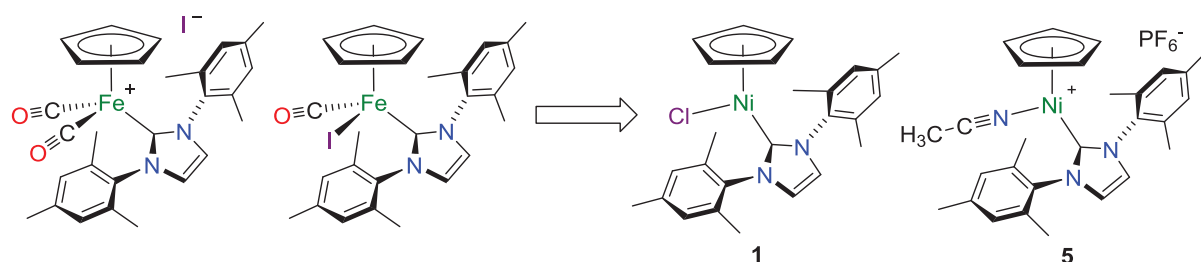
**AIBN (20 mol%), pas de NaOtBu ni (2) : 5% (GC)**

**Schéma 7.**  $\alpha$ -Arylation de la propiophénone avec le 4-bromotoluène en présence d'inhibiteurs et d'initiateurs radicalaires

En conclusion, nous avons démontré que le complexe bon marché et facile à utiliser [Ni(IPr)ClCp] **2** est un pré-catalyseur efficace pour l' $\alpha$ -arylation de cétones acycliques. Cette méthodologie est complémentaire de celles nécessitant Ni(COD)<sub>2</sub>, et permet de travailler avec des charges catalytiques pouvant descendre jusqu'à 1 mol%, ce qui est sans précédent concernant l'emploi de catalyseurs basés sur des métaux non-nobles. En outre, les données mécanistiques recueillies suggèrent un mécanisme radicalaire, même si un intermédiaire nickel-énolate C-lié est peut-être également impliqué.

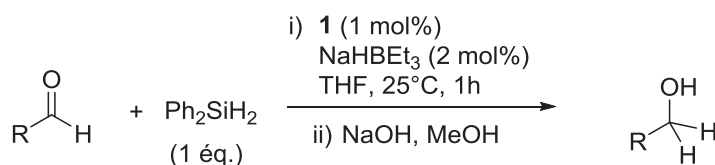
Cette même classe de complexes demi-sandwich a également été évaluée en réaction d'hydrosilylation de carbonyles et d'imines, et les résultats obtenus sont présentés dans le **Chapitre III**. Ces travaux ont découlé d'une collaboration avec l'équipe du Pr. Darcel (Université de Rennes I) qui avait précédemment montré que des complexes demi-sandwich

Fe–NHC sont très actifs en hydrosilylation catalytique de composés (pseudo)carbonylés. L'analogie structurale existante entre ces dérivés du fer et les complexes demi-sandwich de type  $[\text{Ni}(\text{NHC})\text{XCp}]^{(+)}$  nous a ainsi mené à évaluer l'activité de ces derniers dans ces réactions de réduction (**Schéma 8**).



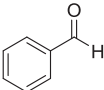
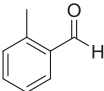
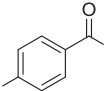
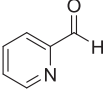
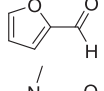
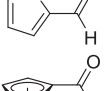
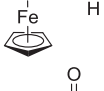
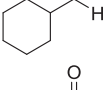
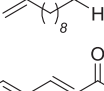
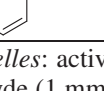
**Schéma 8.** Analogie structurale entre complexes demi-sandwich Fe–NHC utilisés pour l'hydrosilylation de dérivés (pseudo)carbonylés et les complexes demi-sandwich Ni–NHC

Une première étape de cette étude a été d'évaluer l'activité d'une série de complexes, dont le complexe neutre  $[\text{Ni}(\text{IMes})\text{ClCp}]$  **1**, en hydrosilylation de carbonyles. Ce dernier s'est montré relativement actif avec les aldéhydes et les cétones, et après optimisation des conditions réactionnelles, il s'est avéré que l'ajout d'une quantité sub-stoechiométrique de  $\text{NaHBET}_3$  permettait d'observer une activité catalytique plus que satisfaisante. Ainsi, dans le cas des aldéhydes, des rendements modestes à excellents ont pu être obtenus avec une large gamme de substrats en 1 h de réaction en présence de seulement 1 mol% de pré-catalyseur et 2 mol% d'additif (**Schéma 9**). Cette méthodologie est compatible avec une vaste gamme d'aldéhydes qu'ils soient riches ou pauvres en électrons (**Tableau 2**, entrées 1, 3, 4, 6-9, 11-17), et de façon très satisfaisante, tolère de nombreux groupes fonctionnels (entrées 6 à 9), les substrats hétéroaromatiques (entrées 11 à 13) ainsi que les substrats encombrés (entrée 2) sans altération notable de l'activité catalytique.



**Schéma 9.** Hydrosilylation des aldéhydes catalysée par  $[\text{Ni}(\text{IMes})\text{ClCp}]$  **1**

**Tableau 2.** Champ réactionnel de l'hydrosilylation des aldéhydes catalysée par **1**-NaHBET<sub>3</sub><sup>a</sup>

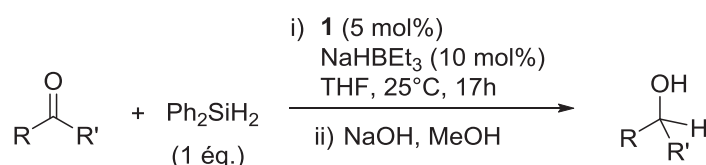
Entrée	Substrat	Conversion (%) <sup>b</sup>	Rendement (%) <sup>c</sup>
1		> 97	88
2		> 97	79
3	 R = Me	> 97	83
4	R = Cl	> 97	76
5	R = Br	13	—
6 <sup>d</sup>	R = OMe	81	70
7 <sup>d</sup>	R = NMe <sub>2</sub>	86	75
8	R = CN	95	68
9	R = NO <sub>2</sub>	70	59
10	R = OH	0	—
11 <sup>d,e</sup>		> 97	—
12 <sup>d</sup>		> 97	86
13 <sup>d</sup>		96	83
14 <sup>d</sup>		> 97	84
15 <sup>e</sup>		96	—
16		75	68
17 <sup>d,f</sup>		88	65

<sup>a</sup> Conditions réactionnelles: activation de **1** (1 mol%) avec NaHBET<sub>3</sub> (2 mol%) dans le THF (4 mL), suivie de l'addition de l'aldéhyde (1 mmol) et Ph<sub>2</sub>SiH<sub>2</sub> (1 mmol), et agitation du milieu réactionnel à 25°C pendant 1 h. <sup>b</sup> Conversions déterminées par RMN <sup>1</sup>H après méthanolyse. <sup>c</sup> Rendements isolés. <sup>d</sup> Réaction effectuée à 70°C. <sup>e</sup> Conversions déterminées par CPG après méthanolyse. <sup>f</sup> Un mélange 75:25 d'alcool cinnamique et de 3-phénylpropan-1-ol a été obtenu.

Il est également important de noter qu'en présence de liaisons Carbone–Carbone doubles conjuguées ou non, la réduction de la fonction carbonyle est majoritaire (entrées 16 et 17). Une limitation de la méthodologie concerne l'emploi d'aldéhydes aromatiques portant un groupement iodure ou bromure, pour lesquels une nette chute d'activité a été observée,

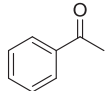
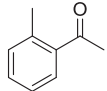
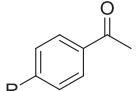
probablement à cause de réactions secondaires de déhalogénéation du substrat (entrées 5 et 6). Enfin, les aldéhydes portant un groupement phénole sont incompatibles avec cette méthodologie (entrée 10).

Dans le cas des cétones, l'optimisation des conditions réactionnelles a permis d'établir qu'en présence de 5 mol% de **1**, 10 mol% de NaHBET<sub>3</sub> dans le THF à 25°C, de très bons rendements sont obtenus pour une large gamme de substrats après 17 h de réaction (**Schéma 10** et **Tableau 3**). Les observations concernant le champ réactionnel sont du même ordre que pour les aldéhydes. En effet, cette méthodologie chimiosélective tolère les substrats riches ou pauvres en électrons, de nombreux groupes fonctionnels, les substrats hétéroaromatiques, les substrats encombrés ainsi que la présence de liaisons Carbone–Carbone doubles. Comme dans le cas des aldéhydes, les cétones aromatiques bromées ou iodées conduisent à des chutes très nettes d'activité.

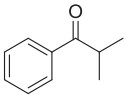
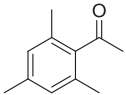
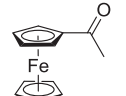
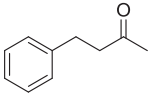
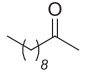
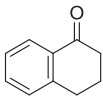
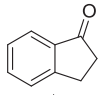
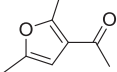
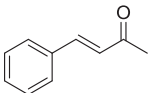


**Schéma 10.** Hydrosilylation des cétones catalysée par [Ni(IMes)ClCp] **1**

**Tableau 3.** Champ réactionnel de l'hydrosilylation des cétones catalysée par **1**-NaHBET<sub>3</sub><sup>a</sup>

Entrée	Substrat	Conversion (%) <sup>b</sup>	Rendement (%)
1		> 97	88
2		> 97	85
3	 R = Me	> 97	79
4	R = Cl	> 97	73
5	R = Br	30	—
6	R = I	14	—
7	R = F	> 97	73
8	R = NO <sub>2</sub>	90	71
9	R = OMe	> 97	88

**Tableau 3. (suite)**

Entrée	Substrat	Conversion (%) <sup>b</sup>	Rendement (%)
10		> 97	75
11		> 97	83
12		> 97	88
13		> 97	83
14		> 97	78
15		> 97	79
16		> 97	86
17		> 97	79
18 <sup>d</sup>		95 <sup>c</sup>	—

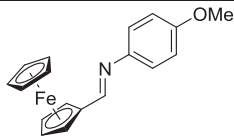
<sup>a</sup> Conditions réactionnelles : activation de **1** (5 mol%) avec NaHBET<sub>3</sub> (10 mol%) dans le THF (4 mL), suivie de l'addition de la cétone (1 mmol) et Ph<sub>2</sub>SiH<sub>2</sub> (1 mmol), et agitation du milieu réactionnel à 25°C pendant 17 h. <sup>b</sup> Conversions déterminées par RMN <sup>1</sup>H après méthanolyse. <sup>c</sup> Un mélange 2:1 de 4-phényl-but-3-èn-2-ol et de 4-phénylbutan-2-ol a été obtenu.

Une deuxième partie de l'étude de la réaction d'hydrosilylation a été d'évaluer l'activité de **1** et de son analogue cationique [Ni(IMes)(NCMe)Cp](PF<sub>6</sub>) **5** (Schéma 8) pour la réduction d'imines. Il a ainsi été déterminé, dans le cas des aldimines, des conditions optimales semblables à celles employées pour les aldéhydes, c'est-à-dire avec 1 mol% de **1** et 2 mol% de NaHBET<sub>3</sub> dans le THF à 25°C, le temps réactionnel étant toutefois de 17 h dans ce cas (Tableau 4). Alternativement, 1 mol% du complexe **5** peut être employé sans additif, dans le THF à 50°C pendant 24 h. Quelque soit le système catalytique employé, des rendements modestes à excellents ont été obtenus avec une vaste gamme d'aldimines aromatiques riches ou pauvres en électrons (entrées 1-3, 5, 6 et 8-30). A nouveau, la limitation majeure reste l'utilisation de substrats iodés ou bromés (entrées 4 et 7).

**Tableau 4.** Champ réactionnel de l'hydrosilylation d'aldimines catalysée par **1**-NaHBET<sub>3</sub> ou **5**<sup>a</sup>

<div style="display: flex; align-items: center; justify-content: center;"> <div style="text-align: center; margin-right: 10px;"> <math display="block">\text{R}-\text{CH}=\text{N}-\text{Ar}</math> </div> <div style="text-align: center; margin-right: 10px;"> <math>+</math> </div> <div style="text-align: center; margin-right: 10px;"> <math>\text{Ph}_2\text{SiH}_2</math> </div> <div style="text-align: center; margin-right: 10px;"> <math>\xrightarrow[\text{ii) NaOH, MeOH}]{\begin{array}{c} \text{i) } \mathbf{1} \text{ (1 mol\%), NaHBET}_3 \text{ (2 mol\%), THF, 25}^\circ\text{C} \\ \text{ou} \\ \mathbf{5} \text{ (1 mol\%), THF, 50}^\circ\text{C} \end{array}}</math> </div> <div style="text-align: center;"> <math>\text{R}-\text{CH}_2-\text{NH}-\text{Ar}</math> </div> </div>					
Entrée	Substrat		Pré-catalyseur	Conversion <sup>b</sup> (%)	Rendement <sup>c</sup> (%)
1		R = Me	<b>1</b>	> 97	83
2		R = Me	<b>5</b>	> 97	—
3		R = OMe	<b>1</b>	> 97	90
4		R = Br	<b>1</b>	20	—
5		R = <i>p</i> -OMe	<b>1</b>	> 97	89
6		R = <i>p</i> -OMe	<b>5</b>	> 97	—
7		R = <i>p</i> -I	<b>1</b>	27	—
8		R = <i>o</i> -OMe	<b>1</b>	28	—
9		R = <i>o</i> -OMe	<b>1</b>	48 <sup>d</sup>	39
10		R = <i>p</i> -OMe	<b>1</b>	> 97	84
11		R = <i>p</i> -OMe	<b>5</b>	> 97	—
12		R = <i>p</i> -NMe <sub>2</sub>	<b>1</b>	77	57
13		R = <i>p</i> -Cl	<b>1</b>	> 97	80
14		R = <i>p</i> -Cl	<b>5</b>	71	—
15		R = <i>p</i> -CO <sub>2</sub> Me	<b>1</b>	95	76
16		R = <i>p</i> -CO <sub>2</sub> Me	<b>5</b>	> 97	83
17		R = <i>p</i> -Cl	<b>1</b>	94 <sup>e</sup>	74
18		R = 3,4,5-OMe	<b>1</b>	93	81
19		R = NHAc	<b>1</b>	70	—
20		R = NHAc	<b>1</b>	90 <sup>d</sup>	72
21		R = NO <sub>2</sub>	<b>1</b>	0	—
22		R = NO <sub>2</sub>	<b>1</b>	40 <sup>f</sup>	—
23			<b>1</b>	20	—
24			<b>1</b>	80 <sup>f</sup>	57
25			<b>1</b>	43	—
26			<b>1</b>	70 <sup>f</sup>	61
27			<b>1</b>	20	—
28			<b>1</b>	60 <sup>f</sup>	—
29			<b>1</b>	87 <sup>f,g</sup>	70

**Tableau 4.** (suite)

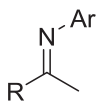
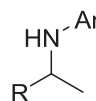
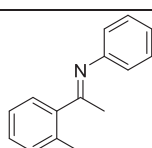
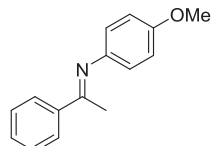
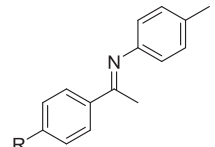
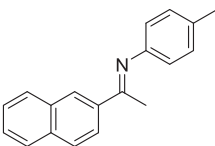
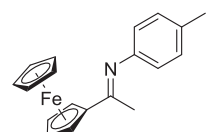
Entrée	Substrat	Pré-catalyseur	Conversion <sup>b</sup> (%)	Rendement <sup>c</sup> (%)
30		<b>1</b>	> 97	85

<sup>a</sup> Conditions réactionnelles : activation de **1** (1 mol%) avec NaHBET<sub>3</sub> (2 mol%) dans le THF (4 mL) à t.a. pendant 5 min, ou dissolution de **5** (1 mol%) dans le THF (4 mL) à t.a., suivie de l'addition de l'aldimine (1 mmol) et Ph<sub>2</sub>SiH<sub>2</sub> (1 mmol), et agitation du milieu réactionnel à 25°C pendant 17 h (**1**) ou à 50°C pendant 24 h (**5**). <sup>b</sup> Conversions déterminées par RMN <sup>1</sup>H après méthanolyse. <sup>c</sup> Rendements isolés. <sup>d</sup> 50°C. <sup>e</sup> 5% de réduction des groupements cyano et aldimine a été observé. <sup>f</sup> 70°C. <sup>g</sup> **1** (5 mol%), NaHBET<sub>3</sub> (10 mol%).

Des conditions un peu plus dures ont été nécessaires pour obtenir des rendements similaires avec les cétimines. Ainsi, il a fallu (i) chauffer à 50°C avec le système **1**-NaHBET<sub>3</sub>, et (ii) augmenter la charge catalytique et celle en Ph<sub>2</sub>SiH<sub>2</sub> à respectivement 5 mol% et 2 équiv. avec le complexe cationique **5** sans additif (**Tableau 5**). Une fois encore, cette méthodologie a pu s'appliquer à un champ réactionnel de cétimines méthyléniques relativement étendu (17 exemples).

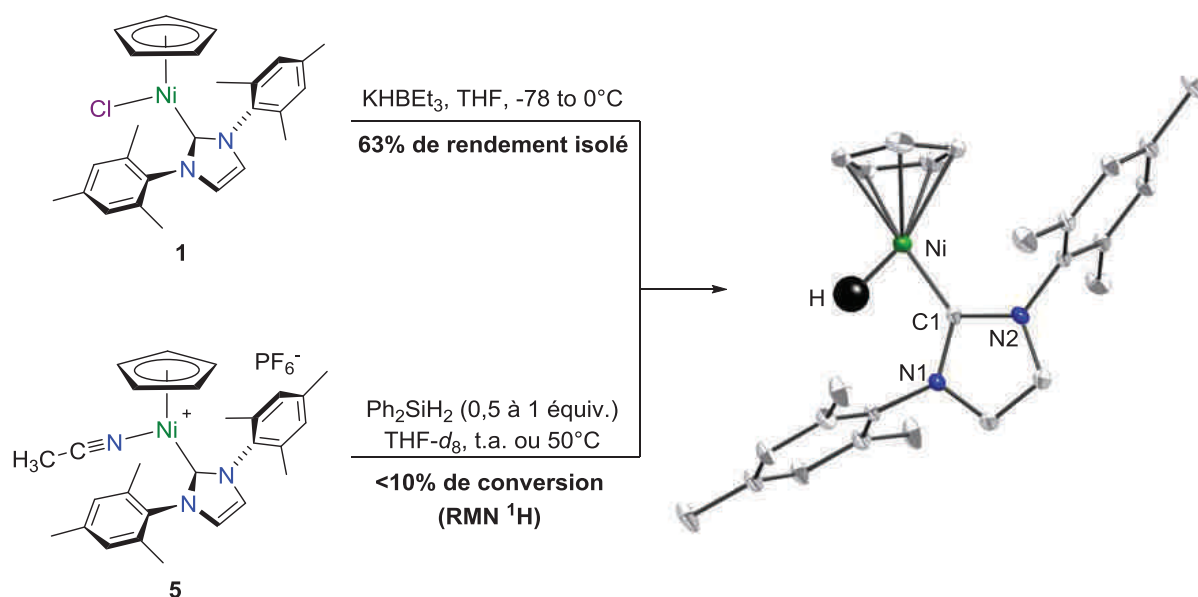
La troisième et dernière partie de cette étude a été centrée sur l'étude du mécanisme réactionnel de ces procédures d'hydrosilylation catalysées par **1**-NaHBET<sub>3</sub> ou **5**. Pour rationaliser le rôle de l'additif dans le système **1**-NaHBET<sub>3</sub>, le complexe **1** a été traité par un équivalent de KHBET<sub>3</sub> dans le THF à froid (**Schéma 11**). La réaction donne lieu à la formation du complexe nickel-hydrure [Ni(IMes)HCp] **6** qui a pu être isolé avec 63% de rendement et caractérisé par diffraction des rayons X sur monocristal. Similairement, la réaction du complexe cationique **5** avec 0,5 ou 1 équiv. de Ph<sub>2</sub>SiH<sub>2</sub> donne également le complexe **6**, mais avec une conversion inférieure à 10% (déterminée par RMN <sup>1</sup>H). Ces observations suggèrent que **6** serait le véritable précurseur catalytique, ce qui a été confirmé par un test catalytique (**Schéma 12**, éqn. 1). Cependant, lorsque **6** a été traité avec le benzaldéhyde en absence de Ph<sub>2</sub>SiH<sub>2</sub>, aucune insertion n'a été observée, et le signal de l'hydrure est resté inchangé (**Schéma 12**, éqn. 2). Ainsi, nous pensons que, bien que **6** soit très probablement le véritable précurseur catalytique, le ligand hydrure ne participe pas directement à ces réactions de réductions, comme l'a conclu Royo *et al.* dans des travaux analogues publiés simultanément aux nôtres (*Adv. Synth. Catal.* **2012**, 354, 2613).

**Tableau 5.** Champ réactionnel de l'hydrosilylation de cétones catalysée par **1**-NaHBEt<sub>3</sub> ou **5**<sup>a</sup>

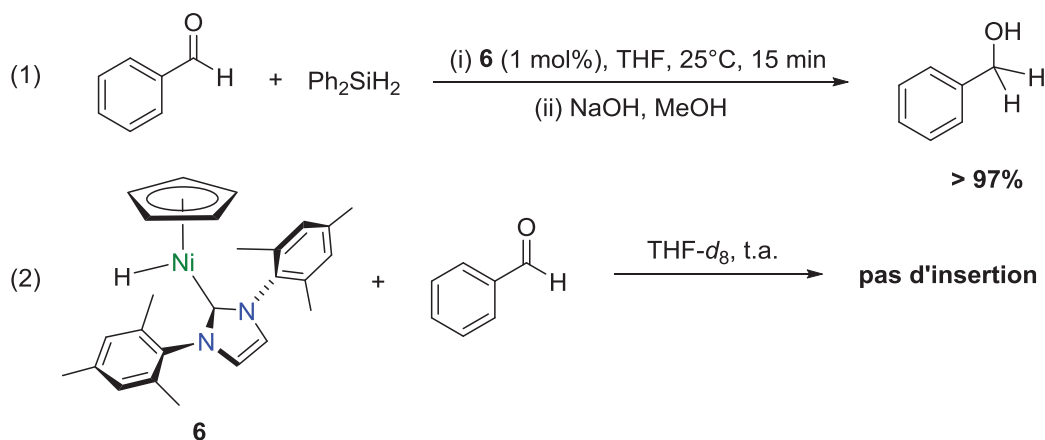
<div style="display: flex; align-items: center; justify-content: center;"><div style="text-align: center; margin-right: 10px;"></div><div style="text-align: center; margin-right: 10px;">+ Ph<sub>2</sub>SiH<sub>2</sub></div><div style="text-align: center; margin-right: 10px;"><math>\xrightarrow[\text{ii) NaOH, MeOH}]{\begin{array}{l} \text{i) } \mathbf{1} \text{ (1 mol\%), NaHBEt}_3 \text{ (2 mol\%), THF, 50}^\circ\text{C} \\ \text{ou} \\ \mathbf{5} \text{ (5 mol\%), THF, 50}^\circ\text{C} \end{array}}</math></div><div style="text-align: center;"></div></div>					
Entrée	Substrat	Pré-catalyseur	Conversion <sup>b</sup> (%)	Rendement <sup>c</sup> (%)	
1		<b>1</b>	> 97	77	
2		<b>1</b>	> 97	78	
3		<b>5</b>	> 97	—	
4		R = H	<b>1</b>	79	63
5		R = Me	<b>1</b>	86	73
6		R = OMe	<b>1</b>	> 97	84
7		R = OMe	<b>5</b>	> 97	—
8		R = Cl	<b>1</b>	90	77
9		R = F	<b>1</b>	90	75
10		R = F	<b>5</b>	> 97	80
11		R = CF <sub>3</sub>	<b>1</b>	30	—
12		R = CF <sub>3</sub>	<b>1</b>	52 <sup>d</sup>	—
13		R = CF <sub>3</sub>	<b>1</b>	85 <sup>d,e</sup>	69
14		<b>1</b>	90	59	
15		<b>1</b>	20	—	
16		<b>1</b>	48 <sup>d</sup>	—	
17		<b>1</b>	80 <sup>d,e</sup>	66	

<sup>a</sup> Conditions réactionnelles : activation de **1** (1 mol%) avec NaHBEt<sub>3</sub> (2 mol%) dans le THF (4 mL) à t.a. pendant 5 min, ou dissolution de **5** (5 mol%) dans le THF (4 mL) à t.a., suivie de l'addition de la cétone (1 mmol) et Ph<sub>2</sub>SiH<sub>2</sub> (1 mmol (**1**) ou 2 mmol (**5**)), et agitation du milieu réactionnel à 50°C pendant 17 h (**1**) ou 24 h (**5**). <sup>b</sup> Conversions déterminées par RMN <sup>1</sup>H après méthanolyse. <sup>c</sup> Rendements isolés. <sup>d</sup> 70°C. <sup>e</sup> **1** (5 mol%), NaHBEt<sub>3</sub> (10 mol%).





**Schéma 11.** Formation du complexe nickel-hydrure **6** à partir de **1** ou de **5**



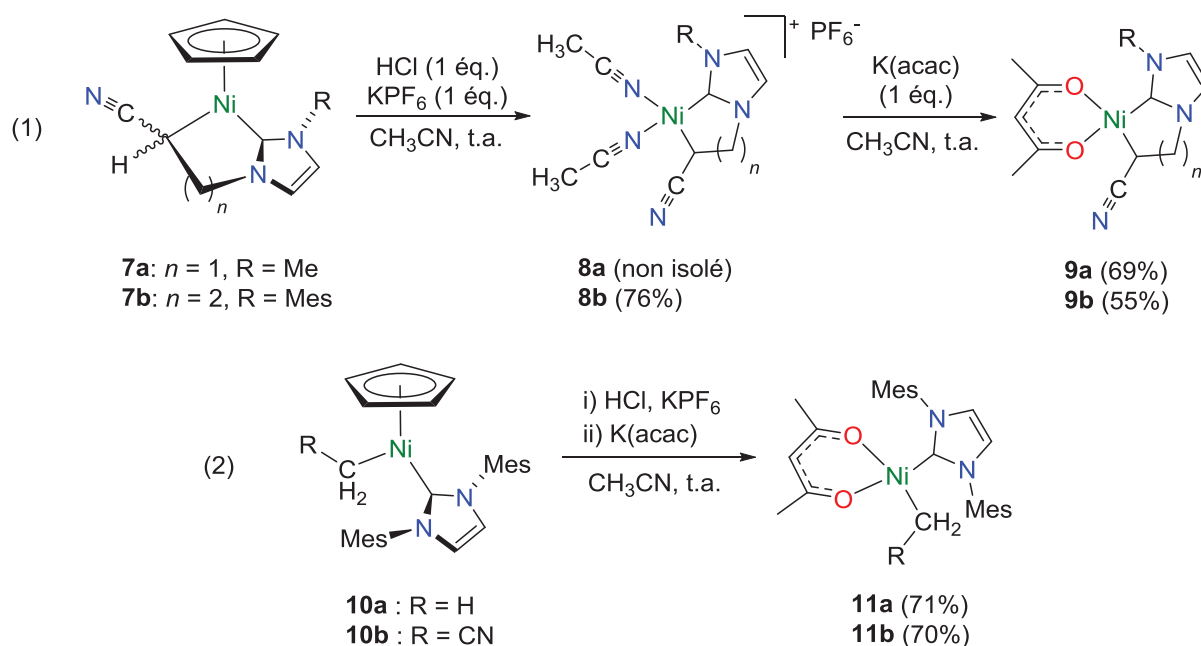
**Schéma 12.** Evaluation de **6** en tant qu'intermédiaire réactionnel

Cette étude nous a donc permis de démontrer que ces complexes demi-sandwich Ni–NHC ne sont pas simplement des pré-catalyseurs efficaces en  $\alpha$ -arylation de cétones, mais plutôt des outils polyvalents puisqu'ils permettent également l'hydrosilylation de carbonyles et d'imines dans des conditions très douces, et avec des charges catalytiques relativement faibles. De plus, ces méthodologies sont chimiosélectives et tolèrent une vaste gamme de substrats, ce qui est tout à fait remarquable lorsqu'on considère les rares exemples décrivant l'utilisation de nickel comme catalyseur. Enfin, ces procédés de réduction tendent à impliquer, comme bien

souvent, la formation d'un complexe nickel–hydrure qui serait à l'origine des activités observées, même si le ligand hydrure ne semble pas participer directement au mécanisme.

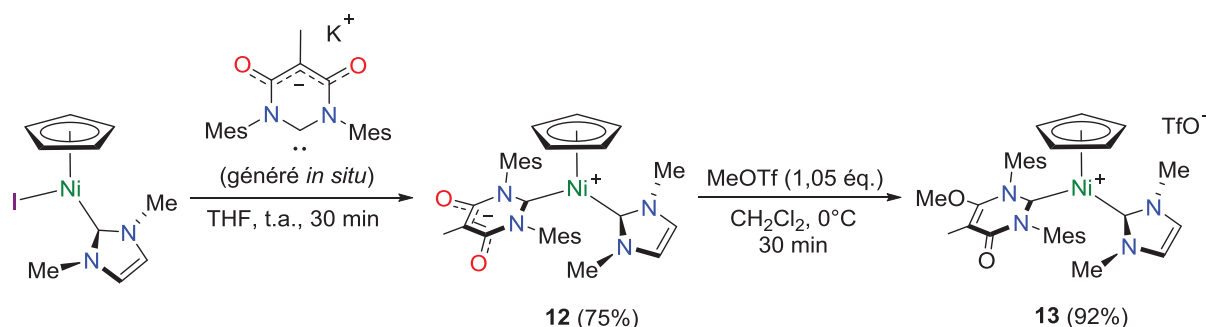
Enfin, dans le quatrième et **dernier chapitre** de cette thèse, nous décrivons la synthèse, la caractérisation et l'évaluation en catalyse de nouveaux complexes Ni–NHC. Cette initiative découle de la volonté de développer des espèces Ni–NHC plus actives et/ou sélectives en catalyse homogène.

Lors de cette étude, il a été démontré dans un premier temps qu'il était possible de labiliser le ligand Cp  $\eta^5$ -coordonné par acidolyse de complexes demi-sandwich alkyl,NHC–Ni, dont la sphère de coordination du nickel est saturée. La réaction s'effectue de manière très sélective, que ce soit dans des dérivés cycliques (**Schéma 13**, éqn. 1) ou acycliques (éqn. 2), pour donner les complexes carré-plan à 16 électrons correspondants avec de bons rendements. Ainsi, dans le cas des complexes cycliques **7a,b**, leur traitement avec 1 équiv. d'HCl et 1 équiv. de KPF<sub>6</sub> dans l'acétonitrile permet la substitution du ligand Cp par deux molécules d'acétonitrile pour donner les complexes cationiques correspondants **8a,b**, dont les deux molécules d'acétonitrile peuvent être aisément substituées par un ligand acétylacétonate (acac) pour donner les complexes carré-plan neutres **9a,b** avec de bons rendements. De façon remarquable, la même méthodologie a pu être appliquée aux dérivés acycliques **10a,b**. Ces réactions qui passent par une protonolyse directe du ligand Cp, comme l'ont montré des expériences de deutération, est remarquable pour un certain nombre de raisons : (i) la démétallation d'un ligand Cp d'un complexe monocyclopentadiényle à 18 électrons en présence d'une source de protons est, à notre connaissance, sans précédent, (ii) cette réaction permet la création de deux sites de coordination potentiellement vacants, comme en témoigne la substitution aisée des ligands acétonitriles des complexes **8a,b**, ce qui est potentiellement un avantage pour une éventuelle application en catalyse, et (iii) elle démontre l'exceptionnelle robustesse des liaisons Ni–carbène et Ni–alkyle de ces complexes.



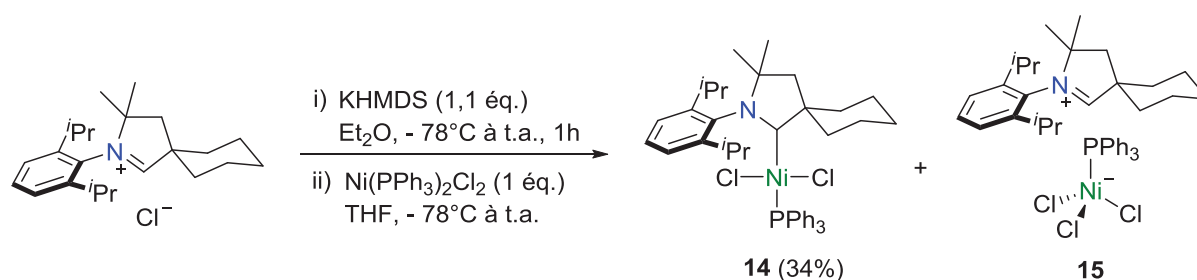
**Schéma 13.** Labilisation du ligand Cp dans les complexes cycliques **7a,b** et acycliques **10a,b**

Parallèlement à ces travaux, le complexe zwitterionique demi-sandwich **12** portant un NHC de type *malo*-pyrimidine a été synthétisé par réaction du *malo*-NHC libre généré *in situ* avec le complexe  $[\text{Ni}(\text{IMe})\text{ICp}]$  (**Schéma 14**). L'intérêt des ligands de type *malo*-NHC en catalyse est la modularité aisée de leurs propriétés électroniques sans affecter leurs propriétés stériques. En effet, le ligand anionique *malo*-NHC de **12** peut être piégé par un vaste choix d'électrophiles, permettant l'adaptation du pouvoir  $\sigma$ -donneur du NHC au besoin, ce que nous avons illustré en le faisant réagir avec MeOTf pour obtenir le complexe cationique **13** (**Schéma 14**). En outre, un complexe zwitterionique comme **12** présente l'intérêt d'avoir une charge négative dirigée en dehors de la sphère de coordination du nickel peut avoir des avantages si la présence d'un autre type d'anion s'avère négative.



**Schéma 14.** Synthèse des complexes *malo*-NHC–Ni zwitterionique **12** et cationique **13**

Enfin, la chimie de coordination encore balbutiante d'un ligand alkyl-amino carbène cyclique (CAAC) au nickel, a également été étudiée. Ces ligands ont un pouvoir  $\sigma$ -donneur encore plus important que les diaminocarbènes classiques et possèdent un environnement stérique différent, ce qui s'est révélé bénéfique dans certaines transformations catalysées par les métaux comme le palladium. Le complexe de nickel **14** portant un ligand CAAC a donc été synthétisé par réaction du CAAC libre généré *in situ* avec  $[\text{Ni}(\text{PPh}_3)_2\text{Cl}_2]$  dans le THF à froid (**Schéma 15**). Lors de cette synthèse, un sous-produit a également été obtenu. Il s'agit du composé ionique **15**, présentant un anion nickelate tétraédrique et un contre-ion azolium.



**Schéma 15.** Synthèse du complexe Ni-CAAC **14** avec la formation de **15**

L'activité en catalyse homogène des nickelacycles **7-9b** et des nouveaux complexes **12-14** a fait l'objet d'une étude préliminaire dans diverses réactions comme le couplage de Suzuki-Miyaura de l'acide phénylboronique avec la 4-bromoacétophénone, l'hydrosilylation du benzaldéhyde et l'arylation oxydative du THF.

En particulier, l'activité des nickelacycles **7-9b** pour le couplage de l'acide phénylboronique et de la 4-bromoacétophénone a été comparée afin d'évaluer l'effet de la substitution du ligand Cp du complexe **7b** sur cette transformation (**Tableau 6**). Comme espéré, les complexes carré-plan **8b** et **9b** se sont révélés plus actifs que **7b**. En outre, le complexe cationique **8b** possédant deux ligands acétonitriles labiles s'est révélé plus actif que le complexe neutre **9b**, ce qui montre que plus les ligands autre que ceux du nickelacycle sont labiles, plus les complexes sont réactifs. Cependant, les activités obtenues n'excèdent pas celles déjà décrites dans la littérature sont réactifs avec certains complexes demi-sandwich de type  $[\text{Ni}(\text{NHC})\text{LCp}^\dagger]^{(+)}$ .

**Tableau 6.** Couplage de Suzuki-Miyaura entre l'acide phénylboronique et la 4-bromoacétophénone catalysée par les complexes Ni(II)–NHC **7-9b** et **12-14**<sup>a</sup>

c1ccccc1B(O)O (1,3 éq.) + BrC1=CC=C(C(=O)C)C=C1
 $\xrightarrow[\text{toluène, 110°C}]{\text{[Ni] (1 - 3 mol\%), K}_3\text{PO}_4 \text{ (2,6 éq.)}}$ 
c1ccccc1C2=CC=C(C(=O)C)C=C2

Entrée	Catalyseur	Temps (min)	Conversion (%) <sup>b</sup>
1	<b>7b</b>	60	20
2	<b>8b</b>	60	58
3	<b>9b</b>	60	45
4	<b>12</b>	60	21
5	<b>13</b>	60	23
6	<b>14</b>	60	13

<sup>a</sup> Conditions réactionnelles : acide phénylboronique (1,3 mmol), 4-bromoacétophénone (1 mmol), K<sub>3</sub>PO<sub>4</sub> (2,6 mmol), [Ni] (3 mol%) dans le toluène (3 mL) à 110°C. <sup>b</sup> Conversions déterminées par RMN <sup>1</sup>H; moyenne de deux expériences.

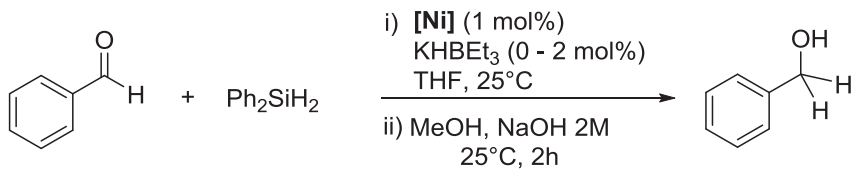
Dans cette même réaction, les complexes *malo*-NHC **12** et **13** ont montré une activité comparable à celle de **7b** (Tableau 6, entrées 1, 4 et 5), ce qui peut sans doute s'expliquer par le fait que la sphère de coordination du nickel est saturée dans les trois cas. Des tentatives de labilisation du ligand Cp en milieu acide n'ont malheureusement aboutit à rien de probant avec les complexes **12** et **13**.

L'activité de ces mêmes complexes a alors été évaluée dans la réaction d'hydrosilylation du benzaldéhyde avec le diphenylsilane, en présence ou non de KHBET<sub>3</sub> comme additif (Tableau 7). Contrairement au couplage du Suzuki-Miyaura, le complexe zwitterionique **12** est deux fois plus actif que son analogue cationique **13**, que ce soit sans ou avec additif (entrées 1 vs. 3 et 2 vs. 4). Néanmoins, **12** reste bien moins efficace que **1** (Tableau 7, entrée 4 vs. Tableau 2, entrée 1).

Notre engouement pour la valorisation de complexes Ni(II)–NHC dans des transformations impliquant la fonctionnalisation de liaisons C–H nous a enfin conduit à tester ces complexes *malo*-NHC dans la réaction d'arylation directe du THF en présence d'acide phénylboronique (Tableau 8). En effet, cette réaction en conditions oxydantes fait intervenir la fonctionnalisation directe du THF qui constitue un défi particulièrement important du fait

de la très grande stabilité du THF. De façon satisfaisante, une activité certes modeste mais non négligeable a été observée, en particulier avec **12**, qui est à nouveau deux fois plus actif que **13** (entrées 1 et 2). Ainsi, ces résultats, même s'ils sont inférieurs à ceux récemment obtenus avec un système Ni(acac)<sub>2</sub>/PPh<sub>3</sub>, tendent à montrer un certain potentiel des complexes *malo*-NHC de nickel, et il est certain qu'un travail de recherche dans l'élaboration d'autres complexes de ce type devrait permettre d'aboutir à des catalyseurs bien plus performants.

**Tableau 7.** Hydrosilylation du benzaldéhyde avec le diphenylsilane catalysée par les complexes Ni(II)–NHC **12-14**<sup>a</sup>

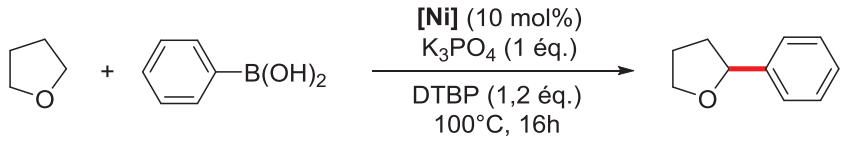
				
Entrée	Catalyseur	Additif (mol%)	Temps (min)	Conversion (%) <sup>b</sup>
1	<b>12</b>	—	60	12
2	<b>12</b>	KHBET <sub>3</sub> (2)	60	61
3	<b>13</b>	—	60	5
4	<b>13</b>	KHBET <sub>3</sub> (2)	60	38
5	<b>14</b>	KHBET <sub>3</sub> (2)	30	31

<sup>a</sup> Conditions réactionnelles : activation de **12-14** avec KHBET<sub>3</sub> dans le THF (4 mL), ou dissolution dans le THF, suivie de l'addition de benzaldéhyde (1 mmol) et Ph<sub>2</sub>SiH<sub>2</sub> (1 mmol), et agitation du milieu réactionnel à 25°C. <sup>b</sup> Conversions déterminées par RMN <sup>1</sup>H après méthanolyse.

De façon décevante, le complexe Ni–CAAC **14** s'est montré peu, voire très peu actif, que ce soit en couplage de Suzuki-Miyaura (**Tableau 6**, entrée 6), en hydrosilylation du benzaldéhyde en présence de KHBET<sub>3</sub> (**Tableau 7**, entrée 5), ou encore en arylation directe du THF (**Tableau 8**, entrée 3). Cette étude n'étant qu'à son commencement, les raisons d'une activité aussi faible dans trois réactions très différentes ne sont pas encore bien comprises. Cependant, l'exposition à l'air d'une solution du complexe **14** dans le THF menant partiellement à la formation du composé zwitterionique **15** tend à montrer une certaine sensibilité de la liaison Ni–CAAC de **14**, ce qui peut être une raison possible de ces observations. Une étude plus approfondie de la chimie de coordination, et de l'activité en catalyse de composés du nickel comportant des ligands de type CAAC est donc nécessaire

afin de mieux comprendre leur comportement, et éventuellement développer des espèces dans lesquelles la présence de CAACs s'avèrerait bénéfique en catalyse.

**Tableau 8.** Arylation directe du THF en présence d'acide phénylboronique et catalysée par les complexes Ni(II)–NHC **12-14**<sup>a</sup>

		
Entrée	Catalyseur	Rendement (%) <sup>b</sup>
1	<b>12</b>	19
2	<b>13</b>	11
3	<b>14</b>	4

<sup>a</sup> Conditions réactionnelles : acide phénylboronique (0,50 mmol), [Ni] (10 mol%) dans le THF (3 mL) à 100°C pendant 16 h. <sup>b</sup> Rendements isolés.

En conclusion, ce travail de thèse a permis d'identifier les complexes demi-sandwich de nickel de type [Ni(NHC)XCp] comme des outils efficaces et polyvalents en catalyse. Leur utilisation a abouti à des activités sans précédent en  $\alpha$ -arylation de cétones acycliques, où des charges en pré-catalyseur allant jusqu'à 1 mol% peuvent être utilisées. Cette méthodologie est complémentaire à celles développées avec des charges importantes de Ni(COD)<sub>2</sub> comme catalyseur, et qui ont été appliquées exclusivement à des cétones cycliques. Une étude du mécanisme tend à démontrer l'implication d'intermédiaires radicalaires dans ce processus d' $\alpha$ -arylation de cétones. De plus, ces complexes sont également des pré-catalyseurs permettant l'emploi de conditions douces dans les réactions d'hydrosilylation chimiosélectives de dérivés carbonylés et d'imines. Le champ réactionnel est remarquablement vaste, et il apparaît qu'un intermédiaire de type nickel–hydrure formé *in situ* serait le véritable précurseur catalytique, même si l'hydrure ne semble pas directement impliqué dans le mécanisme. Par ailleurs, le développement d'une méthodologie de labilisation de ligand Cp dans des complexes alkyle,NHC–Ni a ouvert une voie originale dans l'élaboration de nouveaux complexes carré-plan de nickel, potentiellement plus actifs en catalyse. Cette étude a permis de montrer l'exceptionnelle stabilité des liaisons nickel–NHC et nickel–alkyle de ces complexes, fait qui n'avait jamais été observé dans d'autres complexes alkyle,NHC–Ni. Enfin, la synthèse de nouveaux complexes de nickel portant un ligand *mal*-NHC ou CAAC a également été

réalisée. Ce type de composés n'a encore que très peu été étudié, et les premières études en catalyse montre un certain potentiel, et donc un intérêt à les étudier de façon plus approfondie. Ce travail de thèse démontre le formidable potentiel des complexes Ni(II)–NHC et il ne fait nul doute que des travaux ultérieurs mèneront à des espèces encore plus efficaces en catalyse.



# Contents



## Chapter I. *N*-heterocyclic carbene–nickel complexes: versatile tools for catalysis ..... 1

<b>I. Carbenes and carbene complexes.....</b>	<b>2</b>
I.1. Historical aspects .....	2
I.2. Theoretical aspects.....	3
I.3. NHC as ligands in catalysis .....	6
<b>II. <i>N</i>-heterocyclic carbene–nickel complexes in catalysis .....</b>	<b>9</b>
II.1. Introduction.....	9
II.2. Coupling reactions involving Carbon–Carbon bond formation .....	9
II.2.1. Kumada-Tamao-Corriu coupling .....	9
II.2.2. Suzuki-Miyaura coupling .....	23
II.2.3. Mizoroki-Heck coupling.....	29
II.2.4. Negishi coupling .....	30
II.2.5. Homocoupling reactions.....	31
II.2.6. Other cross-couplings .....	32
II.2.7. Carbon–Carbon bond formation via Carbon–Hydrogen bond functionalization.....	33
II.2.8. Miscellaneous Carbon–Carbon bond formation reactions.....	38
II.3. Coupling reactions involving Carbon–Heteroatom bond formation .....	40
II.3.1. Carbon–Nitrogen bond formation.....	40
II.3.2. Carbon–Sulfur bond formation .....	45
II.4. Reduction reactions.....	48
II.4.1. Dehalogenation reactions.....	48
II.4.2. Carbon–Carbon multiple bond reduction .....	48
II.4.3. Carbon–Heteroatom multiple bond reduction .....	51
II.5. Oxidation reactions .....	53
II.6. Miscellaneous reactions .....	54
<b>III. Conclusions.....</b>	<b>57</b>
<b>IV. References.....</b>	<b>58</b>

## Chapter II. From acetone metalation to the catalytic $\alpha$ -arylation of acyclic ketones with *N*-heterocyclic carbene–nickel(II) complexes.... 69

<b>I. Introduction.....</b>	<b>70</b>
<b>II. Results and Discussion.....</b>	<b>73</b>
II.1. Choice and syntheses of the pre-catalysts.....	73
II.2. Optimization of the catalytic conditions .....	75

II.3. Reaction scope study .....	76
II.4. Mechanistic studies.....	79
<b>III. Conclusion .....</b>	<b>84</b>
<b>IV. Experimental section .....</b>	<b>84</b>
IV.1. General information .....	84
IV.2. Synthesis of [Ni(IPr)(NCMe)Cp](PF <sub>6</sub> ) (8) .....	85
IV.3. Synthesis of [Ni(IMes){CH(CH <sub>3</sub> )C(O)Ph}Cp] (10).....	86
IV.4. Synthesis of [Ni(IMes)PhCp] (11).....	86
IV.5. X-ray diffraction study of (8) and (11): structure determination and refinement.....	87
IV.6. Optimization of the catalytic $\alpha$ -arylation of ketones: solvent and base influence.....	89
IV.7. General procedure for the catalytic $\alpha$ -arylation of ketones .....	89
IV.8. Control experiments.....	90
IV.8.1. Investigation of the mercury effect.....	90
IV.8.2. Reaction of complex (10) with 4-bromotoluene.....	90
IV.8.3. Catalytic $\alpha$ -arylation of propiophenone with (10) as pre-catalyst.....	91
IV.8.4. Reaction of complex (11) with propiophenone .....	91
IV.8.5. Investigation of radical scavenger effect .....	91
IV.8.6. Investigation of radical initiator effect .....	91
IV.9. Spectral data of the coupling products.....	92
<b>V. References.....</b>	<b>97</b>

## Chapter III. Ni–NHC-catalyzed hydrosilylation of Carbon–Heteroatom double bonds..... 101

<b>I. Introduction.....</b>	<b>102</b>
<b>II. Results and Discussion.....</b>	<b>103</b>
II.1. Hydrosilylation of aldehydes <sup>[39]</sup> .....	103
II.2. Hydrosilylation of ketones <sup>[39]</sup> .....	107
II.3. Hydrosilylation of aldimines <sup>[45]</sup> .....	109
II.4. Hydrosilylation of ketimines <sup>[45]</sup> .....	114
II.5. Mechanistic studies <sup>[39,45]</sup> .....	116
II.5.1. (1)-NaHBEt <sub>3</sub> catalytic system.....	116
II.5.2. (4)-no additive catalytic system .....	121
<b>III. Conclusion .....</b>	<b>126</b>
<b>IV. Experimental section .....</b>	<b>126</b>
IV.1. General information .....	126
IV.2. Synthesis of [Ni(IMes)HCp] (9) .....	127
IV.3. Reactions of [Ni(IMes)(NCMe)Cp](PF <sub>6</sub> ) (4) and Ph <sub>2</sub> SiH <sub>2</sub> .....	128

IV.4. X-ray diffraction study of (9): structure determination and refinement .....	129
IV.5. Hydrosilylation of aldehydes and ketones .....	130
IV.5.1. Optimization studies.....	130
IV.5.2. General procedure: nickel-catalyzed hydrosilylation of aldehydes .....	130
IV.5.3. General procedure: nickel-catalyzed hydrosilylation of ketones .....	131
IV.6. Hydrosilylation of aldimines and ketimines .....	131
IV.6.1. Optimization studies.....	131
IV.6.2. General procedure: nickel-catalyzed hydrosilylation of aldimines with (1) and NaHBET <sub>3</sub> .....	132
IV.6.3. General procedure: nickel-catalyzed hydrosilylation of aldimines with (4) ....	133
IV.7. Characterization of the hydrosilylation products .....	133
<b>V. References.....</b>	<b>133</b>

## Chapter IV. Synthesis, characterization and catalysis applications of new N-heterocyclic carbene–nickel complexes..... 137

<b>I. Introduction.....</b>	<b>138</b>
<b>II. Results and discussion .....</b>	<b>142</b>
II.1. Facile displacement of $\eta^5$ -cyclopentadienyl ligands from half sandwich alkyl, NHC–nickel complexes .....	142
II.2. Attempts to synthesize [Ni(IMes)(acac)Cl]: unexpected formation of [IMes.H <sup>+</sup> ] <sub>3</sub> [(NiCl <sub>4</sub> <sup>2-</sup> )(Cl <sup>-</sup> )] .....	149
II.3. Synthesis of <i>malo</i> -NHC–nickel complexes .....	152
II.4. Synthesis of Ni–CAAC complexes .....	157
II.5. Catalysis applications of the new nickel carbene complexes .....	161
<b>III. Conclusion .....</b>	<b>166</b>
<b>IV. Experimental section .....</b>	<b>166</b>
IV.1. General information .....	167
IV.2. Synthesis of [Ni{Mes-NHC-(CH <sub>2</sub> ) <sub>2</sub> CH(CN)}(NCCH <sub>3</sub> ) <sub>2</sub> ] <sup>+</sup> PF <sub>6</sub> <sup>-</sup> (3b) .....	167
IV.3. Deuterium labeling experiment; reaction of (2b) with DCl.....	168
IV.4. Synthesis of [Ni{Mes-NHC-(CH <sub>2</sub> ) <sub>2</sub> CH(CN)}(acac)] (4b) .....	168
IV.5. Synthesis of [Ni{Me-NHC-CH <sub>2</sub> CH(CN)}(acac)] (4a) .....	169
IV.6. Synthesis of [Ni(IMes)(CH <sub>3</sub> )(acac)] (6a).....	170
IV.7. Synthesis of [Ni(IMes)(CH <sub>2</sub> CN)(acac)] (6b).....	171
IV.8. Synthesis of [IMes.H <sup>+</sup> ] <sub>3</sub> [(NiCl <sub>4</sub> <sup>2-</sup> )(Cl <sup>-</sup> )] (7).....	171
IV.9. Synthesis of [Ni(IMes) <sub>2</sub> Cl <sub>2</sub> ] (8) .....	172
IV.10. Synthesis of [Ni(PPh <sub>3</sub> ) <sub>2</sub> ( <i>malo</i> NHC)Cl] (10).....	172
IV.11. Synthesis of [Ni(Ime)( <i>malo</i> NHC)Cp] (12).....	173

IV.12. Synthesis of [Ni(Ime)(MeO-maloNHC)Cp](OTf) (13).....	173
IV.13. Synthesis of [Ni(CAAC)(PPh <sub>3</sub> )Cl <sub>2</sub> ] (15) and of [CAAC.H <sup>+</sup> ][Ni(PPh <sub>3</sub> )Cl <sub>3</sub> <sup>-</sup> ] (16) .....	173
IV.14. X-ray Diffraction Studies. Structure Determination and Refinement.....	174
<b>V. References.....</b>	<b>175</b>

<b>General conclusion .....</b>	<b>181</b>
---------------------------------	------------

<b>Publications.....</b>	<b>185</b>
--------------------------	------------

## **Chapter I.**

# ***N*-Heterocyclic carbene–nickel complexes: versatile tools for catalysis**





# Chapter I.

## ***N*-Heterocyclic carbene–nickel complexes: versatile tools for catalysis**

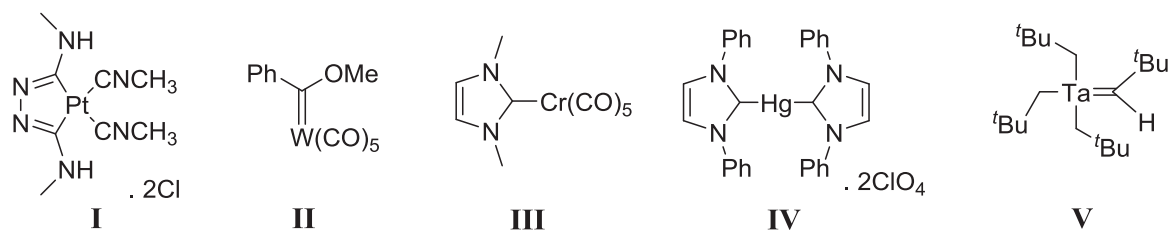
<b>I.</b>	<b>Carbenes and carbene complexes.....</b>	<b>2</b>
I.1.	Historical aspects .....	2
I.2.	Theoretical aspects.....	3
I.3.	NHC as ligands in catalysis .....	6
<b>II.</b>	<b><i>N</i>-heterocyclic carbene–nickel complexes in catalysis .....</b>	<b>9</b>
II.1.	Introduction.....	9
II.2.	Coupling reactions involving Carbon–Carbon bond formation .....	9
II.2.1.	<i>Kumada-Tamao-Corriu coupling .....</i>	<i>9</i>
II.2.2.	<i>Suzuki-Miyaura coupling .....</i>	<i>23</i>
II.2.3.	<i>Mizoroki-Heck coupling.....</i>	<i>29</i>
II.2.4.	<i>Negishi coupling .....</i>	<i>30</i>
II.2.5.	<i>Homocoupling reactions.....</i>	<i>31</i>
II.2.6.	<i>Other cross-couplings.....</i>	<i>32</i>
II.2.7.	<i>Carbon–Carbon bond formation via Carbon–Hydrogen bond functionalization.....</i>	<i>33</i>
II.2.8.	<i>Miscellaneous Carbon–Carbon bond formation reactions.....</i>	<i>38</i>
II.3.	Coupling reactions involving Carbon–Heteroatom bond formation .....	40
II.3.1.	<i>Carbon–Nitrogen bond formation.....</i>	<i>40</i>
II.3.2.	<i>Carbon–Sulfur bond formation .....</i>	<i>45</i>
II.4.	Reduction reactions.....	48
II.4.1.	<i>Dehalogenation reactions.....</i>	<i>48</i>
II.4.2.	<i>Carbon–Carbon multiple bond reduction .....</i>	<i>48</i>
II.4.3.	<i>Carbon–Heteroatom multiple bond reduction .....</i>	<i>51</i>
II.5.	Oxidation reactions .....	53
II.6.	Miscellaneous reactions .....	54
<b>III.</b>	<b>Conclusions.....</b>	<b>57</b>
<b>IV.</b>	<b>References.....</b>	<b>58</b>

## I. Carbenes and carbene complexes

### I.1. Historical aspects

Since the pioneering work of Buchner,<sup>[1]</sup> Staudinger<sup>[2]</sup> and Doering,<sup>[3]</sup> carbenes have become powerful tools in synthetic organic chemistry. However, their relatively high reactivity prevented chemists from isolating them in the free state. Generally, the strategy employed to stabilize and isolate such species was the complexation of the carbene carbon to a metal center.

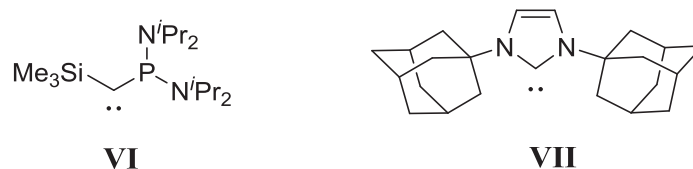
The first carbene complex was introduced to organometallic chemistry in 1915 by Chugaev<sup>[4]</sup> (**I**). However at that time, spectroscopic techniques could not enable an exact structural determination, and this was only confirmed in 1970.<sup>[5,6]</sup> In 1964, Fischer reported and structurally characterized the first carbene complex, which was obtained by treatment of tungsten hexacarbonyl with phenyl lithium and diazomethane (**II**).<sup>[7]</sup> Öfele<sup>[8]</sup> (**III**) and Wanzlick<sup>[9]</sup> (**IV**) described the syntheses of the first diaminocarbene complexes only four years later. Starting from 1971, Lappert very rapidly extended the preparative procedures of the latter compounds and synthesized more than a hundred diaminocarbene complexes of almost all transition metals of groups VI, VIII, IX, X and XI.<sup>[10,11]</sup> In 1974, Schrock developed a new type of alkylidene complex, which was obtained by  $\alpha$ -hydride elimination of a neopentyl ligand in a tantalum complex<sup>[12]</sup> (**V**) (**Figure 1**).



**Figure 1.** Representative examples of the first carbene complexes

Intensive research on the stabilization of free carbenes quickly followed these findings. In the 1980's, Tomioka started to study persistent triplet diarylcarbenes.<sup>[13]</sup>

Remarkably, Bertrand<sup>[14]</sup> (**VI**) and Arduengo<sup>[15]</sup> (**VII**) isolated and characterized the first stable free carbenes in 1988 and 1991, respectively (**Figure 2**).



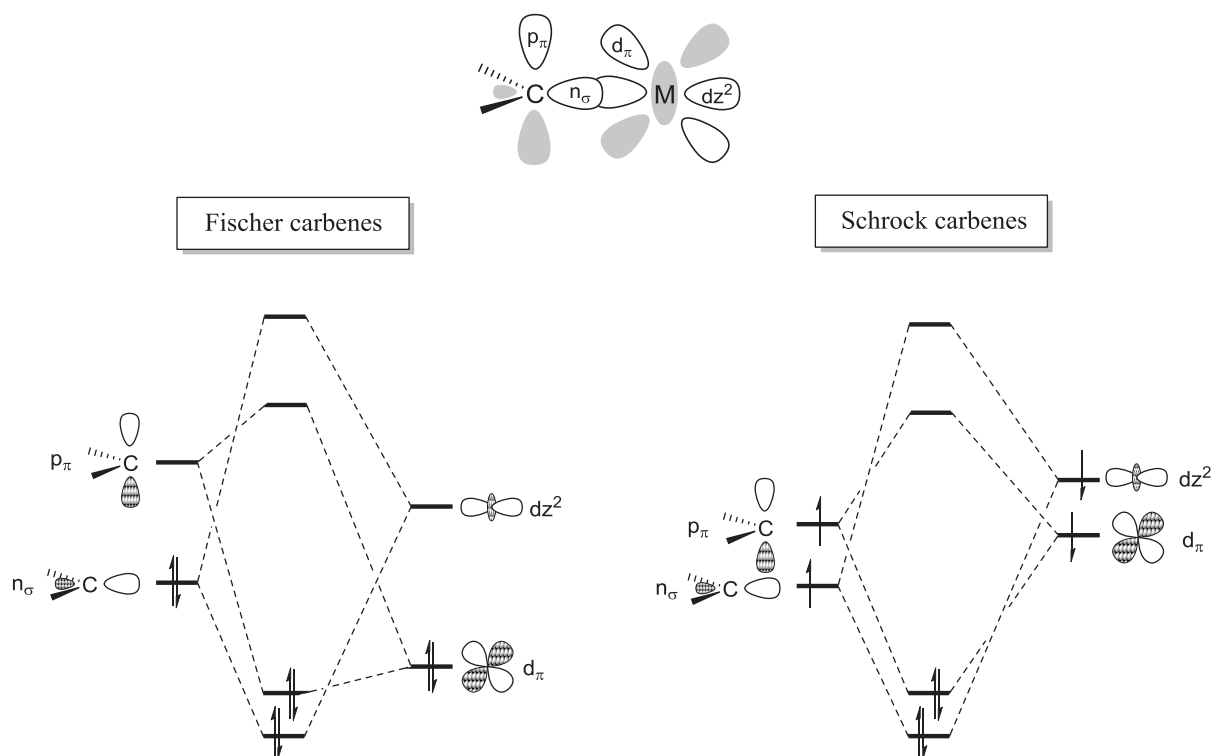
**Figure 2.** First isolated free carbenes

The isolation of carbene **VII** is now commonly recognized as the starting point of the growing impact of this special class of diaminocarbenes, which are more commonly named *N*-heterocyclic carbenes (NHCs).

## I.2. Theoretical aspects

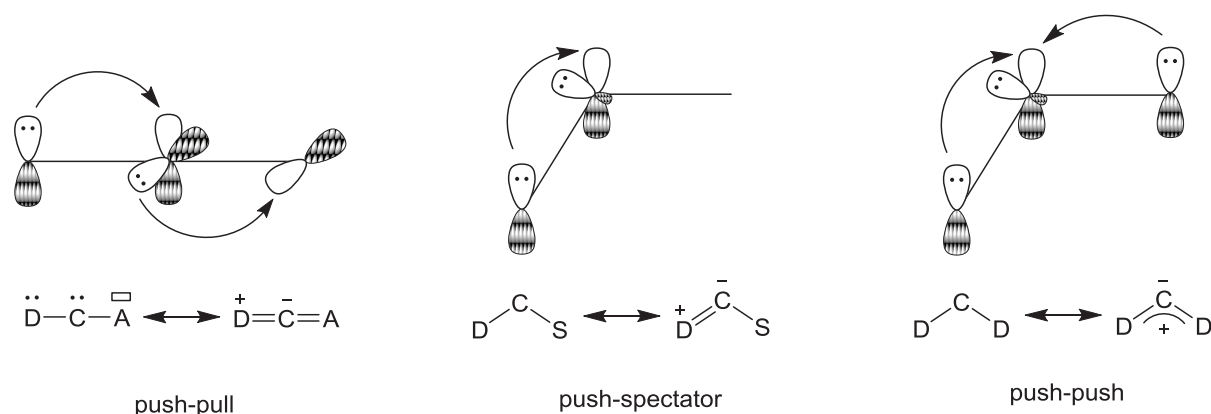
Carbenes are organic species containing a divalent carbon possessing two unshared electrons, and display either electrophilic or nucleophilic reactivity depending on whether these two electrons are unpaired (triplet carbene) or paired (singlet carbene). Even if there is no single way to categorize and rationalize the nature of the metal–carbene bond, three classes of carbenes can be coarsely distinguished: Fischer carbenes, Schrock carbenes, and persistent carbenes.

In the case of Fischer carbenes, the  $\pi$ -donating substituent in  $\alpha$ -position (see **II**, **Figure 1**) will partially fill the  $p_\pi$  orbital of the carbene thus increasing its energy. As a consequence, the difference in energy between the  $n_\sigma$  and  $p_\pi$  orbitals of the carbene (singlet-triplet gap) favors the singlet state. Moreover, the  $p_\pi$  orbital of the carbene is higher in energy than the  $d_\pi$  orbital of the metal. In this case, the metal–carbene bond is polarized  $\delta^+$  on the carbon and  $\delta^-$  on the metal (electrophilic carbene). Conversely, Schrock carbenes (triplet carbene) have a low singlet-triplet gap and the carbene carbon is nucleophilic. The bonding scheme in Schrock carbene complexes is similar to that in carbon–carbon double bonds (**Figure 3**).



**Figure 3.** Partial molecular diagram for Fischer and Schrock carbenes

Persistent carbenes, and more precisely persistent singlet carbenes, are structurally similar to Fischer carbenes. However, they show unique properties and therefore constitute a special class of carbenes. They can be divided into three categories: "push-pull" carbenes, "push-spectator" carbenes and "push-push" carbenes (**Figure 4**).<sup>[16]</sup> "Push-pull" carbenes possess one  $\pi$ -donating substituent D partially filling the vacant  $p_\pi$  orbital of the carbene, and one  $\pi$ -accepting substituent A, which interacts with the occupied orbital of the carbene carbon, giving rise to a quasi-linear geometry around the carbene carbon. A typical example of this category are (phosphino)(silyl)carbenes (see for example **VI**, **Figure 2**),<sup>[17,18]</sup> which behave as electrophiles.<sup>[19]</sup> "Push-spectator" carbenes possess only one strongly  $\pi$ -donating substituent D. These bent carbenes are very reactive and are able to activate small molecules such as  $H_2$ ,  $NH_3$ , CO and  $P_4$ .<sup>[20,21]</sup> This category notably includes (amino)(alkyl)carbenes.<sup>[17,18]</sup> Finally, "push-push" carbenes, which are the most common persistent carbenes, bear two  $\pi$ -donating substituents resulting in a polarized 4e three-center  $\pi$  system.<sup>[22,23]</sup> Consequently, these species are less electrophilic than "push-spectator" carbenes.<sup>[24,25]</sup>



**Figure 4.** Orbital interactions in push-pull, push-spectator and push-push persistent singlet carbenes

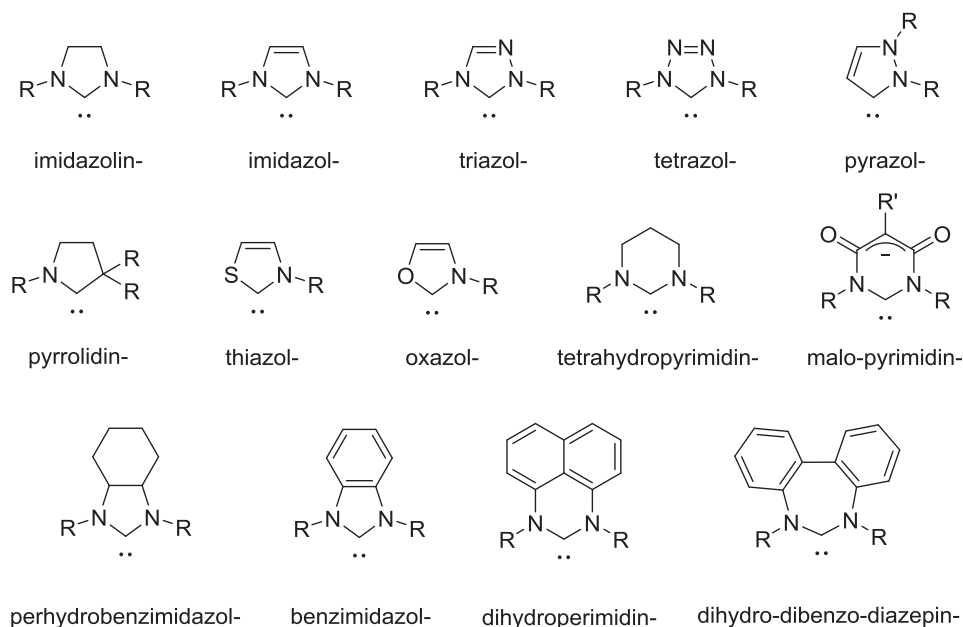
Among these "push-push" carbenes, NHCs constitute the most important family. On one hand, the  $\pi$ -donation of the two nitrogen atoms (orbital overlap) will increase the energy of the  $p_\pi$  orbital of the carbene even more. On the other hand, the inductive attractive effect of both nitrogen atoms stabilizes the  $d_\pi$  orbital (**Figure 5**).<sup>[26–33]</sup>



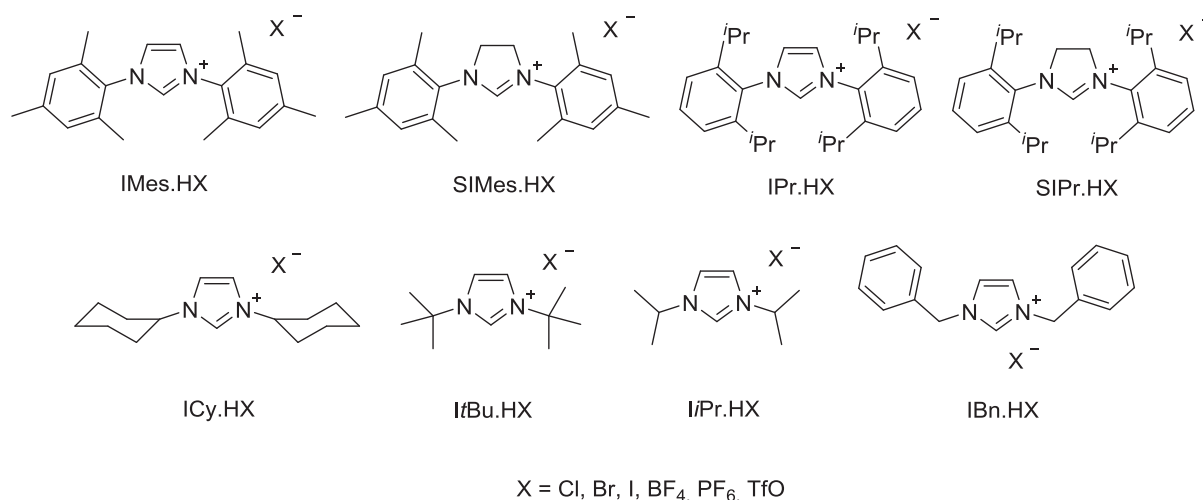
**Figure 5.** Electronic stabilization of NHCs

Consequently the singlet-triplet gap will be even more important than in the Fischer carbenes, thus preventing the  $p_\pi$  and the  $d_\pi$  orbitals from almost any interaction.  $\pi$ -back-donation from the metal to the NHC is therefore relatively low. This is the reason why the metal–NHC bond is commonly represented by a single bond (NHCs are virtually  $\sigma$ -donating ligands) in contrast to Fischer- and Schrock-type carbenes.

NHCs can be divided into several families that are depicted in **Figure 6**. Among the imidazolin-2-ylidenes and imidazol-2-ylidenes families, the most commonly employed NHC precursors are depicted in **Figure 7**.



**Figure 6.** Common families of NHCs (the suffix "ylidene" should be added to obtain the complete name of each family)

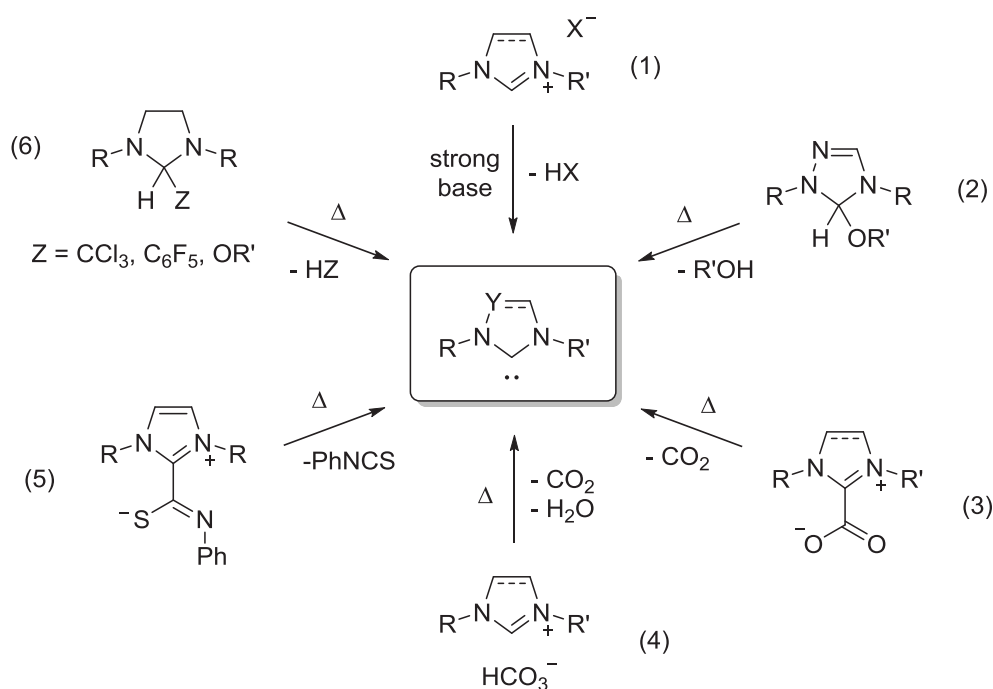


**Figure 7.** Most common imidazolium and imidazolinium salts

### I.3. NHC as ligands in catalysis

The strong  $\sigma$ -donating properties of NHCs often prompted chemists to compare them to phosphine and even cyclopentadienyl (Cp) ligands, which are commonly used ligands in homogeneous catalysis.<sup>[34]</sup> However, NHCs have relatively different properties. Their

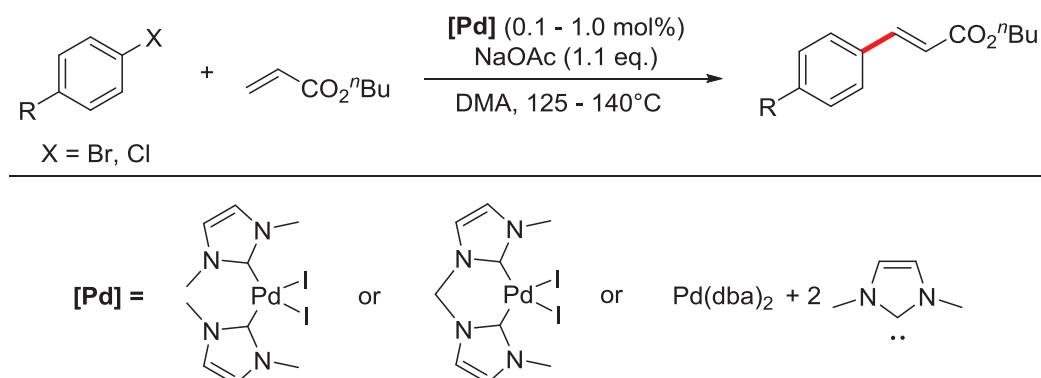
significantly weaker ability to receive  $\pi$ -back-donation from the metal to the ligand renders them electron-rich than any trialkylphosphine. Dissociation of the metal–carbene bond is thus unfavorable, giving rise to more active and stable catalytic systems. Moreover, NHC complexes are easily synthesized by reaction of commercially available metal sources and free carbenes.<sup>[35]</sup> The latter are generally generated by simple deprotonation of air-stable and readily available azolium salts with a strong base (**Scheme 1**, eqn. (1)). However, other methodologies such as the thermal activation of 5-alkoxytriazolines (eqn. (2)),<sup>[36,37]</sup> imidazolium-2-carboxylates (eqn. (3)),<sup>[38–40]</sup> imidazolium hydrogen carbonates (eqn. (4)),<sup>[41]</sup> imidazolium-2-thioisocyanates (eqn. (5)),<sup>[42]</sup> 2-alkoxy-,<sup>[43–45]</sup> 2-pentafluorophenyl-<sup>[46,47]</sup> and 2-trichloromethyl-imidazolidines<sup>[47,48]</sup> (eqn. (6)), efficiently give rise to the targeted free carbenes. Transmetalation with Ag(I)–NHC complex represents another useful method to synthesize metal–NHC complexes due to the weak Ag–carbene bond.<sup>[49]</sup>



**Scheme 1.** Representative methods for generating free carbenes

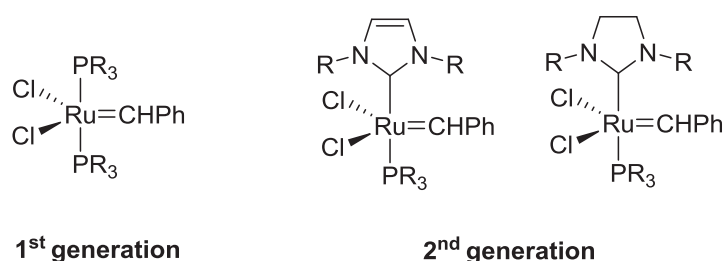
Thus, these species have rapidly evolved from laboratory curiosities to powerful ligands for transition metal-catalyzed processes, notably after the pioneering work of Herrmann in this field. In the first metal–NHC-catalyzed reaction, the Pd–NHC catalysts

showed high thermal and hydrolytic durability, and an excess of ligand was not needed in contrast to phosphine and phosphite-based catalysts (**Scheme 2**).<sup>[50]</sup>



**Scheme 2.** First use of a metal–NHC system in homogeneous catalysis in 1995

Moreover, in the Ru-catalyzed olefin metathesis, replacement of one of the two phosphines of the first generation of Grubbs' catalyst by an NHC led to significantly more active systems for olefin metathesis reactions (**Figure 8**).<sup>[44,51,52]</sup> Such an enhancement in activity can be explained by the increased stability of the resulting second generation catalysts, and by an easier dissociative substitution of the phosphine ligand with the olefinic substrate.<sup>[53]</sup>



**Figure 8.** 1<sup>st</sup> and 2<sup>nd</sup> generations of Grubbs' metathesis catalysts

These two important findings strongly contributed to the democratization of these ligands, which have quickly been applied in association with a notable part of the d-block metals in a very large array of organic transformations.<sup>[54–63]</sup>



## II. *N*-heterocyclic carbene–nickel complexes in catalysis

### II.1. Introduction

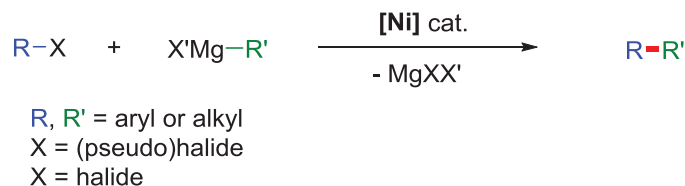
With the discovery of the "nickel effect" by Ziegler and Holzkamp in the mid 1950's,<sup>[64]</sup> the importance of nickel complexes in the field of catalysis has considerably increased. Nevertheless, the study of new nickel catalysts has remained relatively limited compared to noble metals, in particular compared to its  $d^{10}$  counterpart, palladium. Nowadays, however, compelling economical and environmental demands are driving researchers to use more abundant metals such as iron, copper or nickel. As observed for other metal catalysts, the use of NHC ligands in place of phosphines or amines ligands has led to an important enhancement of catalytic activity, and therefore to an important diversification of nickel-based systems. Hence, catalysis applications of Ni–NHC complexes has already been reviewed in several reviews and book chapters.<sup>[60,65–67]</sup> Nevertheless, due to the vast scope of these catalysts, the latter reports often concern a limited number of applications. Herein, we will try to encompass all the examples involving these species, as *in situ* generated or well-defined catalysts in C–C and C–Heteroatom bond forming reactions, as well as in reduction and oxidation reactions, with a special emphasis on the catalytic systems. Rearrangement, cycloaddition and multi-component coupling reactions, as well as polymerization and oligomerization of olefins are excluded from the present review, as they do not fit with the thematic of the rest of this thesis.

### II.2. Coupling reactions involving Carbon–Carbon bond formation

#### II.2.1. Kumada-Tamao-Corriu coupling

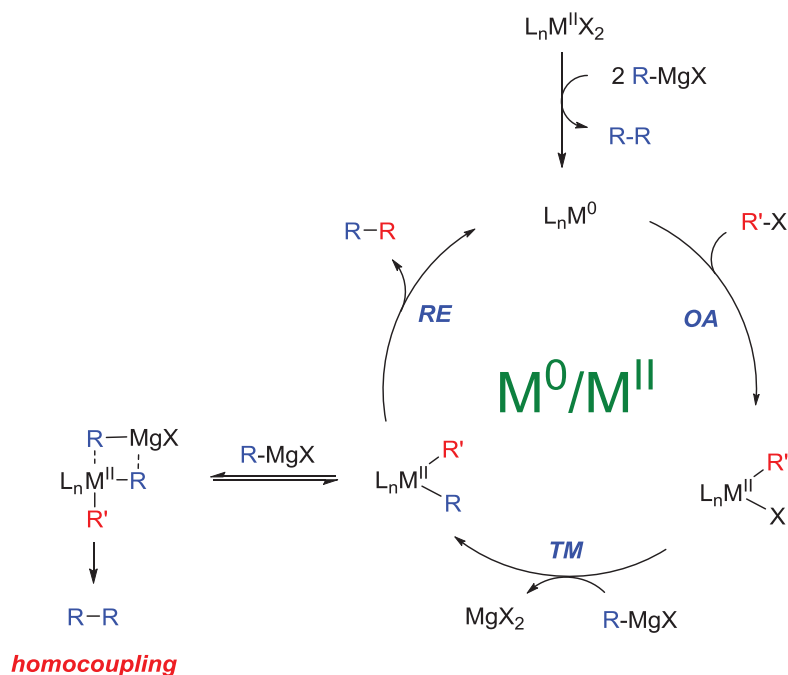
The Kumada-Tamao-Corriu<sup>[68,69]</sup> (KTC) coupling that involves the selective formation of C–C bonds by cross-coupling of Grignard reagents with organic halides, is historically the first cross-coupling reaction that involved nickel compounds as catalysts (**Scheme 3**). Moreover, despite their sensitivity towards air and moisture, Grignard reagents are often precursors of boronic acids, stannanes and organozincs employed for other cross-coupling

methodologies, thus avoiding extra synthetic steps involving stoichiometric amounts of organometallic reagents.



**Scheme 3.** Ni-catalyzed KTC cross-coupling reaction

The classical mechanism of the KTC reaction involves a M(0)/M(II) catalytic cycle (**Scheme 4**). The M(0) species is generally generated by two subsequent transmetallation steps on a di-halogenated metal precursor, followed by a reductive elimination step to form the active M(0) species along with the homocoupling product. Oxidative addition of M(0) on the aryl halide followed by transmetallation with the Grignard reagent and reductive elimination thus affords the coupling product. However, the intermediate before reductive elimination can undergo further reaction with a Grignard reagent, which could result in the formation of notable amounts of the homocoupling product. Suppression of this step is therefore of major importance to obtain selectively the cross-coupling product.

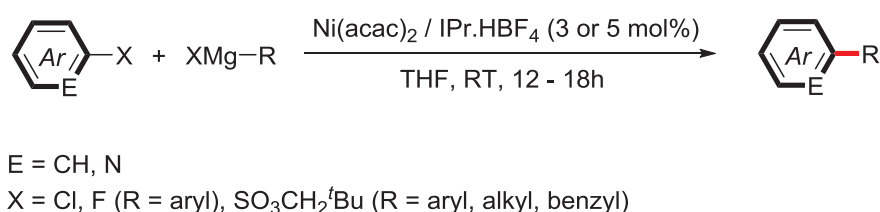


**Scheme 4.** Classical M(0)/M(II) catalytic cycle for KTC coupling

(OA = oxidative addition, TM = transmetallation, RE = reductive elimination)

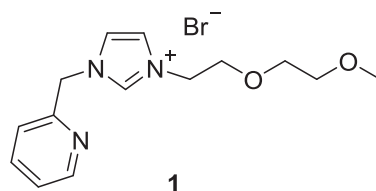
a) *In situ* generated Ni–NHC complexes

From a practical and economical point of view, *in situ* generation of a Ni–NHC complex from a commercial source of nickel and an azolium salt is the method of choice. Such a system was first reported by Herrmann for the KTC coupling of aryl chlorides under mild conditions.<sup>[70]</sup> Remarkably, with only 3 mol% of Ni(acac)<sub>2</sub>/IPr.HBF<sub>4</sub>, moderate to excellent yields (47 - 99%) were obtained with a large array of (hetero)aryl halides and Grignard reagents (**Scheme 5**). Even di-*ortho*-substituted arenes could be efficiently coupled. Of notable interest is that the same catalytic system was also successfully applied with arenesulfonates<sup>[71,72]</sup> and aryl fluorides<sup>[73]</sup> as electrophiles. <sup>13</sup>C NMR spectroscopy analyses of the crude reaction mixtures were consistent with a catalytically active nickel(0) intermediate. Moreover, the lower activity observed for the zerovalent complex Ni(IPr)<sub>2</sub> suggests that a highly reactive 12-electron Ni(IPr) species could act as the real catalyst.<sup>[70]</sup>



**Scheme 5.** KTC coupling with Herrmann's catalytic system

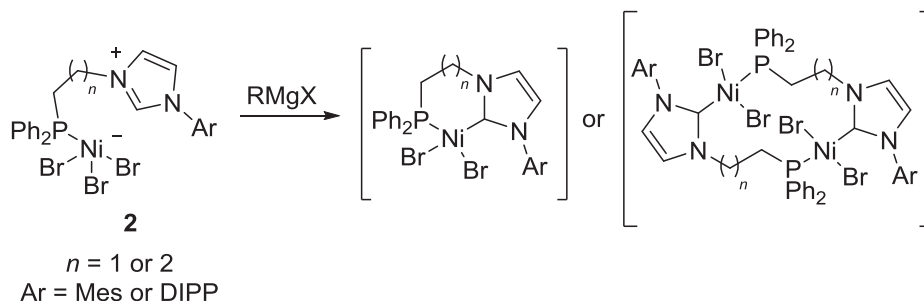
Interestingly, the use of the NHC precursor **1** (**Figure 9**) under slightly different reaction conditions resulted in improved activities compared to IPr.HBF<sub>4</sub>.<sup>[74]</sup>



**Figure 9.** NHC precursor **1**

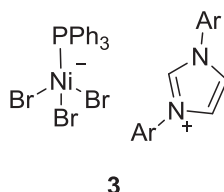
In 2006, Labande and Poli developed zwitterionic complexes **2** containing a phosphine-imidazolium ligand.<sup>[75,76]</sup> The imidazolium counter-anion is deprotonated *in situ* by the Grignard reagent, thus leading to Ni–NHC intermediates in which the phosphine arm remains coordinated (**Scheme 6**). The authors claimed that the activity of these complexes is

similar to Herrmann's system with a slightly improved selectivity for the cross-coupling product.



**Scheme 6.** Plausible intermediates formed during the catalysis starting from complexes **2**

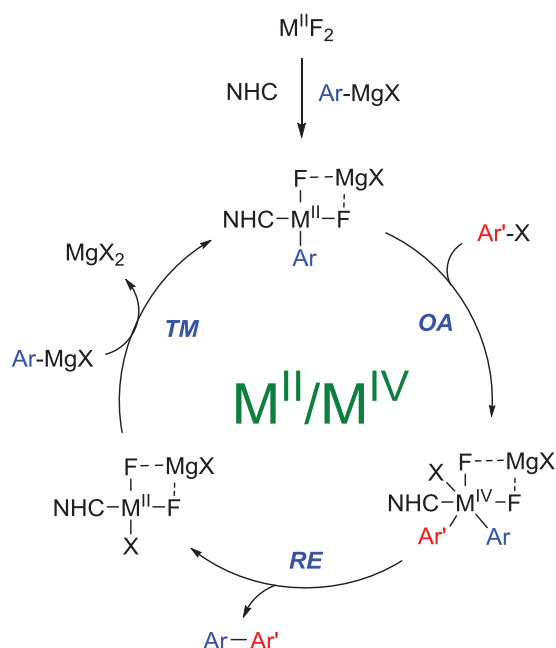
An interesting study on the same reaction showed that nickelate complexes **3** (**Figure 10**) displayed similar activities, demonstrating that the linking between the imidazolium salt and the phosphine is not necessarily required to keep a good activity, thus providing simpler precatalysts.<sup>[77]</sup>



**Figure 10.** Zwitterionic complex **3** employed in the KTC coupling of aryl chlorides

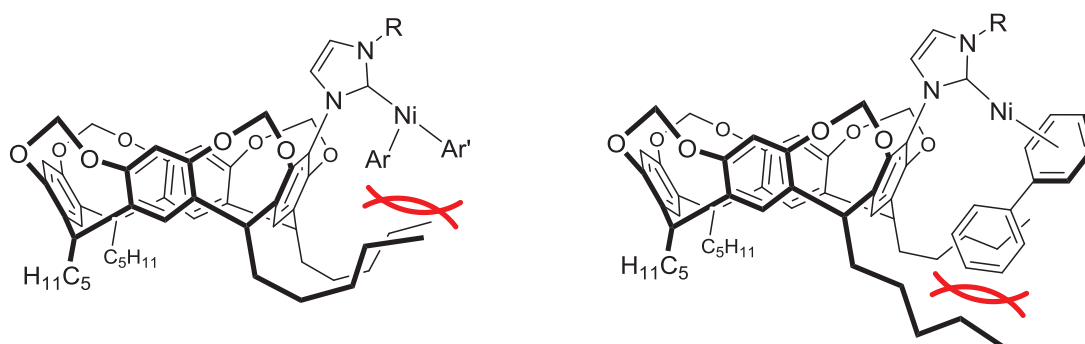
In 2009, Nakamura reported a very efficient "catalytical triad" based on the use of metal difluorides (Fe, Co and Ni) with an NHC ligand (IPr or SIPr) for the coupling of aryl halides with arylmagnesium halides with excellent selectivities for the cross-coupling products.<sup>[78]</sup> Impressively, for activated and unactivated aryl bromides and chlorides, very good to excellent yields (84 - 99%) of the biaryl products were obtained with the appropriate *in situ* generated metal–NHC complex. In the case of the Fe–NHC catalyst, highly selective coupling using various aryl chlorides were achieved, whereas the Co–NHC catalyst was particularly effective in the coupling of heteroaromatics. The Ni–NHC system showed notably high catalytic activity when aryl bromides and hindered substrates were employed. Experimental results and theoretical calculations suggest that a "fluoride effect" would be responsible for the observed excellent selectivities for the cross-coupling products. This effect would consist in strong coordination of the fluoride ligands to the magnesium center, which

would inhibit reduction of the metal by a conventional transmetalation/reductive elimination process. The reaction would therefore proceed *via* a Ni(II)/Ni(IV) catalytic cycle which is less favorable for the formation of the homocoupling product than a Ni(0)/Ni(II) cycle (**Scheme 7**).



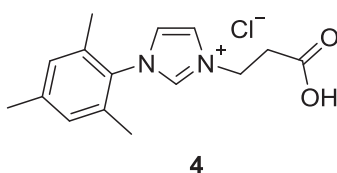
**Scheme 7.** M(II)/M(IV) cycle proposed by Nakamura (M = Ni, Fe, Co)

More recently, Sémeril and Matt described the use of resorcinarenyl-imidazolium salts as efficient pre-ligands for the nickel-catalyzed KTC coupling of aryl bromides and chlorides.<sup>[79]</sup> The best activity was achieved with the flexible pentyl-functionalized derivative that might allow steric interactions in possible *exo*-intermediates, which would favor the reductive elimination process (**Figure 11**).



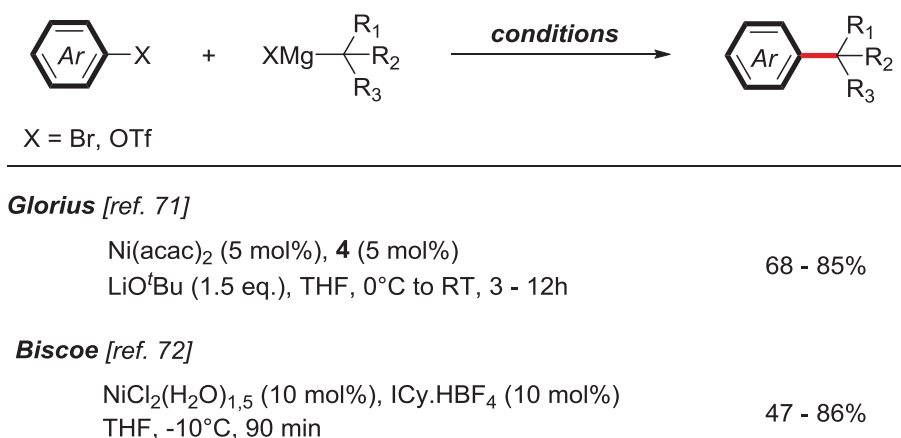
**Figure 11.** Possible Ni(II) and Ni(0) intermediates formed during the catalysis

A great improvement in the Ni–NHC-catalyzed KTC coupling was the possibility of using sterically demanding tertiary alkyl Grignard reagents, which still represents a challenge because of the competitive  $\beta$ -hydride elimination and isomerization reactions.<sup>[80]</sup> In 2011, Glorius reported the use of the flexible NHC precursor **4** (**Figure 12**) that probably acts as a bidentate ligand during the catalysis, thus retarding the  $\beta$ -hydride elimination by occupying an additional coordination site on the nickel.<sup>[81]</sup>



**Figure 12.** NHC precursor **4** employed in the KTC coupling of alkyl tertiary Grignard reagents

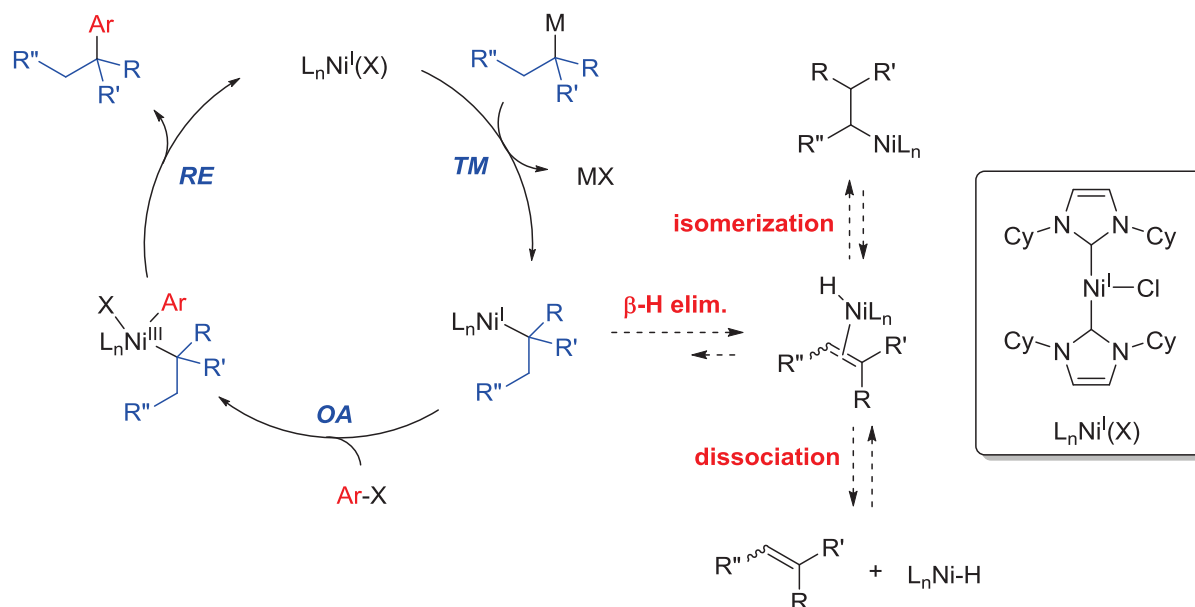
Addition of a base is crucial as it probably helps in the generation of the carbene complex. The catalytic system is therefore relatively active for the coupling of aryl bromides and triflates at room temperature with moderate to good yields (**Scheme 8**).



**Scheme 8.** Ni–NHC-catalyzed KTC coupling of tertiary Grignard reagents

Control experiments in the presence of radical scavengers suggest that radical intermediates are implied in the cross-coupling reaction as the activity was totally inhibited. The same year Biscoe used a simpler system to achieve the selective coupling of tertiary substrates.<sup>[82]</sup> In this

case both the nature of the ligand and the hydration of the nickel source are essential. Although 10 mol% of pre-catalyst were necessary, the reaction proceeded without the need of an additive and at shorter reaction times and lower temperatures. The optimal conditions were found when using  $\text{NiCl}_2 \cdot (\text{H}_2\text{O})_{1.5} / \text{ICy} \cdot \text{HBF}_4$  (1:1), allowing the coupling of a broad scope of aryl bromides (26 examples), and also of some aryl triflates (**Scheme 8**). A Ni(I)/Ni(III) cycle with a T-shape tricoordinate active species has been proposed (**Figure 13**).



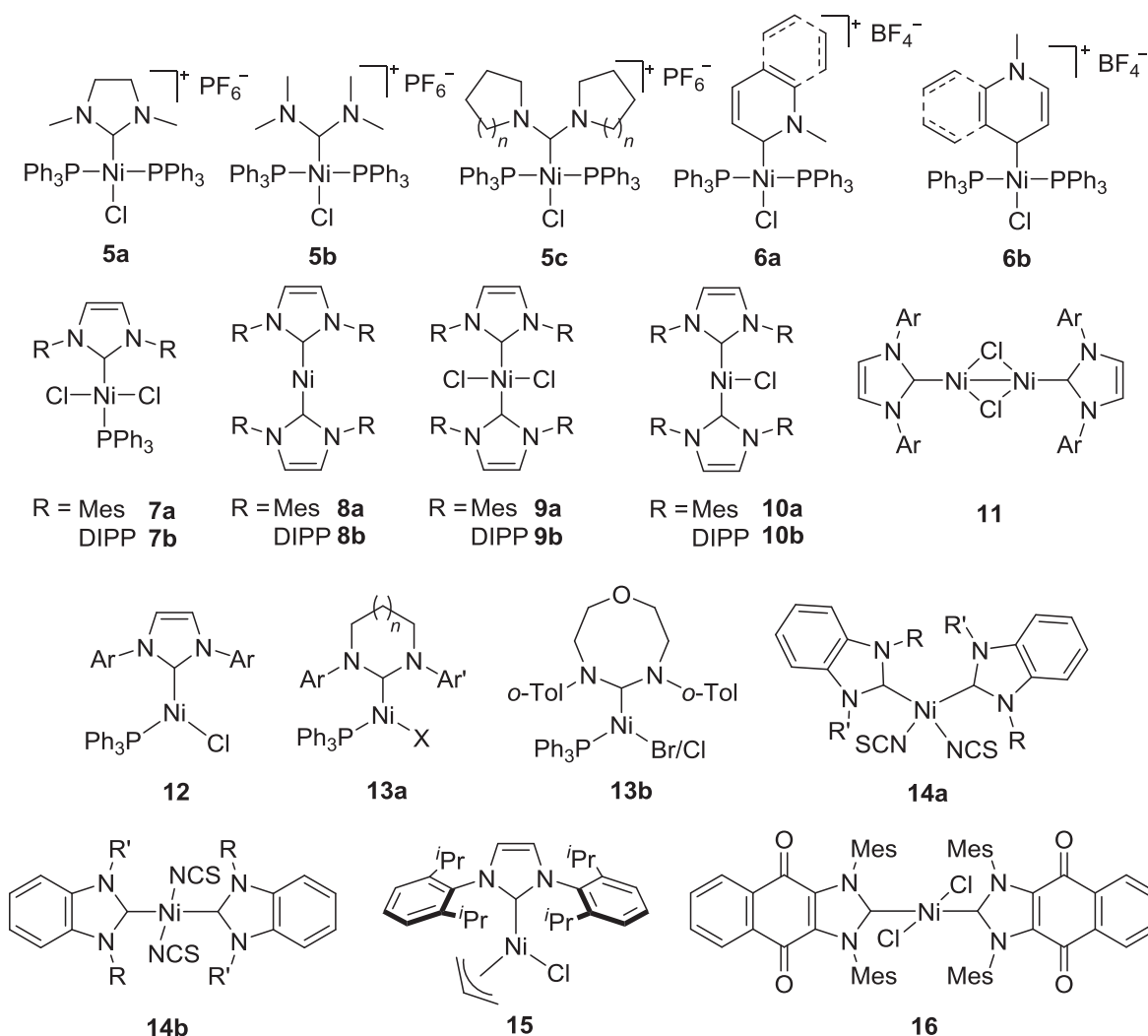
**Figure 13.** Ni(I)/Ni(III) catalytic cycle for the KTC coupling of tertiary Grignard reagents

#### b) Well-defined Ni–NHC complexes: Monodentate NHCs

Whereas *in situ* generated metal catalysts are often preferred, they can give rise to "cocktail-type systems" with different metal species present in solution, and sometimes decreased selectivities.<sup>[83]</sup> The use of well-defined Ni–NHC complexes can tackle this problem, and much efforts has been devoted to the development of monodentate Ni(II)–NHC, Ni(I)–NHC and Ni(0)–NHC complexes (**Figure 14**).

The mixed phosphine/carbene complexes **5a-d** and **6a,b** were prepared by oxidative addition of  $\text{Ni}(\text{PPh}_3)_4$  to the corresponding 2-chloroazolium salt, and were briefly evaluated in the KTC coupling of electron-rich aryl Grignard reagents with aryl chlorides.<sup>[84,85]</sup> The catalytic activities however did not exceed those observed with Herrmann's initial system,<sup>[70]</sup> or even those observed with Matsubara's more classical and easily prepared complex **7b**,

which allowed one to observe quantitative yields with aryl iodides and bromides with only 0.5 mol% of precatalyst within 30 minutes.<sup>[86]</sup> It is interesting that this system is actually better than its analogues Ni(IPr)<sub>2</sub>Cl<sub>2</sub> **9b** and Ni(PPh<sub>3</sub>)<sub>2</sub>Cl<sub>2</sub>.

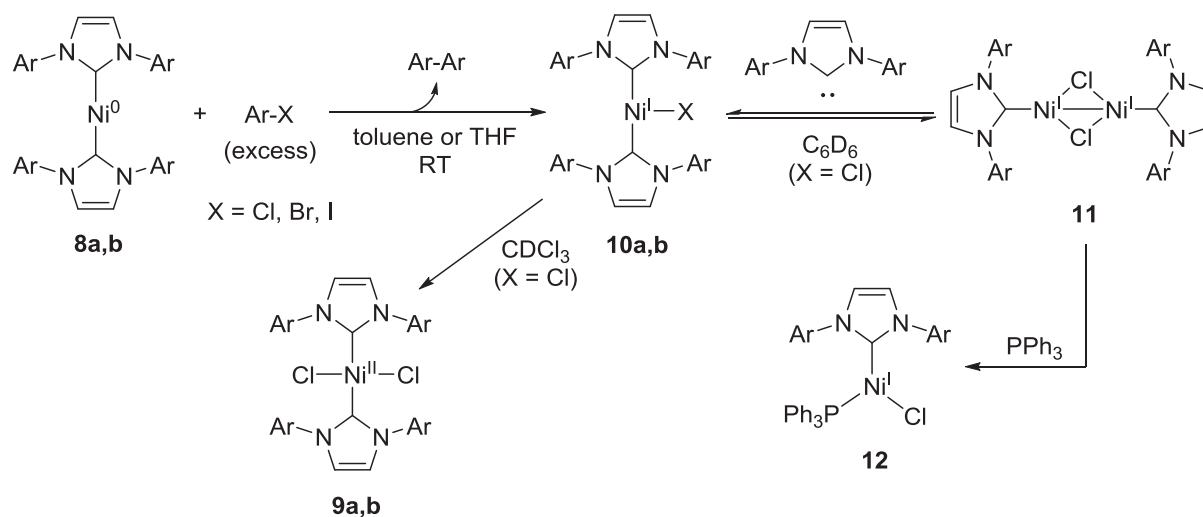


**Figure 14.** Monodentate Ni–NHC complexes applied in the KTC coupling reaction

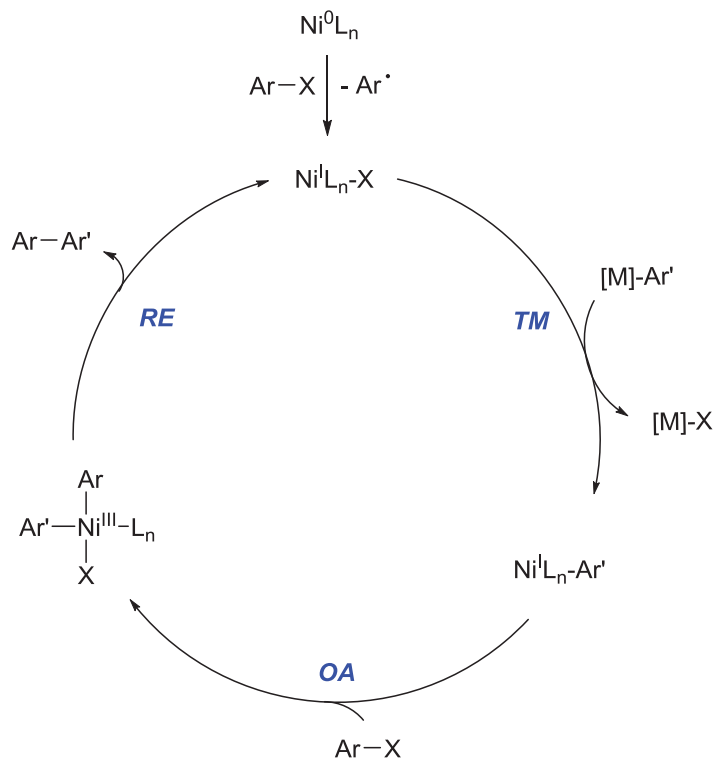
Considering the mechanism, it is important to note that, at the end of 2010, Matsubara<sup>[87]</sup> and Louie<sup>[88]</sup> concurrently described the synthesis of paramagnetic 15-electron nickel(I)–NHC species **10a,b** by reaction of aryl halides with the related zerovalent Ni(NHC)<sub>2</sub> complexes **8a,b** (Scheme 9). These T-shaped complexes were obtained instead of the expected oxidative addition product Ni(NHC)<sub>2</sub>(Ar)X, and show similar activities in the KTC coupling of aryl bromides and chlorides when compared to their Ni(NHC)<sub>2</sub> and Ni(NHC)<sub>2</sub>Cl<sub>2</sub> analogues.<sup>[88]</sup> Additionally, stoichiometric reactions between these species and the cross-



coupling partner suggested that cross-coupling reactions are initiated by a transmetalation reaction between  $\text{Ni}^{\text{I}}(\text{NHC})_n\text{X}$  and the transmetallating reagent.<sup>[88]</sup> The mechanism depicted in **Scheme 10** was therefore proposed.



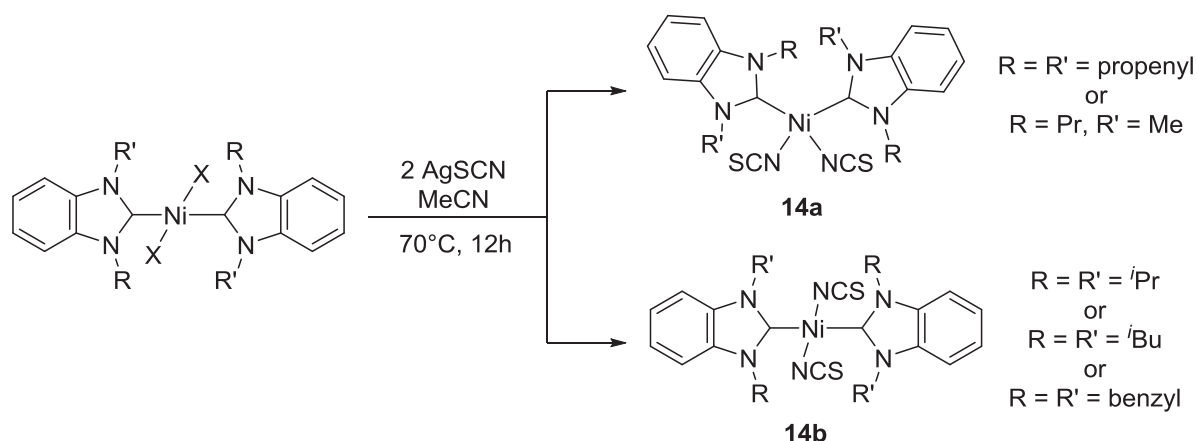
**Scheme 9.** Synthesis of 15-electron Ni–NHC complexes



**Scheme 10.** Plausible mechanism involving Ni(I) intermediates in the KTC reaction

Complexes **10a,b** could also be synthesized by addition of one equivalent of the free carbene to the dinuclear complex **11**.<sup>[87,89]</sup> However, when adding one equivalent of triphenylphosphine to **11**, Y-shaped species **12** were obtained, and these proved to be significantly better catalysts as reaction times could be decreased from 18 to 3 hours.<sup>[89]</sup> More recently, a comparative study with the ring-expanded nickel(I) complexes **13a,b** has shown that the NHC ring has a dramatic influence on catalysis.<sup>[90]</sup> Thus, the six-membered NHC complex **13a** ( $n = 1$ ,  $X = \text{Br}$ ,  $\text{Ar} = \text{Ar}' = \text{Mes}$ ) was found to be the most efficient catalyst of this family, as increasing the size of the ring probably induces too much steric hindrance around the metal. However, prolonged reaction times are required compared to **12**.

Always in the context of valuing new monodentate Ni–NHC complexes in the KTC reaction, Huynh reported the syntheses of diisothiocyanato *bis*-NHC complexes **14a,b** via ligand exchange in the *trans*-dibromo precursor.<sup>[91]</sup> Surprisingly, depending on the nature of the *N*-substituents of the carbene, either *trans*- and *cis*-diisothiocyanato complexes were obtained (**Scheme 11**).

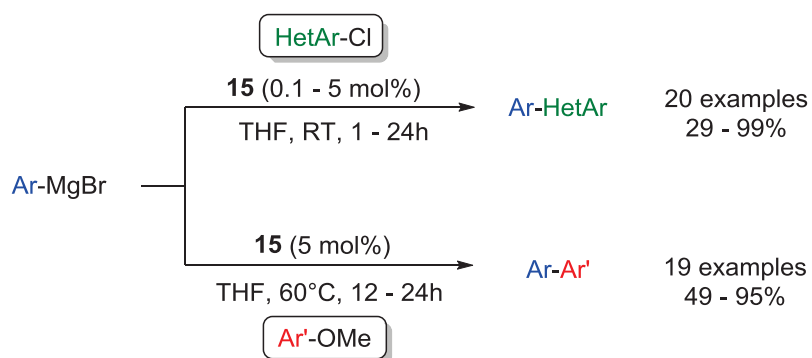


**Scheme 11.** Synthesis of *cis*- and *trans*-diisothiocyanato complexes **14a** and **14b**

The best activity was achieved with **14a** ( $R = R' = \text{propenyl}$ ) which was predictably more efficient than complexes **14b**. Several (hetero)aryl bromides and chlorides were coupled with moderate to excellent yields (49 - 94%) at room temperature with 1 mol% of precatalyst.

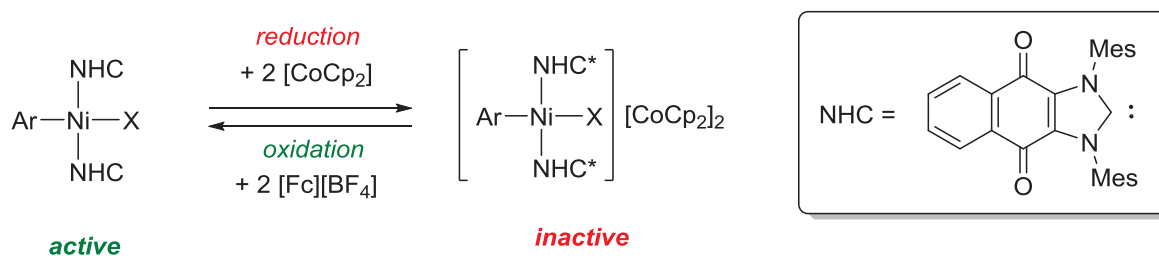
Significant improvement in the Ni–NHC-catalyzed KTC biaryl coupling came up only recently with the use of **15**.<sup>[92]</sup> The latter complex remarkably allowed the use of a vast array of challenging heteroaryl chlorides and anisole derivatives, still with reasonable precatalyst loadings (**Scheme 12**). To the best of our knowledge, this is the only example of a KTC

coupling involving the functionalization of a C<sub>Ar</sub>–O bond by a Ni–NHC catalyst. The observed unprecedented catalytic activity could be explained by the ease of generating an active nickel(0) intermediate starting from a nickel(II)–allyl complex,<sup>[93]</sup> the latter reduction probably occurring in a similar manner to that proposed for palladium(II) analogues.<sup>[94,95]</sup>



**Scheme 12.** KTC coupling of heteroaryl chlorides and anisole derivatives catalyzed by **15**

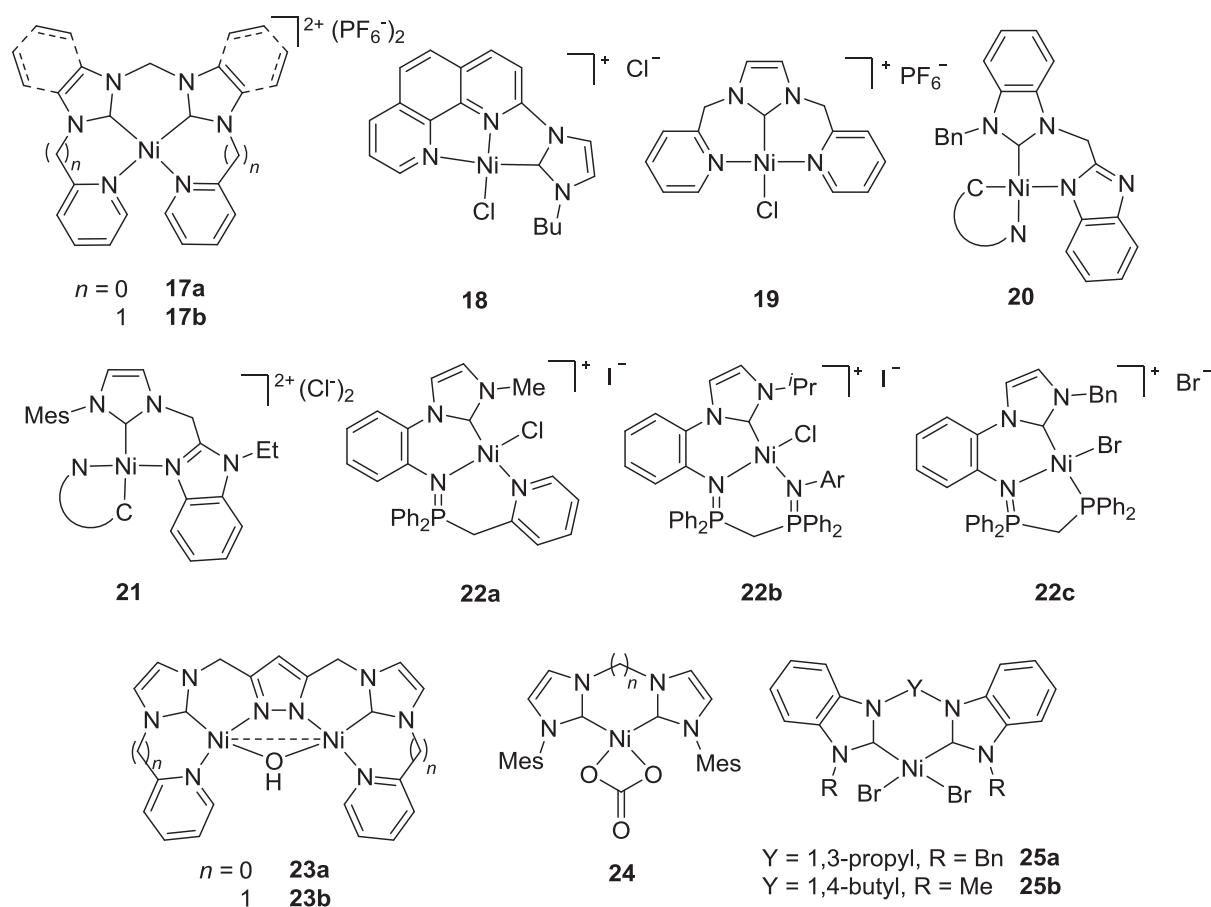
Another breakthrough has been achieved with the use of the naphthoquinone-based NHC complex **16** that can be electronically modified (NHC\*) by an external redox stimulus.<sup>[96]</sup> Impressively, catalysis can be arrested at anytime by reduction of the electronically active NHC upon addition of CoCp<sub>2</sub> (**Scheme 13**). The active state can be restored by simple oxidation with [Fc][BF<sub>4</sub>]. This system represents a significant practical and conceptual progress toward the use of redox-switchable control as an effector of tandem catalysis.



**Scheme 13.** Redox control of the catalytically active species derived from **16**

c) *Well-defined Ni–NHC complexes: Multidentate NHCs*

Compared to monodentate complexes, chelate complexes often give rise to more stable and sometimes more active metal species. This fact was confirmed with the use of the Ni–NHC chelate complexes presented in **Figure 15** in KTC coupling, which are globally more active than the well-defined monodentate Ni–NHC complexes, and thus generally allow one to avoid high reaction temperatures and pre-catalyst loadings.

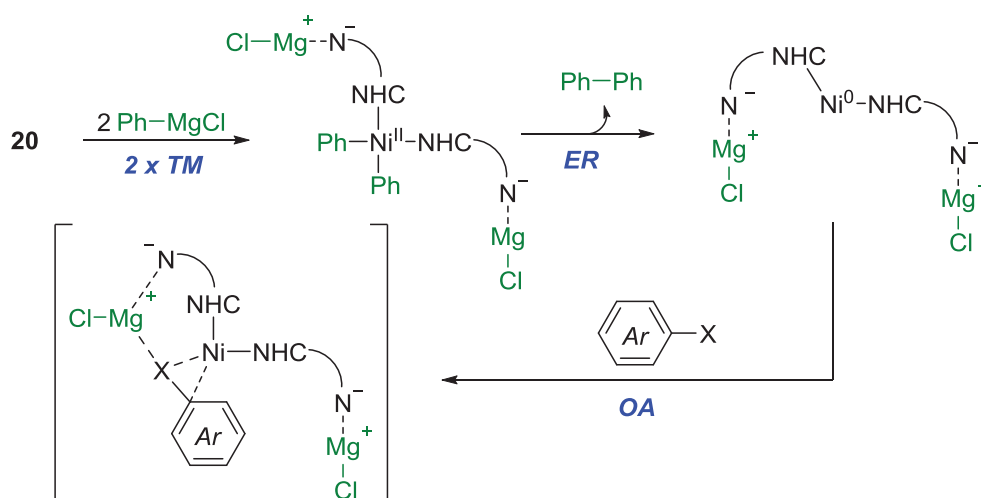


**Figure 15.** Chelate Ni–NHC complexes applied in the KTC coupling reaction

In particular, (*C,N*)-chelate NHC complexes **17a,b**, **18** and **19** with flexible or rigid pyridine/phenanthroline/benzimidazole arms were shown to efficiently catalyze the coupling of aryl chlorides with aryl Grignard reagents at room temperature. More precisely, complexes **17a,b** were able to couple a large array of substrates (best activity with 2 to 4 mol% of **17a**, 32 examples, 62 - 99%) including *ortho*-substituted chloroarenes, vinyl chlorides, and nitrile-

functionalized aryl chlorides without significant loss of activity.<sup>[97]</sup> The more rigid phenanthroline-based complex **18** notably displayed comparable results (1 mol% of **18** for 24 h instead of 2 mol% of **17a** for 12 h) even if the reaction scope was not as broad as for **17a**.<sup>[98]</sup> The use of the flexible *bis*-pyridine functionalized NHC complex **19** allowed a decrease in the precatalyst loading to 0.5 mol% with a comparable efficiency.<sup>[99]</sup> The higher activity of this complex may arise from the ease of generating vacant sites compared to **17a** and the rigid complex **18**.

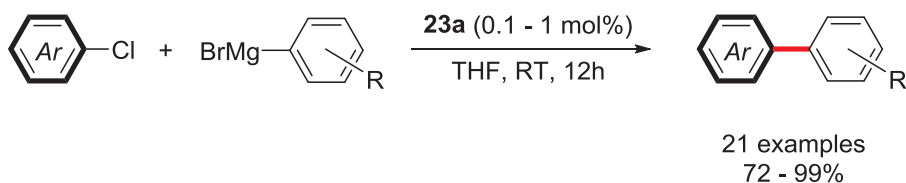
Similarly, although the neutral (**20**)<sup>[100]</sup> and cationic (**21**)<sup>[101]</sup> benzimidazole-tethered Ni–NHC complexes are structurally similar, they behave rather differently during the reaction, as the neutral complex **20** allowed the use of aryl chlorides and even fluorides with much shorter reaction times (12 - 150 minutes) than the cationic complex **21**. The difference of activity would indeed result from the possible de-coordination of the anionic benzimidazole arm of **20**, which would be facilitated by subsequent coordination to a magnesium center (Scheme 14).



**Scheme 14.** Plausible intermediates in the KTC reaction catalyzed by **20**

The structurally related (*C,N,N*)- and (*C,N,P*)-pincer complexes **22a-c**, notably **22a** and **22b** (1 to 4 mol% **22a-c**, THF, RT or 80°C, 16 or 24 h),<sup>[102]</sup> all are very active for the coupling of aryl chlorides. Nevertheless, the bimetallic complex **23a** is certainly among the best active well-defined Ni–NHC precatalysts, as it could be used with loadings as low as 0.1

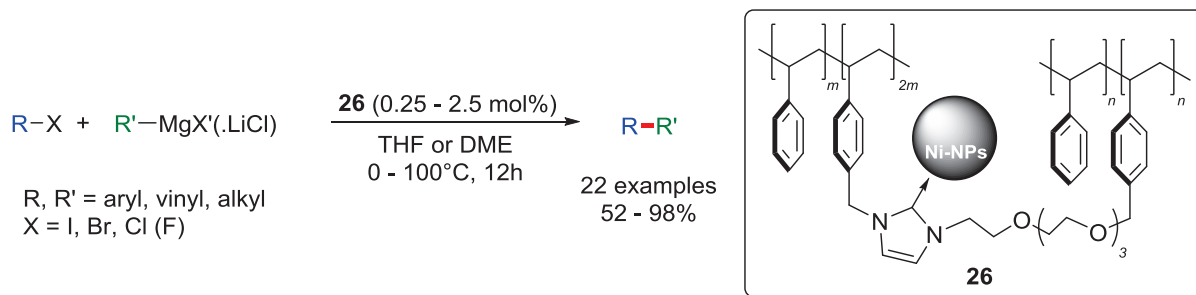
mol% with a large array of aryl chlorides (**Scheme 15**).<sup>[103]</sup> This high activity was attributed to possible bimetallic cooperation ( $d_{\text{Ni-Ni}} = 3.22 \text{ \AA}$ ).



**Scheme 15.** KTC coupling catalyzed by **23a** under mild conditions

*Cis*-chelating *bis*-NHC complexes of nickel are also of interest, as shown by the use of the carbonato complex **24**<sup>[104]</sup> (best for  $n = 3$ ) and of the *cis*-chelating *bis*-benzimidazolyldene complexes **25a**<sup>[105]</sup> and **25b**.<sup>[106]</sup> Thus, loadings of **24** could be lowered to 0.2 mol% (even if long reaction times ranging from 18 to 69 h were required); in addition, **25a,b** tolerate heteroaromatic and di-*ortho*-substituted substrates.

Finally, Kobayashi very elegantly described the use of nickel nanoparticles stabilized by NHC ligands supported on cross-linked polymers **26**.<sup>[107]</sup> This recyclable catalyst surprisingly competes with homogeneous versions of Ni–NHC complexes, as it allows the coupling of aryl iodides and bromides at room temperature (**Scheme 16**). While the coupling of iodides and bromides proceeded very smoothly (0°C or RT), heating at 65 or 100°C was required with chloro substrates in order to obtain a good activity. Exceptionally, tertiary alkyl Grignard reagents were found to be suitable substrates and 4-fluoroiodobenzene was notably used for the double coupling. Simple filtration allowed recovery of **26**, which could be reused up to ten times without notable loss of activity.



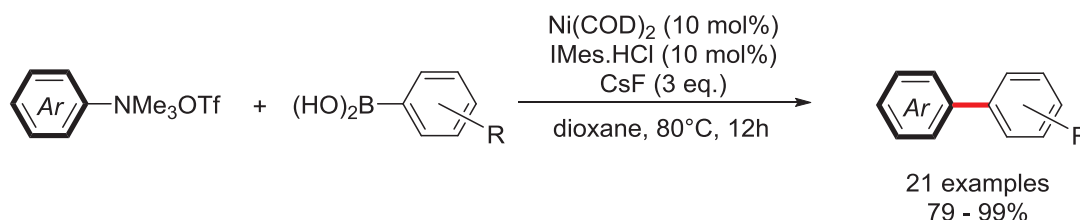
**Scheme 16.** NHC-stabilized Ni-NPs as an heterogeneous catalyst for the KTC reaction

## II.2.2. Suzuki-Miyaura coupling

a) *In situ* generated Ni–NHC complexes

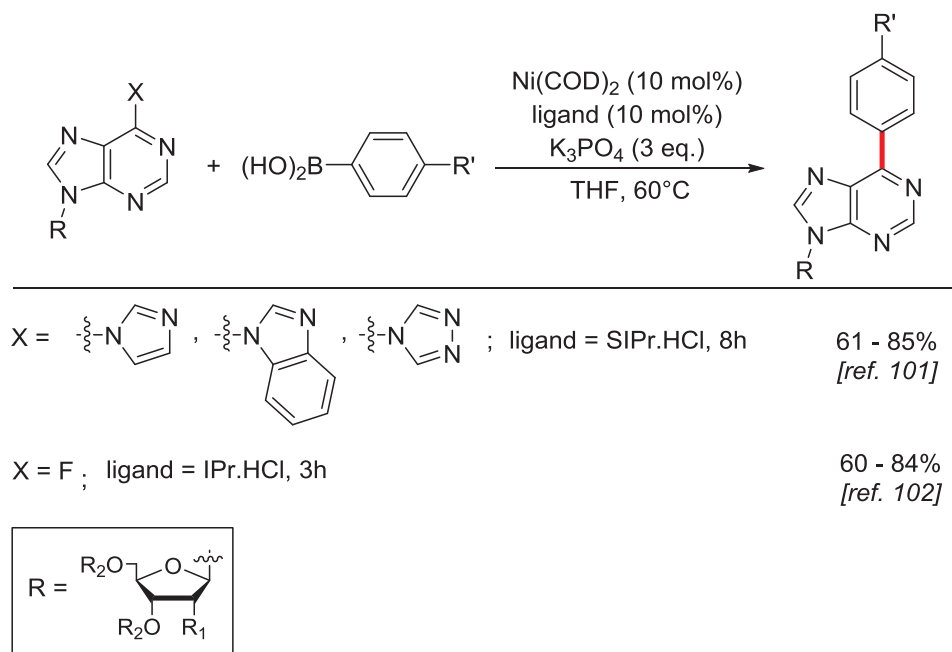
The Suzuki-Miyaura<sup>[108,109]</sup> (SM) cross-coupling is undoubtedly one of the most powerful methodologies available for the formation of aryl–aryl bonds. The most frequently encountered catalysts are based on palladium. However, significant progress has been made in enabling the use of nickel catalysts under mild reaction conditions. In this context, Ni–NHC based systems have shown interesting activities, in particular with the use of *in situ* generated monodentate NHC complexes. In contrast to KTC coupling for which various nickel sources could be used (*vide supra*), Ni(COD)<sub>2</sub> appeared to be the best nickel source for Suzuki coupling, and allowed the coupling of uncommon electrophiles.

For instance, aryl trimethylammonium salts could be used for the first time as coupling partners to give the biaryl products in good to excellent yield with a Ni(COD)<sub>2</sub>/IMes.HCl (1:1) catalytic system (**Scheme 17**).<sup>[110]</sup> Moreover, this system allowed the coupling of mono- and di-*ortho*-substituted coupling partners without significant decrease of yields.



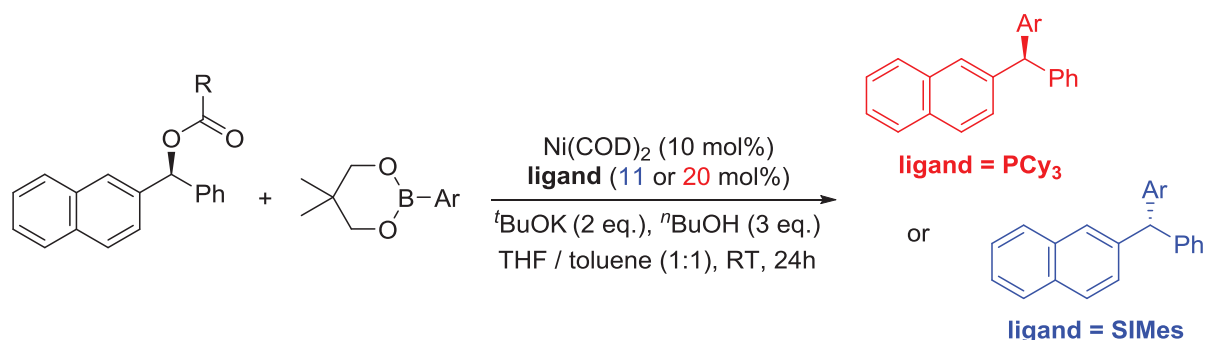
**Scheme 17.** First example of the use of aryl trimethylammonium salts as electrophilic coupling partners in the SM reaction

Robins *et al.* also described the use of uncommon coupling partners, such as azole derivatives of purine ribonucleosides.<sup>[111]</sup> Their coupling with *para*-substituted arylboronic acids efficiently gave 6-arylpurine ribonucleosides which possess cytostatic activities (**Scheme 18**). The same methodology could also be applied to fluoropurine derivatives.<sup>[112]</sup>



**Scheme 18.** Synthesis of 6-arylpurine ribonucleosides described by Robins

With a similar catalytic system, benzylic esters could also be employed as electrophiles for the efficient synthesis of enantioenriched triarylmethanes.<sup>[113]</sup> Remarkably, the stereoselectivity of the reaction could be modulated with achiral ligands. Whereas inversion took place with a Ni/SIMes (1:1) catalyst, the retention product was predominantly obtained with a Ni/PCy<sub>3</sub> (1:2) catalytic system (**Scheme 19**).



**Scheme 19.** Stereoselective synthesis of triarylmethanes

Finally, ionic liquids and silica-immobilized ionic liquids containing a tetrachloronickelate ion were used for the coupling of arylboronic acids with aryl

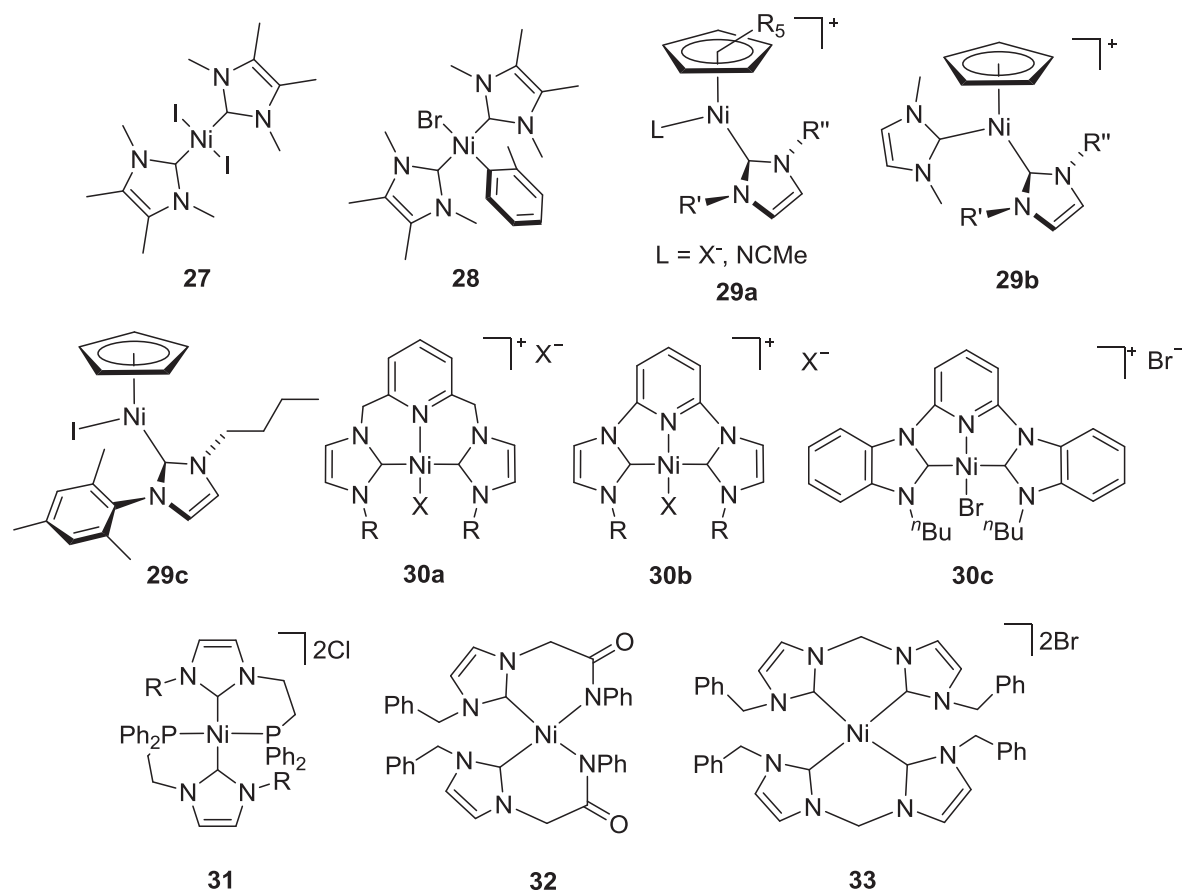


chlorides.<sup>[114]</sup> In the presence of 2 equivalents of PPh<sub>3</sub>, both systems were very efficient, and the immobilized ionic liquid-derivative could be reused up to three cycles without notable loss of activity.

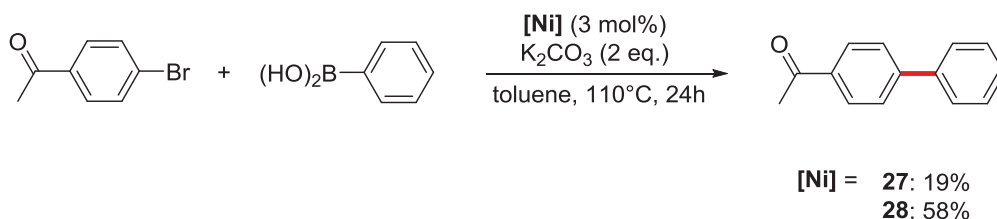
*b) Well-defined Ni–NHC complexes. Monodentate NHCs*

A number of well-defined monodentate NHC complexes of nickel were also shown to have interesting activities in SM reactions, though usually with more classical aryl halides (**Figure 16**).

The first example was described in 1999 by Cavell *et al.* with the use of the *trans*-bis-NHC complexes **27** and **28** in the coupling of 4-bromoacetophenone with phenylboronic acid (**Scheme 20**).<sup>[115]</sup> Notably, the use of **28** resulted in an increased activity thus sustaining the possibility of a Ni(0)/Ni(II) catalytic cycle.

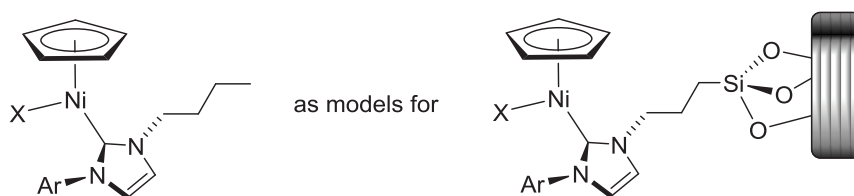


**Figure 16.** Well-defined Ni–NHC complexes employed in SM reaction



**Scheme 20.** First example of a Ni–NHC-catalyzed SM coupling

Cyclopentadienyl (Cp) Ni–NHC complexes **29a–c** were demonstrated to be efficient pre-catalysts for the SM coupling of haloarenes with phenylboronic acid in the presence of  $K_3PO_4$  as the sole additive.<sup>[116]</sup> The methodology was successfully applied to activated haloarenes but a notable loss of activity was observed with unactivated ones. Interestingly, using the more hindered and electron-rich pentamethylcyclopentadienyl (Cp\*) derivatives led to more active systems. In contrast, the cationic or neutral nature of the complexes did not seem to have a significant influence. In comparison, *bis*-NHC complexes **29b** did not allow an efficient SM coupling, probably because they are too stable to induce some reactivity.<sup>[117]</sup> Encouraged by these results, the authors embraced a study aiming at heterogenizing these complexes.<sup>[118]</sup> In this study, while using *N*-aryl,*N'*-butyl-NHC derivatives as models for complexes immobilized on a solid support *via* a three carbon linker (**Figure 17**), they surprisingly uncovered that the iodide complex **29c** was even more active than the Cp\* complexes, and a TOF up to  $352\text{ h}^{-1}$  was observed.



**Figure 17.** Use of *N*-aryl,*N'*-butyl-NHCs of nickel as models for supported derivatives in the SM coupling

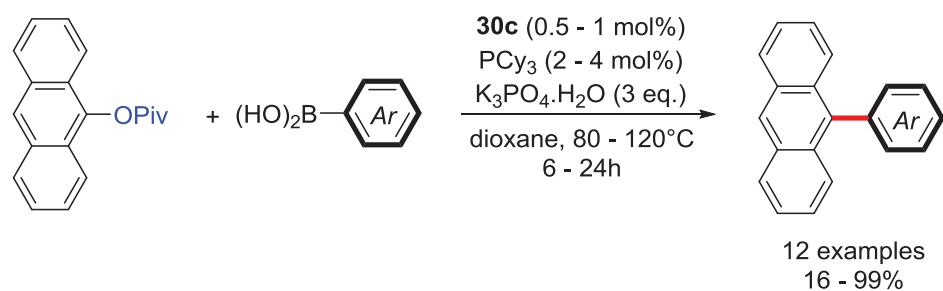
The significant stabilization of the active species, which allowed this very high TOF for a Ni(II) complex under similar conditions, was tentatively attributed to the presence of the voluminous iodide ligand, which would play a protecting role. In contrast, Buchowicz recently showed that the counter-ion has a non-negligible influence on the catalytic activity of cationic half-sandwich complexes.<sup>[119]</sup> Depending on the nature of that counter-ion, efficiency of the reaction could notably be doubled in the best case.

These latter results contrast with that of the *bis*-NHC complexes Ni(0)(NHC)<sub>2</sub> **8**, Ni(II)(NHC)<sub>2</sub>X<sub>2</sub> **9** and Ni(I)(NHC)<sub>2</sub>X **10** in the SM coupling of *para*-substituted bromoarenes. As observed for the KTC coupling, all three complexes display similar activities. Again, the proposed mechanisms involve a nickel(I)–NHC complex as the real intermediate (**Scheme 10**, [M] = B(OH)<sub>2</sub>).

*c) Well-defined Ni–NHC complexes: multidentate NHCs*

Bi- and tridentate chelate Ni–NHC complexes were also employed for SM coupling. This often resulted in good activities with relatively low pre-catalyst loadings, albeit the use of harsher conditions and/or additional triphenylphosphine were generally required. For instance, the cationic tetradentate complexes **17a,b** catalyzed the coupling of phenylboronic acid with *para*-substituted aryl iodides, bromides and chlorides at catalyst loadings of 1 - 3 mol%.<sup>[120,121]</sup> However, except for activated aryl bromides, addition of two equivalents of triphenylphosphine relative to the nickel precursor was crucial to obtain good activities.

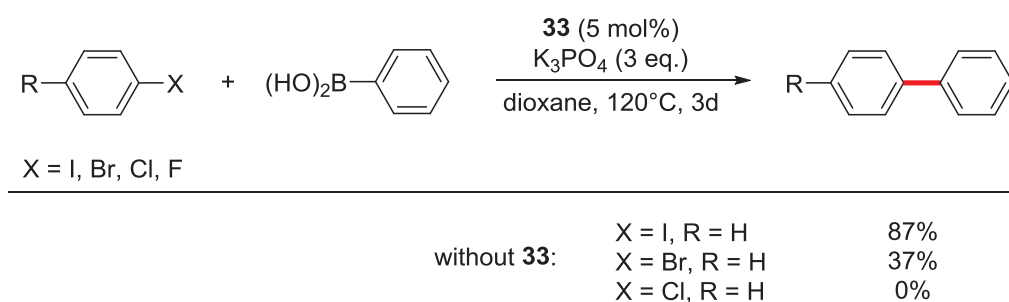
In comparison, the pincer NHC-pyridine systems **30a-c** catalyze the SM coupling of a wider range of substrates. They notably allow the avoidance of triphenylphosphine in most cases. These systems, that have initially been applied to the coupling of simple bromo- and chloroarenes<sup>[122,123]</sup> were later used with more challenging substrates, such as aryl and vinyl tosylates, as well as aryl mesylates.<sup>[124,125]</sup> Comparative studies between complexes **30a** and **30b** showed a better activity with the most rigid system. Further studies in the design of appropriate ligands showed that the benzimidazolylidene derivative **30c** allowed the use of anthracenyl carboxylates as coupling partners to form (hetero)aryl-substituted anthracene derivatives, though the use of phosphine was again required (**Scheme 21**).<sup>[126]</sup>



**Reactivity:** OPiv ~ OCONEt<sub>2</sub> > OCOPh ~ OCOEt > OCOMe ~ OCO<sup>*i*</sup>Pr >> OCOMes >> OCOBn

**Scheme 21.** Formation of (hetero)aryl-substituted anthracene derivatives with **30c**

Other chelate complexes such as **31**<sup>[127]</sup> or **32**<sup>[128]</sup> displayed good activities in the coupling of *para*-substituted aryl bromides and chlorides with 1 to 3 mol% of the precatalyst, but such complexes still suffer from the requirement of an excess of phosphine in addition of a base. It is noteworthy that complex **33**<sup>[129]</sup> also allowed the coupling of some aryl fluorides, though long reaction times as well as high temperatures and catalyst loadings were required (**Scheme 22**).

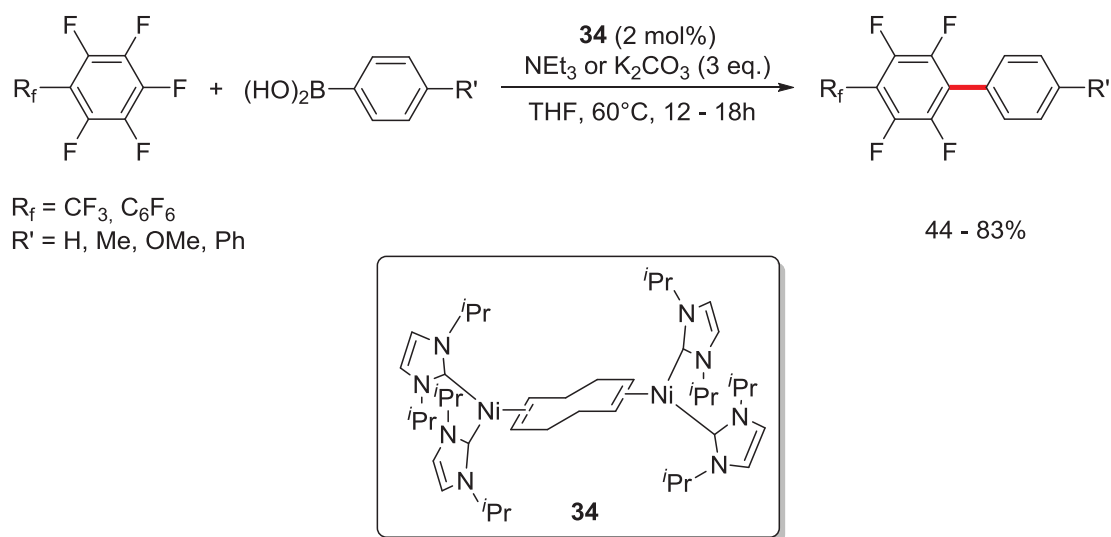


**Scheme 22.** SM coupling of aryl halides with and without **33**

Importantly, this study pointed out the necessity of performing test reactions as aryl iodides and bromides could be coupled without adding the nickel pre-catalyst. As was observed by Leadbeater, sub-ppm levels of Pd found in several bases including K<sub>3</sub>PO<sub>4</sub> are likely responsible for catalyzing the reaction.<sup>[130,131]</sup>

As observed in KTC coupling, homobimetallic complex **23a** was one of the most active complexes for the SM coupling of aryl chlorides, probably due to the bimetallic cooperative effect.<sup>[103]</sup> Thus, pre-catalyst loadings as low as 0.04 mol% could be used with very good efficiency and applicability (20 examples, 78 - 99%). As for the KTC coupling, the catalytic system tolerates hindered substrates and is selective in the presence of other functional groups such as ketones, aldehydes and nitriles. However, the major drawback of this catalyst was, again, the requirement of additional triphenylphosphine (up to five equivalents relative to nickel!).

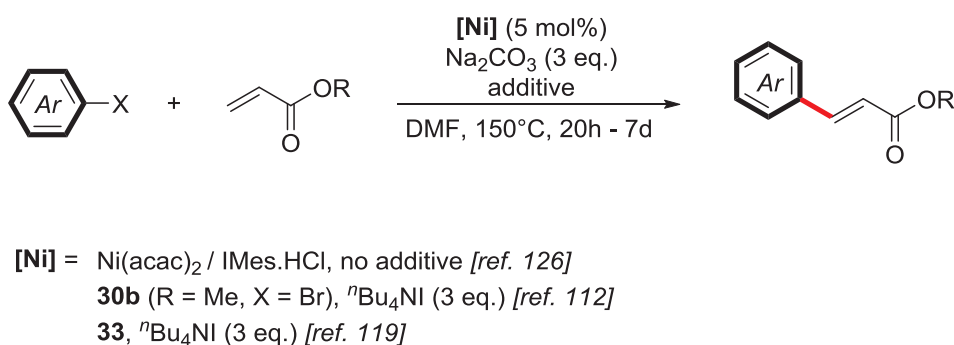
Finally, perhaps the most interesting result was obtained with Radius' Ni(0) homobimetallic complex **34**, which allowed the coupling of aryl chlorides,<sup>[132]</sup> but more importantly for the first selective coupling of perfluoroarenes by C–F activation (**Scheme 23**).<sup>[133]</sup> It is noteworthy that the choice of the base appeared to be highly substrate-dependent.



**Scheme 23.** SM coupling of perfluoroarenes catalyzed by **34**

### II.2.3. Mizoroki-Heck coupling

Ni–NHC catalysts have been scarcely applied in the Mizoroki-Heck<sup>[134,135]</sup> (MH) coupling. Thus, only a few examples on the use of acrylates as sole olefinic substrates have been reported. Moreover, harsh reaction conditions were required to obtain reasonable yields of the *trans*-cross-coupling product (**Scheme 24**).<sup>[122,129,136]</sup>



**Scheme 24.** Ni–NHC-catalyzed MH coupling

Inamoto's *in situ* generated catalytic system from Ni(acac)<sub>2</sub>/IMes.HCl was the first reported example.<sup>[136]</sup> It allowed the efficient coupling of aryl iodides and bromides with

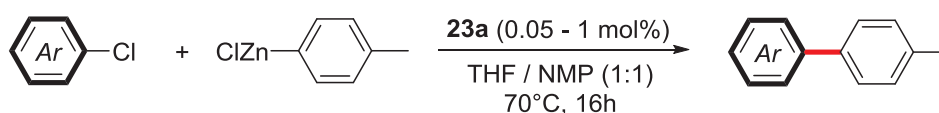
acrylates (**Scheme 24**). Interestingly, the observed long induction period suggested that reduction of the nickel(II) precatalysts to active nickel(0) was rather difficult. Moreover, the mercury drop test resulted in total inhibition of the reaction, thus suggesting the participation of a heterogeneous nickel(0) catalyst.

Later, the use of the (*C,N,C*)-pincer complex **30b** (*R* = Me, *X* = Br) allowed the use of activated aryl chlorides as electrophiles, even though reaction times were longer and an iodide salt was required.<sup>[122]</sup> The cationic complex **33** has been proved to be less active, probably due to a difficult generation of vacant sites.<sup>[129]</sup>

#### II.2.4. Negishi coupling

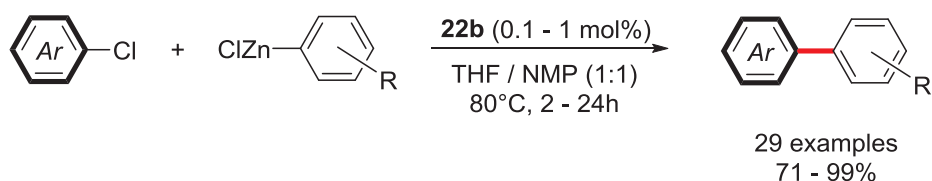
Ni–NHC systems were rarely applied in Negishi coupling,<sup>[137,138]</sup> and to the best of our knowledge, only a couple of examples describing the use of well-defined Ni–NHC complexes for the coupling of aryl chlorides have been reported.

The mononuclear complex **17a**, and most importantly, the versatile bimetallic complex **23a** proved to be able of catalyzing the Negishi coupling of a variety of (hetero)aryl chlorides and vinyl chlorides under mild conditions (**Scheme 25**).<sup>[139]</sup> Again, the bimetallic cooperativity was proposed to be responsible for its higher activity.



**Scheme 25.** Negishi cross-coupling catalyzed by **23a**

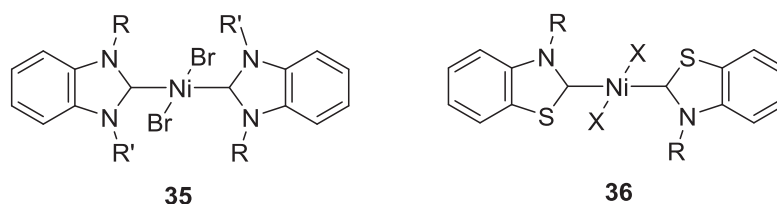
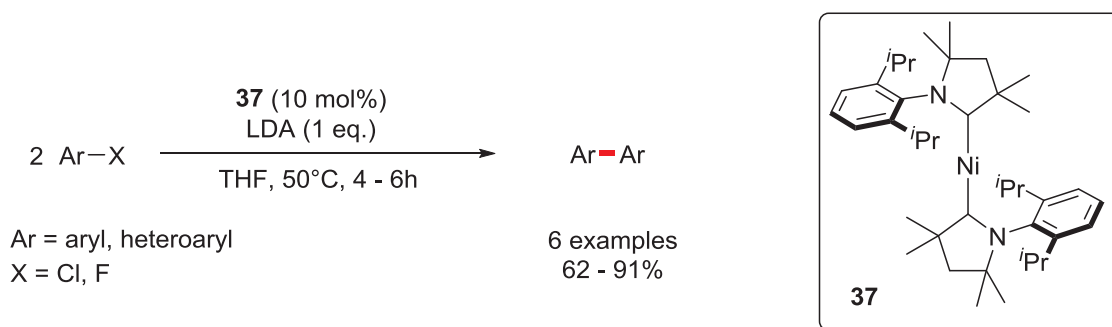
The (*C,N,N*)- and (*C,N,P*)-pincer complexes **22a-c** have also been valued in the Negishi coupling of some activated and unactivated aryl chlorides.<sup>[102]</sup> Among these complexes, **22b** exhibited the highest catalytic activity and allowed catalyst loadings as low as 0.05 - 0.5 mol% for several activated and unactivated aryl chlorides (**Scheme 26**).

**Scheme 26.** Negishi cross-coupling catalyzed by **22b**

Of notable interest, *ortho*-substituted substrates could also be employed even if slightly lower yields were obtained.

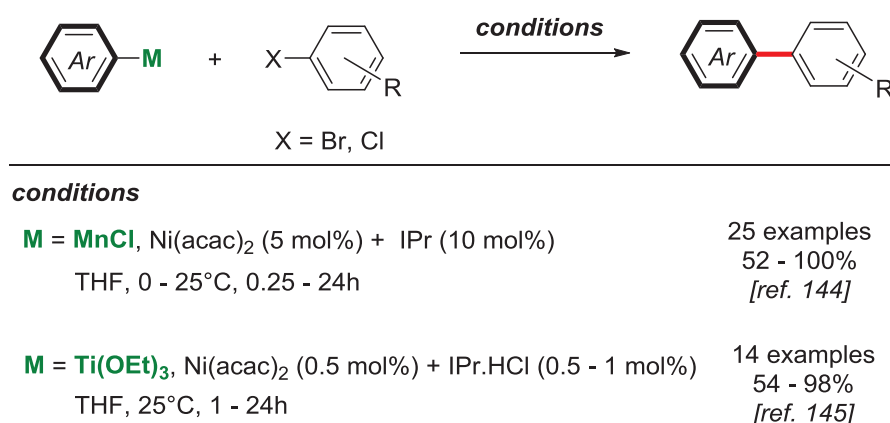
### II.2.5. Homocoupling reactions

The timeless Ullmann homocoupling reaction<sup>[140]</sup> has also seen a small number of successful Ni–NHC catalysts. The reported examples concern the exclusive use of monodentate *bis*-NHC complexes of nickel. While 1 mol% of Ni(II) complexes **35**<sup>[141]</sup> and **36**<sup>[142]</sup> (**Figure 18**) in the presence of Zn powder allowed the use of simple aryl bromides under relatively harsh reaction conditions, employing the zerovalent nickel complex **37** with 1 equivalent of LDA resulted in a clearly better activity, as more challenging aryl chlorides and fluorides were coupled under milder reaction conditions (**Scheme 27**).<sup>[143]</sup> Unfortunately, this methodology suffers from high catalyst loadings.

**Figure 18.** Ni–NHC complexes applied in the catalytic homocoupling reaction**Scheme 27.** Homocoupling of aryl chlorides and fluorides catalyzed by **37**

## II.2.6. Other cross-couplings

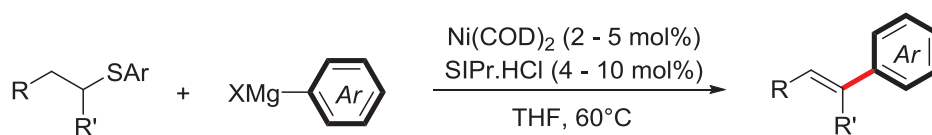
An alternative to the KTC, SM and Negishi couplings is the use of less expensive organomanganese and titanium reagents. Thus, the combination of Ni(acac)<sub>2</sub> with 2 equivalents of IPr was demonstrated to provide an efficient catalyst for the cross-coupling of aryl bromides and organomanganese reagents under very mild conditions (**Scheme 28**).<sup>[144]</sup> Moreover, the procedure appears to be suitable for electron-deficient and electron-rich aryl bromides, as well as for sterically hindered ones. Similarly, Ni(acac)<sub>2</sub> and 1-2 equivalents of IPr were demonstrated to be an efficient catalytic combination for the cross coupling of aryl titanium(IV) alkoxides and various aryl halides (**Scheme 28**).<sup>[145]</sup> Of notable interest is the much lower catalyst loading required (0.5 - 1 mol%) compared to the previous reaction. A limitation, however, concerns the use of electron-rich aryl halides, which could be overcome by employing the *tris*-(2,4,6-trimethoxyphenyl)phosphine ligand instead of IPr.



**Scheme 28.** Other C–C bond formation methodologies to form biaryl compounds

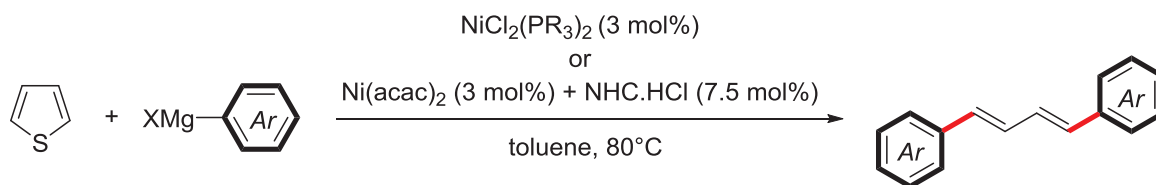
Other alternatives to traditional cross-coupling reactions involve the use of alternative electrophiles to the traditional organohalides, such as organosulfur compounds which have received far less attention in spite of the seminal publications of Wenkert<sup>[146]</sup> and Takei.<sup>[147]</sup> Thus, another Ni–NHC-catalyzed cross-coupling reaction was the alkenylative coupling of alkyl aryl sulfides with aryl Grignard reagents to produce alkenyl-aryls in high yields by using Ni(COD)<sub>2</sub> and 2 equivalents of SIPr (**Scheme 29**).<sup>[148]</sup>





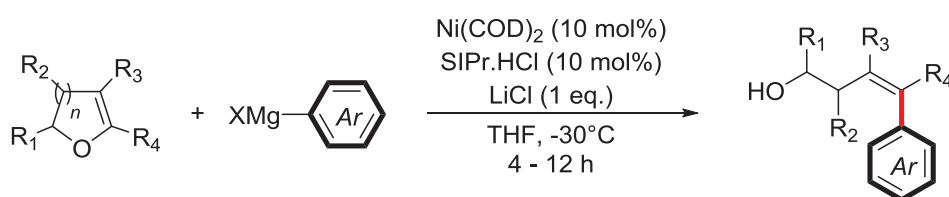
**Scheme 29.** Ni–NHC-catalyzed alkenylative coupling of alkyl aryl sulfides

Similarly, the use of  $\text{Ni}(\text{acac})_2$  in the presence of 2.5 equivalents of  $\text{IMes.HCl}$ ,  $\text{iPr.HCl}$  or of a nickel phosphine complex allowed the direct and scalable synthesis of (*E,E*)-1,4-diaryl-1,3-butadienes by the coupling of thiophene with aryl Grignard reagents (**Scheme 30**).<sup>[149]</sup>



**Scheme 30.** Ni-catalyzed Wenkert arylation of thiophene

Finally, a  $\text{Ni}(\text{COD})_2/\text{SIPr.HCl}$  (1:1) catalyst was employed for the C–O arylation of 2,3-dihydrofurans with arylmagnesium bromides.<sup>[150]</sup> The reaction proceeded with high chemoselectivity, allowing the efficient preparation of (*Z*)-homoallylic alcohols (**Scheme 31**).

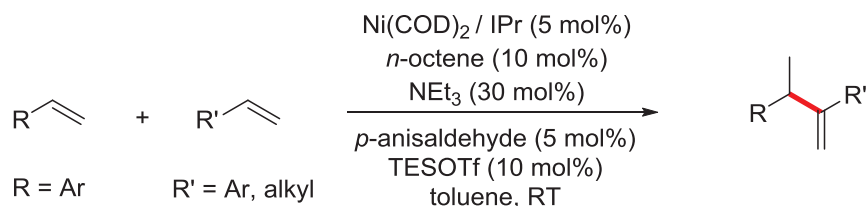


**Scheme 31.** C–O arylation of 2,3-dihydrofurans

### II.2.7. Carbon–Carbon bond formation *via* Carbon–Hydrogen bond functionalization

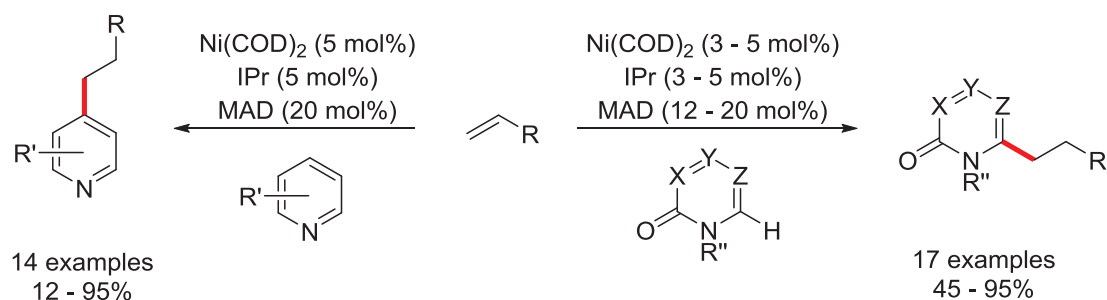
The use of Ni–NHC systems for the functionalization of C–H bonds has mainly involved olefinic substrates. In 2010, Ho *et al.* reported for the first time the highly selective

intermolecular tail-to-tail hetero-hydroalkenylation of vinyl arenes with unactivated  $\alpha$ -olefins.<sup>[151]</sup> Remarkably, branched terminal 1,1-disubstituted olefins were predominantly obtained thanks to an *in situ* generated Ni(IPr)-hydride derivative "[IPr-Ni-H]OTf" (**Scheme 32**). The same catalyst was also proved to be efficient in the head-to-tail vinylsilane- $\alpha$ -olefin hydroalkenylation.<sup>[152]</sup>



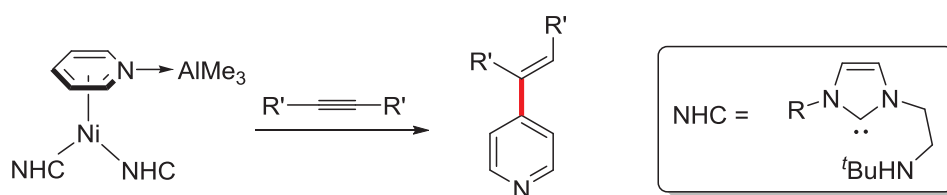
**Scheme 32.** Selective tail-to-tail hydroalkenylation of olefins

The hydroalkenylation of pyridines<sup>[153]</sup> and pyridones<sup>[154]</sup> has also been described. Remarkably, a Ni(COD)<sub>2</sub>/IPr catalyst in combination with MAD (methyl aluminium *bis*-(2,6-di-*tert*-butyl-4-methylphenoxide) as a Lewis acid led to selective C4-alkylation and C6-alkylation of pyridines and pyridones, respectively (**Scheme 33**). The observed selectivities were strongly dependent on the Lewis acid. The very bulky MAD gave the best results.



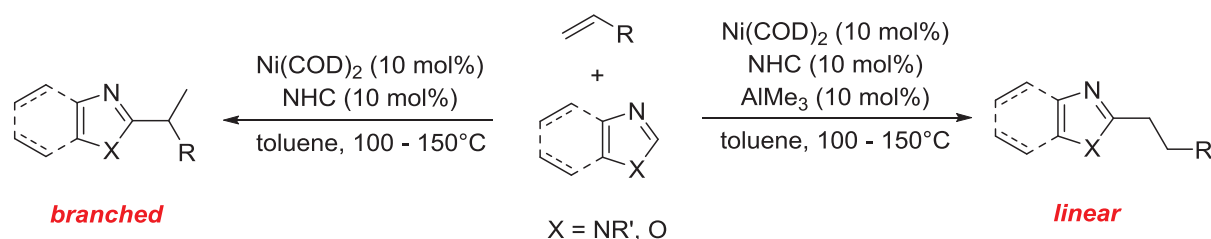
**Scheme 33.** Selective C4- and C6-hydroalkenylation of pyridines and pyridones

In a related example, an amino-NHC Ni-Al complex allowed the C4-hydroalkynylation of pyridines with symmetrical alkynes.<sup>[155]</sup> Of notable interest was the isolation of a  $\eta^2, \eta^1$ -pyridine nickel aluminum intermediate prior to the C–H activation step (**Scheme 34**), which supports bimetallic catalysis.



**Scheme 34.** Ni–NHC–pyridine active intermediate

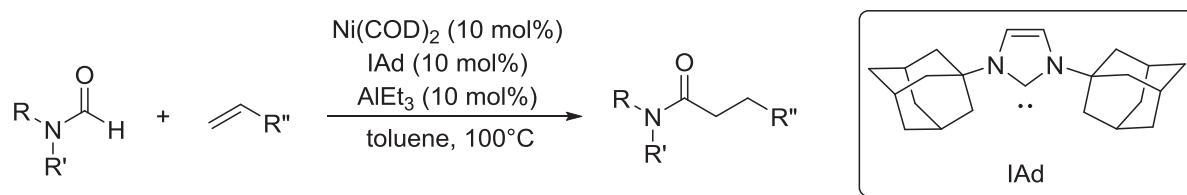
Similar catalytic systems also catalyze the hydroalkenylation at the C2-position ofazole derivatives.<sup>[156,157]</sup> Remarkably, in these cases, the regioselectivity of the reaction could be switched, depending on the presence or absence of trimethylaluminium, to obtain the branched instead of the linear product (**Scheme 35**).



**Scheme 35.** Selective C2-hydroalkenylation of azoles

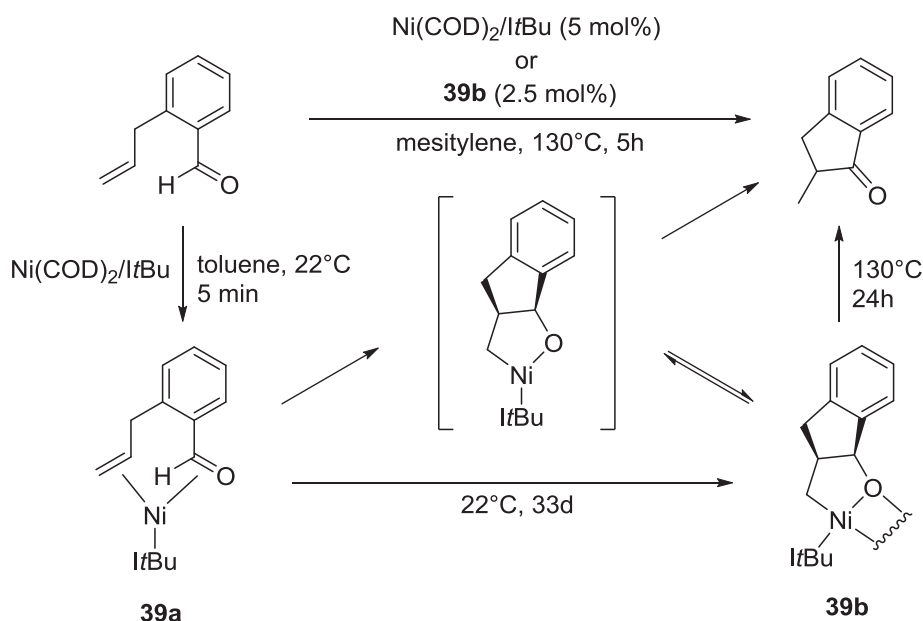
A last example involving a Ni–Al bimetallic cooperation has been reported for the cyanative aldehyde–alkene coupling catalyzed by a  $Ni(IPr)-Et_2AlCN$  catalyst with high *cis*-selectivities at room temperature.<sup>[158]</sup>

$\alpha$ -Alkenes were also valued in transformations involving formamides and aldehydes (**Scheme 36**). These reactions required the use of very bulky NHC ligands. In the case of formamides,  $Ni(COD)_2/IAAd$  (1:1) in combination with triethylaluminium resulted in the formation linear amides.<sup>[159]</sup> However a limitation of this methodology is the use of aryl formamides for which a drastic decrease of catalytic activity was observed.



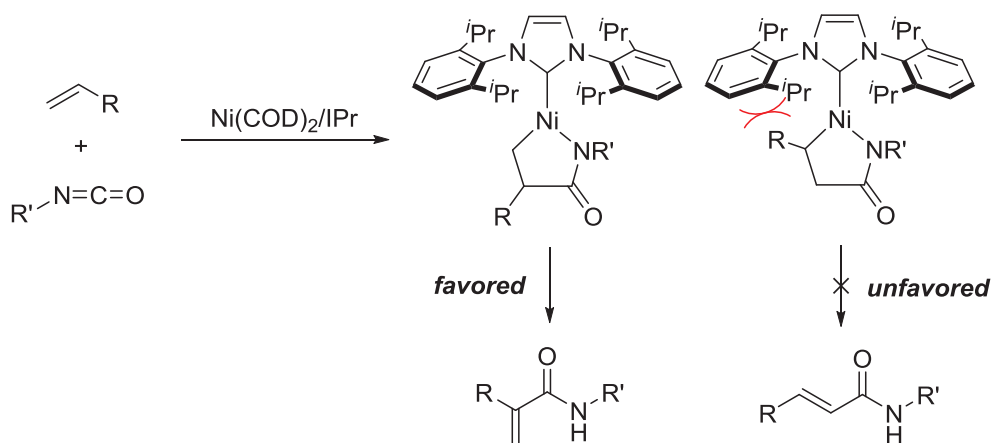
**Scheme 36.** Regioselective hydrocarbamoylation of 1-alkenes

Remarkably, the intramolecular hydroacylation of alkenes was achieved with a  $\text{Ni}(\text{COD})_2/\text{ItBu}$  system to afford indanones and tetralones derivatives in good to excellent yields.<sup>[160]</sup> Of notable interest is the isolation of two complexes **39a** and **39b**, which are likely to be real active species, as confirmed by control experiments (**Scheme 37**).



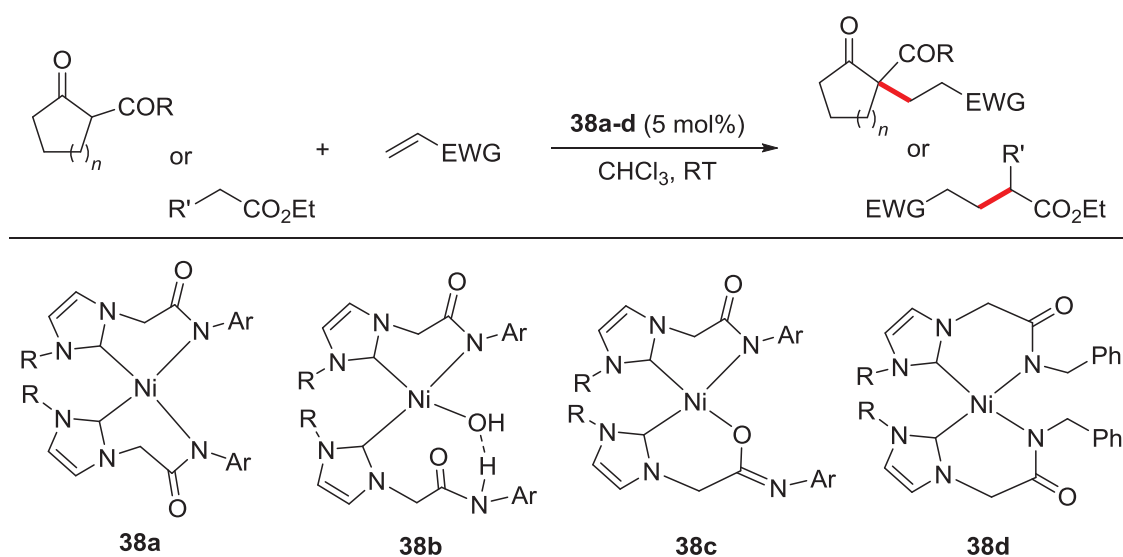
**Scheme 37.** Plausible intermediates involved in the intramolecular hydroacylation of alkenes

$\alpha$ -olefins were also employed for the Ni–NHC-catalyzed coupling with isocyanates to form acrylamides, which are important building blocks in the polymer industry.<sup>[161]</sup> The predominant formation of the *exo* product was explained by steric factors (**Scheme 38**).



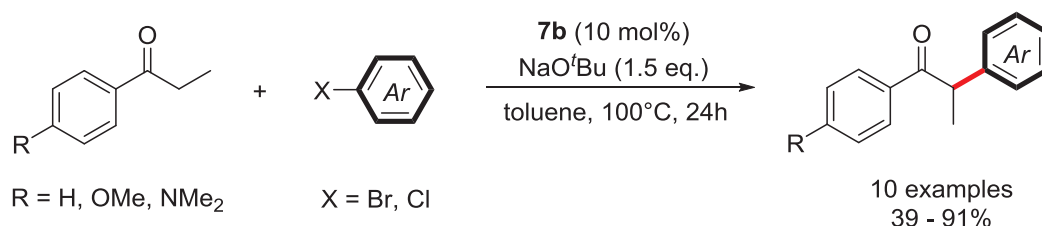
**Scheme 38.** Plausible intermediates involved in the coupling of  $\alpha$ -olefins and isocyanates

Other C–C bond formation methodologies involving the functionalization of C–H bonds notably include the Michael reaction of  $\beta$ -dicarbonyl,  $\beta$ -diester,  $\beta$ -keto ester and  $\alpha$ -cyano ester compounds with  $\alpha,\beta$ -unsaturated carbonyl compounds, catalyzed by the well-defined Ni–NHC complexes **38a–d** (Scheme 39).<sup>[162–164]</sup> The main advantage of this methodology is the avoidance of a base, which consequently suppresses side reactions such as the aldol-cyclization or the retro-Claisen type decomposition. Moreover, the reaction is performed in air and at room temperature.



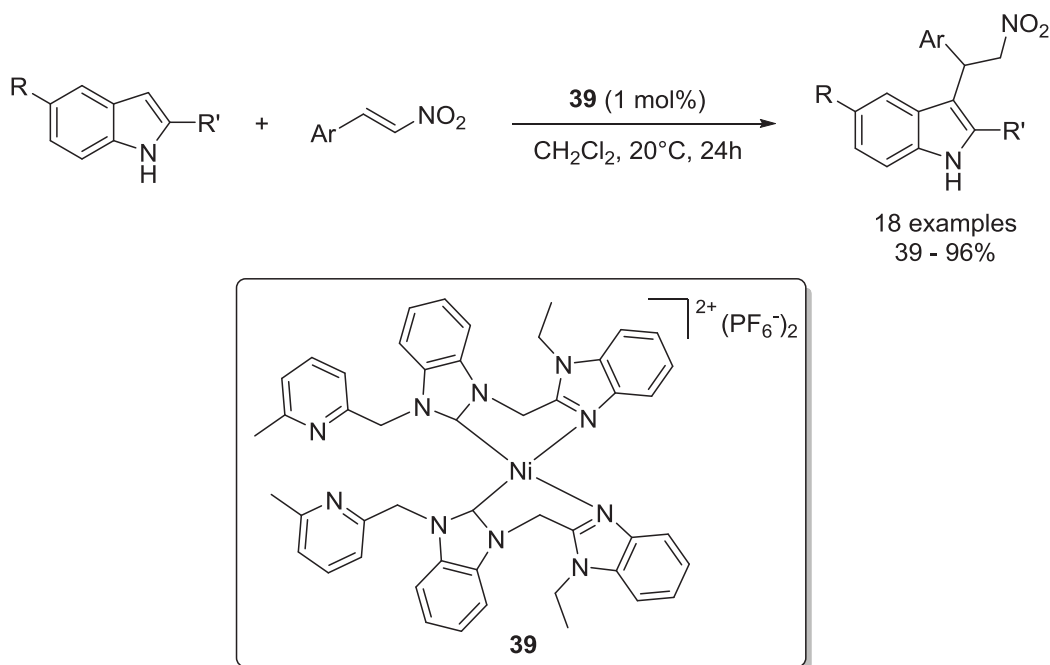
**Scheme 39.** Ni–NHC-catalyzed base-free Michael reaction

The  $\alpha$ -arylation of propiophenone derivatives catalyzed by **7b** constitute another attractive methodology for the formation of C–C bonds *via* C–H functionalization (Scheme 40).<sup>[165]</sup> Although high precatalyst loadings were required, some aryl bromides and chlorides could be converted into the corresponding  $\alpha$ -aryl ketone in reasonable yields. Of notable interest is the use of the air- and moisture-stable complex **7b**, which does not require the addition of any reductant.



**Scheme 40.**  $\alpha$ -Arylation of propiophenone derivatives catalyzed by **7b**

Finally, the well-defined Ni–NHC complex **39** has been proved to be catalytically active in the Friedel-Crafts reaction of indoles with  $\beta$ -nitrostyrenes (**Scheme 41**).<sup>[166]</sup>



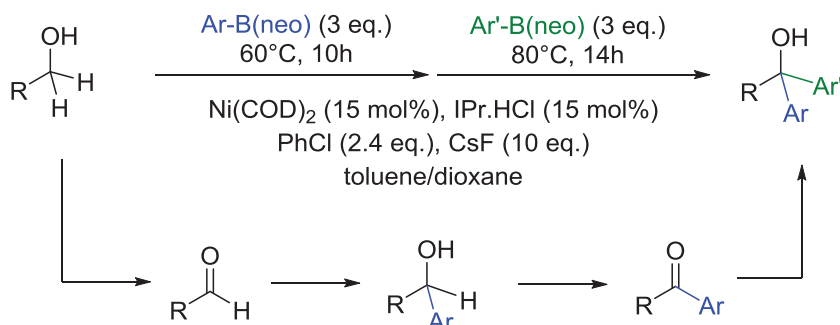
**Scheme 41.** Friedel-Crafts alkylation of indoles with  $\beta$ -nitrostyrenes

### II.2.8. Miscellaneous Carbon–Carbon bond formation reactions

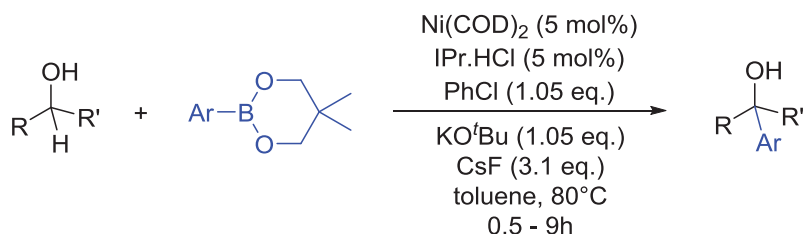
In 2009, Navarro described the Ni–NHC-catalyzed oxidation of secondary alcohols<sup>[167]</sup> (see *Oxidations* section). The same year, Itami concurrently described the use of a similar catalytic system for addition of organoboronate esters to ketones and aldehyde to yield tertiary alcohols.<sup>[168]</sup> As a consequence, these two groups later and independently reported the efficient one-pot oxidation-addition of secondary alcohols with boronic esters (**Scheme 42**).<sup>[169,170]</sup> The rate-determining step is the addition of the boronic compound, which depends on its electronic and steric nature.<sup>[170]</sup> By using slightly different reaction conditions than Navarro, Itami was able to employ primary alcohols for a controlled sequential double oxidation-addition process.<sup>[169]</sup> The key of this remarkable reaction seems to be the use of an excess of cesium fluoride in a toluene/dioxane media (**Scheme 42**). This

strategy notably allowed the one-pot synthesis of flumecinol, a hepatic microsomal enzyme reducer.

**Itami**

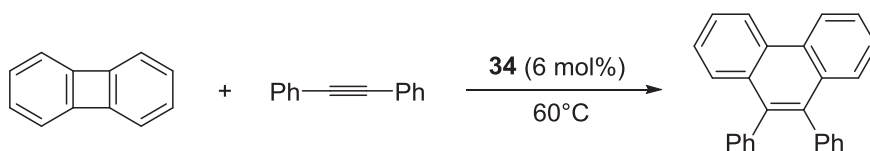


**Navarro**



**Scheme 42.** Domino synthesis of tertiary alcohols from primary and secondary alcohols

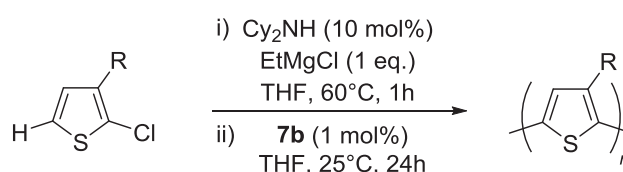
In a totally different context, complex **34** has been shown to be able to activate not only C–F bonds, but also C–C bonds.<sup>[171]</sup> Indeed, the reaction of diphenylacetylene with biphenylene led to the product formed by alkyne insertion into the 2,2' bond of biphenylene (**Scheme 43**).



**Scheme 43.** Catalytic C–C activation by **34**

Finally, Mori elegantly described the use of **7b** for the polycondensation of chlorothiophenes in the presence of stoichiometric or catalytically generated magnesium amide (**Scheme 44**).<sup>[172]</sup> The methodology is atom-efficient, and operates under mild

conditions to efficiently give polythiophenes, that are valuable building blocks in materials chemistry. The same strategy has been employed for the coupling of thiophene derivatives with polyhalogenated thiophenes or arenes to give the corresponding multi-coupled product,<sup>[173]</sup> as well as for the synthesis of polythienylenearylenes.<sup>[174]</sup>

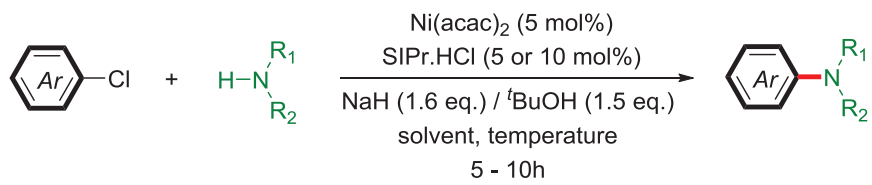


**Scheme 44.** Ni–NHC-catalyzed polycondensation of thiophenes

### II.3. Coupling reactions involving Carbon–Heteroatom bond formation

#### II.3.1. Carbon–Nitrogen bond formation

The Ni–NHC-catalyzed amination of aryl halides was first reported by Fort and co-workers in 2001.<sup>[175]</sup> The combination of Ni(acac)<sub>2</sub> (5 mol%), SIPr.HCl (10 mol%), <sup>t</sup>BuOH and an excess of NaH resulted in the formation of subnanoparticles of NHC–Ni(0), which were possibly responsible for the observed catalytic activity. Remarkably, this system already allowed for the coupling of aryl chlorides with anilines and primary alkylamines, even if the catalytic activity slightly decreased with the latter substrates. One year later, the same group extended the methodology to a broader scope of substrates by using slightly modified reaction conditions, notably with anilines (**Scheme 45**).<sup>[176]</sup> Finally, this methodology was also applied in an intramolecular version, to build 5- to 7-membered heterocycles.<sup>[177]</sup>



**Conditions:**

*secondary amines:* THF, 65°C

25 examples  
53 - 99%

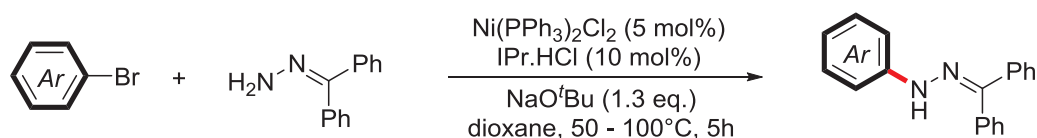
*anilines:* dioxane, 100°C

22 examples  
47 - 99%

**Scheme 45.** *In situ* catalytic amination of aryl chlorides

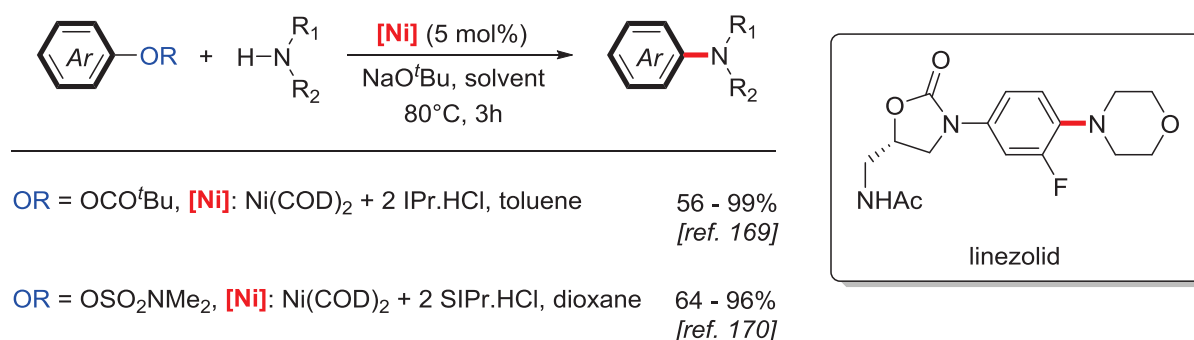


Very recently, the use of  $\text{NiCl}_2(\text{PPh}_3)_2/\text{IPr.HCl}$  (1:2) under conditions similar to these developed by Fort *et al.* allowed the coupling of benzophenone hydrazine with bromoarenes (**Scheme 46**).<sup>[178]</sup>



**Scheme 46.** Ni–NHC-catalyzed amination of bromoarenes with benzophenone hydrazine

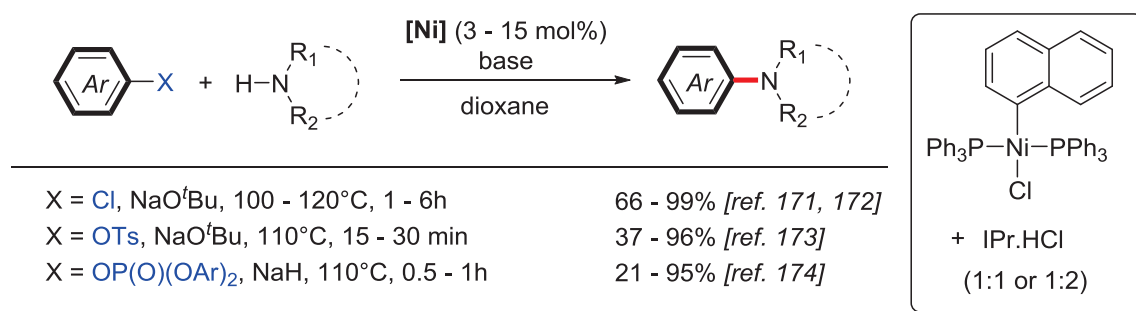
The direct use of a nickel(0) source with an imidazolium salt in the presence of a base also proved to be very efficient. Thus, the combination of  $\text{Ni}(\text{COD})_2$ ,  $\text{IPr.HCl}$  or  $\text{SIPr.HCl}$  and  $\text{NaO}^t\text{Bu}$  was shown to promote the amination of aryl carboxylates<sup>[179]</sup> and sulfamates,<sup>[180]</sup> which are very interesting electrophiles due to their ease of preparation and handling, pronounced stability, low toxicity and low cost (**Scheme 47**). Remarkably, the methodology with aryl sulfamates could be used for the expeditious synthesis of linezolid, an antibacterial drug.<sup>[180]</sup> Both reactions allowed the arylation of cyclic and acyclic secondary amines and anilines with various arenes, and in the case of sulfamates, heteroarenes.



**Scheme 47.** Catalytic amination of aryl sulfamates and carbonates

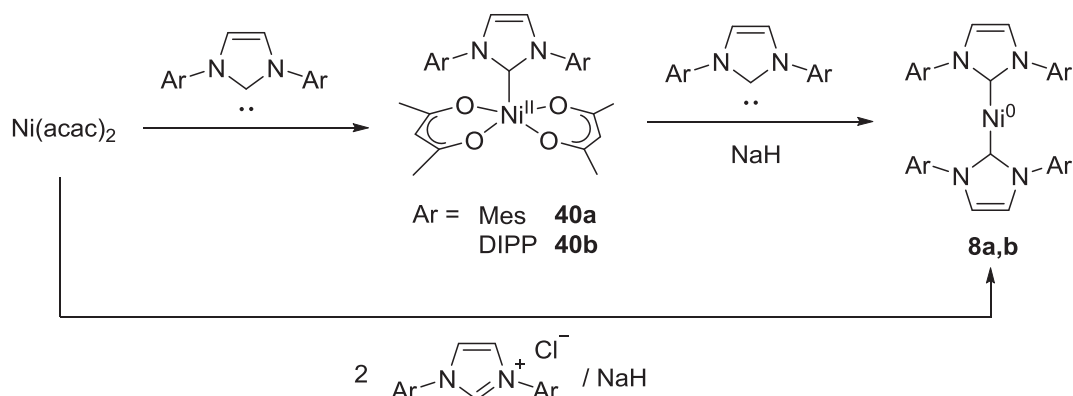
$\sigma$ -Aryl nickel(II) complexes, which are readily available and easy to modulate, were demonstrated to be an alternative source of nickel to *in situ* generate active  $\text{Ni}(0)$ –NHC complexes without need for an additional reductant. Initially, such a system was successfully applied in the amination of aryl chlorides with cyclic dialkylamines and anilines.<sup>[181,182]</sup>

Rapidly, it was also used with aryl tosylates, which required slightly higher catalyst loadings but much shorter reaction times.<sup>[183]</sup> More recently, this system also proved to be useful when using aryl phosphates as coupling partners.<sup>[184]</sup> Interestingly, the reaction has a wider scope of substrates than other C–O bond functionalization methodologies with respect to the amine. Thus, primary alkylamines were efficiently functionalized under these conditions (**Scheme 48**).



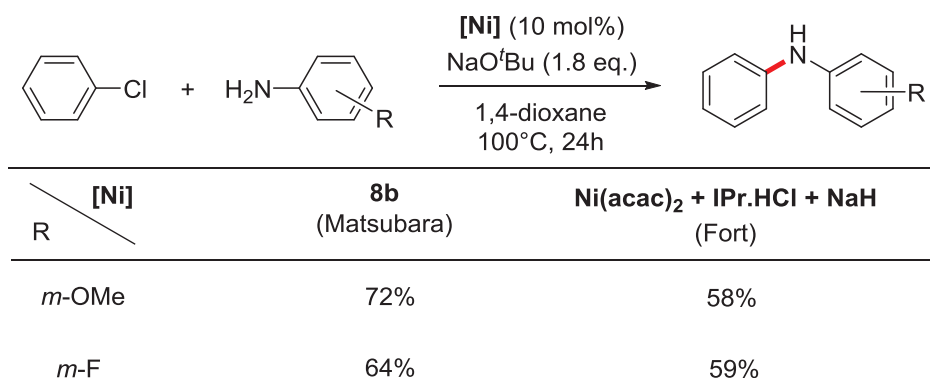
**Scheme 48.** Use of  $\sigma$ -aryl nickel(II) complexes in the formation of C–N bonds

Matsubara *et al.* isolated the well-defined 18-electron (**40a,b**), and 14-electron (**8a,b**) Ni(NHC)<sub>2</sub> complexes starting from Ni(acac)<sub>2</sub>, an *in situ* generated NHC ligand, and NaH, which are the reagents employed by Fort and co-workers to *in situ* generate Ni(0)–NHC complexes (**Scheme 49**).<sup>[185]</sup>



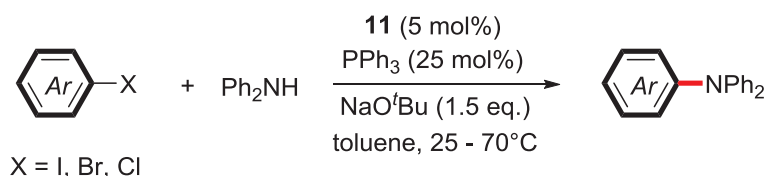
**Scheme 49.** Synthesis of **40a,b** and **8a,b** described by Matsubara

Catalytic amination of chlorobenzene, carried out in the presence of **8a**, gave slightly higher yields than with Fort's *in situ* generated Ni(0)–NHC generation process, which suggests that **8a** is very close to the active species (**Scheme 50**).



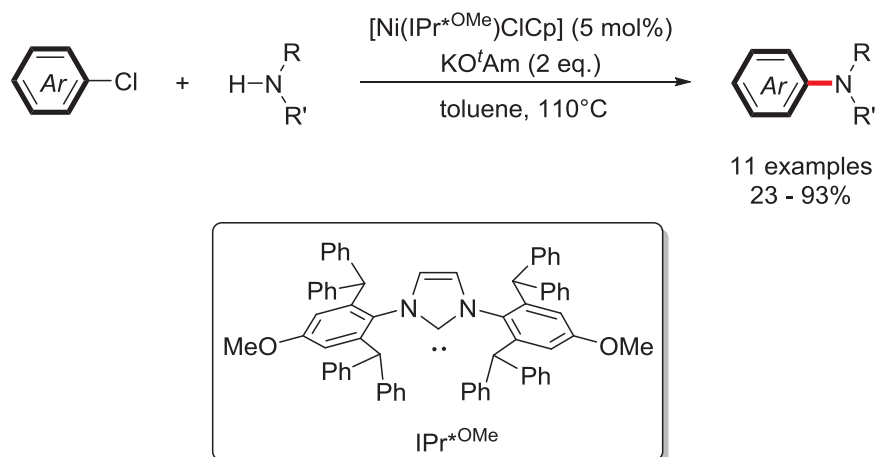
**Scheme 50.** Comparative study between Fort's results and complex **8b** in the catalytic amination of aryl chlorides

In another work, the same authors reported the use of the 15-electron electron mixed phosphine/NHC complex **12** (Ar = DIPP), *in situ* generated from **11** and an excess of triphenylphosphine.<sup>[89]</sup> These pre-catalyst efficiently catalyzes the Buchwald-Hartwig coupling of diphenylamine with aryl halides under relatively mild reaction conditions (**Scheme 51**).



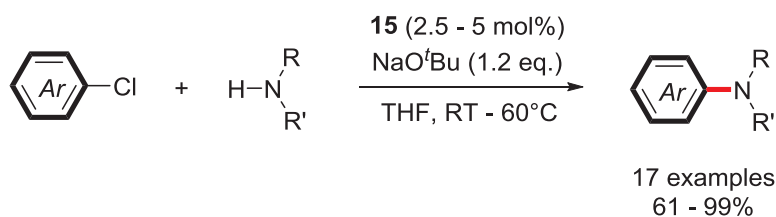
**Scheme 51.** Ni–NHC-catalyzed diphenylamination of aryl halides

The half-sandwich complexes **30** bearing (S)IPr and (S)IMes ligands also showed some activity in the amination of a very restricted number of aryl bromides and chlorides with morpholine.<sup>[186]</sup> More recently, it was found that using the bulkier IPr\*<sup>OMe</sup> ligand (**Scheme 52**) led to a significant increase of activity, probably due to a better steric protection of the active species that prevents its decomposition.<sup>[187]</sup>



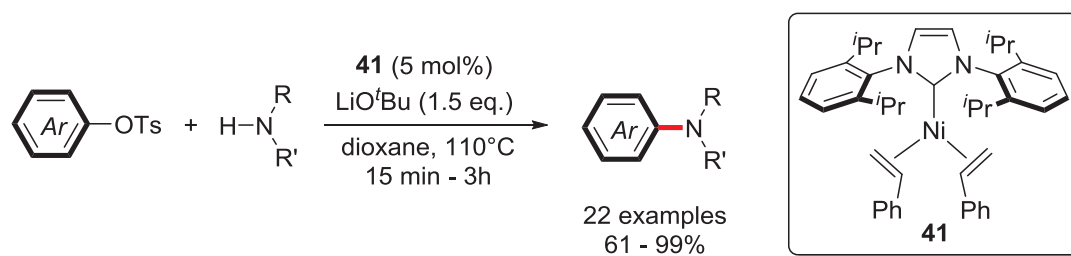
**Scheme 52.** Buchwald-Hartwig amination of aryl chlorides catalyzed by  $[\text{Ni}(\text{IPr}^*\text{OMe})\text{ClCp}]$

The related 16-electron  $\pi$ -allyl nickel complex **15** is not only very efficient for KTC cross-coupling,<sup>[92]</sup> but also for the formation of Carbon–Heteroatom bonds.<sup>[93]</sup> In particular, the Buchwald-Hartwig amination of heteroaromatic chlorides with secondary amines and anilines proceeded smoothly at room temperature to give the cross-coupling products in good to excellent yields (61 - 99%) (**Scheme 53**). The better results obtained with **15** compared to complexes **30** could be explained by presence of the allyl moiety in **15**, which would help reducing Ni(II) to Ni(0) probably in a way similar to that proposed for Pd(II) analogues.<sup>[94,95]</sup> Again, replacement of the IPr ligand by the bulkier  $\text{IPr}^*\text{OMe}$ , this time in **15**, resulted in increased activities.<sup>[188]</sup>



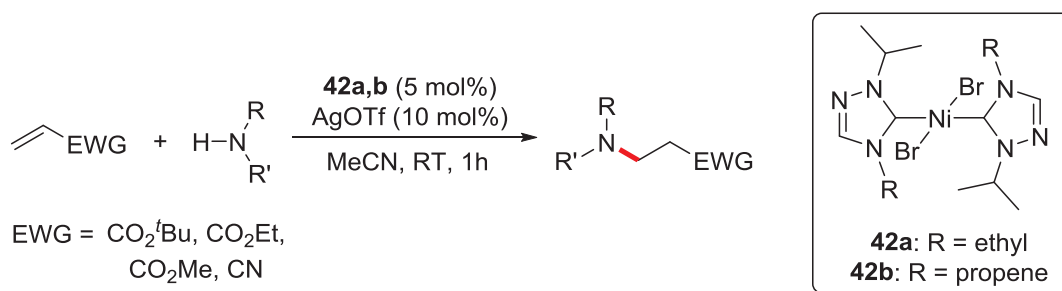
**Scheme 53.** Buchwald-Hartwig amination of aryl chlorides catalyzed by **15**

A remarkable improvement has been reported when using the *bis*-styrene Ni(0)–IPr complex **41**. The latter indeed allows the coupling of aryl tosylates with secondary cyclic amines and anilines in short reaction times (**Scheme 54**).<sup>[189]</sup> Interestingly, the catalytic system worked well with sterically-hindered anilines.



**Scheme 54.** Buchwald-Hartwig amination of aryl tosylates catalyzed by **41**

Finally, complexes **42a,b** showed moderate activities in the hydroamination of electron-poor  $\alpha$ -alkenes (**Scheme 55**).<sup>[190]</sup> Remarkably, these nickel complexes were found to be more efficient than their palladium analogues.

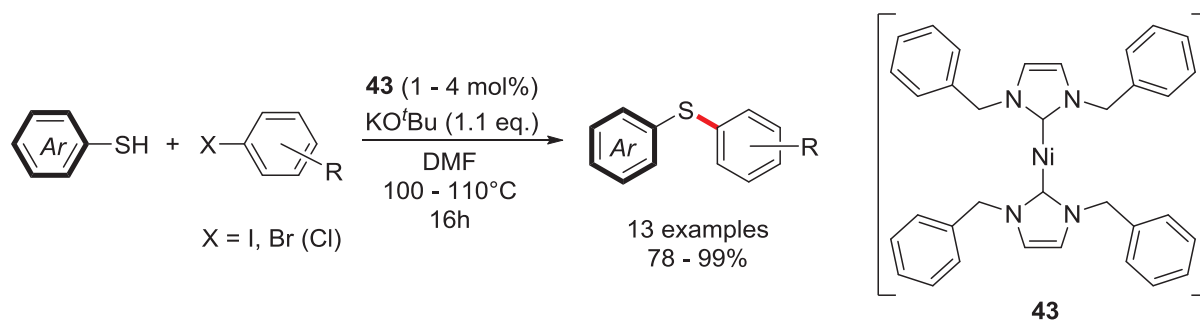


**Scheme 55.** Hydroamination of electron-poor  $\alpha$ -olefins catalyzed by **42a,b**

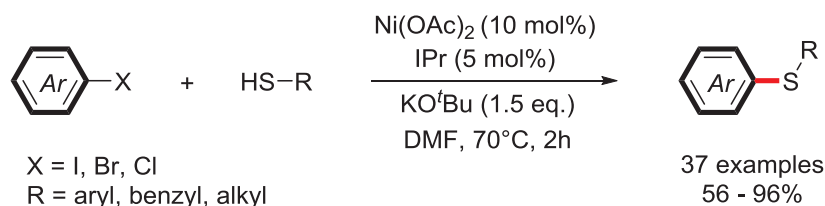
### II.3.2. Carbon–Sulfur bond formation

C–S couplings have been much less studied than C–N couplings. Nevertheless, a few Ni–NHC systems have been shown to promote the formation of C–S bonds between thiol derivatives and electrophiles.

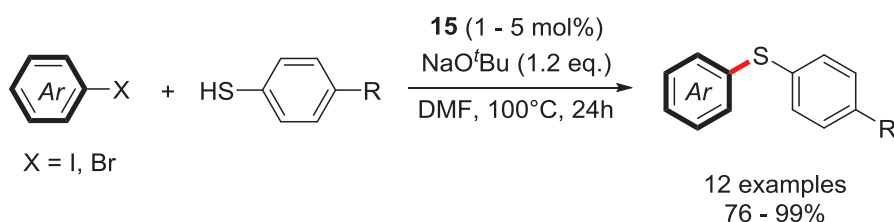
The first example was only described in 2007 when the *bis*-NHC-nickel(0) complex **43**, which would be formed by reaction of Ni(COD)<sub>2</sub> with two equivalents of the IBn ligand, was reported to efficiently couple arylthiols with aryl iodides and bromides (**Scheme 56**).<sup>[191]</sup>

**Scheme 56.** First Ni–NHC-catalyzed arylthiolation of aryl halides

More recently, the readily available and easy-to-handle  $\text{Ni}(\text{OAc})_2$  was reported to catalyze the C–S coupling of a large array of aryl-, benzyl- and alkylthiols with aryl iodides, bromides and electron-deficient aryl chlorides in the presence of IPr and  $\text{KO}^t\text{Bu}$  (**Scheme 57**).<sup>[192]</sup>

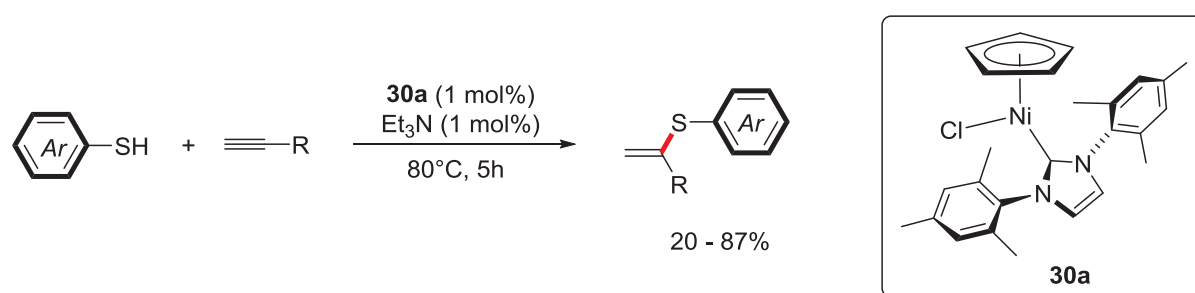
**Scheme 57.** Aryl-, benzyl- and alkylthiolation of haloarenes

As observed for the formation of Carbon–Nitrogen bonds, monodentate Ni–NHC complexes appeared to be the only well-defined Ni–NHC complexes that are suitable for these transformations. Thus, the air-stable complex **15**, which is highly active in aryl amination (see **Scheme 53**), also shows interesting activities in the thiolation of aryl iodides and bromides in the presence of  $\text{NaO}^t\text{Bu}$  as the sole additive (**Scheme 58**).<sup>[93]</sup> Interestingly, it appears to be more active than the *in situ* generated complex **43**. Again, replacement of the IPr ligand in **15** by an  $\text{IPr}^*\text{OMe}$  ligand resulted in increased activities.<sup>[188]</sup>

**Scheme 58.** Arylthiolation of aryl iodides and bromides catalyzed by **15**

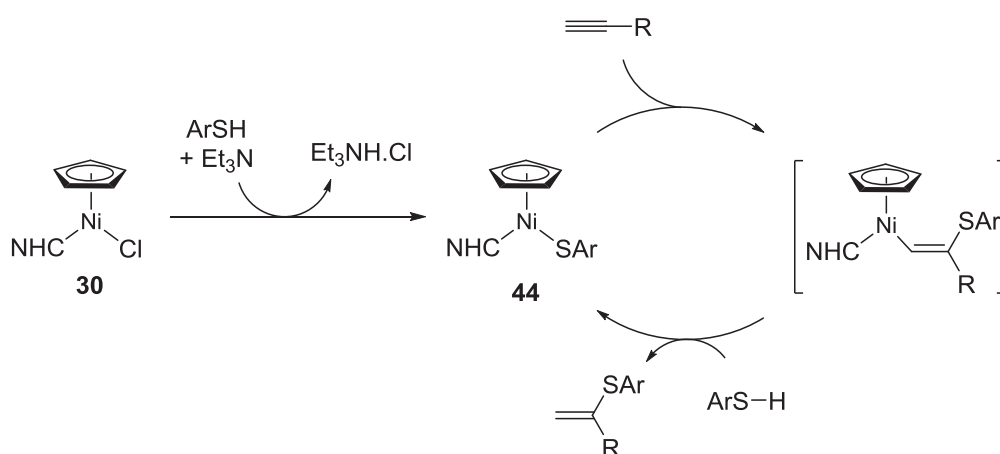
Recyclable Ni–NHC complexes immobilized on Magnetite/Silica nanoparticles have been applied in the thiolation of aryl iodides.<sup>[193]</sup> Catalyst recovery was achieved with the assistance of an external magnet after each run, and the catalyst could be reused up to three cycles without notable decrease of activity.

Finally, the CpNi–NHC complexes **30** are efficient pre-catalysts for the atom-efficient hydrothiolation of alkynes (**Scheme 59**).<sup>[194]</sup> The reaction was performed with good selectivities for the Markovnikov addition product and displays good functional group-tolerance, when employing the IMes derivative **30a**.



**Scheme 59.** Hydrothiolation of alkynes catalyzed by complex **30a**

Mechanistic investigations revealed that the thiol complexes **44**, which are formed by reaction of **30** with one equivalent of thiol in the presence of NEt<sub>3</sub>, may act as active intermediates in a Ni(II)/Ni(II) catalytic cycle (**Scheme 60**). These intermediates would react by alkyne insertion to yield an unstable thioalkenyl intermediate. The latter would then be trapped by another equivalent of thiol to yield the desired product and regenerate the active species.

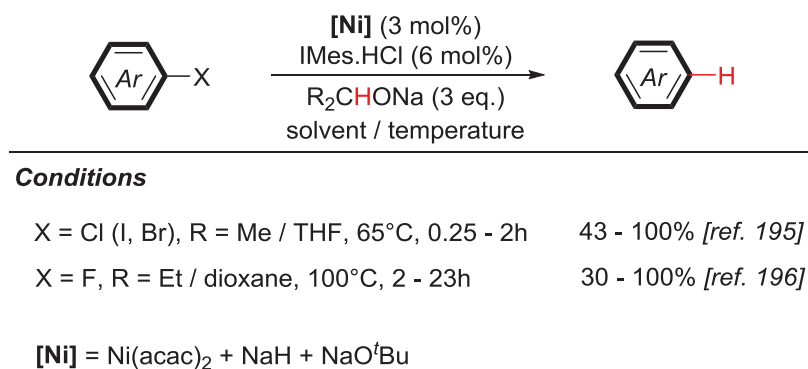


**Scheme 60.** Catalytic cycle proposed by Nolan

## II.4. Reduction reactions

### II.4.1. Dehalogenation reactions

The dehalogenation of aryl halides was a side reaction observed by Fort and co-workers during their studies on the Ni-catalyzed amination of aryl halides (see **Scheme 45**).<sup>[176]</sup> By addition of alkoxide as a hydrogen-donor, the same catalytic system proved to be efficient for the dehalogenation of aryl iodides, bromides, chlorides<sup>[195]</sup> and even fluorides<sup>[196]</sup> (**Scheme 61**).



**Scheme 61.** Catalytic dehalogenation of aryl halides

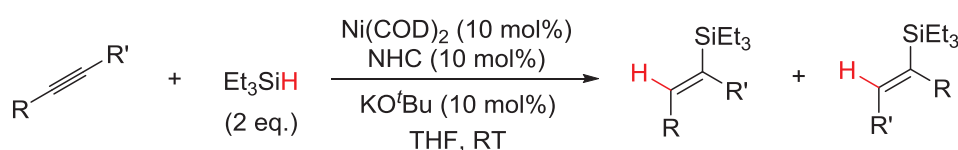
The well-defined half-sandwich complexes **30** also catalyze the dehalogenation of *para*-bromotoluene in the presence of sodium isopropoxide.<sup>[186]</sup> However, their efficiency is very limited as a maximum of 40% conversion was observed with a catalyst loading of 5 mol% in THF or 1,4-dioxane at reflux. Much better yields were observed at room temperature with the nickel(I) complex **7a** (*n* = 1) under otherwise similar conditions.<sup>[197]</sup> However, the substrate scope was not studied.

### II.4.2. Carbon–Carbon multiple bond reduction

Montgomery was the first to apply a Ni–NHC system to the reduction of Carbon–Carbon multiple bonds in 2006.<sup>[198]</sup> Generating a catalyst *in situ* starting from Ni(COD)<sub>2</sub> and IMes.HCl or IPr.HCl allowed the hydrosilylation of internal and terminal alkynes under mild conditions (**Scheme 62**). It is noteworthy that a key to avoid the formation

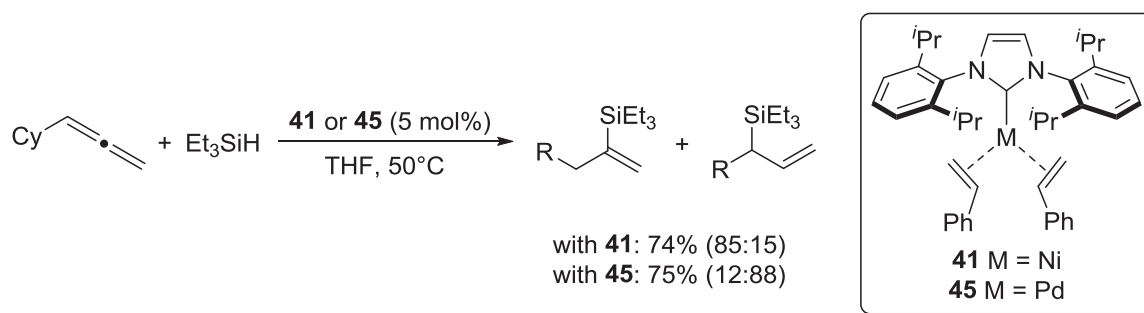


of 2:1 coupling products of the alkyne and the silane is the slow addition of the alkyne over 20 min. With asymmetric alkynes, the regioselectivity depended on the structures of the alkyne, silane and NHC ligand. The impact of these variables on the regioselectivity of the reaction was compared to that on the regioselectivity of the closely related three-component coupling of alkynes, aldehydes and silanes. The result suggests that alkyne hydrometallation is not a common first step in both reaction.



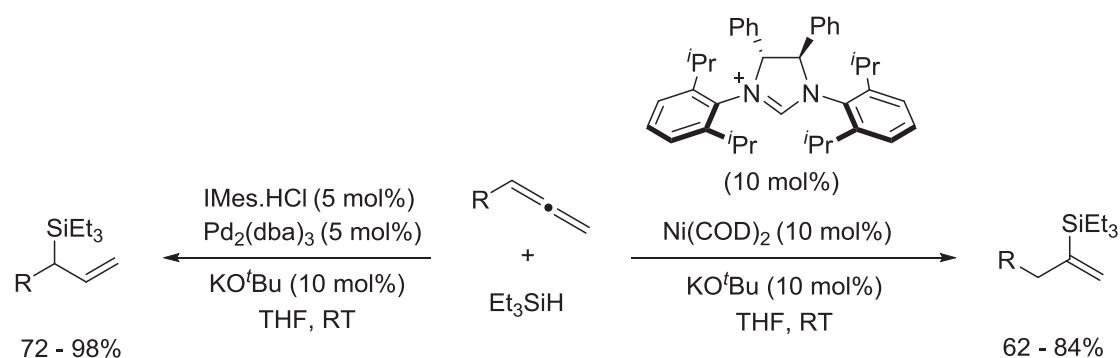
**Scheme 62.** Hydrosilylation of alkynes catalyzed by a Ni(COD)<sub>2</sub>/NHC (1:1) system

In a very elegant study, Montgomery recently extended this reaction to the more challenging allenes.<sup>[199]</sup> Impressively, they observed that the regioselectivity of the reaction could be reversed by changing the nature of the metal, within complexes that possess a common ligand scaffold. Thus, the nickel complex **41** provided the alkenyl silane as the major product, whereas the Pd complex **45** provided the allyl silane as the major product (**Scheme 63**).



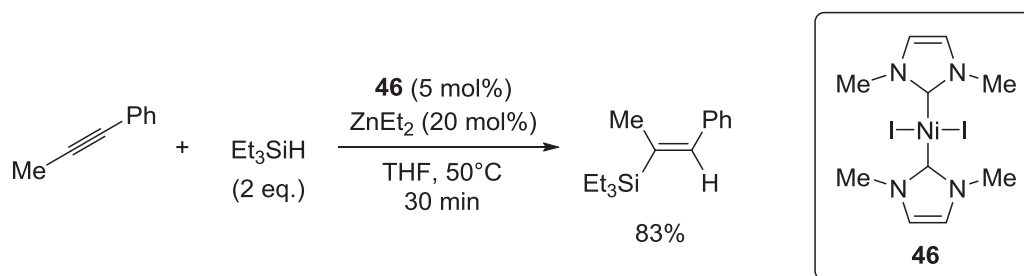
**Scheme 63.** Metal-induced selective hydrosilylation of allenes

Further optimization of the procedure led to slight ligand variation for both nickel- and palladium-catalyzed hydrosilylations, and *in situ* generated complexes were preferred for practical convenience (**Scheme 64**).



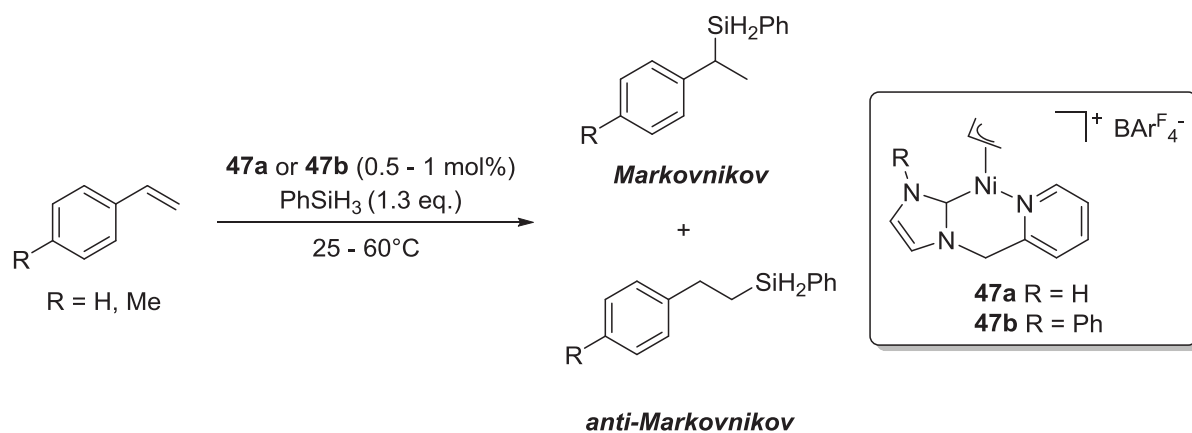
**Scheme 64.** Optimized selective hydrosilylation of allenes

Well-defined Ni(II)–NHCs were also used for the hydrosilylation of alkynes and alkenes. Thus a number of nickel(II) dihalide complexes **35** and **46** of the type [Ni(NHC)<sub>2</sub>X<sub>2</sub>] with small monodentate NHCs were shown to be catalytically active in the hydrosilylation of internal alkynes in the presence of ZnEt<sub>2</sub> as a reductant. In all cases, the catalytic activity yielded the *syn* product selectively, and the asymmetric alkyne 1-phenyl-1-propyne gave (*E*)-1-phenyl-2-(triethylsilyl)propene as the major product (**Scheme 65**).<sup>[200]</sup>



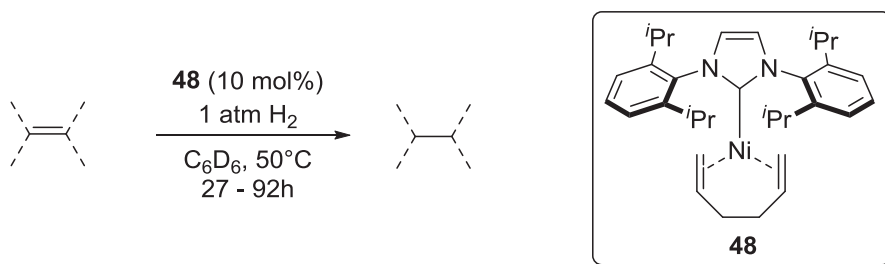
**Scheme 65.** Hydrosilylation of internal alkynes catalyzed by **46**

The chelate  $\pi$ -allyl complexes **47a,b** are efficient tools for the selective reduction of styrene and 4-methylstyrene in the presence of phenyl silane to obtain the Markovnikov addition product (**Scheme 66**).<sup>[201]</sup> Yields were moderate however. <sup>1</sup>H NMR monitoring of the reaction clearly showed several signals in the metal-hydride region, indicating the presence of Ni–H intermediates.



**Scheme 66.** Hydrosilylation of styrene derivatives catalyzed by **47a,b** and selectively yielding Markovnikov addition products

The thermally stable nickel(0) complex **48** can be notably used as a synthon to synthesize several Ni(0) and Ni(II) complexes.<sup>[202]</sup> Moreover it is active in the hydrogenation of several olefins (**Scheme 67**). Although relatively high pre-catalyst loadings were required, the reaction interestingly proceeded under only 1 atm of hydrogen at 50°C. The negative mercury test and the formation of hexane during the catalysis suggest the formation of a 12-electron Ni(0)–IPr active species.

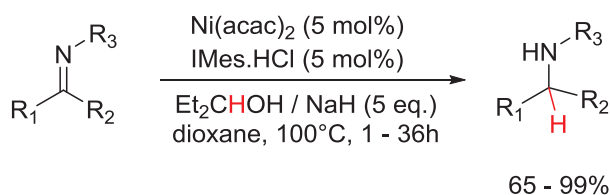


**Scheme 67.** Hydrogenation of simple alkenes catalyzed by **48**

#### II.4.3. Carbon–Heteroatom multiple bond reduction

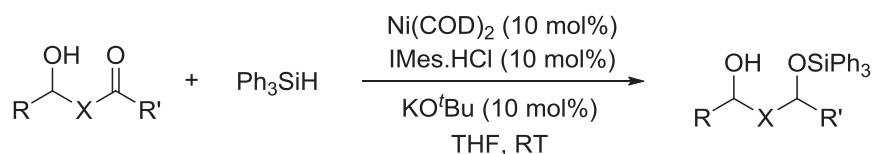
Fort's versatile catalytic Ni(0)–NHC (see *C–N couplings*, **Scheme 45** and *Dehalogenation reactions*, **Scheme 61**) system has also been successfully applied in the transfer hydrogenation of aldimines and ketimines.<sup>[203]</sup> Thus, the combination of Ni(acac)<sub>2</sub>, IMes.HCl and NaH allowed the reduction of a relatively broad range of imines in good to

excellent yields in the presence of NaOCH<sub>2</sub>Et<sub>2</sub> (**Scheme 68**), which is assumed to have a 3-fold role: (i) it could deprotonate IMes.HCl to form the free carbene, that would then coordinate to the nickel; (ii) it could activate NaH for the *in situ* reduction of Ni(II) into Ni(0); and (iii) it could act as an hydrogen-donor.



**Scheme 68.** Ni–NHC-catalyzed reduction of imines by transfer hydrogenation

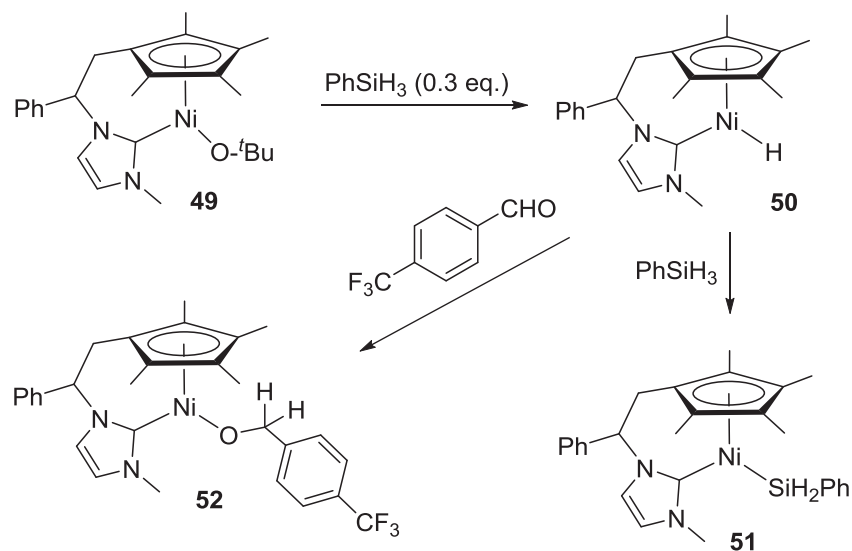
The reduction of C=O multiple bonds has also been targeted. Thus, a chemoselective method for the hydrosilylation of ketones has recently been developed, using Ni(COD)<sub>2</sub> and IMes.HCl with Ph<sub>3</sub>SiH. The most notable feature of this process is that free hydroxy groups are largely unaffected, thus providing an efficient one-step method for the conversion of these species to mono-protected diols, wherein the protecting group is exclusively installed on the ketone-derived hydroxyl group (**Scheme 69**).<sup>[204]</sup> Interestingly, the direct use of air-sensitive Ni(COD)<sub>2</sub> could be avoided by generating this complex *in situ* by reducing Ni(acac)<sub>2</sub> with DIBAL-H in the presence of cyclooctadiene.



**Scheme 69.** Chemoselective hydrosilylation of hydroxyketones

The use of the well-defined half-sandwich chelate complex **49** with PhSiH<sub>3</sub> allowed a significant improvement of the catalytic activity.<sup>[205]</sup> Thus, hydrosilylation of aldehydes and ketones was performed smoothly at 25°C with lower pre-catalyst loadings ranging between 0.5 and 2 mol%, and showed good functional group tolerance (although hydroxy groups were not tested). Reaction of **49** with 0.3 equiv. of PhSiH<sub>3</sub> led to the formation of the nickel-

hydride complex **50**. Further reaction of **50** with  $\text{PhSiH}_3$  yielded the diphenylsilyl complex **51**, and reaction with 4-trifluoromethylbenzaldehyde yielded the corresponding Ni–alkoxide insertion product **52** (**Scheme 70**). However, deuterium labeling studies indicated that the hydride ligand does not directly participate in the reduction reaction, thus ruling out the conventional hydride mechanism.<sup>[206]</sup>

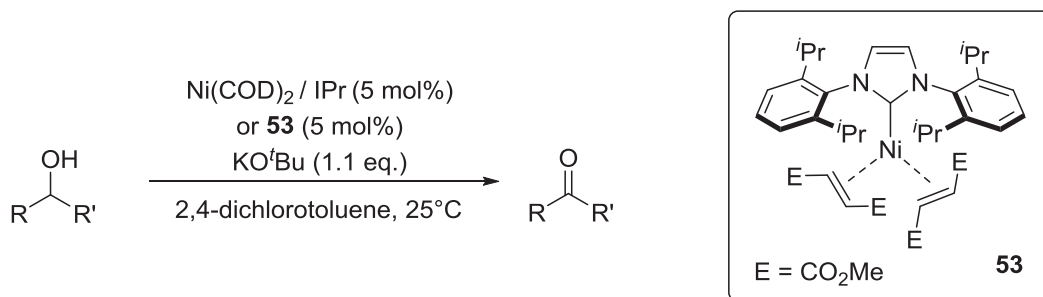


**Scheme 70.** Stoichiometric experiments

## II.5. Oxidation reactions

In 2009, Navarro started to study the catalytic oxidation of secondary alcohols catalyzed by a Ni–NHC complex *in situ* generated from equimolar amounts of  $\text{Ni}(\text{COD})_2$  and  $\text{IPr}\cdot\text{HCl}$  (see *Miscellaneous C–C bond formations*, **Scheme 42**).<sup>[167]</sup> Actually, this methodology refers to Fort's system employed for the dehalogenation of aryl halides, in which a secondary alcoholate is used as a hydrogen-donor to form the corresponding ketone as a by-product.<sup>[195]</sup> Thus, in the presence of chlorobenzene as an oxidant and  $\text{KO}^t\text{Bu}$  as a base, alcohols were converted in 17 to 26 h at  $60^\circ\text{C}$  to the corresponding ketones in good to excellent yields.<sup>[167]</sup> Secondary alcohols bearing an aryl group were mostly studied but the reaction was also efficient when using aliphatic secondary alcohols. However, primary alcohols were found to be unsuitable substrates. Of notable interest, this reaction can be performed under milder reaction conditions and in much shorter reaction times (15 - 120 min) by using dichlorotoluene as both the solvent and the oxidant (**Scheme 71**).<sup>[207]</sup> In addition, the

air-stable Ni(0) complex **53** was also shown to be active under these conditions. Although longer reaction times were required, it avoided the use of the highly air-sensitive and pyrophoric Ni(COD)<sub>2</sub> (**Scheme 71**).

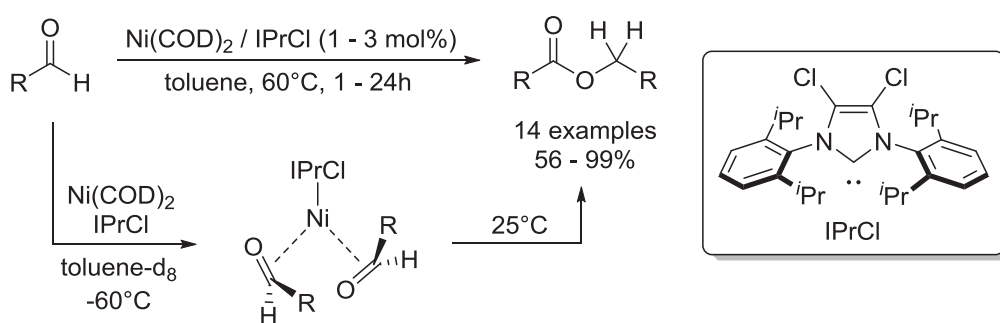


**Scheme 71.** Ni–NHC-catalyzed oxidation of secondary alcohols

In another context, a nickel-containing ionic liquid immobilized on mesoporous silica has been applied as heterogeneous catalyst for the oxidation of styrene with H<sub>2</sub>O<sub>2</sub> to produce benzaldehyde.<sup>[208]</sup> Interestingly, the reaction proceeded under solvent-free conditions, but a better activity was observed in acetonitrile. In both cases the method is very selective for the formation of benzaldehyde, and yields are among the highest reported in the literature (37% in CH<sub>3</sub>CN) with only *ca.* 0.4 mol% of nickel.

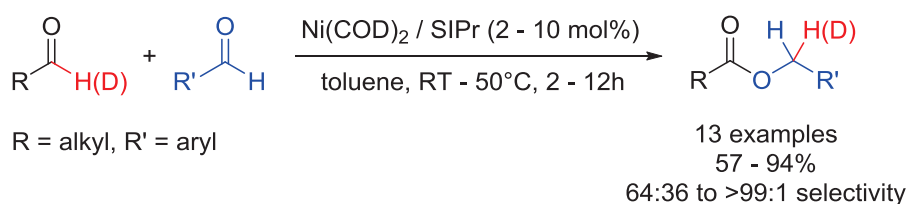
## II.6. Miscellaneous reactions

The use of an *in situ* generated Ni–NHC catalytic system has been successful in the Tischenko reaction.<sup>[209–211]</sup> Thus, the Ni(COD)<sub>2</sub>/IPrCl (1:1) catalyst was able to promote the homo-dimerization of (hetero)aryl and alkyl aldehydes in toluene at 60°C, in moderate to excellent yields (**Scheme 72**). Monitoring the reaction by <sup>1</sup>H NMR spectroscopy at –60°C showed the formation of a Ni(0)–IPrCl complex with two coordinated molecules of aldehydes, which probably acts as a key intermediate, as warming up the reaction to 25°C gave quantitatively the homo-dimer ester (**Scheme 72**).



**Scheme 72.** Ni–NHC-catalyzed Tischenko reaction yielding homo-dimer esters

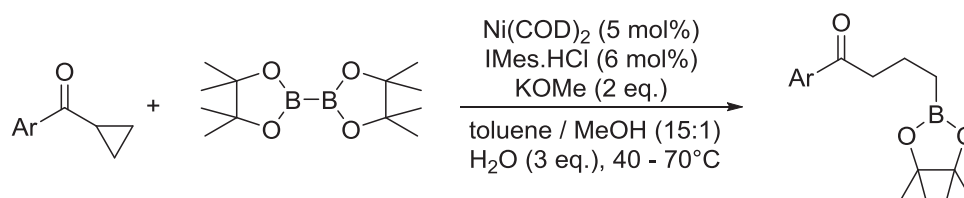
By a simple change of ligand, the methodology was notably extended to the crossed Tischenko reaction between an aryl aldehyde and an alkyl aldehyde (**Scheme 73**).<sup>[210]</sup> Thus, by using a Ni(COD)<sub>2</sub>/SIPr (1:1) catalyst, the corresponding cross-coupled esters were obtained under fairly mild reaction conditions. Mechanistic studies revealed that, as for the homo-dimerization of aldehydes, the active species might include two aldehyde molecules, and deuterium labeling experiments suggest that, from the two hydrogen atoms of the formed methylene function, one comes from the aryl aldehyde, and the other from the alkyl aldehyde (**Scheme 73**). The mechanism of this reaction has later been supported by DFT calculations, and mono-carbonyl activation, in which the carbonyl group of the alkyl aldehyde would be activated by oxidative addition, is likely to occur.<sup>[211]</sup>



**Scheme 73.** Ni–NHC-catalyzed Tischenko reaction yielding cross-coupled esters

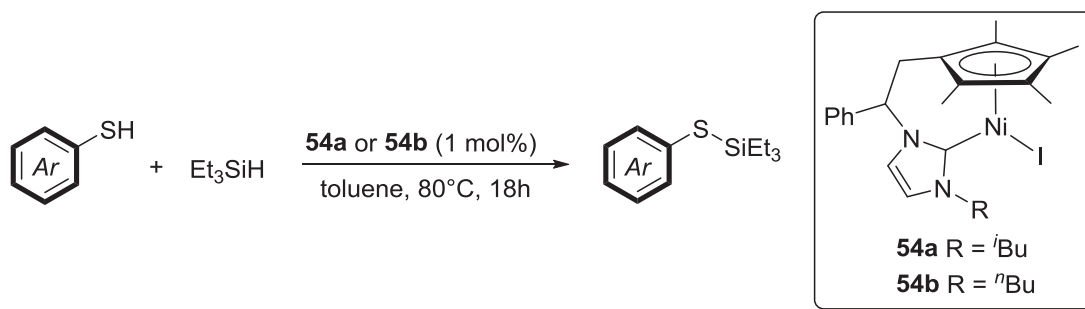
In a reaction similar to the rearrangement of vinylcyclopropanes, aryl cyclopropyl ketones were found to undergo a C–C cleavage of the cyclopropyl ring under Ni–NHC catalysis. In the presence of *bis*-(pinacolato)diboron, the borylative ring opening of the cyclopropyl aryl ketones efficiently occurred to yield 4-oxoalkylboronates in poor to excellent yields (**Scheme 74**). Importantly, aryl cyclopropyl ketones possessing an additional substituent on the cyclopropyl ring were used without notable decrease in selectivity, as the cleavage of

the C–C bond mainly takes place on the less sterically hindered side. It is noteworthy that the Ni(COD)<sub>2</sub>/IMes.HCl (1:1) catalyst gave superior results to the Pd(OAc)<sub>2</sub>/IMes (1:1) catalyst.



**Scheme 74.** Borylative ring-opening of aryl cyclopropyl ketones

Cyclopentadienyl-linked NHC complexes of nickel, that were described as efficient pre-catalysts for the hydrosilylation of aldehydes and ketones,<sup>[205]</sup> are also able to catalyze the dehydrogenative coupling of aromatic thiols with Et<sub>3</sub>SiH (**Scheme 75**).<sup>[212]</sup> Thus, using only 1 mol% of either complex **54a** or **54b** allowed the formation of the corresponding silylthioethers in moderate to excellent yields (60 - 96%). However, the use of alkyl- and benzylthiols resulted in an important decrease of activity.

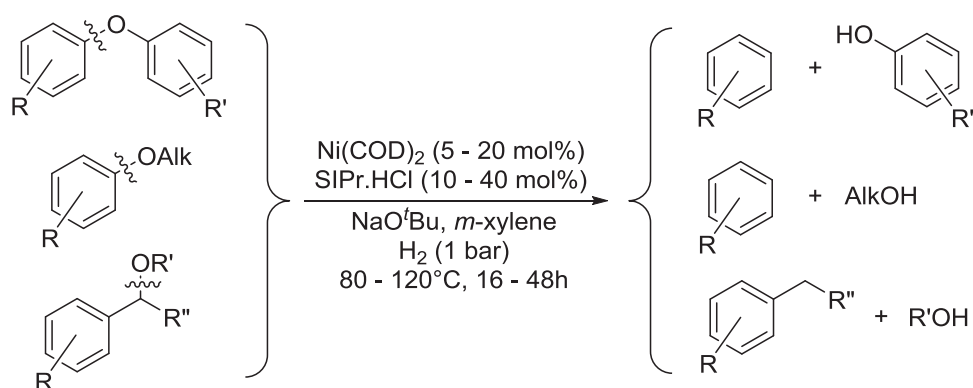


**Scheme 75.** Dehydrogenative coupling of aromatic thiols catalyzed by **54a,b**

Finally, probably the most elegant Ni–NHC-catalyzed process was described in 2011 for the hydrogenolysis of aryl ethers.<sup>[213]</sup> Thus, the use of a simple Ni(COD)<sub>2</sub>/SIPr.HCl (1:2) system impressively allowed the selective cleavage of aromatic C–O bonds in alkyl aryl, benzyl and diaryl ethers at "only" 80 to 120°C, under 1 bar of dihydrogen (**Scheme 76**). Indeed, this transformation usually required heterogeneous catalysts that operate at high temperature and pressure, resulting in the formation of products stemming from competing



hydrogenolysis of aliphatic C–O bonds and hydrogenation of the arene. Remarkably, in the case of unsymmetrical diaryl ethers, C–O cleavage occurred preferentially at the C–O bond adjacent to the more electron-poor aryl ring, while in the case of alkyl aryl ethers and benzyl ethers, hydrogenation selectively occurred at the C<sub>Ar</sub>–O bond and at the C<sub>benz</sub>–O bond, respectively. To rationalize the observed unprecedented selectivity and catalytic activity, the hydrogenolysis of diphenyl ether and 2-methoxynaphtalene was conducted in the presence of a 300-fold excess of elemental mercury with respect to the Ni catalyst. No decrease in product yields was observed. Thus, the homogeneous nature of the catalyst would be responsible for the relatively mild reaction conditions employed, and for the selectivities. This process is therefore of major importance for the conversion of oxygen-rich lignocellulosic plant biomass to deoxygenated fuels and commercial chemicals.



**Scheme 76.** Selective hydrogenolysis of aryl ethers

### III. Conclusions

Since the discovery of NHCs as powerful ligands for transition metal-catalyzed organic transformations, the field of nickel catalysis has increased exponentially. Over the last fifteen years, considerable efforts have been directed towards the development of Ni–NHC systems as cheaper alternatives to noble metal-based catalysts. Intensive work has impressively demonstrated a very broad scope of applicability of these Ni–NHC catalysts, as demonstrated by the number of topics discussed above. However, further contributions in ligand design, and scope applicability are still needed in order to valorize these systems, so that they will constitute not just cheap and *versatile* tools, but also *very efficient* tools for

catalysis. In this regard, the very recent Ni(COD)<sub>2</sub>/SIPr.HCl (1:2)-catalyzed selective hydrogenolysis of aryl ethers undoubtedly represents the most encouraging result (see *Miscellaneous reactions*). This example perfectly demonstrates the potential of these systems, which will probably become inescapable reagents for synthetic organic chemistry.

### IV. References

- [1] E. Buchner, L. Feldmann, *Berichte Dtsch. Chem. Ges.* **1903**, 36, 3509–3517.
- [2] H. Staudinger, O. Kupfer, *Berichte Dtsch. Chem. Ges.* **1912**, 45, 501–509.
- [3] W. von E. Doering, A. K. Hoffmann, *J. Am. Chem. Soc.* **1954**, 76, 6162–6165.
- [4] L. Chugaev and M. Skanavy-Grigorieva, *J. Russ. Chem. Soc.* **1915**, 47, 776.
- [5] G. Rouschias, B. L. Shaw, *J. Chem. Soc. Chem. Commun.* **1970**, 183–183.
- [6] A. Burke, A. L. Balch, J. H. Enemark, *J. Am. Chem. Soc.* **1970**, 92, 2555–2557.
- [7] E. O. Fischer, A. Massbol, *Angew. Chem. Int. Ed. Engl.* **1964**, 3, 580–581.
- [8] K. Öfele, *J. Organomet. Chem.* **1968**, 12, P42–P43.
- [9] H.-W. Wanzlick, H.-J. Schönherr, *Angew. Chem. Int. Ed. Engl.* **1968**, 7, 141–142.
- [10] D. J. Cardin, B. Cetinkaya, M. F. Lappert, L. Manojlović-Muir, K. W. Muir, *J. Chem. Soc. Chem. Commun.* **1971**, 400–401.
- [11] D. J. Cardin, B. Cetinkaya, M. F. Lappert, *Chem. Rev.* **1972**, 72, 545–574.
- [12] R. R. Schrock, *J. Am. Chem. Soc.* **1974**, 96, 6796–6797.
- [13] H. Tomioka, *Acc. Chem. Res.* **1997**, 30, 315–321.
- [14] A. Igau, H. Grutzmacher, A. Baceiredo, G. Bertrand, *J. Am. Chem. Soc.* **1988**, 110, 6463–6466.
- [15] A. J. Arduengo, R. L. Harlow, M. Kline, *J. Am. Chem. Soc.* **1991**, 113, 361–363.
- [16] Y. Canac, S. Conejero, B. Donnadieu, W. W. Schoeller, G. Bertrand, *J. Am. Chem. Soc.* **2005**, 127, 7312–7313.
- [17] D. Bourissou, G. Bertrand, in *Adv. Organomet. Chem.* (Ed.: Robert West and Anthony F. Hill), Academic Press, **1999**, pp. 175–219.
- [18] Y. Canac, M. Soleilhavoup, S. Conejero, G. Bertrand, *J. Organomet. Chem.* **2004**, 689, 3857–3865.
- [19] S. Goumri-Magnet, O. Polishchuk, H. Gornitzka, C. J. Marsden, A. Baceiredo, G. Bertrand, *Angew. Chem. Int. Ed.* **1999**, 38, 3727–3729.

- [20] V. Lavallo, Y. Canac, B. Donnadieu, W. W. Schoeller, G. Bertrand, *Angew. Chem. Int. Ed.* **2006**, *45*, 3488–3491.
- [21] G. D. Frey, V. Lavallo, B. Donnadieu, W. W. Schoeller, G. Bertrand, *Science* **2007**, *316*, 439–441.
- [22] C. Heinemann, T. Müller, Y. Apeloig, H. Schwarz, *J. Am. Chem. Soc.* **1996**, *118*, 2023–2038.
- [23] C. Boehme, G. Frenking, *J. Am. Chem. Soc.* **1996**, *118*, 2039–2046.
- [24] T. W. Hudnall, C. W. Bielawski, *J. Am. Chem. Soc.* **2009**, *131*, 16039–16041.
- [25] U. Siemeling, C. Färber, C. Bruhn, M. Leibold, D. Selent, W. Baumann, M. von Hopffgarten, C. Goedecke, G. Frenking, *Chem. Sci.* **2010**, *1*, 697–704.
- [26] D. Bourissou, O. Guerret, F. P. Gabbaï, G. Bertrand, *Chem. Rev.* **2000**, *100*, 39–92.
- [27] L. Cavallo, A. Correa, C. Costabile, H. Jacobsen, *J. Organomet. Chem.* **2005**, *690*, 5407–5413.
- [28] S. Díez-González, S. P. Nolan, *Coord. Chem. Rev.* **2007**, *251*, 874–883.
- [29] H. Jacobsen, A. Correa, A. Poater, C. Costabile, L. Cavallo, *Coord. Chem. Rev.* **2009**, *253*, 687–703.
- [30] U. Radius, F. M. Bickelhaupt, *Coord. Chem. Rev.* **2009**, *253*, 678–686.
- [31] D. G. Gusev, *Organometallics* **2009**, *28*, 6458–6461.
- [32] D. G. Gusev, E. Peris, *Dalton Trans.* **2013**, *42*, 7359–7364.
- [33] D. J. Nelson, S. P. Nolan, *Chem. Soc. Rev.* **2013**, *42*, 6723–6753.
- [34] R. H. Crabtree, *J. Organomet. Chem.* **2005**, *690*, 5451–5457.
- [35] L. Benhamou, E. Chardon, G. Lavigne, S. Bellemin-Laponnaz, V. César, *Chem. Rev.* **2011**, *111*, 2705–2733.
- [36] D. Enders, K. Breuer, G. Raabe, J. Runsink, J. H. Teles, J.-P. Melder, K. Ebel, S. Brode, *Angew. Chem. Int. Ed. Engl.* **1995**, *34*, 1021–1023.
- [37] O. Coulembier, B. G. G. Lohmeijer, A. P. Dove, R. C. Pratt, L. Mespouille, D. A. Culkin, S. J. Benight, P. Dubois, R. M. Waymouth, J. L. Hedrick, *Macromolecules* **2006**, *39*, 5617–5628.
- [38] A. M. Voutchkova, M. Feliz, E. Clot, O. Eisenstein, R. H. Crabtree, *J. Am. Chem. Soc.* **2007**, *129*, 12834–12846.
- [39] H. A. Duong, T. N. Tekavec, A. M. Arif, J. Louie, *Chem. Commun.* **2004**, 112–113.
- [40] M. Smiglak, C. C. Hines, R. D. Rogers, *Green Chem.* **2010**, *12*, 491–501.

- [41] M. Fèvre, J. Pinaud, A. Leteneur, Y. Gnanou, J. Vignolle, D. Taton, K. Miqueu, J.-M. Sotiropoulos, *J. Am. Chem. Soc.* **2012**, *134*, 6776–6784.
- [42] B. C. Norris, D. G. Sheppard, G. Henkelman, C. W. Bielawski, *J. Org. Chem.* **2011**, *76*, 301–304.
- [43] H.-W. Wanzlick, F. Esser, H.-J. Kleiner, *Chem. Ber.* **1963**, *96*, 1208–1212.
- [44] M. Scholl, S. Ding, C. W. Lee, R. H. Grubbs, *Org. Lett.* **1999**, *1*, 953–956.
- [45] O. Coulembier, A. P. Dove, R. C. Pratt, A. C. Sentman, D. A. Culkin, L. Mespouille, P. Dubois, R. M. Waymouth, J. L. Hedrick, *Angew. Chem. Int. Ed.* **2005**, *44*, 4964–4968.
- [46] A. P. Blum, T. Ritter, R. H. Grubbs, *Organometallics* **2007**, *26*, 2122–2124.
- [47] G. W. Nyce, S. Csihony, R. M. Waymouth, J. L. Hedrick, *Chem. Eur. J.* **2004**, *10*, 4073–4079.
- [48] T. M. Trnka, J. P. Morgan, M. S. Sanford, T. E. Wilhelm, M. Scholl, T.-L. Choi, S. Ding, M. W. Day, R. H. Grubbs, *J. Am. Chem. Soc.* **2003**, *125*, 2546–2558.
- [49] I. J. B. Lin, C. S. Vasam, *Coord. Chem. Rev.* **2007**, *251*, 642–670.
- [50] W. A. Herrmann, M. Elison, J. Fischer, C. Köcher, G. R. J. Artus, *Angew. Chem. Int. Ed. Engl.* **1995**, *34*, 2371–2374.
- [51] M. Scholl, T. M. Trnka, J. P. Morgan, R. H. Grubbs, *Tetrahedron Lett.* **1999**, *40*, 2247–2250.
- [52] R. H. Grubbs, *Angew. Chem. Int. Ed.* **2006**, *45*, 3760–3765.
- [53] T. Weskamp, F. J. Kohl, W. Hieringer, D. Gleich, W. A. Herrmann, *Angew. Chem. Int. Ed.* **1999**, *38*, 2416–2419.
- [54] W. A. Herrmann, *Angew. Chem. Int. Ed.* **2002**, *41*, 1290–1309.
- [55] E. Peris, R. H. Crabtree, *Coord. Chem. Rev.* **2004**, *248*, 2239–2246.
- [56] J. A. Mata, M. Poyatos, E. Peris, *Coord. Chem. Rev.* **2007**, *251*, 841–859.
- [57] W. J. Sommer, M. Weck, *Coord. Chem. Rev.* **2007**, *251*, 860–873.
- [58] E. A. B. Kantchev, C. J. O'Brien, M. G. Organ, *Angew. Chem. Int. Ed.* **2007**, *46*, 2768–2813.
- [59] N. Marion, S. Díez-González, S. P. Nolan, *Angew. Chem. Int. Ed.* **2007**, *46*, 2988–3000.
- [60] S. Díez-González, N. Marion, S. P. Nolan, *Chem. Rev.* **2009**, *109*, 3612–3676.
- [61] M. Poyatos, J. A. Mata, E. Peris, *Chem. Rev.* **2009**, *109*, 3677–3707.

- [62] C. Valente, S. Çalimsiz, K. H. Hoi, D. Mallick, M. Sayah, M. G. Organ, *Angew. Chem. Int. Ed.* **2012**, *51*, 3314–3332.
- [63] K. V. S. Ranganath, S. Onitsuka, A. K. Kumar, J. Inanaga, *Catal. Sci. Technol.* **2013**, *3*, 2161–2181.
- [64] K. Ziegler, E. Holzkamp, H. Breil, H. Martin, *Angew. Chem.* **1955**, *67*, 541–547.
- [65] Y. Fort, C. Comoy, in *N-Heterocycl. Carbenes* (Ed.: S. Díez-González), Royal Society Of Chemistry, Cambridge, **2010**, pp. 284–326.
- [66] S. Gu, P. Ni, W. Chen, *Chin. J. Catal.* **2010**, *31*, 875–886.
- [67] S. P. Nolan, *N-Heterocyclic Carbenes in Synthesis*, Wiley-VCH; John Wiley, Weinheim; Chichester, **2006**.
- [68] K. Tamao, K. Sumitani, M. Kumada, *J. Am. Chem. Soc.* **1972**, *94*, 4374–4376.
- [69] R. J. P. Corriu, J. P. Masse, *J. Chem. Soc., Chem. Commun.* **1972**, 144a–144a.
- [70] V. P. W. Böhm, T. Weskamp, C. W. K. Gstöttmayr, W. A. Herrmann, *Angew. Chem. Int. Ed.* **2000**, *39*, 1602–1604.
- [71] C.-B. Kim, H. Jo, B.-K. Ahn, C. K. Kim, K. Park, *J. Org. Chem.* **2009**, *74*, 9566–9569.
- [72] H.-J. Jo, C.-B. Kim, T.-Y. Ryoo, B.-K. Ahn, K.-Y. Park, *Bull. Korean Chem. Soc.* **2010**, *31*, 3749–3754.
- [73] V. P. W. Böhm, C. W. K. Gstöttmayr, T. Weskamp, W. A. Herrmann, *Angew. Chem. Int. Ed.* **2001**, *40*, 3387–3389.
- [74] K. Mitsudo, Y. Doi, S. Sakamoto, H. Murakami, H. Mandai, S. Suga, *Chem. Lett.* **2011**, *40*, 936–938.
- [75] J. Wolf, A. Labande, M. Natella, J.-C. Daran, R. Poli, *J. Mol. Catal. Chem.* **2006**, *259*, 205–212.
- [76] J. Wolf, A. Labande, J.-C. Daran, R. Poli, *J. Organomet. Chem.* **2006**, *691*, 433–443.
- [77] Y.-C. Xu, J. Zhang, H.-M. Sun, Q. Shen, Y. Zhang, *Dalton Trans.* **2013**, *42*, 8437–8445.
- [78] T. Hatakeyama, S. Hashimoto, K. Ishizuka, M. Nakamura, *J. Am. Chem. Soc.* **2009**, *131*, 11949–11963.
- [79] N. Şahin, D. Sémeril, E. Brenner, D. Matt, İ. Özdemir, C. Kaya, L. Toupet, *Eur. J. Org. Chem.* **2013**, *2013*, 4443–4449.
- [80] A. Joshi-Pangu, M. R. Biscoe, *Synlett* **2012**, *23*, 1103–1107.
- [81] C. Lohre, T. Dröge, C. Wang, F. Glorius, *Chem. Eur. J.* **2011**, *17*, 6052–6055.

- [82] A. Joshi-Pangu, C.-Y. Wang, M. R. Biscoe, *J. Am. Chem. Soc.* **2011**, *133*, 8478–8481.
- [83] A. S. Kashin, V. P. Ananikov, *J. Org. Chem.* **2013**, *78*, 11117–11125.
- [84] D. Kremzow, G. Seidel, C. W. Lehmann, A. Fürstner, *Chem. Eur. J.* **2005**, *11*, 1833–1853.
- [85] S. K. Schneider, C. F. Rentzsch, A. Krüger, H. G. Raubenheimer, W. A. Herrmann, *J. Mol. Catal. A* **2007**, *265*, 50–58.
- [86] K. Matsubara, K. Ueno, Y. Shibata, *Organometallics* **2006**, *25*, 3422–3427.
- [87] S. Miyazaki, Y. Koga, T. Matsumoto, K. Matsubara, *Chem. Commun.* **2010**, *46*, 1932–1934.
- [88] K. Zhang, M. Conda-Sheridan, S. R. Cooke, J. Louie, *Organometallics* **2011**, *30*, 2546–2552.
- [89] S. Nagao, T. Matsumoto, Y. Koga, K. Matsubara, *Chem. Lett.* **2011**, *40*, 1036–1038.
- [90] M. J. Page, W. Y. Lu, R. C. Poulten, E. Carter, A. G. Algarra, B. M. Kariuki, S. A. Macgregor, M. F. Mahon, K. J. Cavell, D. M. Murphy, M. K. Whittlesey, *Chem. Eur. J.* **2013**, *19*, 2158–2167.
- [91] R. Jothibasu, K.-W. Huang, H. V. Huynh, *Organometallics* **2010**, *29*, 3746–3752.
- [92] M. J. Iglesias, A. Prieto, M. C. Nicasio, *Org. Lett.* **2012**, *14*, 4318–4321.
- [93] M. J. Iglesias, A. Prieto, M. C. Nicasio, *Adv. Synth. Catal.* **2010**, *352*, 1949–1954.
- [94] N. Marion, O. Navarro, J. Mei, E. D. Stevens, N. M. Scott, S. P. Nolan, *J. Am. Chem. Soc.* **2006**, *128*, 4101–4111.
- [95] O. Navarro, N. Marion, J. Mei, S. P. Nolan, *Chem. Eur. J.* **2006**, *12*, 5142–5148.
- [96] A. G. Tennyson, V. M. Lynch, C. W. Bielawski, *J. Am. Chem. Soc.* **2010**, *132*, 9420–9429.
- [97] Z. Xi, B. Liu, W. Chen, *J. Org. Chem.* **2008**, *73*, 3954–3957.
- [98] S. Gu, W. Chen, *Organometallics* **2009**, *28*, 909–914.
- [99] C. Chen, H. Qiu, W. Chen, *J. Organomet. Chem.* **2012**, *696*, 4166–4172.
- [100] J. Berding, T. F. van Dijkman, M. Lutz, A. L. Spek, E. Bouwman, *Dalton Trans.* **2009**, 6948–6955.
- [101] F. Li, J. J. Hu, L. L. Koh, T. S. A. Hor, *Dalton Trans.* **2010**, *39*, 5231–5241.
- [102] C. Zhang, Z.-X. Wang, *Organometallics* **2009**, *28*, 6507–6514.
- [103] Y. Zhou, Z. Xi, W. Chen, D. Wang, *Organometallics* **2008**, *27*, 5911–5920.

- [104] J. Guo, L. Lv, X. Wang, C. Cao, G. Pang, Y. Shi, *Inorg. Chem. Commun.* **2013**, *31*, 74–78.
- [105] J. Berding, M. Lutz, A. L. Spek, E. Bouwman, *Organometallics* **2009**, *28*, 1845–1854.
- [106] H. Vinh Huynh, R. Jothibas, *Eur. J. Inorg. Chem.* **2009**, 2009, 1926–1931.
- [107] J.-F. Soulé, H. Miyamura, S. Kobayashi, *J. Am. Chem. Soc.* **2013**, *135*, 10602–10605.
- [108] N. Miya, K. Yamada, A. Suzuki, *Tetrahedron Lett.* **1979**, *20*, 3437–3440.
- [109] N. Miya, A. Suzuki, *J. Chem. Soc., Chem. Commun.* **1979**, 866–867.
- [110] S. B. Blakey, D. W. C. MacMillan, *J. Am. Chem. Soc.* **2003**, *125*, 6046–6047.
- [111] J. Liu, M. J. Robins, *Org. Lett.* **2004**, *6*, 3421–3423.
- [112] J. Liu, M. J. Robins, *Org. Lett.* **2005**, *7*, 1149–1151.
- [113] M. R. Harris, L. E. Hanna, M. A. Greene, C. E. Moore, E. R. Jarvo, *J. Am. Chem. Soc.* **2013**, *135*, 3303–3306.
- [114] C. Zhong, T. Sasaki, M. Tada, Y. Iwasawa, *J. Catal.* **2006**, *242*, 357–364.
- [115] D. S. McGuinness, K. J. Cavell, B. W. Skelton, A. H. White, *Organometallics* **1999**, *18*, 1596–1605.
- [116] V. Ritleng, A. M. Oertel, M. J. Chetcuti, *Dalton Trans.* **2010**, *39*, 8153–8160.
- [117] A. M. Oertel, V. Ritleng, L. Burr, M. J. Chetcuti, *Organometallics* **2011**, *30*, 6685–6691.
- [118] A. M. Oertel, V. Ritleng, M. J. Chetcuti, *Organometallics* **2012**, *31*, 2829–2840.
- [119] W. Buchowicz, Ł. Banach, J. Conder, P. A. Guńka, D. Kubicki, P. Buchalski, *Dalton Trans.* **2014**, *43*, 5847–5857.
- [120] P. L. Chiu, C.-L. Lai, C.-F. Chang, C.-H. Hu, H. M. Lee, *Organometallics* **2005**, *24*, 6169–6178.
- [121] Z. Xi, X. Zhang, W. Chen, S. Fu, D. Wang, *Organometallics* **2007**, *26*, 6636–6642.
- [122] K. Inamoto, J. Kuroda, K. Hiroya, Y. Noda, M. Watanabe, T. Sakamoto, *Organometallics* **2006**, *25*, 3095–3098.
- [123] K. Inamoto, J. Kuroda, E. Kwon, K. Hiroya, T. Doi, *J. Organomet. Chem.* **2009**, *694*, 389–396.
- [124] J. Kuroda, K. Inamoto, K. Hiroya, T. Doi, *Eur. J. Org. Chem.* **2009**, 2009, 2251–2261.
- [125] T. Tu, H. Mao, C. Herbert, M. Xu, K. H. Dötz, *Chem. Commun.* **2010**, *46*, 7796–7798.
- [126] M. Xu, X. Li, Z. Sun, T. Tu, *Chem. Commun.* **2013**, *49*, 11539–11541.
- [127] C.-C. Lee, W.-C. Ke, K.-T. Chan, C.-L. Lai, C.-H. Hu, H. M. Lee, *Chem. Eur. J.* **2007**, *13*, 582–591.



- [128] C.-Y. Liao, K.-T. Chan, Y.-C. Chang, C.-Y. Chen, C.-Y. Tu, C.-H. Hu, H. M. Lee, *Organometallics* **2007**, *26*, 5826–5833.
- [129] T. A. P. Paulose, S.-C. Wu, J. A. Olson, T. Chau, N. Theaker, M. Hassler, J. W. Quail, S. R. Foley, *Dalton Trans.* **2012**, *41*, 251–260.
- [130] N. E. Leadbeater, M. Marco, *J. Org. Chem.* **2003**, *68*, 5660–5667.
- [131] R. K. Arvela, N. E. Leadbeater, M. S. Sangi, V. A. Williams, P. Granados, R. D. Singer, *J. Org. Chem.* **2005**, *70*, 161–168.
- [132] T. Zell, M. Feierabend, B. Halfter, U. Radius, *J. Organomet. Chem.* **2011**, *696*, 1380–1387.
- [133] T. Schaub, M. Backes, U. Radius, *J. Am. Chem. Soc.* **2006**, *128*, 15964–15965.
- [134] T. Mizoroki, K. Mori, A. Ozaki, *Bull. Chem. Soc. Jpn.* **1971**, *44*, 581–581.
- [135] R. F. Heck, J. P. Nolley, *J. Org. Chem.* **1972**, *37*, 2320–2322.
- [136] K. Inamoto, J. Kuroda, T. Danjo, T. Sakamoto, *Synlett* **2005**, 1624–1626.
- [137] A. O. King, N. Okukado, E. Negishi, *J. Chem. Soc., Chem. Commun.* **1977**, 683–684.
- [138] V. B. Phapale, D. J. Cárdenas, *Chem. Soc. Rev.* **2009**, *38*, 1598–1607.
- [139] Z. Xi, Y. Zhou, W. Chen, *J. Org. Chem.* **2008**, *73*, 8497–8501.
- [140] F. Ullmann, J. Bielecki, *Berichte Dtsch. Chem. Ges.* **1901**, *34*, 2174–2185.
- [141] H. V. Huynh, L. R. Wong, P. S. Ng, *Organometallics* **2008**, *27*, 2231–2237.
- [142] N. Ding, J. Zhang, T. S. A. Hor, *Dalton Trans.* **2009**, 1853–1858.
- [143] K. C. Mondal, P. P. Samuel, Y. Li, H. W. Roesky, S. Roy, L. Ackermann, N. S. Sidhu, G. M. Sheldrick, E. Carl, S. Demeshko, S. De, P. Parameswaran, L. Ungur, L. F. Chibotaru, D. M. Andrada, *Eur. J. Inorg. Chem.* **2014**, *2014*, 818–823.
- [144] A. Leleu, Y. Fort, R. Schneider, *Adv. Synth. Catal.* **2006**, *348*, 1086–1092.
- [145] G. Manolikakes, N. Dastbaravardeh, P. Knochel, *Synlett* **2007**, *2007*, 2077–2080.
- [146] E. Wenkert, T. W. Ferreira, E. L. Michelotti, *J. Chem. Soc., Chem. Commun.* **1979**, 637–638.
- [147] H. Takei, M. Miura, H. Sugimura, H. Okamura, *Chem. Lett.* **1979**, *8*, 1447–1450.
- [148] K. Ishizuka, H. Seike, T. Hatakeyama, M. Nakamura, *J. Am. Chem. Soc.* **2010**, *132*, 13117–13119.
- [149] L. Hintermann, M. Schmitz, Y. Chen, *Adv. Synth. Catal.* **2010**, *352*, 2411–2415.
- [150] J. Cornella, R. Martin, *Org. Lett.* **2013**, *15*, 6298–6301.
- [151] C.-Y. Ho, L. He, *Angew. Chem. Int. Ed.* **2010**, *49*, 9182–9186.



- [152] C.-Y. Ho, L. He, *Chem. Commun.* **2012**, 48, 1481–1483.
- [153] Y. Nakao, Y. Yamada, N. Kashiwara, T. Hiyama, *J. Am. Chem. Soc.* **2010**, 132, 13666–13668.
- [154] R. Tamura, Y. Yamada, Y. Nakao, T. Hiyama, *Angew. Chem. Int. Ed.* **2012**, 51, 5679–5682.
- [155] C.-C. Tsai, W.-C. Shih, C.-H. Fang, C.-Y. Li, T.-G. Ong, G. P. A. Yap, *J. Am. Chem. Soc.* **2010**, 132, 11887–11889.
- [156] W.-C. Shih, W.-C. Chen, Y.-C. Lai, M.-S. Yu, J.-J. Ho, G. P. A. Yap, T.-G. Ong, *Org. Lett.* **2012**, 14, 2046–2049.
- [157] W.-C. Lee, C.-H. Wang, Y.-H. Lin, W.-C. Shih, T.-G. Ong, *Org. Lett.* **2013**, 15, 5358–5361.
- [158] C.-Y. Ho, *Chem. Commun.* **2010**, 46, 466–468.
- [159] Y. Miyazaki, Y. Yamada, Y. Nakao, T. Hiyama, *Chem. Lett.* **2012**, 41, 298–300.
- [160] Y. Hoshimoto, Y. Hayashi, H. Suzuki, M. Ohashi, S. Ogoshi, *Angew. Chem. Int. Ed.* **2012**, 51, 10812–10815.
- [161] K. D. Schleicher, T. F. Jamison, *Org. Lett.* **2007**, 9, 875–878.
- [162] M. K. Samantaray, M. M. Shaikh, P. Ghosh, *Organometallics* **2009**, 28, 2267–2275.
- [163] S. Ray, M. M. Shaikh, P. Ghosh, *Eur. J. Inorg. Chem.* **2009**, 1932–1941.
- [164] S. Kumar, A. Narayanan, M. N. Rao, M. M. Shaikh, P. Ghosh, *J. Organomet. Chem.* **2012**, 696, 4159–4165.
- [165] K. Matsubara, K. Ueno, Y. Koga, K. Hara, *J. Org. Chem.* **2007**, 72, 5069–5076.
- [166] G. Huang, H. Sun, X. Qiu, Y. Shen, J. Jiang, L. Wang, *J. Organomet. Chem.* **2011**, 696, 2949–2957.
- [167] C. Berini, D. F. Brayton, C. Mocka, O. Navarro, *Org. Lett.* **2009**, 11, 4244–4247.
- [168] J. Bouffard, K. Itami, *Org. Lett.* **2009**, 11, 4410–4413.
- [169] T. Maekawa, H. Sekizawa, K. Itami, *Angew. Chem. Int. Ed.* **2011**, 50, 7022–7026.
- [170] C. Berini, O. Navarro, *Chem. Commun.* **2012**, 48, 1538–1540.
- [171] T. Schaub, M. Backes, U. Radius, *Organometallics* **2006**, 25, 4196–4206.
- [172] S. Tamba, K. Shono, A. Sugie, A. Mori, *J. Am. Chem. Soc.* **2011**, 133, 9700–9703.
- [173] S. Tanaka, G. Tatsuta, A. Sugie, A. Mori, *Tetrahedron Lett.* **2013**, 54, 1976–1979.
- [174] S. Tamba, Y. Okubo, A. Sugie, A. Mori, *Polym. J.* **2012**, 44, 1209–1213.
- [175] B. Gradel, E. Brenner, R. Schneider, Y. Fort, *Tetrahedron Lett.* **2001**, 42, 5689–5692.
- [176] C. Desmarets, R. Schneider, Y. Fort, *J. Org. Chem.* **2002**, 67, 3029–3036.

- [177] R. Omar-Amrani, A. Thomas, E. Brenner, R. Schneider, Y. Fort, *Org. Lett.* **2003**, *5*, 2311–2314.
- [178] W. Wu, X.-H. Fan, L.-P. Zhang, L.-M. Yang, *RSC Adv.* **2014**, *4*, 3364–3367.
- [179] T. Shimasaki, M. Tobisu, N. Chatani, *Angew. Chem. Int. Ed.* **2010**, *49*, 2929–2932.
- [180] S. D. Ramgren, A. L. Silberstein, Y. Yang, N. K. Garg, *Angew. Chem. Int. Ed.* **2011**, *50*, 2171–2173.
- [181] C. Chen, L.-M. Yang, *J. Org. Chem.* **2007**, *72*, 6324–6327.
- [182] X.-H. Fan, G. Li, L.-M. Yang, *J. Organomet. Chem.* **2011**, *696*, 2482–2484.
- [183] C.-Y. Gao, L.-M. Yang, *J. Org. Chem.* **2008**, *73*, 1624–1627.
- [184] J.-H. Huang, L.-M. Yang, *Org. Lett.* **2011**, *13*, 3750–3753.
- [185] K. Matsubara, S. Miyazaki, Y. Koga, Y. Nibu, T. Hashimura, T. Matsumoto, *Organometallics* **2008**, *27*, 6020–6024.
- [186] R. A. Kelly III, N. M. Scott, S. Díez-González, E. D. Stevens, S. P. Nolan, *Organometallics* **2005**, *24*, 3442–3447.
- [187] A. R. Martin, Y. Makida, S. Meiries, A. M. Z. Slawin, S. P. Nolan, *Organometallics* **2013**, *32*, 6265–6270.
- [188] A. R. Martin, D. J. Nelson, S. Meiries, A. M. Z. Slawin, S. P. Nolan, *Eur. J. Org. Chem.* **2014**, DOI: 10.1002/ejoc.201402022.
- [189] M. J. Iglesias, J. F. Blandez, M. R. Fructos, A. Prieto, E. Álvarez, T. R. Belderrain, M. C. Nicasio, *Organometallics* **2012**, *31*, 6312–6316.
- [190] C. Dash, M. M. Shaikh, R. J. Butcher, P. Ghosh, *Dalton Trans.* **2010**, *39*, 2515–2524.
- [191] Y. Zhang, K. C. Ngeow, J. Y. Ying, *Org. Lett.* **2007**, *9*, 3495–3498.
- [192] P. Guan, C. Cao, Y. Liu, Y. Li, P. He, Q. Chen, G. Liu, Y. Shi, *Tetrahedron Lett.* **2012**, *53*, 5987–5992.
- [193] H.-J. Yoon, J.-W. Choi, H. Kang, T. Kang, S.-M. Lee, B.-H. Jun, Y.-S. Lee, *Synlett* **2010**, 2518–2522.
- [194] D. A. Malyshev, N. M. Scott, N. Marion, E. D. Stevens, V. P. Ananikov, I. P. Beletskaya, S. P. Nolan, *Organometallics* **2006**, *25*, 4462–4470.
- [195] C. Desmarets, S. Kuhl, R. Schneider, Y. Fort, *Organometallics* **2002**, *21*, 1554–1559.
- [196] S. Kuhl, R. Schneider, Y. Fort, *Adv. Synth. Catal.* **2003**, *345*, 341–344.
- [197] C. J. E. Davies, M. J. Page, C. E. Ellul, M. F. Mahon, M. K. Whittlesey, *Chem. Commun.* **2010**, *46*, 5151–5153.

- [198] M. R. Chaulagain, G. M. Mahandru, J. Montgomery, *Tetrahedron* **2006**, *62*, 7560–7566.
- [199] Z. D. Miller, W. Li, T. R. Belderrain, J. Montgomery, *J. Am. Chem. Soc.* **2013**, *135*, 15282–15285.
- [200] J. Berding, J. A. van Paridon, V. H. S. van Rixel, E. Bouwman, *Eur. J. Inorg. Chem.* **2011**, *2011*, 2450–2458.
- [201] L. Benítez Junquera, M. C. Puerta, P. Valerga, *Organometallics* **2012**, *31*, 2175–2183.
- [202] J. Wu, J. W. Faller, N. Hazari, T. J. Schmeier, *Organometallics* **2012**, *31*, 806–809.
- [203] S. Kuhl, R. Schneider, Y. Fort, *Organometallics* **2003**, *22*, 4184–4186.
- [204] M. L. Lage, S. J. Bader, K. Sa-ei, J. Montgomery, *Tetrahedron* **2013**, *69*, 5609–5613.
- [205] L. Postigo, B. Royo, *Adv. Synth. Catal.* **2012**, *354*, 2613–2618.
- [206] O. G. Shirobokov, L. G. Kuzmina, G. I. Nikonov, *J. Am. Chem. Soc.* **2011**, *133*, 6487–6489.
- [207] C. Berini, O. H. Winkelmann, J. Otten, D. A. Vicic, O. Navarro, *Chem. Eur. J.* **2010**, *16*, 6857–6860.
- [208] G. Liu, M. Hou, J. Song, Z. Zhang, T. Wu, B. Han, *J. Mol. Catal. A* **2010**, *316*, 90–94.
- [209] S. Ogoshi, Y. Hoshimoto, M. Ohashi, *Chem. Commun.* **2010**, *46*, 3354–3356.
- [210] Y. Hoshimoto, M. Ohashi, S. Ogoshi, *J. Am. Chem. Soc.* **2011**, *133*, 4668–4671.
- [211] H. Yu, Y. Fu, *Chem. Eur. J.* **2012**, *18*, 16765–16773.
- [212] L. Postigo, R. Lopes, B. Royo, *Dalton Trans.* **2014**, *43*, 853–858.
- [213] A. G. Sergeev, J. F. Hartwig, *Science* **2011**, *332*, 439–443.

## **Chapter II.**

**From acetone metalation to the catalytic  
 $\alpha$ -arylation of acyclic ketones with  
*N*-heterocyclic carbene–nickel(II) complexes**



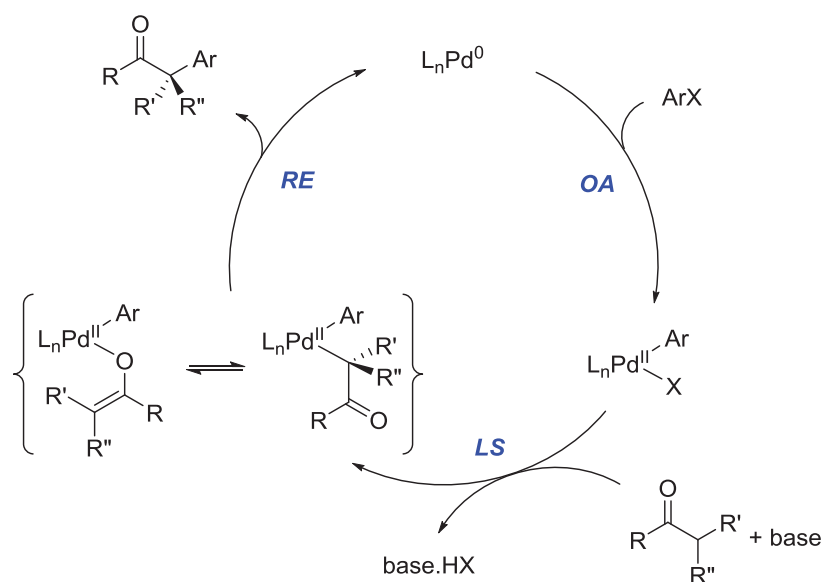
# Chapter II.

## From acetone metalation to the catalytic $\alpha$ -arylation of acyclic ketones with *N*-heterocyclic carbene–nickel(II) complexes

<b>I.</b>	<b>Introduction .....</b>	<b>70</b>
<b>II.</b>	<b>Results and Discussion .....</b>	<b>73</b>
II.1.	Choice and syntheses of the pre-catalysts .....	73
II.2.	Optimization of the catalytic conditions.....	75
II.3.	Reaction scope study .....	76
II.4.	Mechanistic studies .....	79
<b>III.</b>	<b>Conclusion .....</b>	<b>84</b>
<b>IV.</b>	<b>Experimental section .....</b>	<b>84</b>
IV.1.	General information.....	84
IV.2.	Synthesis of [Ni(IPr)(NCMe)Cp](PF <sub>6</sub> ) (8).....	85
IV.3.	Synthesis of [Ni(IMes){CH(CH <sub>3</sub> )C(O)Ph}Cp] (10) .....	86
IV.4.	Synthesis of [Ni(IMes)PhCp] (11) .....	86
IV.5.	X-ray diffraction study of (8) and (11): structure determination and refinement .....	87
IV.6.	Optimization of the catalytic $\alpha$ -arylation of ketones: solvent and base influence .....	89
IV.7.	General procedure for the catalytic $\alpha$ -arylation of ketones.....	89
IV.8.	Control experiments .....	90
IV.8.1.	<i>Investigation of the mercury effect</i> .....	90
IV.8.2.	<i>Reaction of complex (10) with 4-bromotoluene</i> .....	90
IV.8.3.	<i>Catalytic <math>\alpha</math>-arylation of propiophenone with (10) as pre-catalyst</i> .....	91
IV.8.4.	<i>Reaction of complex (11) with propiophenone</i> .....	91
IV.8.5.	<i>Investigation of radical scavenger effect</i> .....	91
IV.8.6.	<i>Investigation of radical initiator effect</i> .....	91
IV.9.	Spectral data of the coupling products .....	92
<b>V.</b>	<b>References .....</b>	<b>96</b>

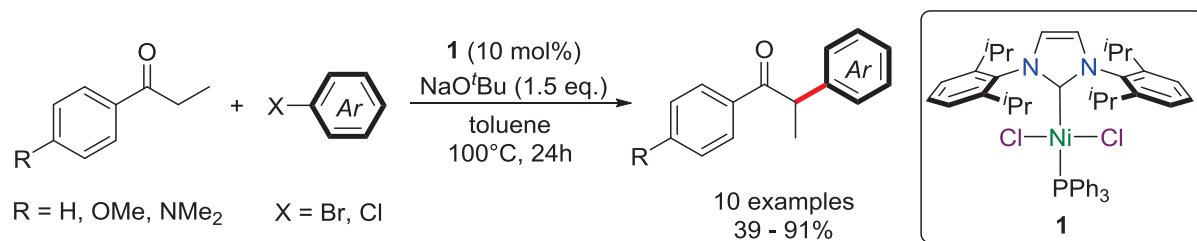
## I. Introduction

The sustainable formation of  $\alpha$ -aryl carbonyl compounds has remained a challenge for years. The adopted strategies often included conventional nucleophilic aromatic substitution, which is limited to the use of highly activated aryl halides.<sup>[1]</sup> Another approach consisted in using a preformed enolate derivative in a metal-mediated process requiring stoichiometric amounts of catalysts.<sup>[2–4]</sup> However, these methods generally suffered from the high cost and toxicity of the metal sources, and the limited functional-group compatibility. In 1997, Miura,<sup>[5]</sup> Buchwald<sup>[6]</sup> and Hartwig<sup>[7]</sup> concurrently reported the serendipitous discovery of the palladium-catalyzed  $\alpha$ -arylation of ketones,<sup>[8–11]</sup> which proceeds *via* the direct functionalization of a C–H bond  $\alpha$  to the ketone (*i.e.* without a preformed metal-enolate). At that time, the methodology already included aromatic and aliphatic ketones with aryl iodides and bromides, and very soon chlorides.<sup>[12]</sup> Since then, significant progress has been realized in this field, as other carbonyl compounds can be functionalized this way, such as esters,<sup>[13–21]</sup> amides,<sup>[22–28]</sup> aldehydes<sup>[29–34]</sup> and nitriles.<sup>[35–37]</sup> Moreover, the challenging aryl mesylates recently also proved to be suitable electrophiles in the  $\alpha$ -arylation of ketones.<sup>[38]</sup> Finally, it is noteworthy that efforts from the group of Hartwig has allowed to shed some light on the mechanism of the Pd-catalyzed  $\alpha$ -arylation process, which possibly proceeds *via* the catalytic cycle depicted in **Scheme 1**.<sup>[39,40]</sup>



**Scheme 1.** Plausible catalytic cycle for the Pd-catalyzed  $\alpha$ -arylation of ketones  
(OA = oxidative addition, LS = ligand substitution, RE = reductive elimination)

Despite this considerable progress, the TM-catalyzed  $\alpha$ -arylation of carbonyl derivatives suffers from the high costs of Pd and its associated ligands, as well as from a certain lack of catalyst variety, as almost only Pd is used. It is therefore of major interest to develop suitable alternatives in terms of both cost and catalyst variety. In this regard, very recent efforts have been directed towards the use of copper catalysts, but this field is only at its infancy,<sup>[41]</sup> and another alternative to palladium may be its 1<sup>st</sup> row counterpart, nickel, with which the direct  $\alpha$ -arylation of ketone and esters enolates were actually first reported in the 1970s.<sup>[42,43]</sup> Nevertheless, since then, almost all of the few reported examples involves the use of high loadings (5 - 10 mol%) of sensitive and pyrophoric Ni(COD)<sub>2</sub> for the  $\alpha$ -arylation of cyclic ketones (exclusively).<sup>[40,44–46]</sup> Thus, to the best of our knowledge, the only example of an air- and moisture-stable nickel(II) pre-catalyst for this transformation has been described by Matsubara *et al.* in 2007 (**Scheme 2**).<sup>[47]</sup> In this paper, the mixed phosphine–, *N*-heterocyclic carbene–nickel(II) complex [Ni(IPr)(PPh<sub>3</sub>)Cl<sub>2</sub>] **1** was reported to catalyze the coupling of some aryl bromides and chlorides with propiophenone derivatives. However, here too, relatively demanding conditions (10 mol% of **1**) were required to observe respectable yields.

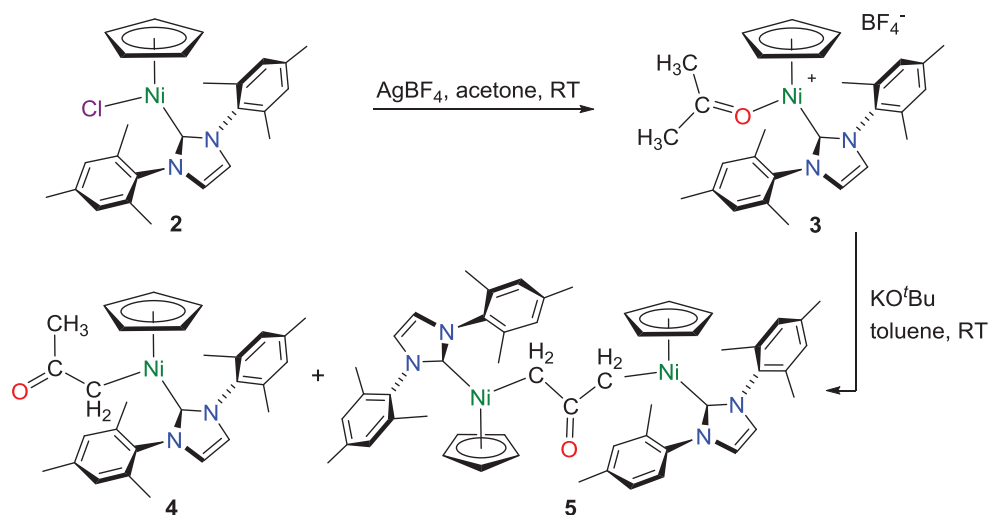


**Scheme 2.**  $\alpha$ -Arylation of acyclic ketones catalyzed by [Ni(IPr)(PPh<sub>3</sub>)Cl<sub>2</sub>] **1**

In this context, our group recently reported that cyclopentadienyl (Cp) nickel–*N*-heterocyclic carbene complexes are able to activate C–H bonds of labile acetonitrile<sup>[48,49]</sup> and acetone<sup>[50]</sup> ligands in the presence of stoichiometric amounts of a strong base. Of notable interest, the latter reaction led to the formation of a rare example of the nickel-acetonyl complex **4**, as well as to the unique formation of the dinickel-oxyallyl complex **5**, resulting from the mono and double base-promoted nickelation of acetone, respectively (**Scheme 3**). Indeed, in contrast to the heavier group 10 elements, Pd and Pt, where metal-acetonyl or so-

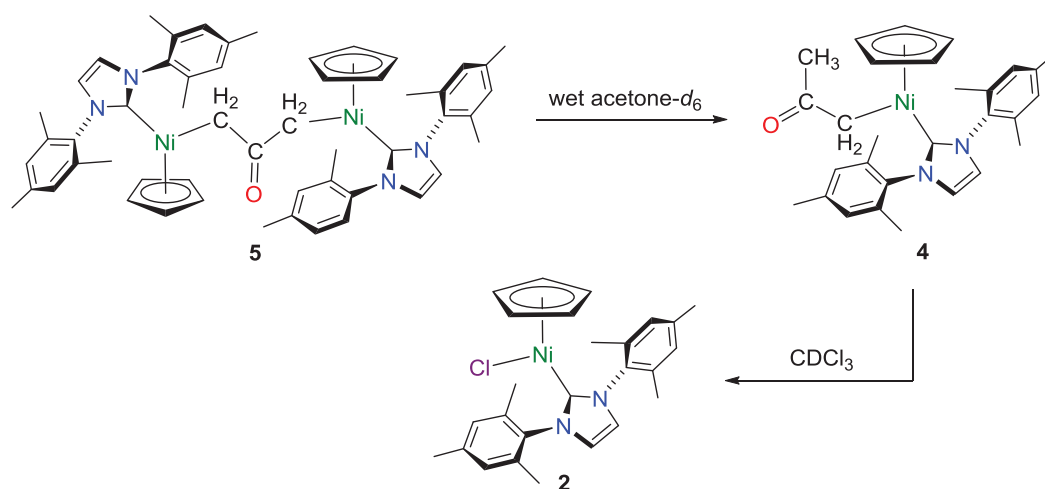


called C-bound enolate complexes are prevalent,<sup>[51–55]</sup> the latter have rarely been reported for nickel,<sup>[56–58]</sup> as similar reactions usually generate O-bound enolate nickel complexes.<sup>[59–62]</sup>



**Scheme 3.** Base-assisted nickelation of acetone

The isolation of such nickel-C-bound enolate complexes, which are important intermediates in the  $\alpha$ -arylation of carbonyl derivatives (see **Scheme 1**), coupled with the fact they could be protonated back from **5** to **4**, and from **4** to **2** (**Scheme 4**), suggested that this family of CpNi(II)–NHC complexes might be used as catalyst precursors in such C(sp<sup>2</sup>)–C(sp<sup>3</sup>) couplings *via* C–H bond cleavage. Herein, we show that these air-stable complexes exhibit high catalytic activity for the  $\alpha$ -arylation of acyclic ketones at concentration as low as 1 mol%, and give insights to the mechanism of this catalytic process.

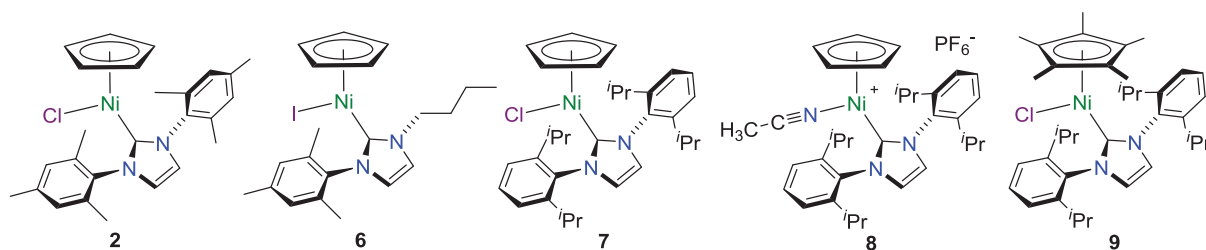


**Scheme 4.** Reprotonation of complexes **4** and **5**

## II. Results and Discussion

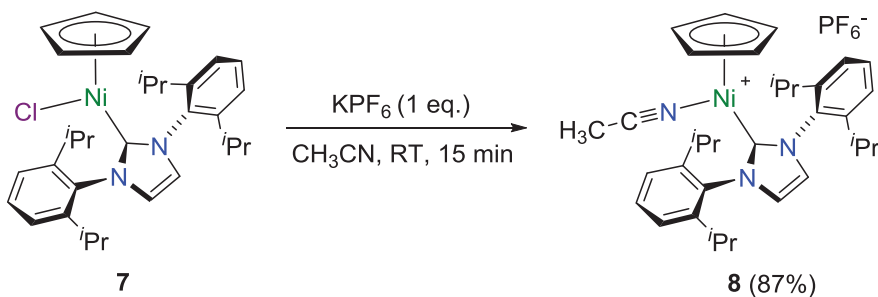
### II.1. Choice and syntheses of the pre-catalysts

Selected half-sandwich Ni–NHC complexes for the catalytic study are depicted in **Figure 1**.



**Figure 1.** Selected half-sandwich Ni–NHC complexes

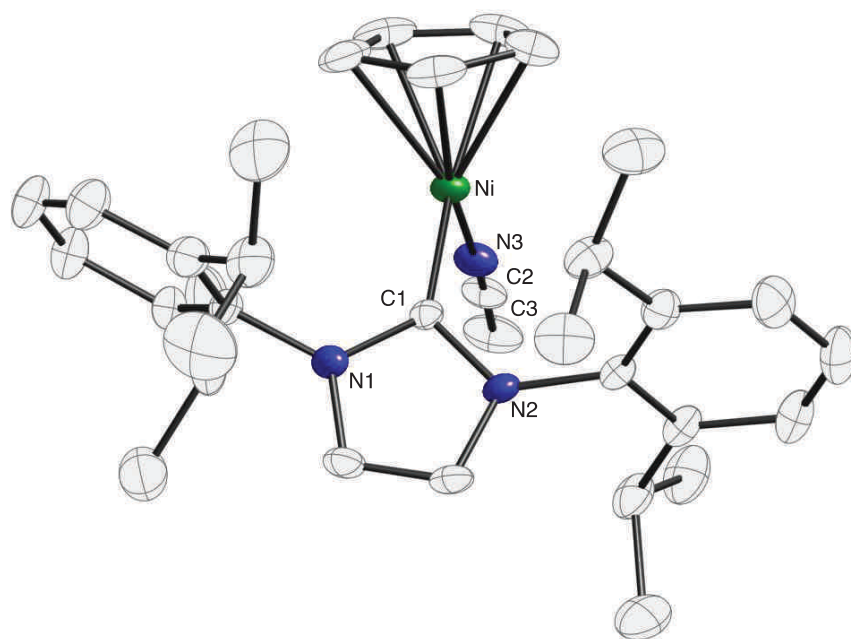
Complexes  $[\text{Ni}(\text{IMes})\text{ClCp}]$  **2**,<sup>[63]</sup>  $[\text{Ni}(\text{Mes-NHC-nBu})\text{ICp}]$  **6**,<sup>[64]</sup>  $[\text{Ni}(\text{IPr})\text{ClCp}]$  **7**<sup>[65]</sup> and  $[\text{Ni}(\text{IPr})\text{ClCp}^*]$  **9**<sup>[66]</sup> were prepared according to the published methods. The cationic complex  $[\text{Ni}(\text{IPr})(\text{NCMe})\text{Cp}](\text{PF}_6)$  **8** was synthesized by treatment of an acetonitrile solution of the neutral complex **7** with 1 equivalent of  $\text{KPF}_6$  (**Scheme 5**). Thus, the chloride atom was abstracted, and the cationic complex **8** was isolated as a dark yellow air-stable solid in 87% yield. Complex **8** was characterized by  $^1\text{H}$  and  $^{13}\text{C}\{^1\text{H}\}$  NMR spectroscopy, IR spectroscopy, elemental analyses and X-ray diffraction.



**Scheme 5.** Synthesis of  $[\text{Ni}(\text{IPr})(\text{NCMe})\text{Cp}](\text{PF}_6)$  **8**

The  $^1\text{H}$  and  $^{13}\text{C}\{^1\text{H}\}$  NMR spectra of **8** in  $\text{CD}_3\text{CN}$  are straightforward as they clearly show the presence of one  $\eta^5\text{-Cp}$  ligand and one IPr ligand. As for the neutral complex **7**, the spectra reveal that an effective plane of symmetry that bisects the molecule exists in solution on the NMR time scale. This effective mirror plane contains the acetonitrile ligand, the nickel center and the NHC carbene carbon atom, as well as the Cp ring centroid. Free  $\text{CH}_3\text{CN}$  that results from the exchange with  $\text{CD}_3\text{CN}$  is seen in the NMR spectrum, indicating that the acetonitrile ligand of the cationic species is labile in solution. It is noteworthy that the carbene carbon atom in **8** appears at 162.7 ppm (in  $\text{CD}_3\text{CN}$ ). This signal is slightly upfield of the signal seen at 169.3 ppm (in  $\text{CDCl}_3$ ) for its neutral derivative **7**, as was observed for all other cationic complexes of this type in comparison to their neutral derivatives.<sup>[67]</sup>

Crystals of **8** suitable for an X-ray structure determination were grown from an acetonitrile/diethylether solution at  $4^\circ\text{C}$ . The molecular structure of its cationic part is shown in **Figure 2**. Crystallographic data and data collection parameters are listed in **Table 4** (see *Experimental Section*), and a list of selected bond lengths and angles appear in **Figure 2's** legend.



**Figure 2.** Molecular structure of the cationic part of **8** showing all non-H atoms. Ellipsoids are shown at the 50% probability level and key atoms are labelled. Selected distances ( $\text{\AA}$ ) and angles ( $^\circ$ ) for both cations contained in the asymmetric unit: Ni–C1, 1.8885(19)/1.8912(19); Ni–N3, 1.863(2)/1.8637(19); Ni–Cp<sub>cent</sub>, 1.746/1.749; C1–Ni–N3, 97.24(8)/96.29(8); C1–Ni–Cp<sub>cent</sub>, 134.55/135.25; N3–Ni–Cp<sub>cent</sub>, 127.89/128.16.

This structure is strikingly similar to that of both its neutral and Cp\* analogues, **7**<sup>[65]</sup> and [Ni(IPr)(NCMe)Cp\*](PF<sub>6</sub>), and deserves no particular comment.<sup>[67]</sup> Indeed, all distances and angles are in the same range to that of these two analogous complexes, with a nickel atom laying at the center of a trigonal plan, with the same range of significant departures from the 120° angles of a trigonal structure.

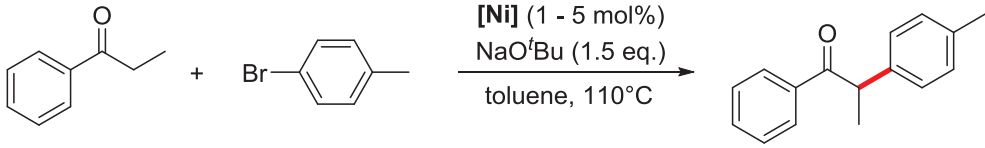
## II.2. Optimization of the catalytic conditions

Our initial efforts focused on the coupling of propiophenone with 4-bromotoluene in toluene at 110°C in the presence of 1.5 equiv. of NaO<sup>t</sup>Bu as a base and of 5 mol% of a pre-catalyst, *i.e.* under conditions similar to those of Matsubara, but with a lower pre-catalyst loading (**Table 1**). Complex **6** was first tested, as this pre-catalyst is highly active in the Suzuki-Miyaura cross-coupling reaction.<sup>[64]</sup> However, it was totally inert in this  $\alpha$ -arylation process (**Table 1**, entry 2). Switching to complex **2**, which bears the more bulky IMes ligand and a chloride instead of an iodide ligand, gave an encouraging 25% GC yield after 24 h (entry 1). Moving to the bulkier pre-catalyst **7** allowed a further yield enhancement to 65% (entry 3). However, using the cationic **8** and Cp\* **9** derivatives of **7** yielded no further improvement (entries 4 and 5). Using commercial sources of nickel such as nickelocene (entry 6) or Ni(acac)<sub>2</sub> (entry 7) without additional ligands resulted in an important decrease or total loss of activity, and attempting the reaction without any nickel catalyst resulted in no conversion at all (entry 8).

Unexpectedly, decreasing the pre-catalyst loading from 5 to 3 mol% showed a significant yield improvement to 78% (entry 9). A plausible explanation could be that **7** likely catalyzes side-reactions at too high loadings. Indeed, **7** was shown to be active in the catalytic dehalogenation of aryl bromides under similar conditions (see **Chapter I.**, *Dehalogenation reactions*).<sup>[65]</sup> Decreasing the loading even further to 1 mol% still allowed the arylation process to proceed, although with a slightly decreased activity (entry 10). It is noteworthy, however, that this conversion observed with 1 mol% of **7** after 24 h of reaction (60%) is similar to that observed with 10 mol% of Matsubara's complex after the same reaction time (65%) (entries 10 vs. 12). Moreover, quantitative yields were obtained by extending the reaction time from 24 to 48 h (entry 11), which shows that the active species is long-lived.

These results thus make of the **7**-NaO<sup>t</sup>Bu mixture in toluene the most efficient nickel-based system reported to date for the  $\alpha$ -arylation of ketones in terms of pre-catalyst loading.

**Table 1.** Nickel(II)-catalyzed  $\alpha$ -arylation of propiophenone with 4-bromotoluene<sup>a</sup>

			
Entry	Catalyst (mol%)	Time (h)	Yield (%) <sup>b</sup>
1	<b>2</b> (5)	24	25
2	<b>6</b> (5)	24	< 1
3	<b>7</b> (5)	24	65
4	<b>8</b> (5)	24	60
5	<b>9</b> (5)	24	61
6	NiCp <sub>2</sub> (5)	24	8
7	Ni(acac) <sub>2</sub> (5)	24	< 1
8	–	24	< 1
9	<b>7</b> (3)	24	78
10	<b>7</b> (1)	24	60
11	<b>7</b> (1)	48	> 97
12	<b>1</b> (10)	24	65 <sup>c</sup>

<sup>a</sup> Reaction conditions: propiophenone (1.2 mmol), 4-bromotoluene (1 mmol), NaO<sup>t</sup>Bu (1.5 mmol), [Ni] (1 - 5 mol%) in toluene (3 mL) at 110°C. <sup>b</sup> Yields determined by GC; average of two runs. <sup>c</sup> temperature = 100°C

### II.3. Reaction scope study

With these optimized conditions in hand (3 mol% of **7**, 1.5 equiv. NaO<sup>t</sup>Bu, toluene, 110°C, 24 h), we then examined the scope of the  $\alpha$ -arylation reaction (**Table 2**). A first part of this study concerned the use of propiophenone with various aryl halides (entries 1 - 12). As expected, aryl iodides gave excellent results (entry 3) whereas aryl chlorides proved to be totally unreactive under these reaction conditions (entry 2). This allowed us to obtain 2-(*p*-chlorophenyl)propiophenone selectively in 89% yield from 4-iodo-chlorobenzene (entry 7).

The presence of electron-withdrawing or -donating groups at the *para* position of the tested aryl bromides seems to have little influence, as moderate yields were obtained in all cases after 24 h of reaction (entries 8, 10 and 12). Nevertheless, running the reactions for 48 h allowed us to obtain very good yields with *p*-methoxy- and *p*-*tert*-butylbromobenzene (entries 9 and 11). Finally, the sterically hindered 2-bromotoluene gave poor yields, even after 48 h of reaction (entries 5 and 6).

**Table 2.**  $\alpha$ -Arylation of ketones with aryl halides catalyzed by **7**<sup>a</sup>

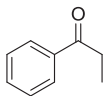
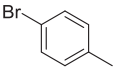
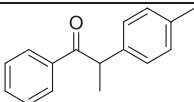
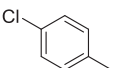
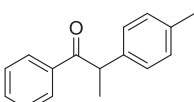
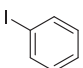
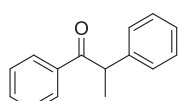
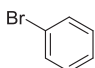
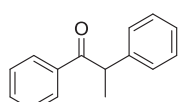
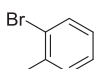
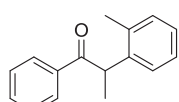
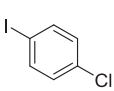
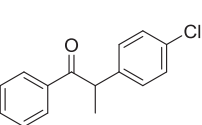
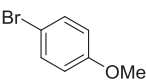
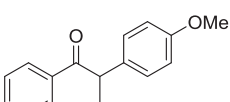
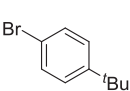
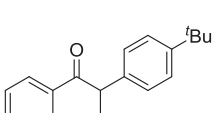
$  \begin{array}{c}  \text{R}-\text{C}(=\text{O})-\text{CH}_2-\text{R}' + \text{X}-\text{Ar} \xrightarrow[\text{toluene, 110}^\circ\text{C, 24-48h}]{\text{7 (3 mol\%), NaO}^t\text{Bu (1.5 eq.)}} \text{R}-\text{C}(=\text{O})-\text{CH}(\text{Ar})-\text{R}'  \end{array}  $					
Entry	Ketone	Aryl halide	Coupling product	Time (h)	Yield (%) <sup>b</sup>
1				24	73
2				24	< 1 <sup>c</sup>
3				24	92
4				24	65
5				24	10
6				48	17
7				24	89
8				24	53
9				48	93
10				24	52
11				48	85

Table 2. (continued)<sup>a</sup>

12				24	42
13				24	66
14				48	89
15				24	71
16				24	84
17				48	92
18				24	13
19				48	21
20				24	< 1
21				24	68
22				48	79
23				24	55 <sup>d</sup>
24				24	< 1 <sup>e</sup>

<sup>a</sup> Reaction conditions: ketone (1.2 mmol), 4-bromotoluene (1 mmol), NaO<sup>t</sup>Bu (1.5 mmol), **7** (3 mol%) in toluene (3 mL) at 110°C for 24 or 48 h. <sup>b</sup> Isolated yields; average value of two runs. <sup>c</sup> Yield determined by GC; average value of two runs. <sup>d</sup> A 2:1 mixture of 2-(*p*-tolyl)-4-methyl-pentan-3-one and 2-(*p*-tolyl)-2-methyl-pentan-3-one was obtained. <sup>e</sup> Aldol condensation products were observed.

We next studied the reaction of 4-bromotoluene with various ketones (entries 13 - 24). Good to excellent yields were obtained with electron-rich and -poor propiophenone derivatives in 24 and/or 48 h (entries 13 - 17). Interestingly, the reaction of 3-pentanone with

4-bromotoluene selectively gave the monoarylated product with up to 79% yield (entries 21 - 22). In contrast, a 2:1 mixture of 2-(*p*-tolyl)-4-methyl-pentan-3-one and 2-(*p*-tolyl)-2-methyl-pentan-3-one was obtained with 2-methyl-pentan-3-one (entry 23). The use of the sterically encumbered *iso*-butyrophenone gave poor yields (entries 18 and 19), thus highlighting the relative sensitivity of our catalytic system to bulky substrates. Surprisingly, no conversion was observed when employing a cyclic ketone (entry 20). The latter result makes our system complementary to Ni(COD)<sub>2</sub>/ligand-based catalysts, which only achieve the  $\alpha$ -arylation of cyclic ketones.<sup>[40,44–46]</sup> Finally, as observed by Matsubara *et al.* with complex **1**, acetophenone was found to be an unsuitable substrate because of the competitive aldol condensation reaction (entry 24).

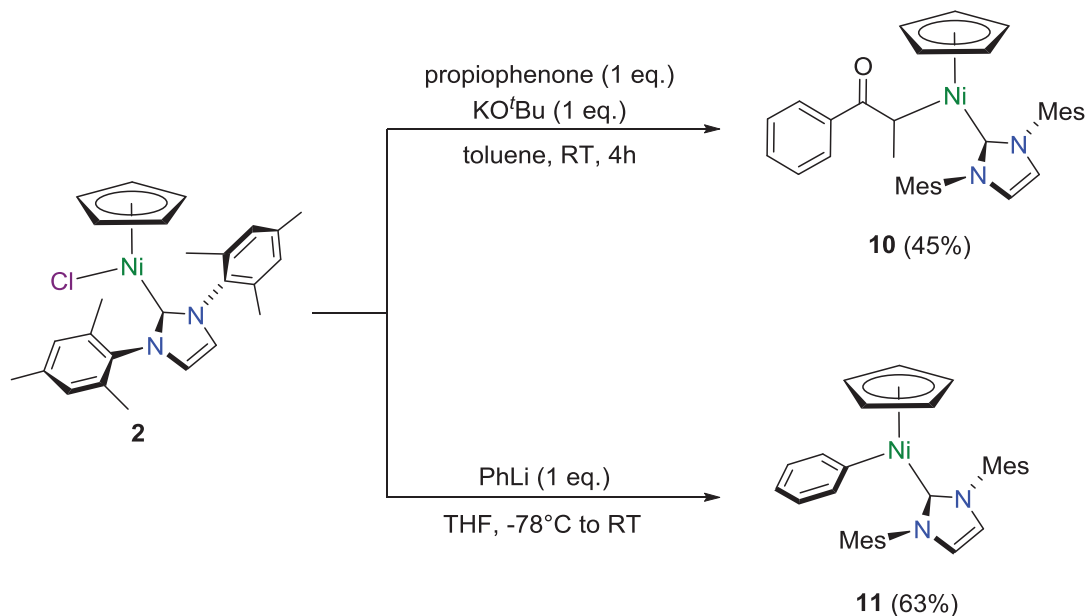
#### II.4. Mechanistic studies

To get an insight into the mechanism, we first checked whether the  $\alpha$ -arylation process was the result of a true homogeneous catalysis by conducting the coupling of propiophenone with 4-bromotoluene in the presence of a 100-fold excess of elemental mercury relative to the nickel.<sup>[68,69]</sup> No inhibition was observed, and thus a process catalyzed by nickel nanoparticles seems unlikely.

This being established, we then considered the mechanism of the Pd-catalyzed  $\alpha$ -arylation reaction (see **Scheme 1**), and attempted to synthesize an enolate derivative of complex **7**. For that purpose, we conducted a series of stoichiometric reactions in toluene with **7** in the presence of propiophenone. However, using either NaO<sup>*t*</sup>Bu or KO<sup>*t*</sup>Bu as the base, or working at room temperature or at 100°C always led to the formation of complicated mixtures, which prevented the isolation of an enolate nickel complex. The strategy employed for the base assisted C–H activation of acetone (see **Scheme 3**), which consisted in chloride abstraction with AgBF<sub>4</sub> with the ketone acting as both the solvent and the reactant, followed by treatment of the resulting cationic ketone complex with KO<sup>*t*</sup>Bu, proved also unsuccessful. We thus thought that the steric hindrance induced by the IPr ligand might not favor the isolation of such species. Consequently, similar reactions were performed with the less bulky IMes complex **2**, and the target complex, [Ni(IMes){CH(CH<sub>3</sub>)C(O)Ph}] **10**, could be isolated after reaction with KO<sup>*t*</sup>Bu and propiophenone (1 equiv. of each) in toluene, at room temperature (**Scheme 6**). Complex **10** was obtained as an air- and thermally-sensitive reddish



solid in 45% yield. The latter was characterized by means of  $^1\text{H}$  and  $^{13}\text{C}\{^1\text{H}\}$  NMR spectroscopy and elemental analysis. Unfortunately, we were not able to get suitable crystals for an X-ray diffraction study. Nevertheless, the C-bonded enolate nature of **10** was corroborated, in the  $^1\text{H}$  NMR spectrum, by the signals of the  $\alpha$ -proton and of the  $\beta$ -methyl group, which appear at 2.57 and 0.72 ppm as a quadruplet and a doublet integrating for 1 and 3 protons, respectively. In the  $^{13}\text{C}\{^1\text{H}\}$  NMR spectrum, the carbonyl carbon appears at 207.8 ppm.

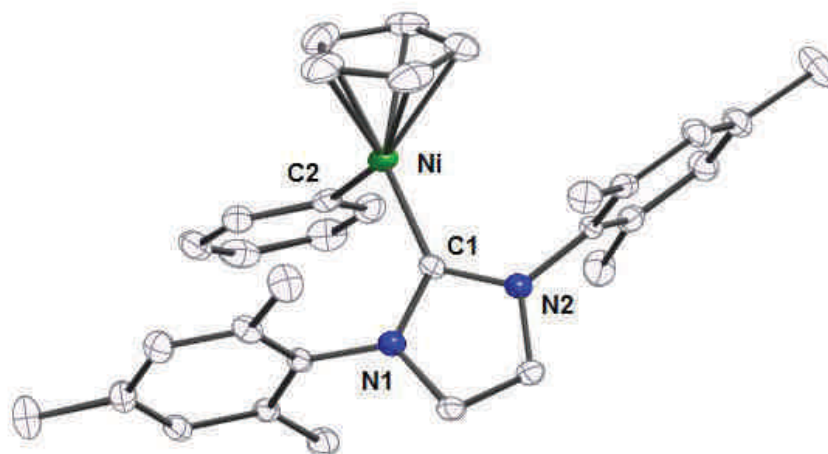


**Scheme 6.** Synthesis of complexes **10** and **11** from **2**, as possible intermediates of the  $\alpha$ -arylation process

We also synthesized the nickel–phenyl complex **11** by treatment of **2** with phenyllithium, as a nickel–aryl species may also be implied in the reaction mechanism (**Scheme 1**). The phenyl derivative of **2**,  $[\text{Ni}(\text{IMes})\text{PhCp}]$  **11**, was isolated as air-stable crystals in 63% yield after work-up (**Scheme 5**), and characterized by  $^1\text{H}$  and  $^{13}\text{C}\{^1\text{H}\}$  NMR spectroscopy, elemental analysis and X-ray diffraction. The NMR spectra of **11** clearly show the presence of one NHC ligand, one Cp ligand, and one phenyl group. This is consistent with the X-ray diffraction study, that was conducted with a single crystal selected from a batch of crystals obtained at room temperature from a toluene/pentane solution, and which allowed us to determine the molecular structure of **11** (**Figure 3** and **Table 4**).

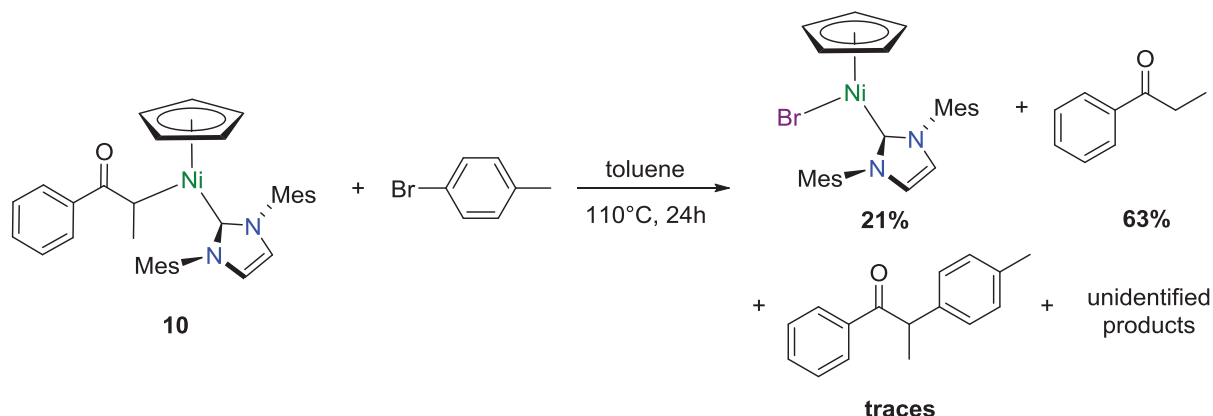
The latter is closely related to those established for similar  $[\text{Ni}(\text{NHC})\text{XCp}]$  complexes, such as **8** (see **Figure 2**). Thus, the nickel atom is bonded to a  $\eta^5\text{-Cp}$  group, a NHC moiety

and a phenyl group, and if one consider the Cp group as a single ligand, the metal lies at the center of a pseudo-trigonal plane with significant departures from the idealized  $120^\circ$  angles of a trigonal planar structure (**Figure 3**'s legend). The carbenoid carbon C1 and the phenyl carbon C2 subtend an angle of  $95.4^\circ$  at the nickel atom. This value is in the range of the C1–Ni–N3, angle observed for **8** for which values of  $97.2/96.3^\circ$  have been determined (see **Figure 2**).



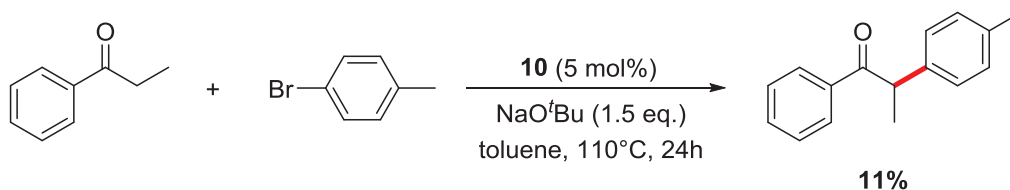
**Figure 3.** Molecular structure of **11** showing all non-H atoms. Ellipsoids are shown at the 50% probability level and key atoms are labeled. Selected distances (Å) and angles ( $^\circ$ ): Ni–C1, 1.875(2); Ni–C2, 1.908(2); Ni–Cp<sub>cent</sub>, 1.785; C1–Ni–C2, 95.35(9); C1–Ni–Cp<sub>cent</sub>, 136.45; C2–Ni–Cp<sub>cent</sub>, 128.18.

We next assessed the viability of complex **10** and **11** as intermediates in the catalytic process by conducting a series of control experiments. The stoichiometric reaction of **10** with 4-bromotoluene in refluxing toluene gave a complicated mixture, from which a violet complex, which we have identified as [Ni(IMes)BrCp] by comparison of its NMR data with those of [Ni(IMes)ClCp]<sup>[70]</sup> and by its mass spectrum (see *Experimental section*), was isolated in 21% yield (**Scheme 7**). The latter would mostly result from the dehalogenation of 4-bromotoluene, as propiophenone was the major organic product, but could also partly result from the coupling of the C-bound propiophenone enolate and 4-bromotoluene, as traces of the expected product were identified by  $^1\text{H}$  NMR spectroscopy in one organic fraction.



**Scheme 7.** Stoichiometric reaction of **10** with 4-bromotoluene

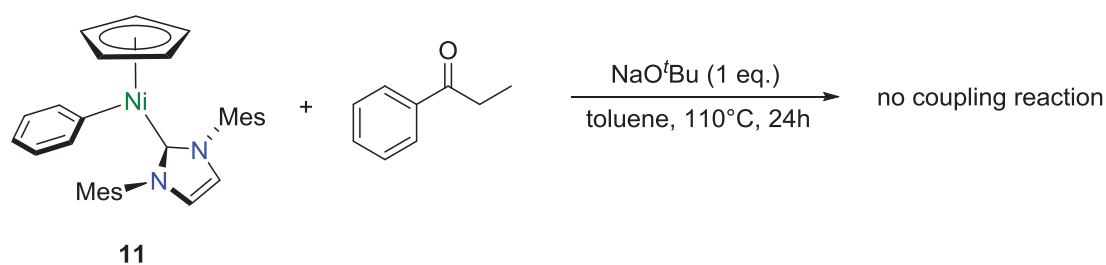
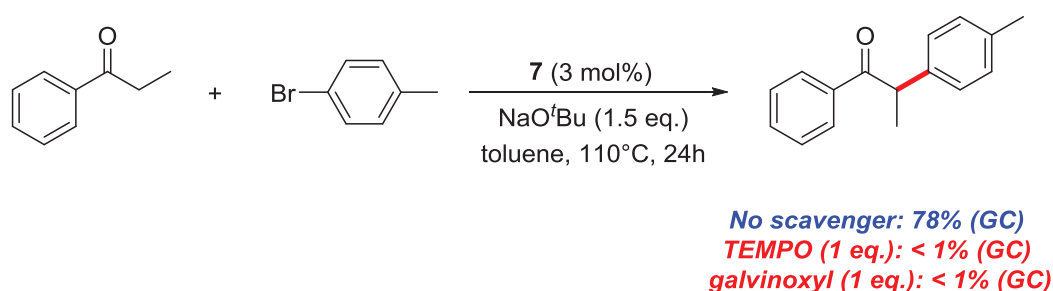
To verify this latter hypothesis, we conducted the coupling of propiophenone and 4-bromotoluene in the presence of a sub-stoichiometric amount of **10**, and an 11% yield of 1-phenyl-2-(*p*-tolyl)propan-1-one was measured by GC (**Scheme 8**). This result suggests that **10** is a possible intermediate in the Ni-catalyzed  $\alpha$ -arylation, but the higher yield observed with [Ni(IMes)ClCp] **2** as a catalyst precursor (25%, see **Table 1**, entry 1) suggests that at least some of the product is formed *via* another intermediate and/or *via* a different type of mechanism.



**Scheme 8.**  $\alpha$ -Arylation of propiophenone catalyzed by **10**

To assess the possibility of **11** being an intermediate in the  $\alpha$ -arylation process, we reacted it with stoichiometric amounts of propiophenone and NaO<sup>t</sup>Bu in refluxing toluene (**Scheme 9**). No coupling product was formed and most of the propiophenone was recovered, thus ruling out **11** as an intermediate.

These results and recent reports on Ni-catalyzed organic transformations led us to suspect a competing radical pathway.<sup>[71]</sup> Experiments performed in the presence of radical scavengers supported this hypothesis. Thus, the addition of 1 equivalent of TEMPO or galvinoxyl completely inhibited the reaction (**Scheme 10**).

**Scheme 9.** Stoichiometric reaction of **11** with propiophenone**Scheme 10.** Effect of radical inhibitors

Moreover, a "metal-free" version of the reaction using AIBN as a radical initiator – although far less efficient – led to some conversion, as a 5% yield was measured by GC when the reaction was run with 20 mol% of AIBN and no other additive (**Table 3**, entry 4).

**Table 3.**  $\alpha$ -Arylation of propiophenone with 4-bromotoluene catalyzed by **7** and/or AIBN.<sup>a</sup>

Entry	Catalyst (mol%)	NaO <sup>t</sup> Bu (equiv.)	Yield (%) <sup>b</sup>
1 <sup>c</sup>	<b>7</b> (3)	1.5	78
2	<b>7</b> (3) + AIBN (20)	1.5	< 1
3	AIBN (20)	1.5	< 1
4	AIBN (20)	0	5

<sup>a</sup> Reaction conditions: propiophenone (1.2 mmol), 4-bromotoluene (1 mmol), NaO<sup>t</sup>Bu (0 or 1.5 mmol), **7** (0 or 3 mol%), AIBN (0 or 20 mol%) in toluene (3 mL) at 110 °C for 24 h. <sup>b</sup> Yields determined by GC; average value of two runs.

Consequently, we believe that the principal mechanism at work in this Ni-catalyzed  $\alpha$ -arylation process is of a radical nature, and that a C-bound ketone enolate derivative of **7**, if involved, only plays a minor role.

### III. Conclusion

In summary, we have demonstrated that the inexpensive and easy-to-handle complex, [Ni(IPr)ClCp] **7**, is an efficient pre-catalyst for the  $\alpha$ -arylation of acyclic ketones, and the most productive nickel-based catalyst reported to date, as loadings as low as 1 mol% could be used. Indeed, we are aware of only five previous examples describing the use of nickel, where relatively high loadings of the highly sensitive and pyrophoric nickel(0) complex, Ni(COD)<sub>2</sub>, or high loadings of a nickel(II) complex were used. Our methodology is thus superior in terms of practicality and cost, and allows the use of aromatic or aliphatic enolizable acyclic ketones to give the corresponding coupling product in moderate to excellent yields. We also isolated the C-bound enolate complex **10**, which could act as an active intermediate, although other mechanistic studies indicate that a radical pathway is more likely.

### IV. Experimental section

#### IV.1. General information

All reactions were carried out using standard Schlenk techniques under an atmosphere of dry argon. Solvents were distilled from appropriate drying agents under argon.

Solution NMR spectra were recorded at 298K on FT-Bruker Ultra Shield 300 and Bruker Spectrospin 400 spectrometers operating at 300.13 or 400.14 MHz for <sup>1</sup>H, at 75.47 or 100.61 MHz for <sup>13</sup>C{<sup>1</sup>H} and at 376 MHz for <sup>19</sup>F{<sup>1</sup>H}. DEPT <sup>13</sup>C spectra and/or <sup>1</sup>H/<sup>13</sup>C HSQC correlations were recorded for the new complex [Ni(IPr)(NCMe)Cp](PF<sub>6</sub>) **8** and for the 2:1 mixture of 2-(4-methylphenyl)-4-methyl-3-pentanone and 2-(4-methylphenyl)-2-methyl-3-pentanone to help in the <sup>13</sup>C signal assignments. The chemical shifts are referenced to the residual deuterated or <sup>13</sup>C solvent peaks. Chemical shifts ( $\delta$ ) and coupling constants ( $J$ ) are expressed in ppm and Hz respectively.

The IR spectrum of **7** was recorded on a FT-IR Nicolet 380 spectrometer equipped with a diamond SMART-iTR ATR. Vibrational frequencies are expressed in  $\text{cm}^{-1}$ .

Elemental analyses were performed at the Services d'Analyses, de Mesures Physiques et de Spectroscopie Optique, UMR CNRS 7177, Institut de Chimie, Strasbourg.

GC analyses were performed with an Agilent 7820A GC system equipped with a 30-m capillary column (Agilent HP-5, cross-linked 5% phenyl silicone gum, 30 m  $\times$  0.32 mm  $\times$  0.25  $\mu\text{m}$ ).  $\text{H}_2$ /air was used as a vector gas. The following GC conditions were employed: initial temperature 40°C, for 2 min, then ramped up at a rate of 10°C/min until 200°C, and 20°C/min until 280°C. 1,3,5-trimethoxybenzene was used as an internal standard.

Commercial compounds were used as received. Coupling products that have been previously reported were isolated in greater than 95% purity, as determined by  $^1\text{H}$  et  $^{13}\text{C}$  NMR spectroscopy. New coupling products were characterized by  $^1\text{H}$  and  $^{13}\text{C}$  NMR spectroscopy, and elemental analyses or high-resolution mass spectrometry. Nickelocene,<sup>[72]</sup> complexes  $[\text{Ni}(\text{IMes})\text{ClCp}]$  **2**,<sup>[63]</sup>  $[\text{Ni}(\text{Mes-NHC-nBu})\text{ICp}]$  **6**,<sup>[64]</sup>  $[\text{Ni}(\text{IPr})\text{ClCp}]$  **7**<sup>[65]</sup> and  $[\text{Ni}(\text{IPr})\text{ClCp}^*]$  **9**<sup>[66]</sup> were prepared according the published methods.

#### IV.2. Synthesis of $[\text{Ni}(\text{IPr})(\text{NCMe})\text{Cp}](\text{PF}_6)$ (**8**)

**7** (500 mg, 0.913 mmol) and  $\text{KPF}_6$  (168 mg, 0.913 mmol) were suspended in acetonitrile (10 mL), and the resulting mixture was stirred at room temperature. A quick color change from violet to dark yellow was observed. After 15 min, the reaction mixture was filtered through Celite, concentrated to *ca.* 3 mL, and treated with diethylether (10 mL) to yield a dark yellow solid that was washed with diethylether (3  $\times$  10 mL), and dried under vacuum to give **8** (557 mg, 0.798 mmol, 87%).

Anal. Calcd for  $\text{C}_{34}\text{H}_{44}\text{F}_6\text{N}_3\text{NiP}$ : C, 58.47; H, 6.35; N, 6.02. Found: C, 58.08; H, 6.36; N, 6.11.

$^1\text{H}$  NMR ( $\text{CD}_3\text{CN}$ , 400.14 MHz):  $\delta$  7.66 (t,  $^3J = 8.0$  Hz, 2H, *p*-H), 7.59 (s, 2H, NCH), 7.52 (d,  $^3J = 8.0$  Hz, 4H, *m*-H), 4.74 (s, 5H,  $\text{C}_5\text{H}_5$ ), 2.55 (qq,  $^3J = 6.8$  Hz, 4H,  $\text{CHMe}_2$ ), 1.38 (d,  $^3J = 6.8$  Hz, 12H,  $\text{CHMe}_2$ ), 1.14 (d,  $^3J = 6.8$  Hz, 12H,  $\text{CHMe}_2$ ).<sup>a</sup>

$^{13}\text{C}\{^1\text{H}\}$  NMR ( $\text{CD}_3\text{CN}$ , 100.61 MHz):  $\delta$  162.7 (NCN), 147.0 (*ipso*- or *o*- $\text{C}_{\text{Ar}}$ ), 136.7 (*o*- or *ipso*- $\text{C}_{\text{Ar}}$ ), 131.8 (*p*- $\text{C}_{\text{Ar}}$ ), 128.6 (NCH), 125.3 (*m*- $\text{C}_{\text{Ar}}$ ), 94.4 ( $\text{C}_5\text{H}_5$ ), 29.6 ( $\text{CHMe}_2$ ), 26.3 and 22.5 ( $\text{CHMe}_2$ ). FT-IR:  $\nu(\text{CH})$  2963 (m), 2928 (w), 2866 (w);  $\nu(\text{P-F})$  835 (s).

<sup>a</sup> Free CH<sub>3</sub>CN that results from exchange with CD<sub>3</sub>CN is seen as a singlet at 1.96 ppm, on the downfield side of the multiplet due to the residual CHD<sub>2</sub>CN observed at 1.94 ppm.

### IV.3. Synthesis of [Ni(IMes){CH(CH<sub>3</sub>)C(O)Ph}Cp] (**10**)

Toluene (5 mL) was added to **2** (500 mg, 1.08 mmol), KO<sup>t</sup>Bu (121 mg, 1.08 mmol) and propiophenone (145  $\mu$ L, 1.08 mmol). The resulting suspension was stirred at room temperature for 4 h during which a color change from violet to red-brown was observed. Volatiles were then removed *in vacuo*. Addition of pentane (20 mL) to the residue gave a solid that was collected on a frit, washed with pentane until the washings were colorless, extracted with THF (40 mL) and filtered over Celite. Concentration of the filtrate to *ca.* 5 mL and addition of 20 mL of pentane then gave a reddish solid that was washed with pentane until the washings were colorless. Recrystallization from THF/pentane (1:5) at  $-28^{\circ}\text{C}$  finally afforded **10** (273 mg, 0.486 mmol, 45%) as red-brown crystals.

Anal. Calcd for C<sub>35</sub>H<sub>38</sub>N<sub>2</sub>NiO: C, 74.88; H, 6.82; N, 4.99. Found: C, 73.54; H, 6.69; N, 4.99.

<sup>1</sup>H NMR (CDCl<sub>3</sub>, 300.13 MHz):  $\delta$  7.40 (d, <sup>3</sup>*J* = 7.5 Hz, 2H, Ph), 7.28 (m, 1H, Ph), 7.12 (m, 4H, Ph and *m*-H), 6.97 (br. s, 2H, *m*-H), 6.95 (s, 2H, NCH), 4.28 (s, 5H, C<sub>5</sub>H<sub>5</sub>), 2.57 (q, <sup>3</sup>*J* = 6.0 Hz, 1H, CH(CH<sub>3</sub>)), 2.38 (s, 6H, *o*- or *p*-Me), 2.31 (s, 6H, *o*- or *p*-Me), 1.94 (s, 6H, *o*-Me), 0.72 (d, <sup>3</sup>*J* = 6.0 Hz, 3H, CH(CH<sub>3</sub>)).

<sup>13</sup>C{<sup>1</sup>H} NMR (CDCl<sub>3</sub>, 75.47 MHz):  $\delta$  207.8 (CO), 178.2 (NCN), 142.0, 139.1, 137.4, 136.0, 135.5, 129.6, 129.5, 127.6, 127.3, 124.4 (C<sub>Ar</sub> and NCH), 92.2 (C<sub>5</sub>H<sub>5</sub>), 21.2 (*p*-Me), 20.8 (CH(CH<sub>3</sub>)), 19.1 (*o*-Me), 18.3 (*o*-Me), 10.2 (CH(CH<sub>3</sub>)).

### IV.4. Synthesis of [Ni(IMes)PhCp] (**11**)

A solution of **2** (500 mg, 1.08 mmol) in THF (10 mL) was cooled to  $-78^{\circ}\text{C}$  before drop-wise addition of PhLi (1.8 M in Bu<sub>2</sub>O, 0.60 mL, 1.08 mmol). The reaction medium was then allowed to warm to room temperature, during which time a color change from violet to brown was observed. The reaction mixture was subsequently filtered over Celite, concentrated under vacuum to *ca.* 3 mL and treated with pentane (10 mL), to yield brown crystals after standing at  $-28^{\circ}\text{C}$  for 16 h. The crystals were washed with pentane (2  $\times$  10 mL) and dried under vacuum to give **11** (343 mg, 0.679 mmol, 63%).

Anal. Calcd for C<sub>32</sub>H<sub>34</sub>N<sub>2</sub>Ni: C, 76.06; H, 6.78; N, 5.54. Found: C, 75.96; H, 6.98; N, 5.38.

$^1\text{H}$  NMR ( $\text{CDCl}_3$ , 300.13 MHz):  $\delta$  6.98 (s, 4H, *m*-H), 6.83 (s, 2H, NCH), 6.80 (dd,  $^3J = 7.8$  Hz,  $^4J = 1.5$  Hz, 2H, Ph), 6.52 (tt,  $^3J = 7.1$  Hz,  $^4J$  n.r., 1H, Ph), 6.39 (t,  $^3J = 7.2$  Hz, 2H, Ph), 4.65 (s, 5H,  $\text{C}_5\text{H}_5$ ), 2.41 (s, 6H, *p*-Me), 1.98 (s, 12H, *o*-Me).

$^{13}\text{C}\{^1\text{H}\}$  NMR ( $\text{CDCl}_3$ , 75.47 MHz):  $\delta$  181.2 (NCN), 143.3, 141.5, 138.5, 137.4, 136.0, 129.1, 124.1, 123.1, 120.5 ( $\text{C}_{\text{Ar}}$  and NCH), 90.5 ( $\text{C}_5\text{H}_5$ ), 21.3 (*p*-Me), 18.4 (*o*-Me).

#### IV.5. X-ray diffraction study of (8) and (11): structure determination and refinement

Single crystals of **8** and **11** suitable for X-ray diffraction studies were selected from batches of crystals obtained at 4°C from an acetonitrile/diethylether solution, and at room temperature from a toluene/pentane solution, respectively. Diffraction data were collected at 173(2) K on a Bruker APEX II DUO KappaCCD area detector diffractometer equipped with an Oxford Cryosystem liquid  $\text{N}_2$  device using Mo- $\text{K}\alpha$  radiation ( $\lambda = 0.71073$  Å). A summary of crystal data, data collection parameters and structure refinements is given in **Table 4**. The crystal-detector distance was 38 mm. The cell parameters were determined (APEX2 software) from reflections taken from three sets of twelve frames, each at 10 s exposure. The structure was solved using direct methods with SHELXS-97 and refined against  $F^2$  for all reflections using the SHELXL-97 software.<sup>[73]</sup> A semi-empirical absorption correction was applied using SADABS in APEX2. All non-hydrogen atoms were refined with anisotropic displacement parameters, using weighted full-matrix least-squares on  $F^2$ . Hydrogen atoms were included in calculated positions and treated as riding atoms using SHELXL default parameters.

The asymmetric unit of **8** contains two independent cations of  $[\text{Ni}\{(i\text{Pr}_2\text{Ph})_2\text{NHC}\}(\text{NCMe})\text{Cp}]^+$ , two  $\text{PF}_6^-$  anions, and one molecule of acetonitrile. Squeeze instruction was used to suppress a second molecule of acetonitrile that exhibits too much disorder.



**Table 4.** X-Ray Crystallographic Data and Data Collection Parameters for **8** and **11**.

Complex	<b>8</b>	<b>11</b>
Empirical formula	$2(\text{C}_{34}\text{H}_{44}\text{N}_3\text{Ni}) \cdot 2(\text{F}_6\text{P}) \cdot \text{C}_2\text{H}_3\text{N}$	$\text{C}_{32}\text{H}_{34}\text{N}_2\text{Ni}$
Formula weight	1437.86	505.32
Crystal system	Monoclinic	Monoclinic
Space group	$\text{P}2_1/\text{c}$	$\text{P}2_1/\text{c}$
$a$ (Å)	36.2607 (19)	21.3657 (16)
$b$ (Å)	16.6530 (9)	8.2297 (7)
$c$ (Å)	12.6625 (7)	15.7213 (12)
$\beta$ (°)	97.198 (1)	104.982 (2)
$V$ (Å <sup>3</sup> )	7586.0 (7)	2670.4 (4)
$Z$	4	4
$D_{\text{calcd}}$ (Mg.m <sup>-3</sup> )	1.259	1.257
Absorp coeff (mm <sup>-1</sup> )	0.610	0.749
Crystal habit, color	Prism, green	Prism, red
Crystal size (mm)	$0.45 \times 0.25 \times 0.20$	$0.28 \times 0.20 \times 0.15$
$h, k, l_{\text{max}}$	47, 22, 16	29, 5, 21
$T_{\text{min}}, T_{\text{max}}$	0.771, 0.888	0.818, 0.896
Reflns collected	96242	19927
$R$ [ $I > 2\sigma(I)$ ]	0.0485	0.0432
$wR^2$ (all data)	0.1099	0.1136
GOF on $F^2$	1.058	1.004

IV.6. Optimization of the catalytic  $\alpha$ -arylation of ketones: solvent and base influence**Table 5.** Optimization for the  $\alpha$ -arylation of propiophenone with 4-bromotoluene catalyzed by **7**.<sup>a</sup>

Entry	Base	Solvent	Yield (%) <sup>b</sup>
1 <sup>c</sup>	-	Toluene	0
2	LiO <sup>t</sup> Bu	Toluene	21
3	LiO <sup>t</sup> Bu	Dioxane	21
4	NaO <sup>t</sup> Bu	Toluene	65
5 <sup>c</sup>	NaO <sup>t</sup> Bu	Toluene	78
6 <sup>d</sup>	NaO <sup>t</sup> Bu	Toluene	0
7	NaO <sup>t</sup> Bu	Dioxane	3
8	KO <sup>t</sup> Bu	Toluene	0
9	KO <sup>t</sup> Bu	Dioxane	0
10	NaH	Toluene	24
11	NaH	Dioxane	0
12	NaOH	Toluene	4
13	NaOH	Dioxane	0
14	Cs <sub>2</sub> CO <sub>3</sub>	Toluene	0
15	Cs <sub>2</sub> CO <sub>3</sub>	Dioxane	0
16	K <sub>3</sub> PO <sub>4</sub>	Toluene	1
17	K <sub>3</sub> PO <sub>4</sub>	Dioxane	0

<sup>a</sup> Reaction conditions: propiophenone (1.2 mmol), 4-bromotoluene (1.0 mmol), base (1.5 mmol), **7** (5 mol%), solvent (3 mL), reflux, 24 h. <sup>b</sup> Yields determined by GC; average value of two runs. <sup>c</sup> **7** (3 mol%). <sup>d</sup> Reactions run in the absence of **7**.

IV.7. General procedure for the catalytic  $\alpha$ -arylation of ketones

A 10 mL oven-dried Schlenk tube containing a stirring bar was loaded with **7** (16 mg, 0.03 mmol), NaO<sup>t</sup>Bu (144 mg, 1.50 mmol), the aryl halide (1.00 mmol), the ketone (1.20 mmol) and toluene (3 mL). The resulting suspension was stirred in a preheated oil bath at 110°C for 24 or 48 h. The reaction mixture was then quenched by the addition of a solution of

saturated aqueous  $\text{NH}_4\text{Cl}$  (10 mL), and the product extracted with  $\text{CH}_2\text{Cl}_2$  ( $3 \times 10$  mL). The combined organic layers were dried over anhydrous  $\text{MgSO}_4$ , filtered and concentrated under vacuum. The residue was then purified by column chromatography on silica gel (40–63  $\mu\text{m}$ ), eluting with toluene to provide the  $\alpha$ -arylated ketone. All yields are the average of at least two runs.

### IV.8. Control experiments

Each experiment described hereafter was performed twice.

#### IV.8.1. Investigation of the mercury effect

The experiment was performed as per the general procedure using 4-bromotoluene (171 mg, 1.00 mmol), propiophenone (160  $\mu\text{L}$ , 1.20 mmol), **7** (27 mg, 0.05 mmol), and mercury (100 mg, 0.50 mmol). GC analysis indicated 59% yield of 1-phenyl-2-(4-methylphenyl)-propan-1-one (*vs.* 65% yield without Hg).

#### IV.8.2. Reaction of complex (**10**) with 4-bromotoluene

A suspension of **10** (100 mg, 0.178 mmol) and 4-bromotoluene (31 mg, 0.181 mmol) in toluene (5 mL) was stirred at  $110^\circ\text{C}$  for 24 h, during which a color change from reddish to brown as well as the formation of a black solid were observed. The reaction medium was purified by flash silica column chromatography using toluene as eluent. Two fractions were collected: one contained propiophenone (15 mg, 0.112 mmol, 63%) and traces of 1-phenyl-2-(4-methylphenyl)-propan-1-one, and another yielded  $[\text{Ni}(\text{IMes})\text{BrCp}]$  as a violet solid after solvent removal.

ESI-MS:  $m/z$   $[\text{M}]^+$  calcd for  $\text{C}_{26}\text{H}_{29}\text{N}_2\text{NiBr}$  506.09, found 506.08; calcd for  $\text{C}_{26}\text{H}_{29}\text{N}_2\text{Ni}$  427.17, found 427.16.

$^1\text{H}$  NMR ( $\text{CDCl}_3$ , 300.13 MHz):  $\delta$  7.11 (s, 4H, *m*-H), 7.07 (s, 2H, NCH), 4.63 (s, 5H,  $\text{C}_5\text{H}_5$ ), 2.43 (s, 6H, *p*-Me), 2.19 (s, 12H, *o*-Me).

$^{13}\text{C}\{^1\text{H}\}$  NMR ( $\text{CDCl}_3$ , 75.47 MHz):  $\delta$  167.6 (NCN), 139.2, 136.8, 136.0, 129.4 ( $\text{C}_{\text{Ar}}$ ), 124.7 (NCH), 92.5 ( $\text{C}_5\text{H}_5$ ), 21.4 (*p*-Me), 18.9 (*o*-Me).

### IV.8.3. Catalytic $\alpha$ -arylation of propiophenone with **10** as pre-catalyst

The experiment was performed as per the general procedure using 4-bromotoluene (171 mg, 1.00 mmol), propiophenone (160  $\mu$ L, 1.20 mmol), and **10** (28 mg, 0.05 mmol). GC analysis indicated 11% yield of 1-phenyl-2-(4-methylphenyl)-propan-1-one (*vs.* 25% yield with **2**).

### IV.8.4. Reaction of complex **11** with propiophenone

To a suspension of **11** (70 mg, 0.139 mmol) and NaO<sup>t</sup>Bu (13 mg, 0.135 mmol) in toluene (5 mL) was added propiophenone (20  $\mu$ L, 0.150 mmol). The resulting mixture was stirred at 110°C for 24 h. No color change was observed. The reaction was then quenched by the addition of a saturated aqueous solution of NH<sub>4</sub>Cl (10 mL), and the product extracted with CH<sub>2</sub>Cl<sub>2</sub> (3  $\times$  10 mL). The combined organic layers were dried over anhydrous MgSO<sub>4</sub>, filtered and concentrated under vacuum. The resulting residue was then purified by flash silica column chromatography using toluene as eluent. No coupling product was collected, and 12 mg propiophenone (0.089 mmol, 59%) was recovered.

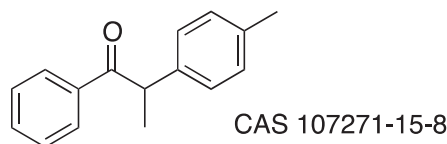
### IV.8.5. Investigation of radical scavenger effect

The experiments were performed as per the general procedure using 4-bromotoluene (171 mg, 1.00 mmol), propiophenone (160  $\mu$ L, 1.20 mmol), and TEMPO (156 mg, 1.00 mmol) or galvinoxyl (422 mg, 1.00 mmol). GC analyses indicated no conversion to 1-phenyl-2-(4-methylphenyl)-propan-1-one in both cases.

### IV.8.6. Investigation of radical initiator effect

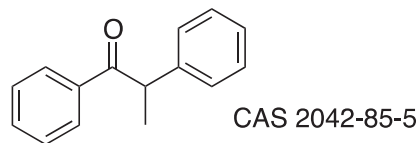
The experiments were performed as per the general procedure using 4-bromotoluene (171 mg, 1.00 mmol), propiophenone (160  $\mu$ L, 1.20 mmol), and AIBN (34 mg, 0.20 mmol), but without NaO<sup>t</sup>Bu and **7**. GC analyses indicated 5% yield of 1-phenyl-2-(4-methylphenyl)-propan-1-one. In the presence of **7** (16 mg, 0.03 mmol) and/or NaO<sup>t</sup>Bu (144 mg, 1.50 mmol), GC analyses indicated no conversion.

## IV.9. Spectral data of the coupling products

**1-phenyl-2-(4-methylphenyl)-propan-1-one**<sup>[74]</sup> (Table 2, entries 1 and 2)

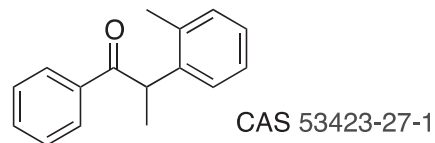
<sup>1</sup>H NMR (CDCl<sub>3</sub>, 300.13 MHz):  $\delta$  7.95 (d, <sup>3</sup>J = 7.2 Hz, 2H, H<sub>Ar</sub>), 7.47 (t, <sup>3</sup>J = 7.2 Hz, 1H, H<sub>Ar</sub>), 7.37 (d, <sup>3</sup>J = 7.3 Hz, 2H, H<sub>Ar</sub>), 7.17 (d, <sup>3</sup>J = 8.1 Hz, 2H, H<sub>Ar</sub>), 7.10 (d, <sup>3</sup>J = 7.8 Hz, 2H, H<sub>Ar</sub>), 4.65 (q, <sup>3</sup>J = 6.9 Hz, 1H, CH(CH<sub>3</sub>)), 2.28 (s, 3H, CH<sub>3</sub>), 1.51 (d, <sup>3</sup>J = 6.9 Hz, 3H, CH(CH<sub>3</sub>)).

<sup>13</sup>C{<sup>1</sup>H} NMR (CDCl<sub>3</sub>, 75.47 MHz):  $\delta$  200.5 (CO), 138.6, 136.7, 136.6, 132.8, 129.8, 128.9, 128.6, 127.7 (C<sub>Ar</sub>), 47.6 (CH(CH<sub>3</sub>)), 21.1 (CH<sub>3</sub>), 19.6 (CH(CH<sub>3</sub>)).

**1,2-diphenylpropan-1-one**<sup>[74]</sup> (Table 2, entries 3 and 4)

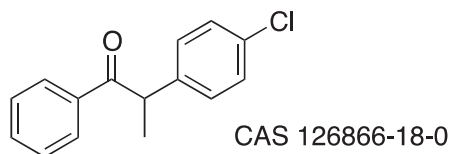
<sup>1</sup>H NMR (CDCl<sub>3</sub>, 300.13 MHz):  $\delta$  7.93 (d, <sup>3</sup>J = 7.2 Hz, 2H, H<sub>Ar</sub>), 7.45 (t, <sup>3</sup>J = 7.5 Hz, 1H, H<sub>Ar</sub>), 7.35 (t, <sup>3</sup>J = 7.5 Hz, 2H, H<sub>Ar</sub>), 7.27–7.24 (m, 4H, H<sub>Ar</sub>), 7.19 (m, 1H, H<sub>Ar</sub>), 4.66 (q, <sup>3</sup>J = 6.9 Hz, 1H, CH(CH<sub>3</sub>)), 1.51 (d, <sup>3</sup>J = 6.9 Hz, 3H, CH(CH<sub>3</sub>)).

<sup>13</sup>C{<sup>1</sup>H} NMR (CDCl<sub>3</sub>, 75.47 MHz):  $\delta$  200.4 (CO), 141.6, 136.6, 132.9, 129.1, 128.9, 128.6, 127.9, 127.0 (C<sub>Ar</sub>), 48.0 (CH(CH<sub>3</sub>)), 19.6 (CH(CH<sub>3</sub>)).

**1-phenyl-2-(2-methylphenyl)-propan-1-one**<sup>[74]</sup> (Table 2, entries 5 and 6)

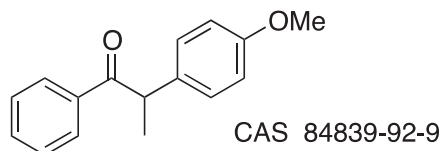
<sup>1</sup>H NMR (CDCl<sub>3</sub>, 400.14 MHz):  $\delta$  7.82 (d, <sup>3</sup>J = 7.2 Hz, 2H, H<sub>Ar</sub>), 7.45 (t, <sup>3</sup>J = 7.4 Hz, 1H, H<sub>Ar</sub>), 7.35 (t, <sup>3</sup>J = 7.8 Hz, 2H, H<sub>Ar</sub>), 7.20 (d, <sup>3</sup>J = 6.8 Hz, 1H, H<sub>Ar</sub>), 7.10 (m, 2H, H<sub>Ar</sub>), 7.02 (dd, <sup>3</sup>J = 7.2 Hz, <sup>4</sup>J = 2.0 Hz, 1H, H<sub>Ar</sub>), 4.76 (q, <sup>3</sup>J = 6.8 Hz, 1H, CH(CH<sub>3</sub>)), 2.50 (s, 3H, CH<sub>3</sub>), 1.47 (d, <sup>3</sup>J = 6.8 Hz, 3H, CH(CH<sub>3</sub>)).

<sup>13</sup>C{<sup>1</sup>H} NMR (CDCl<sub>3</sub>, 100.61 MHz):  $\delta$  201.1 (CO), 140.3, 136.7, 134.7, 132.8, 131.1, 128.6, 127.1, 127.0, 126.9 (C<sub>Ar</sub>), 44.7 (CH(CH<sub>3</sub>)), 19.8 and 18.2 (*o*-CH<sub>3</sub> and CH(CH<sub>3</sub>)).

**1-phenyl-2-(4-chlorophenyl)-propan-1-one**<sup>[75]</sup> (Table 2, entry 7)

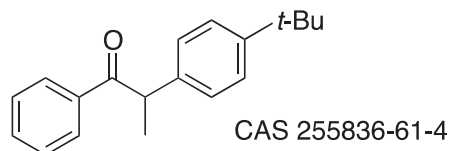
<sup>1</sup>H NMR (CDCl<sub>3</sub>, 300.14 MHz):  $\delta$  7.93 (d, <sup>3</sup>*J* = 7.2 Hz, 2H, H<sub>Ar</sub>), 7.50 (t, <sup>3</sup>*J* = 7.4 Hz, 1H, H<sub>Ar</sub>), 7.39 (t, <sup>3</sup>*J* = 7.4 Hz, 2H, H<sub>Ar</sub>), 7.27 (d, <sup>3</sup>*J* = 8.7 Hz, 2H, H<sub>Ar</sub>), 7.22 (d, <sup>3</sup>*J* = 8.7 Hz, 2H, H<sub>Ar</sub>), 4.67 (q, <sup>3</sup>*J* = 6.8 Hz, 1H, CH(CH<sub>3</sub>)), 1.52 (d, <sup>3</sup>*J* = 6.9 Hz, 3H, CH(CH<sub>3</sub>)).

<sup>13</sup>C{<sup>1</sup>H} NMR (CDCl<sub>3</sub>, 75.47 MHz):  $\delta$  200.1 (CO), 140.0, 136.4, 133.1, 133.0, 129.3, 128.8, 128.7 (C<sub>Ar</sub>), 47.3 (CH(CH<sub>3</sub>)), 19.6 (CH(CH<sub>3</sub>)).

**1-phenyl-2-(4-methoxyphenyl)-propan-1-one**<sup>[74]</sup> (Table 2, entries 8 and 9)

<sup>1</sup>H NMR (CDCl<sub>3</sub>, 400.14 MHz):  $\delta$  7.95 (d, <sup>3</sup>*J* = 7.6 Hz, 2H, H<sub>Ar</sub>), 7.47 (t, <sup>3</sup>*J* = 7.2 Hz, 1H, H<sub>Ar</sub>), 7.38 (t, <sup>3</sup>*J* = 7.6 Hz, 2H, H<sub>Ar</sub>), 7.20 (d, <sup>3</sup>*J* = 8.4 Hz, 2H, H<sub>Ar</sub>), 6.83 (d, <sup>3</sup>*J* = 8.8 Hz, 2H, H<sub>Ar</sub>), 4.64 (q, <sup>3</sup>*J* = 6.8 Hz, 1H, CH(CH<sub>3</sub>)), 3.75 (s, 3H, OCH<sub>3</sub>), 1.51 (d, <sup>3</sup>*J* = 6.8 Hz, 3H, CH(CH<sub>3</sub>)).

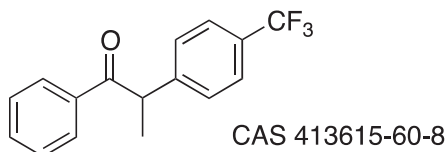
<sup>13</sup>C{<sup>1</sup>H} NMR (CDCl<sub>3</sub>, 100.61 MHz):  $\delta$  200.7 (CO), 158.6 (OC<sub>Ar</sub>), 136.7, 133.6, 132.8, 128.9, 128.9, 128.6, 114.5 (C<sub>Ar</sub>), 55.4 (OCH<sub>3</sub>), 47.1 (CH(CH<sub>3</sub>)), 19.7 (CH(CH<sub>3</sub>)).

**1-phenyl-2-(4-*tert*-butylphenyl)-propan-1-one**<sup>[75]</sup> (Table 2, entries 10 and 11)

<sup>1</sup>H NMR (CDCl<sub>3</sub>, 300.13 MHz):  $\delta$  7.98 (d, <sup>3</sup>*J* = 7.2 Hz, 2H, H<sub>Ar</sub>), 7.49 (t, <sup>3</sup>*J* = 7.3 Hz, 1H, H<sub>Ar</sub>), 7.39 (t, <sup>3</sup>*J* = 7.3 Hz, 2H, H<sub>Ar</sub>), 7.31 (d, <sup>3</sup>*J* = 8.4 Hz, 2H, H<sub>Ar</sub>), 7.22 (d, <sup>3</sup>*J* = 8.4 Hz, 2H, H<sub>Ar</sub>), 4.69 (q, <sup>3</sup>*J* = 6.9 Hz, 1H, CH(CH<sub>3</sub>)), 1.53 (d, <sup>3</sup>*J* = 6.9 Hz, 3H, CH(CH<sub>3</sub>)), 1.28 (s, 9H, C(CH<sub>3</sub>)<sub>3</sub>).

<sup>13</sup>C{<sup>1</sup>H} NMR (CDCl<sub>3</sub>, 75.47 MHz):  $\delta$  200.6 (CO), 149.8, 138.3, 136.7, 132.8, 128.6, 128.6, 127.5, 126.0 (C<sub>Ar</sub>), 47.3 (CH(CH<sub>3</sub>)), 34.5 (C(CH<sub>3</sub>)<sub>3</sub>), 31.4 (C(CH<sub>3</sub>)<sub>3</sub>), 19.6 (CH(CH<sub>3</sub>)).

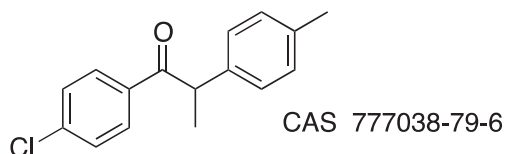
**1-phenyl-2-[(4-trifluoromethyl)phenyl]-propan-1-one**<sup>[76]</sup> (Table 2, entry 12)



<sup>1</sup>H NMR (CDCl<sub>3</sub>, 300.13 MHz):  $\delta$  7.94 (dt, <sup>3</sup>*J* = 7.2 Hz, <sup>4</sup>*J* n.r., 2H, H<sub>Ar</sub>), 7.56 (d, <sup>3</sup>*J* = 8.4 Hz, 2H, H<sub>Ar</sub>), 7.50 (d, <sup>3</sup>*J* = 7.2 Hz, <sup>4</sup>*J* n.r., 1H, H<sub>Ar</sub>), 7.43–7.38 (m, 4H, H<sub>Ar</sub>), 4.77 (q, <sup>3</sup>*J* = 6.9 Hz, 1H, CH(CH<sub>3</sub>)), 1.56 (d, <sup>3</sup>*J* = 6.9 Hz, 3H, CH(CH<sub>3</sub>)).

<sup>13</sup>C{<sup>1</sup>H} NMR (CDCl<sub>3</sub>, 100.61 MHz):  $\delta$  199.8 (CO), 145.5, 136.3, 133.3, 132.8, 128.9, 128.8, 128.3 (C<sub>Ar</sub>), 126.1 (q, <sup>1</sup>*J*<sub>CF</sub> = 3.2 Hz, CF<sub>3</sub>), 47.7 (CH(CH<sub>3</sub>)), 19.6 (CH(CH<sub>3</sub>)).

**1-(4-chlorophenyl)-2-(4-methylphenyl)-propan-1-one** (Table 2, entries 13 and 14)

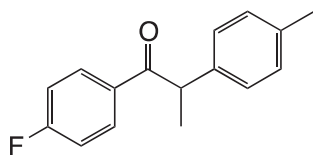


ESI-HRMS: *m/z* [M]<sup>+</sup> calcd for C<sub>16</sub>H<sub>15</sub>ClONa 281.0704, found 281.0695.

<sup>1</sup>H NMR (CDCl<sub>3</sub>, 300.13 MHz):  $\delta$  7.87 (ddd, <sup>3</sup>*J* = 8.7 Hz, <sup>4</sup>*J* = 2.4 Hz, <sup>5</sup>*J* = 2.0 Hz, 2H, H<sub>Ar</sub>), 7.33 (ddd, <sup>3</sup>*J* = 8.7 Hz, <sup>4</sup>*J* = 2.4 Hz, <sup>5</sup>*J* = 2.0 Hz, 2H, H<sub>Ar</sub>), 7.12 (m, 4H, H<sub>Ar</sub>), 4.57 (q, <sup>3</sup>*J* = 6.9 Hz, 1H, CH(CH<sub>3</sub>)), 2.29 (s, 3H, CH<sub>3</sub>), 1.50 (d, <sup>3</sup>*J* = 6.9 Hz, 3H, CH(CH<sub>3</sub>)).

<sup>13</sup>C{<sup>1</sup>H} NMR (CDCl<sub>3</sub>, 100.61 MHz):  $\delta$  199.3 (CO), 139.2, 138.3, 136.9, 134.9, 130.3, 129.9, 128.9, 127.7 (C<sub>Ar</sub>), 47.8 (CH(CH<sub>3</sub>)), 21.2 (CH<sub>3</sub>), 19.6 (CH(CH<sub>3</sub>)).

**1-(4-fluorophenyl)-2-(4-methylphenyl)-propan-1-one** (Table 2, entry 15)



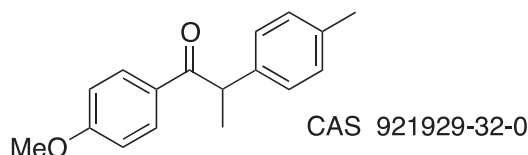
Anal. Calcd for C<sub>16</sub>H<sub>15</sub>FO: C, 79.32; H, 6.24. Found: C, 79.34; H, 6.38.

<sup>1</sup>H NMR (CDCl<sub>3</sub>, 400.14 MHz):  $\delta$  7.89 (m, <sup>3</sup>*J* = 8.8 Hz, <sup>4</sup>*J* = 2.0 Hz, <sup>4</sup>*J*<sub>HF</sub> = 5.6 Hz, 2H, H<sub>ArF</sub>), 7.07 (d, <sup>3</sup>*J* = 8.2 Hz, 2H, H<sub>Ar</sub>), 7.02 (d, <sup>3</sup>*J* = 8.2 Hz, 2H, H<sub>Ar</sub>), 6.95 (m, <sup>3</sup>*J* = 8.8 Hz, <sup>4</sup>*J* = 2.0 Hz, <sup>3</sup>*J*<sub>HF</sub> = 6.6 Hz, 2H, H<sub>ArF</sub>), 4.51 (q, <sup>3</sup>*J* = 6.8 Hz, 1H, CH(CH<sub>3</sub>)), 2.21 (s, 3H, CH<sub>3</sub>), 1.42 (d, <sup>3</sup>*J* = 6.8 Hz, 3H, CH(CH<sub>3</sub>)).

<sup>13</sup>C{<sup>1</sup>H} NMR (CDCl<sub>3</sub>, 75.47 MHz):  $\delta$  198.9 (CO), 165.5 (d, <sup>1</sup>*J*<sub>CF</sub> = 254.4 Hz, C<sub>ArF</sub>), 138.5, 136.8 (C<sub>Ar</sub>), 133.0 (d, <sup>4</sup>*J*<sub>CF</sub> = 2.4 Hz, C<sub>ArF</sub>), 131.5 (d, <sup>3</sup>*J*<sub>CF</sub> = 9.3 Hz, C<sub>ArF</sub>), 129.9, 127.7 (C<sub>Ar</sub>),

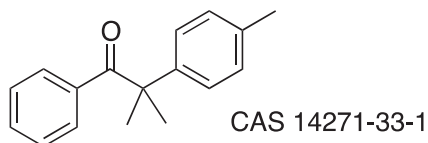
115.7 (d,  $^2J_{\text{CF}} = 21.9$  Hz,  $\text{C}_{\text{ArF}}$ ), 47.7 ( $\text{CH}(\text{CH}_3)$ ), 21.1 ( $\text{CH}_3$ ), 19.6 ( $\text{CH}(\text{CH}_3)$ ).  $^{19}\text{F}\{^1\text{H}\}$  NMR ( $\text{CDCl}_3$ , 376 MHz):  $\delta$  –105.70 (s, F).

**1-(4-methoxyphenyl)-2-(4-methylphenyl)-propan-1-one**<sup>[77]</sup> (Table 2, entries 16 and 17)



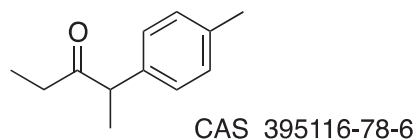
$^1\text{H}$  NMR ( $\text{CDCl}_3$ , 400.14 MHz):  $\delta$  7.95 (d,  $^3J = 8.8$  Hz, 2H,  $\text{H}_{\text{Ar}}$ ), 7.18 (d,  $^3J = 8.0$  Hz, 2H,  $\text{H}_{\text{Ar}}$ ), 7.10 (d,  $^3J = 8.0$  Hz, 2H,  $\text{H}_{\text{Ar}}$ ), 6.85 (d,  $^3J = 8.8$  Hz, 2H,  $\text{H}_{\text{Ar}}$ ), 4.61 (q,  $^3J = 6.8$  Hz, 1H,  $\text{CH}(\text{CH}_3)$ ), 3.81 (s, 3H,  $\text{OCH}_3$ ), 2.28 (s, 3H,  $\text{CH}_3$ ), 1.50 (d,  $^3J = 6.8$  Hz, 3H,  $\text{CH}(\text{CH}_3)$ ).  $^{13}\text{C}\{^1\text{H}\}$  NMR ( $\text{CDCl}_3$ , 100.61 MHz):  $\delta$  199.1 (CO), 163.2 ( $\text{OC}_{\text{Ar}}$ ), 139.0, 136.5, 131.1, 129.7, 129.6, 127.7, 113.7 ( $\text{C}_{\text{Ar}}$ ), 55.5 ( $\text{OCH}_3$ ), 47.2 ( $\text{CH}(\text{CH}_3)$ ), 21.1 ( $\text{CH}_3$ ), 19.7 ( $\text{CH}(\text{CH}_3)$ ).

**1-phenyl-2-methyl-2-(4-methylphenyl)-propan-1-one**<sup>[78]</sup> (Table 2, entries 18 and 19)



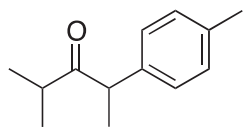
$^1\text{H}$  NMR ( $\text{CDCl}_3$ , 300.13 MHz):  $\delta$  7.49 (dd,  $^3J = 8.4$  Hz, 2H,  $\text{H}_{\text{Ar}}$ ), 7.36 (tt,  $^3J = 7.3$  Hz, 1H,  $\text{H}_{\text{Ar}}$ ), 7.25–7.14 (m, 6H,  $\text{H}_{\text{Ar}}$ ), 2.34 (s, 3H,  $\text{CH}_3$ ), 1.58 (s, 6H,  $\text{C}(\text{CH}_3)_2$ ).  $^{13}\text{C}\{^1\text{H}\}$  NMR ( $\text{CDCl}_3$ , 100.61 MHz):  $\delta$  204.1 (CO), 142.3, 136.5, 131.7, 129.8, 128.9, 128.0, 125.7 ( $\text{C}_{\text{Ar}}$ ), 51.2 ( $\text{C}(\text{CH}_3)_2$ ), 28.0 ( $\text{C}(\text{CH}_3)_2$ ), 21.2 ( $\text{CH}_3$ ).

**2-(4-methylphenyl)-pentan-3-one**<sup>[79]</sup> (Table 2, entries 21 and 22)



$^1\text{H}$  NMR ( $\text{CDCl}_3$ , 300.13 MHz):  $\delta$  7.14 (d,  $^3J = 8.4$  Hz, 2H,  $\text{H}_{\text{Ar}}$ ), 7.09 (d,  $^3J = 8.4$  Hz, 2H,  $\text{H}_{\text{Ar}}$ ), 3.72 (q,  $^3J = 6.9$  Hz, 1H,  $\text{CH}(\text{CH}_3)$ ), 2.37 (m,  $^3J = 7.5$  Hz, 2H,  $\text{CH}_2\text{CH}_3$ ), 2.33 (s, 3H,  $\text{CH}_3$ ), 1.37 (d,  $^3J = 6.9$  Hz, 3H,  $\text{CH}(\text{CH}_3)$ ), 0.96 (t,  $^3J = 7.5$  Hz, 3H,  $\text{CH}_2\text{CH}_3$ ).  $^{13}\text{C}\{^1\text{H}\}$  NMR ( $\text{CDCl}_3$ , 100.61 MHz):  $\delta$  211.9 (CO), 138.1, 136.9, 129.7, 127.8 ( $\text{C}_{\text{Ar}}$ ), 52.4 ( $\text{CH}(\text{CH}_3)$ ), 34.3 ( $\text{CH}_2\text{CH}_3$ ), 21.2 ( $\text{CH}_3$ ), 17.7 ( $\text{CH}(\text{CH}_3)$ ), 8.1 ( $\text{CH}_2\text{CH}_3$ ).

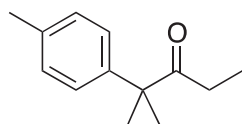


**2-(4-methylphenyl)-4-methyl-pentan-3-one** (Table 2, entry 23)

ESI-HRMS:  $m/z$   $[M]^+$  calcd for  $C_{13}H_{18}ONa$  213.1250, found 213.1241.

$^1H$  NMR ( $CDCl_3$ , 400.14 MHz):  $\delta$  7.16–7.08 (m, 4H,  $H_{Ar}$ ), 3.88 (q,  $^3J = 6.8$  Hz, 1H,  $CH(CH_3)$ ), 2.68 (sept.,  $^3J = 6.8$  Hz, 1H,  $CH(CH_3)_2$ ), 2.32 (s, 3H,  $CH_3$ ), 1.35 (d,  $^3J = 6.8$  Hz, 3H,  $CH(CH_3)$ ), 1.07 (d,  $^3J = 6.8$  Hz, 3H,  $CH(CH_3)_2$ ), 0.91 (d,  $^3J = 6.8$  Hz, 3H,  $CH(CH_3)_2$ ).

$^{13}C\{^1H\}$  NMR ( $CDCl_3$ , 100.61 MHz):  $\delta$  215.0 (CO), 137.9, 136.8, 129.7, 128.0 ( $C_{Ar}$ ), 50.9 ( $CH(CH_3)$ ), 39.2 ( $CH(CH_3)_2$ ), 21.2 ( $CH_3$ ), 19.4 ( $CH(CH_3)_2$ ), 18.4 and 18.3 ( $CH(CH_3)_2$  and  $CH(CH_3)$ ).

**2-(4-methylphenyl)-2-methyl-pentan-3-one** (Table 2, entry 23)

ESI-HRMS:  $m/z$   $[M]^+$  calcd for  $C_{13}H_{18}ONa$  213.1250, found 213.1241.

$^1H$  NMR ( $CDCl_3$ , 400.14 MHz):  $\delta$  7.16–7.08 (m, 4H,  $H_{Ar}$ ), 2.33 (s, 3H,  $CH_3$ ), 2.22 (q,  $^3J = 7.4$  Hz, 2H,  $CH_2CH_3$ ), 1.46 (s, 6H,  $C(CH_3)_2$ ), 0.93 (t,  $^3J = 7.4$  Hz, 3H,  $CH_2CH_3$ ).

$^{13}C\{^1H\}$  NMR ( $CDCl_3$ , 100.61 MHz):  $\delta$  214.3 (CO), 141.5, 136.5, 129.5, 126.0 ( $C_{Ar}$ ), 52.0 ( $C(CH_3)_2$ ), 30.7 ( $CH_2CH_3$ ), 25.4 ( $C(CH_3)_2$ ), 21.1 ( $CH_3$ ), 8.8 ( $CH_2CH_3$ ).

**V. References**

- [1] R. K. Norris, in *Compr. Org. Synth.* (Eds.: B.M. Trost, I. Fleming), Pergamon, Oxford, **1991**, pp. 451–482.
- [2] J. Morgan, J. T. Pinhey, B. A. Rowe, *J. Chem. Soc. Perkin Trans I* **1997**, 1005–1008.
- [3] J. H. Ryan, P. J. Stang, *Tetrahedron Lett.* **1997**, 38, 5061–5064.
- [4] T. Mino, T. Matsuda, K. Maruhashi, M. Yamashita, *Organometallics* **1997**, 16, 3241–3242.
- [5] T. Satoh, Y. Kawamura, M. Miura, M. Nomura, *Angew. Chem., Int. Ed. Engl.* **1997**, 36, 1740–1742.
- [6] M. Palucki, S. L. Buchwald, *J. Am. Chem. Soc.* **1997**, 119, 11108–11109.

- [7] B. C. Hamann, J. F. Hartwig, *J. Am. Chem. Soc.* **1997**, *119*, 12382–12383.
- [8] M. Miura, M. Nomura, in *Cross-Coupling React.*, Springer, **2002**, pp. 211–241.
- [9] D. A. Culkin, J. F. Hartwig, *Acc. Chem. Res.* **2003**, *36*, 234–245.
- [10] C. C. C. Johansson, T. J. Colacot, *Angew. Chem. Int. Ed.* **2010**, *49*, 676–707.
- [11] F. Bellina, R. Rossi, *Chem. Rev.* **2010**, *110*, 1082–1146.
- [12] D. W. Old, J. P. Wolfe, S. L. Buchwald, *J. Am. Chem. Soc.* **1998**, *120*, 9722–9723.
- [13] T. Satoh, J. Inoh, Y. Kawamura, Y. Kawamura, M. Miura, M. Nomura, *Bull. Chem. Soc. Jpn.* **1998**, *71*, 2239–2246.
- [14] W. A. Moradi, S. L. Buchwald, *J. Am. Chem. Soc.* **2001**, *123*, 7996–8002.
- [15] O. Gaertzen, S. L. Buchwald, *J. Org. Chem.* **2002**, *67*, 465–475.
- [16] H. N. Nguyen, X. Huang, S. L. Buchwald, *J. Am. Chem. Soc.* **2003**, *125*, 11818–11819.
- [17] M. R. Biscoe, S. L. Buchwald, *Org. Lett.* **2009**, *11*, 1773–1775.
- [18] S. Lee, N. A. Beare, J. F. Hartwig, *J. Am. Chem. Soc.* **2001**, *123*, 8410–8411.
- [19] X. Liu, J. F. Hartwig, *Org. Lett.* **2003**, *5*, 1915–1918.
- [20] T. Hama, J. F. Hartwig, *Org. Lett.* **2008**, *10*, 1545–1548.
- [21] T. Hama, J. F. Hartwig, *Org. Lett.* **2008**, *10*, 1549–1552.
- [22] K. H. Shaughnessy, B. C. Hamann, J. F. Hartwig, *J. Org. Chem.* **1998**, *63*, 6546–6553.
- [23] S. Lee, J. F. Hartwig, *J. Org. Chem.* **2001**, *66*, 3402–3415.
- [24] T. Hama, D. A. Culkin, J. F. Hartwig, *J. Am. Chem. Soc.* **2006**, *128*, 4976–4985.
- [25] J. Cossy, A. de Filippis, D. G. Pardo, *Org. Lett.* **2003**, *5*, 3037–3039.
- [26] A. de Filippis, D. Gomez Pardo, J. Cossy, *Tetrahedron* **2004**, *60*, 9757–9767.
- [27] T. Y. Zhang, H. Zhang, *Tetrahedron Lett.* **2002**, *43*, 193–195.
- [28] C. Zhang, J. Huang, M. L. Trudell, S. P. Nolan, *J. Org. Chem.* **1999**, *64*, 3804–3805.
- [29] H. Muratake, H. Nakai, *Tetrahedron Lett.* **1999**, *40*, 2355–2358.
- [30] H. Muratake, M. Natsume, H. Nakai, *Tetrahedron* **2004**, *60*, 11783–11803.
- [31] Y. Terao, Y. Fukuoka, T. Satoh, M. Miura, M. Nomura, *Tetrahedron Lett.* **2002**, *43*, 101–104.
- [32] G. D. Vo, J. F. Hartwig, *Angew. Chem. Int. Ed.* **2008**, *47*, 2127–2130.
- [33] R. Martín, S. L. Buchwald, *Angew. Chem. Int. Ed.* **2007**, *46*, 7236–7239.
- [34] V. Lavallo, Y. Canac, C. Präsang, B. Donnadieu, G. Bertrand, *Angew. Chem. Int. Ed.* **2005**, *44*, 5705–5709.
- [35] J. You, J. G. Verkade, *J. Org. Chem.* **2003**, *68*, 8003–8007.

- [36] J. You, J. G. Verkade, *Angew. Chem. Int. Ed.* **2003**, *42*, 5051–5053.
- [37] L. Wu, J. F. Hartwig, *J. Am. Chem. Soc.* **2005**, *127*, 15824–15832.
- [38] P. G. Alsabeh, M. Stradiotto, *Angew. Chem. Int. Ed.* **2013**, *52*, 7242–7246.
- [39] D. A. Culkin, J. F. Hartwig, *J. Am. Chem. Soc.* **2001**, *123*, 5816–5817.
- [40] X. Liao, Z. Weng, J. F. Hartwig, *J. Am. Chem. Soc.* **2008**, *130*, 195–200.
- [41] G. Danoun, A. Tlili, F. Monnier, M. Taillefer, *Angew. Chem. Int. Ed.* **2012**, *51*, 12815–12819.
- [42] M. F. Semmelhack, R. D. Stauffer, T. D. Rogerson, *Tetrahedron Lett.* **1973**, *14*, 4519–4522.
- [43] M. F. Semmelhack, B. P. Chong, R. D. Stauffer, T. D. Rogerson, A. Chong, L. D. Jones, *J. Am. Chem. Soc.* **1975**, *97*, 2507–2516.
- [44] D. J. Spielvogel, S. L. Buchwald, *J. Am. Chem. Soc.* **2002**, *124*, 3500–3501.
- [45] G. Chen, F. Y. Kwong, H. O. Chan, W.-Y. Yu, A. S. C. Chan, *Chem. Commun.* **2006**, 1413–1415.
- [46] S. Ge, J. F. Hartwig, *J. Am. Chem. Soc.* **2011**, *133*, 16330–16333.
- [47] K. Matsubara, K. Ueno, Y. Koga, K. Hara, *J. Org. Chem.* **2007**, *72*, 5069–5076.
- [48] A. M. Oertel, V. Ritleng, M. J. Chetcuti, L. F. Veiros, *J. Am. Chem. Soc.* **2010**, *132*, 13588–13589.
- [49] A. M. Oertel, J. Freudenreich, J. Gein, V. Ritleng, L. F. Veiros, M. J. Chetcuti, *Organometallics* **2011**, *30*, 3400–3411.
- [50] A. M. Oertel, V. Ritleng, A. Busiah, L. F. Veiros, M. J. Chetcuti, *Organometallics* **2011**, *30*, 6495–6498.
- [51] M. A. Bennett, G. B. Robertson, P. O. Whimp, T. Yoshida, *J. Am. Chem. Soc.* **1973**, *95*, 3028–3030.
- [52] Y.-S. Lin, H. Misawa, J. Yamada, K. Matsumoto, *J. Am. Chem. Soc.* **2001**, *123*, 569–575.
- [53] D. A. Culkin, J. F. Hartwig, *Organometallics* **2004**, *23*, 3398–3416.
- [54] J. Vicente, A. Arcas, J. M. Fernández-Hernández, A. Sironi, N. Masciocchi, *Chem. Commun.* **2005**, 1267–1269.
- [55] J. Vicente, A. Arcas, J. M. Fernández-Hernández, D. Bautista, *Organometallics* **2008**, *27*, 3978–3985.
- [56] E. R. Burkhardt, R. G. Bergman, C. H. Heathcock, *Organometallics* **1990**, *9*, 30–44.

- [57] J. Cámpora, C. M. Maya, P. Palma, E. Carmona, E. Gutiérrez-Puebla, C. Ruiz, *J. Am. Chem. Soc.* **2003**, *125*, 1482–1483.
- [58] J. Cámpora, C. M. Maya, P. Palma, E. Carmona, E. Gutiérrez, C. Ruiz, C. Graiff, A. Tiripicchio, *Chem. Eur. J.* **2005**, *11*, 6889–6904.
- [59] D. Matt, M. Huhn, J. Fischer, A. D. Cian, W. Kläui, I. Tkatchenko, M. C. Bonnet, *J. Chem. Soc. Dalton Trans.* **1993**, 1173–1178.
- [60] J. Cámpora, C. M. Maya, P. Palma, E. Carmona, C. Graiff, A. Tiripicchio, *Chem. Commun.* **2003**, 1742–1743.
- [61] B. E. Ketz, X. G. Ottenwaelder, R. M. Waymouth, *Chem. Commun.* **2005**, 5693–5695.
- [62] J. Cámpora, I. Matas, P. Palma, E. Álvarez, C. Graiff, A. Tiripicchio, *Organometallics* **2007**, *26*, 5712–5721.
- [63] C. D. Abernethy, H. Alan, R. A. Jones, *J. Organomet. Chem.* **2000**, *596*, 3–5.
- [64] A. M. Oertel, V. Ritleng, M. J. Chetcuti, *Organometallics* **2012**, *31*, 2829–2840.
- [65] R. A. Kelly III, N. M. Scott, S. Díez-González, E. D. Stevens, S. P. Nolan, *Organometallics* **2005**, *24*, 3442–3447.
- [66] V. Ritleng, C. Barth, E. Brenner, S. Milosevic, M. J. Chetcuti, *Organometallics* **2008**, *27*, 4223–4228.
- [67] V. Ritleng, A. M. Oertel, M. J. Chetcuti, *Dalton Trans.* **2010**, *39*, 8153–8160.
- [68] J. A. Widegren, R. G. Finke, *J. Mol. Catal. A* **2003**, *198*, 317–341.
- [69] R. H. Crabtree, *Chem. Rev.* **2012**, *112*, 1536–1554.
- [70] C. D. Abernethy, Alan H, Cowley, R. A. Jones, *J. Organomet. Chem.* **2000**, *596*, 3–5.
- [71] S. L. Zultanski, G. C. Fu, *J. Am. Chem. Soc.* **2013**, *135*, 624–627.
- [72] V. Ritleng, E. Brenner, M. J. Chetcuti, *J. Chem. Educ.* **2008**, *85*, 1646–1648.
- [73] G. M. Sheldrick, *Acta Crystallogr. A* **2008**, *64*, 112–122.
- [74] G. Adjabeng, T. Brenstrum, C. S. Frampton, A. J. Robertson, J. Hillhouse, J. McNulty, A. Capretta, *J. Org. Chem.* **2004**, *69*, 5082–5086.
- [75] G. A. Grasa, T. J. Colacot, *Org. Lett.* **2007**, *9*, 5489–5492.
- [76] N. Marion, E. C. Ecarnot, O. Navarro, D. Amoroso, A. Bell, S. P. Nolan, *J. Org. Chem.* **2006**, *71*, 3816–3821.
- [77] L. Ackermann, J. H. Spatz, C. J. Gschrei, R. Born, A. Althammer, *Angew. Chem. Int. Ed.* **2006**, *45*, 7627–7630.
- [78] J. A. Landgrebe, A. G. Kirk, *J. Org. Chem.* **1967**, *32*, 3499–3506.
- [79] A. Ehrentraut, A. Zapf, M. Beller, *Adv. Synth. Catal.* **2002**, *344*, 209–217.

## **Chapter III.**

# **Ni–NHC-catalyzed hydrosilylation of Carbon–Heteroatom double bonds**



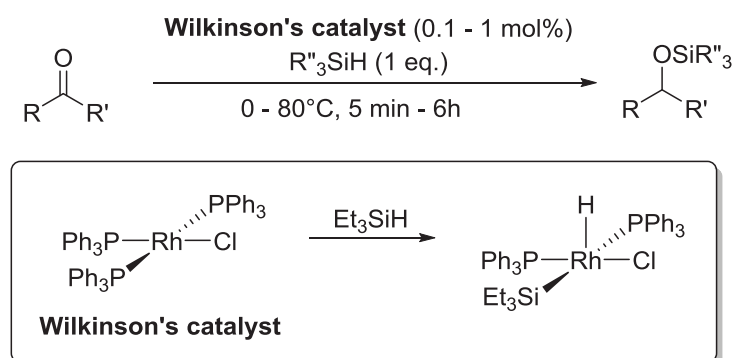
# Chapter III.

## Ni–NHC-catalyzed hydrosilylation of Carbon–Heteroatom double bonds

<b>I.</b>	<b>Introduction .....</b>	<b>102</b>
<b>II.</b>	<b>Results and Discussion .....</b>	<b>103</b>
II.1.	Hydrosilylation of aldehydes <sup>[39]</sup> .....	103
II.2.	Hydrosilylation of ketones <sup>[39]</sup> .....	107
II.3.	Hydrosilylation of aldimines <sup>[45]</sup> .....	109
II.4.	Hydrosilylation of ketimines <sup>[45]</sup> .....	114
II.5.	Mechanistic studies <sup>[39,45]</sup> .....	116
	<i>II.5.1. (1)-NaHBEt<sub>3</sub> catalytic system .....</i>	<i>116</i>
	<i>II.5.2. (4)-no additive catalytic system.....</i>	<i>120</i>
<b>III.</b>	<b>Conclusion .....</b>	<b>125</b>
<b>IV.</b>	<b>Experimental section .....</b>	<b>125</b>
IV.1.	General information.....	125
IV.2.	Synthesis of [Ni(IMes)HCp] (9).....	126
IV.3.	Reactions of [Ni(IMes)(NCMe)Cp](PF <sub>6</sub> ) (4) and Ph <sub>2</sub> SiH <sub>2</sub> .....	127
IV.4.	X-ray diffraction study of (9): structure determination and refinement.....	128
IV.5.	Hydrosilylation of aldehydes and ketones.....	129
	<i>IV.5.1. Optimization studies.....</i>	<i>129</i>
	<i>IV.5.2. General procedure: nickel-catalyzed hydrosilylation of aldehydes.....</i>	<i>129</i>
	<i>IV.5.3. General procedure: nickel-catalyzed hydrosilylation of ketones.....</i>	<i>130</i>
IV.6.	Hydrosilylation of aldimines and ketimines .....	130
	<i>IV.6.1. Optimization studies.....</i>	<i>130</i>
	<i>IV.6.2. General procedure: nickel-catalyzed hydrosilylation of aldimines with (1) and NaHBEt<sub>3</sub>.....</i>	<i>131</i>
	<i>IV.6.3. General procedure: nickel-catalyzed hydrosilylation of aldimines with (4) .....</i>	<i>131</i>
IV.7.	Characterization of the hydrosilylation products .....	132
<b>V.</b>	<b>References .....</b>	<b>132</b>

## I. Introduction

Catalytic reduction of carbonyl and pseudocarbonyl compounds is one of the most fundamental transformation in organic chemistry.<sup>[1]</sup> Main group metal hydrides can accomplish this transformation,<sup>[2,3]</sup> but they are relatively air- and water-sensitive and are required in stoichiometric amounts, which raises practical, environmental and economical problems. Transition metal-catalyzed reduction processes represent a more suitable alternative, especially in hydrogenation reactions. However, the latter transformation often requires harsh conditions with high temperatures and/or high dihydrogen pressures, and this can sometimes affect selectivities in the formation of the desired product. In 1972, Ojima *et al.* discovered that Wilkinson's catalyst,  $[\text{Rh}(\text{PPh}_3)_3\text{Cl}]$ , also shows high catalytic activity in the hydrosilylation of carbonyl compounds. Moreover, they isolated and characterized the rhodium-silyl-hydride complex  $[\text{Rh}(\text{PPh}_3)_2(\text{H})(\text{SiEt}_3)\text{Cl}]$  (**Scheme 1**),<sup>[4,5]</sup> resulting from the oxidative addition of the silane to the rhodium catalyst.

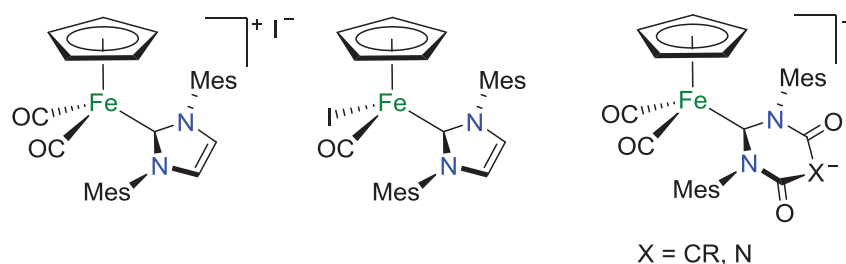


**Scheme 1.** Hydrosilylation of aldehydes and ketones catalyzed by Wilkinson's catalyst

Since this remarkable finding, milder reaction conditions can be employed in these C=O and C=N double bonds reductions with the notable attenuation of the formation of over-reduced products. Indeed, the hydrosilylation reaction can be regarded as a superior method, as it provides a reduction/protection sequence in a single step. A simple subsequent deprotection step allows one to obtain the corresponding alcohols or amines. Consequently, much effort has been directed towards the development of efficient hydrosilylation catalysts, especially with precious metals, and in particular, rhodium.<sup>[6]</sup> During the last decade, however, the development of hydrosilylation reactions based on inexpensive earth-abundant transition metals has become an important area of research as the natural reserves of precious



metals decline, and their prices increase tremendously. In particular, considerable attention has been devoted to the use of metals such as iron,<sup>[7–10]</sup> zinc,<sup>[11–14]</sup> titanium<sup>[15–17]</sup> or copper<sup>[18–20]</sup> for the reduction of carbonyl and pseudocarbonyl derivatives *via* hydrosilylation. In contrast, nickel, which is another attractive surrogate for precious metals in terms of its abundance and low cost, has been much less studied in this area.<sup>[21–27]</sup> This rarity coupled with the research of Sortais, Darcel and co-workers on iron-catalyzed hydrosilylation,<sup>[28–30]</sup> notably with the half-sandwich iron complexes of type  $[\text{Fe}(\text{NHC})\text{L}_2\text{Cp}]^{(+)}$  ( $\text{L} = \text{CO}, \text{I}^-$ ) (**Figure 1**),<sup>[31–38]</sup> which are structurally similar to our half-sandwich compounds, prompted both of our groups to collaboratively investigate the hydrosilylation of carbonyls and imines catalyzed by the closely related half-sandwich complexes of type  $[\text{Ni}(\text{NHC})\text{LCp}^\dagger]$  ( $\text{L} = \text{NCMe}, \text{Cl}^-$ ;  $\text{Cp}^\dagger = \text{Cp} (\eta^5\text{-C}_5\text{H}_5), \text{Cp}^* = (\eta^5\text{-C}_5\text{Me}_5)$ ).



**Figure 1.** Half-sandwich Fe–NHC complexes applied in the hydrosilylation of carbonyl compounds

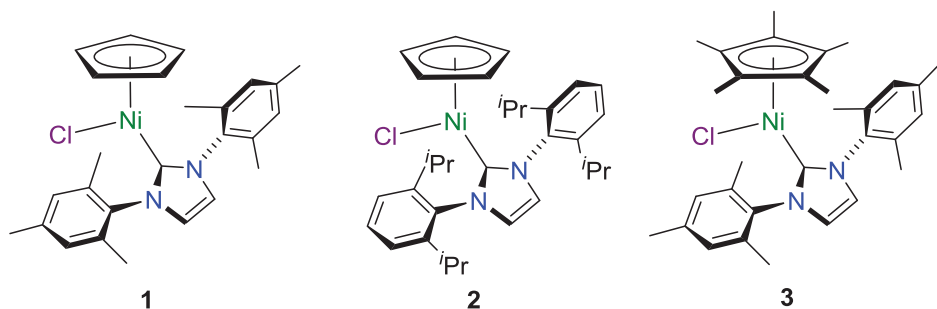
## II. Results and Discussion

*Note:* The optimization procedures, as well as the scope studies of the different nickel-catalyzed hydrosilylations have been performed by the group of Darcel at the University of Rennes I (UMR CNRS 6226), while mechanistic studies were carried out by our group in Strasbourg.

### II.1. Hydrosilylation of aldehydes<sup>[39]</sup>

Three half-sandwich nickel complexes, which have already been shown to catalyze a variety of reactions, such as the Suzuki-Miyaura cross-coupling (see **Chapter I**),<sup>[40]</sup> the  $\alpha$ -arylation of acyclic ketones (see **Chapter II**),<sup>[41]</sup> the dehalogenation of 4-bromotoluene (see

**Chapter I**),<sup>[42]</sup> the arylation of aryl halides (see **Chapter I**)<sup>[42]</sup> and even the polymerization of styrene,<sup>[43,44]</sup> were selected for the present study: complexes **1** and **2** bear a Cp ring and, respectively, the 1,3-dimesitylimidazol-2-ylidene (IMes) and 1,3-bis(2,6-diisopropylphenyl)imidazol-2-ylidene (IPr) as NHC ligands, and complex **3**, incorporates the Cp\* analogue of complex **1** (**Figure 2**).



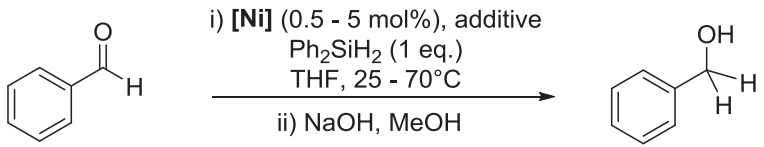
**Figure 2.** Selected half-sandwich NHC-nickel complexes

Initial studies focused on the reduction of benzaldehyde with one equivalent of  $\text{Ph}_2\text{SiH}_2$  in THF in the presence of catalytic amounts of complexes **1–3** under various conditions, in order to optimize the reaction parameters (**Table 1**). At 70°C, benzaldehyde was fully reduced to the corresponding alcohol after 22 h of reaction and a hydrolysis step, in the presence of only 5 mol% of complex **1** (**Table 1**, entry 1). This promising result prompted us to decrease the reaction temperature to 25°C, but no conversion was observed after 17 h (entry 2). Addition of 10 mol% of  $\text{KPF}_6$  as a chloride scavenger led to 38% conversion under otherwise unchanged conditions (entry 3). In light of this result and of the involvement of nickel hydride species in the rare examples of nickel-catalyzed hydrosilylations of carbonyl functionalities,<sup>[24,25]</sup> we then decided to activate **1** with 2 equivalents of  $\text{NaHBET}_3$ . Satisfyingly, the hydrosilylation of benzaldehyde was complete within 1 h with only 1 mol% of **1** and 2 mol% of  $\text{NaHBET}_3$  (entry 4). Moreover, the reaction time could be decreased to 15 min (TOF of 400  $\text{h}^{-1}$ ) (entry 5) and the catalyst loading could be lowered to 0.5 mol% without affecting the reaction (entry 6).

The catalytic activities of the three complexes were then compared under the conditions of entry 4. A lower conversion was obtained with complex **2** bearing the bulkier IPr ligand (40%, entry 7), but a good conversion (90%, entry 8) was observed with the more electron-rich complex **3** bearing a Cp\* ligand. Various other silanes and solvents were then

screened with **1** (see **Table 10** in *Experimental section*), but the combination of  $\text{Ph}_2\text{SiH}_2$  and THF was found to be the best.

**Table 1.** Optimization for the reduction of benzaldehyde with catalysts **1-3**.<sup>a</sup>

<div style="text-align: center;">  </div>				
Entry	Precatalyst (mol%)	Additive (mol%)	Time (h)	Conversion (%) <sup>b</sup>
1 <sup>c</sup>	<b>1</b> (5)	—	22	> 97
2	<b>1</b> (5)	—	17	0
3	<b>1</b> (5)	KPF <sub>6</sub> (10)	17	38
4	<b>1</b> (1)	NaHBET <sub>3</sub> (2)	1	> 97
5	<b>1</b> (1)	NaHBET <sub>3</sub> (2)	0.25	> 97
6	<b>1</b> (0.5)	NaHBET <sub>3</sub> (1)	1	95
7	<b>2</b> (1)	NaHBET <sub>3</sub> (2)	1	40
8	<b>3</b> (1)	NaHBET <sub>3</sub> (2)	1	90

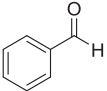
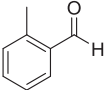
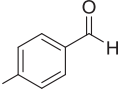
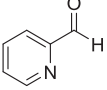
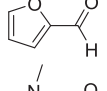
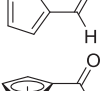
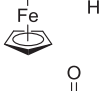
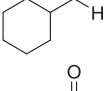
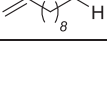
<sup>a</sup> Typical procedure: activation of **1-3** with the additive in THF (4 mL) was followed by addition of benzaldehyde (1 mmol) and  $\text{Ph}_2\text{SiH}_2$  (1 mmol), and the reaction mixture was stirred at 25°C. <sup>b</sup> Conversions determined by GC after methanolysis (MeOH, 2M NaOH) and extraction with  $\text{Et}_2\text{O}$ . <sup>c</sup> Reaction run at 70°C.

With these optimized conditions in hand, we then examined the scope of the hydrosilylation of various aldehydes with the nickel complex **1** (**Table 2**). The reaction proceeds with high conversions for *ortho*- and *para*-methylbenzaldehydes (**Table 2**, entries 2 and 3). For halogenated benzaldehydes, the *para*-chloro derivative was fully reduced without dehalogenation (entry 4), whereas *para*-bromobenzaldehyde gives low conversion (entry 5) and a quick deactivation of the catalyst, which can be visually monitored by a color change from red-orange, which is the color of the active species generated by the reaction of **1** and NaHBET<sub>3</sub> (*vide infra*), to purple-pink, which is that of complex **1**, thus suggesting dehalogenation of the substrate.

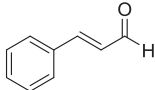
With electron-donating-substituted aldehydes such as *para*-methoxy- and *para*-dimethylaminobenzaldehydes, the reaction proceeds more slowly and needs 17 h to reach good conversions (entries 6 and 7). In contrast, with electro-deficient aldehydes such as *para*-cyano- and *para*-nitrobenzaldehydes, moderate to good conversions were reached within 1 h, and the functional groups remained unchanged (entries 8 and 9). However, the presence of a

phenol group is incompatible with our nickel catalyst (entry 10). Interestingly, with heteroaromatic aldehydes, the corresponding alcohols were obtained with good yields (entries 11-13). Moreover, ferrocene-carboxaldehyde and cyclohexanecarboxaldehyde were also reduced with good yields (entries 14 and 15). Finally, an excellent chemoselectivity toward non-conjugated C=C double bonds was observed, as shown by the sole reduction of the C=O double bond of undecenaldehyde (entry 16), and a moderate one was seen toward the conjugated C=C double bond of cinnamaldehyde (entry 17).<sup>[28]</sup>

**Table 2.** Scope of the nickel-catalyzed hydrosilylation of aldehydes with complex **1**-NaHBEt<sub>3</sub>.<sup>a</sup>

Entry	Substrate	Conversion (%) <sup>b</sup>	Yield (%) <sup>c</sup>
1		> 97	88
2		> 97	79
3	 R = Me	> 97	83
4	R = Cl	> 97	76
5	R = Br	13	—
6 <sup>d</sup>	R = OMe	81	70
7 <sup>d</sup>	R = NMe <sub>2</sub>	86	75
8	R = CN	95	68
9	R = NO <sub>2</sub>	70	59
10	R = OH	0	—
11 <sup>d,e</sup>		> 97	—
12 <sup>d</sup>		> 97	86
13 <sup>d</sup>		96	83
14 <sup>d</sup>		> 97	84
15 <sup>e</sup>		96	—
16		75	68

**Table 2.** (continued)

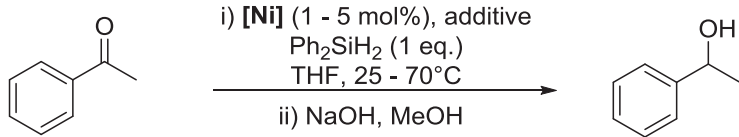
Entry	Substrate	Conversion (%) <sup>b</sup>	Yield (%) <sup>c</sup>
17 <sup>d,f</sup>		88	65

<sup>a</sup> Typical procedure: activation of **1** (1 mol%) with NaHBET<sub>3</sub> (2 mol%) in THF (4 mL) was followed by addition of aldehyde (1 mmol) and Ph<sub>2</sub>SiH<sub>2</sub> (1 mmol), and the reaction mixture was stirred at 25°C for 1 h. <sup>b</sup> Conversions determined by <sup>1</sup>H NMR after methanolysis. <sup>c</sup> Isolated yields. <sup>d</sup> Reaction run at 70°C. <sup>e</sup> Conversions determined by GC after methanolysis. <sup>f</sup> A 75:25 mixture of cinnamyl alcohol and 3-phenylpropan-1-ol was obtained.

## II.2. Hydrosilylation of ketones<sup>[39]</sup>

We explored the reduction of ketones, starting with acetophenone as the model substrate and Ph<sub>2</sub>SiH<sub>2</sub> as the hydrogen source (**Table 3**). With 5 mol% of **1** in refluxing THF, the conversion was modest without any additives, but could be increased to 57% by the addition of KPF<sub>6</sub> (**Table 3**, entries 1 and 2). The activation of **1** with 10 mol% of NaHBET<sub>3</sub> allowed the reduction to proceed to full conversion in 17 h at 25°C (entry 3). However, in contrast to the reduction of aldehydes, decreasing the catalyst and activator loadings led to diminished conversions (entries 4 and 5). Furthermore, complex **2** is as effective as **1** here, while the Cp\* complex **3** gives a lower conversion (entries 6 and 7).

**Table 3.** Optimization for the reduction of acetophenone with catalysts **1-3**.<sup>a</sup>

				
Entry	Precatalyst (mol%)	Additive (mol%)	Time (h)	Conversion (%) <sup>b</sup>
1 <sup>c</sup>	<b>1</b> (5)	—	24	26
2 <sup>c</sup>	<b>1</b> (5)	KPF <sub>6</sub> (10)	24	57
3	<b>1</b> (5)	NaHBET <sub>3</sub> (10)	17	97
4	<b>1</b> (3)	NaHBET <sub>3</sub> (6)	17	94
5	<b>1</b> (1)	NaHBET <sub>3</sub> (2)	17	58
6	<b>2</b> (5)	NaHBET <sub>3</sub> (10)	17	> 97
7	<b>3</b> (5)	NaHBET <sub>3</sub> (10)	17	73

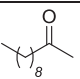
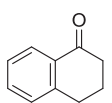
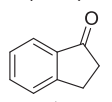
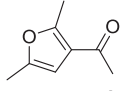
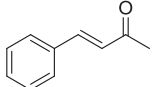
<sup>a</sup> Typical procedure: activation of **1-3** with the additive in THF (4 mL) was followed by addition of acetophenone (1 mmol) and Ph<sub>2</sub>SiH<sub>2</sub> (1 mmol), and the reaction mixture was stirred at 25°C. <sup>b</sup> Conversions determined by GC after methanolysis (MeOH, 2M NaOH) and extraction with Et<sub>2</sub>O. <sup>c</sup> Reaction run at 70°C.

The scope of the reaction was then investigated with 5 mol% of **1** and 10 mol% of NaHBET<sub>3</sub> in THF at room temperature (**Table 4**). High conversions were obtained with both electron-rich and electron-poor acetophenone derivatives (**Table 4**, entries 2-4 and 7-9). As observed with *para*-bromobenzaldehyde (**Table 2**, entry 5), the active species was deactivated with *para*-iodoacetophenones, and low conversions were obtained (**Table 4**, entries 5 and 6). It is noteworthy that sterically encumbered acetophenones did not hamper the reaction as full reduction still occurred (entries 2, 10 and 11). Linear aliphatic ketones, cyclic ketones and furfuryl derivatives were also hydrosilylated with good yields under these conditions (entries 13-17). Unfortunately, the chemoselectivity toward conjugated C=C double bonds was even less efficient than in the case of aldehydes, as shown by the 2:1 mixture of 4-phenylbut-3-en-2-ol and 4-phenylbutan-2-ol obtained from the reduction of benzylideneacetone (entry 18).

**Table 4.** Scope of the nickel-catalyzed hydrosilylation of ketones with complex **1**-NaHBET<sub>3</sub>.<sup>a</sup>

Entry	Substrate	Conversion (%) <sup>b</sup>	Yield (%) <sup>c</sup>
1		> 97	88
2		> 97	85
3		> 97	79
4	R = Cl	> 97	73
5	R = Br	30	—
6	R = I	14	—
7	R = F	> 97	73
8	R = NO <sub>2</sub>	90	71
9	R = OMe	> 97	88
10		> 97	75
11		> 97	83
12		> 97	88
13		> 97	83

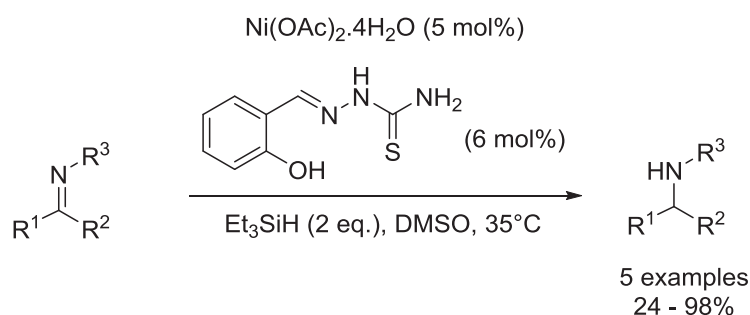
**Table 4.** (continued)

Entry	Substrate	Conversion (%) <sup>b</sup>	Yield (%) <sup>c</sup>
14		> 97	78
15		> 97	79
16		> 97	86
17		> 97	79
18 <sup>d</sup>		95	—

<sup>a</sup> Typical procedure: activation of **1** (5 mol%) with NaHBEt<sub>3</sub> (10 mol%) in THF (4 mL) was followed by addition of ketone (1 mmol) and Ph<sub>2</sub>SiH<sub>2</sub> (1 mmol), and the reaction mixture was stirred at 25°C for 17 h. <sup>b</sup> Conversions determined by <sup>1</sup>H NMR after methanolysis. <sup>c</sup> A 2:1 mixture 4-phenyl-but-3-en-2-ol and 4-phenylbutan-2-ol was obtained.

### II.3. Hydrosilylation of aldimines<sup>[45]</sup>

Transition metal-catalyzed hydrosilylation of aldimines and ketimines is also an interesting target due to the significance and omnipresence of the resulting amines in the field of natural products, pharmaceuticals and agronomical compounds.<sup>[46–48]</sup> Encouraged by our results in the hydrosilylation of aldehydes and ketones, and the extreme scarcity of nickel catalysts for the hydrosilylation of imines, both of our groups decided to pursue the study of half-sandwich nickel–NHC complexes as pre-catalysts for the related hydrosilylation of imines. Before our work, we were aware of only one example where Ni catalysts formed *in situ* from [Ni(OAc)<sub>2</sub>·4H<sub>2</sub>O] and an (*O,N,S*)-pincer ligand (1:1 ratio) were shown to reduce a small array of imines via hydrosilylation (**Scheme 2**).<sup>[49]</sup>

**Scheme 2.** First Ni-catalyzed hydrosilylation of imines

Initial studies focused on the hydrosilylation of *N*-benzylidene-4-methoxyaniline **5** with one equivalent of  $\text{Ph}_2\text{SiH}_2$  in THF in the presence of catalytic amounts of complex **1** under various conditions, in order to optimize the reaction parameters (**Table 5**). In the sole presence of the neutral complex **1** (5 mol%), 70°C was required to observe 50% conversion of the aldimine **5** to the corresponding amine **6** after 24 h of reaction and basic quenching (**Table 5**, entries 1 and 2). Addition of 10 mol% of  $\text{KPF}_6$  as a chloride scavenger led to full conversion under otherwise unchanged conditions (entry 3). This promising and rather surprising result, with respect to what was observed with aldehydes (**Table 1**, entry 3), led us to use the well-defined cationic acetonitrile complex  $[\text{Ni}(\text{IMes})(\text{NCMe})\text{Cp}](\text{PF}_6)$  **4** (5 mol%), with which complete reduction was also observed after 24 h at 70°C (entry 4). Reducing the catalytic loading to 1 mol% of **4** also allowed the reaction to reach full conversion (entry 6), which contrasts with the result obtained with 1 mol% of the *in situ* generated cationic complex from **1** and  $\text{KPF}_6$  (40% conversion, entry 5). One possible explanation is that **4** is generated in THF instead of acetonitrile, and that THF does not have sufficient coordinating ability to stabilize such cationic species. Indeed, no cationic complex of the type  $[\text{Ni}(\text{NHC})\text{LCp}]^+$  has ever been isolated when the halide was scavenged in a weakly coordinating solvent. Interestingly, the temperature can even be decreased to 50°C without loss of catalytic activity (entry 7). However, further lowering of the reaction temperature to 25°C led to a dramatic drop in activity, as only 10% conversion was detected after 17 h (entry 8). Nevertheless, as observed for the hydrosilylation of aldehydes and ketones, the combination of **1** and  $\text{NaHBEt}_3$  resulted in high catalytic activity. Using 1 mol% of this combination allowed us to observe a full conversion when performing the reaction at 25°C for 17 h (entry 9). Decreasing either the reaction time to 8 h or else the catalytic loading to 0.5 mol% allowed us to obtain 90% conversion (entries 11 and 12). Various other silanes and solvents were also screened (see **Tables 11** and **12** in *Experimental section*), but the combination of  $\text{Ph}_2\text{SiH}_2$  and THF was again found to be optimal.

With these optimized conditions in hand (1 equiv. of  $\text{Ph}_2\text{SiH}_2$ , 1 mol% of **1**, 2 mol%  $\text{NaHBEt}_3$ , THF, 25°C; or 1 equiv. of  $\text{Ph}_2\text{SiH}_2$ , 1 mol% of **4**, no additive, THF, 50°C, 24 h), we then explored the scope of the hydrosilylation of aldimines (**Table 6**).



**Table 5.** Optimization for the reduction of aldimines with **1** and **4**<sup>a</sup>

Entry	Precatalyst (mol%)	Additive (mol%)	Temp. (°C)	Time (h)	Conversion <sup>b</sup> (%)
1	<b>1</b> (5)	—	25	18	0
2	<b>1</b> (5)	—	70	24	50
3	<b>1</b> (5)	KPF <sub>6</sub> (10)	70	24	> 97
4	<b>4</b> (5)	—	70	24	> 97
5	<b>1</b> (1)	KPF <sub>6</sub> (2)	70	24	40
6	<b>4</b> (1)	—	70	24	> 97
7	<b>4</b> (1)	—	50	24	> 97
8	<b>4</b> (1)	—	25	17	10
9	<b>1</b> (1)	NaHBET <sub>3</sub> (2)	25	17	> 97
10	—	NaHBET <sub>3</sub> (2)	25	17	0
11	<b>1</b> (1)	NaHBET <sub>3</sub> (2)	25	8	90
12	<b>1</b> (0.5)	NaHBET <sub>3</sub> (1)	25	24	90

<sup>a</sup> Typical procedure: activation of **1** with the additive in THF (4 mL) at RT for 5 min or dissolution of **4** in THF (4 mL) at RT was followed by the addition of **5** (1 mmol) and Ph<sub>2</sub>SiH<sub>2</sub> (1 mmol), and the reaction mixture was stirred at 25, 50 or 70°C for 8 to 24 h. <sup>b</sup> Conversions determined by <sup>1</sup>H NMR spectroscopy after methanolysis: 2M NaOH (2 mL), MeOH (2 mL), RT, 2 h.

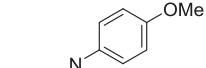
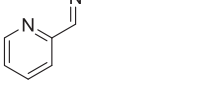
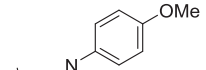
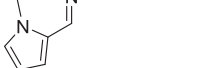
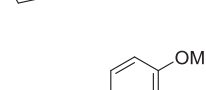
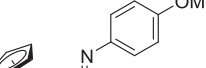
Electronic effects at the *para*-position of the benzylidene or aniline moiety were generally minor (**Table 6**, entries 1-3, 5-6 and 10-20). Thus, aldimines bearing an electron-donating group gave the corresponding amines with good to excellent conversions (entries 1-3, 5-6 and 10-12). Interestingly, no dehalogenation occurred with a chloro-substituted aldimine irrespective of the catalytic system used, **1**-NaHBET<sub>3</sub> or **4**-no additive (entries 13 and 14), and the corresponding amine was isolated in good yields (80%, entry 13). However, with bromo- or iodo-substituted aldimines, low conversions were obtained, probably due to a rapid catalyst deactivation, as observed for the hydrosilylation of aldehydes and ketones (entries 4 and 7 vs. **Table 2**, entry 5, and **Table 4**, entries 5 and 6). Strikingly, functional carbonyl-groups such as esters and amides were not affected under these catalytic conditions irrespective of the catalytic system used, **1**-NaHBET<sub>3</sub> or **4**-no additive (entries 15-16 and 19-20), and the corresponding secondary amines were isolated in good yields (83 and 72%, entries 16 and 20). Moreover, although 5% of fully reduced compound was detected in the crude reaction mixture, the cyano functional group was also well tolerated, and the *N*-(4-

cyanobenzyl)-*p*-toluidine resulting from the selective reduction of the 4-cyanobenzylidene derivative was isolated in 74% yield (entry 17). In contrast, only a moderate conversion was observed for the hydrosilylation of 4-methoxy-*N*-(4-nitrobenzylidene)aniline under forcing conditions, and a mixture of products resulting from the reduction of the nitro group was observed (entries 21 and 22).

**Table 6.** Scope of the reduction of aldimines with **1**-NaHBEt<sub>3</sub> and **4**<sup>a</sup>

$\text{R}-\text{CH}=\text{N}-\text{Ar} + \text{Ph}_2\text{SiH}_2 \xrightarrow[\text{ii) NaOH, MeOH}]{\begin{array}{c} \text{i) } \mathbf{1} \text{ (1 mol\%), NaHBEt}_3 \text{ (2 mol\%), THF, 25}^\circ\text{C} \\ \text{or} \\ \mathbf{4} \text{ (1 mol\%), THF, 50}^\circ\text{C} \end{array}} \text{R}-\text{CH}_2-\text{NH}-\text{Ar}$					
Entry	Substrate	Precatalyst	Conversion <sup>b</sup> (%)	Yield <sup>c</sup> (%)	
1		R = Me	<b>1</b>	> 97	83
2		R = Me	<b>4</b>	> 97	—
3		R = OMe	<b>1</b>	> 97	90
4		R = Br	<b>1</b>	20	—
5		R = <i>p</i> -OMe	<b>1</b>	> 97	89
6		R = <i>p</i> -OMe	<b>4</b>	> 97	—
7		R = <i>p</i> -I	<b>1</b>	27	—
8		R = <i>o</i> -OMe	<b>1</b>	28	—
9		R = <i>o</i> -OMe	<b>1</b>	48 <sup>d</sup>	39
10		R = <i>p</i> -OMe	<b>1</b>	> 97	84
11		R = <i>p</i> -OMe	<b>4</b>	> 97	—
12		R = <i>p</i> -NMe <sub>2</sub>	<b>1</b>	77	57
13		R = <i>p</i> -Cl	<b>1</b>	> 97	80
14		R = <i>p</i> -Cl	<b>4</b>	71	—
15		R = <i>p</i> -CO <sub>2</sub> Me	<b>1</b>	95	76
16		R = <i>p</i> -CO <sub>2</sub> Me	<b>4</b>	> 97	83
17		R = <i>p</i> -CN	<b>1</b>	94 <sup>e</sup>	74
18		R = 3,4,5-OMe	<b>1</b>	93	81
19		R = NHAc	<b>1</b>	70	—
20		R = NHAc	<b>1</b>	90 <sup>d</sup>	72
21		R = NO <sub>2</sub>	<b>1</b>	0	—
22		R = NO <sub>2</sub>	<b>1</b>	40 <sup>f</sup>	—
23			<b>1</b>	20	—
24			<b>1</b>	80 <sup>f</sup>	57

**Table 6.** (continued)<sup>a</sup>

$  \begin{array}{c}  \text{R}-\text{CH}=\text{N}-\text{Ar} \\  + \quad \text{Ph}_2\text{SiH}_2  \end{array}  \xrightarrow[\text{ii) NaOH, MeOH}]{\begin{array}{c} \text{i) } \mathbf{1} \text{ (1 mol\%), NaHBET}_3 \text{ (2 mol\%), THF, 25}^\circ\text{C} \\ \text{or} \\ \mathbf{4} \text{ (1 mol\%), THF, 50}^\circ\text{C} \end{array}}  \begin{array}{c}  \text{R}-\text{CH}_2-\text{NH}-\text{Ar}  \end{array}  $				
Entry	Substrate	Precatalyst	Conversion <sup>b</sup> (%)	Yield <sup>c</sup> (%)
25		<b>1</b>	43	—
26		<b>1</b>	70 <sup>f</sup>	61
27		<b>1</b>	20	—
28		<b>1</b>	60 <sup>f</sup>	—
29		<b>1</b>	87 <sup>f,g</sup>	70
30		<b>1</b>	> 97	85

<sup>a</sup> Typical procedure: activation of **1** (1 mol%) with NaHBET<sub>3</sub> (2 mol%) in THF (4 mL) at RT for 5 min or dissolution of **4** (1 mol%) in THF (4 mL) at rt was followed by the addition of the aldimine (1 mmol) and Ph<sub>2</sub>SiH<sub>2</sub> (1 mmol), and the reaction mixture was stirred at 25°C for 17 h (**1**) or at 50°C for 24 h (**4**). <sup>b</sup> Conversions determined by <sup>1</sup>H NMR spectroscopy after methanolysis: 2M NaOH (2 mL), MeOH (2 mL), RT, 2 h. <sup>c</sup> Isolated yields. <sup>d</sup> 50°C. <sup>e</sup> 5% reduction of both the aldimine and the cyano group was also observed. <sup>f</sup> 70°C. <sup>g</sup> **1** (5 mol%), NaHBET<sub>3</sub> (10 mol%).

Substitution at the *ortho*-position of the aniline moiety seems to have an inhibiting effect, most probably for steric reasons, as shown by the moderate conversion observed for the reduction of benzylidene-*o*-methylaniline, even at 50°C (entries 8 and 9). Substitution at the *meta*-position of the benzylidene moiety seems, in contrast, to have no notable effect (entry 18).

As observed with carbonyl derivatives (Table 2, entries 11-13; Table 4, entry 17), this reduction can also be conducted with heteroaromatic substrates such as 5-methylfur-2-yl-, pyridin-2-yl- and *N*-methylpyrrol-2-yl-4-methoxyaniline, but at higher temperature (50°C or 70°C), and the corresponding amines were isolated in moderate yields (57 - 70%, entries 23-29). Finally, 4-methyl-*N*-(ferrocenylmethylidene)aniline was totally reduced and led to the corresponding amine in good yield (85%, entry 30).

II.4. Hydrosilylation of ketimines<sup>[45]</sup>

Given the high activity of both catalytic systems for aldimines, we then investigated their potential for the hydrosilylation of ketimines, with *N*-(1-phenylethylidene)-4-methoxyaniline **7** as the model substrate (**Table 7**). To obtain similar activities, slightly harsher conditions had to be used, either by performing the reaction at high temperatures (with **1**-NaHBEt<sub>3</sub>, entries 5-9), or else by using higher precatalyst and Ph<sub>2</sub>SiH<sub>2</sub> loadings (with **4**, entries 3 and 4). Thus, to observe full conversion of **7** to the corresponding amine **8** after a methanolysis step, 50°C for 17 h was required in the presence of 1 mol% of **1** and 2 mol% of NaHBEt<sub>3</sub> (entry 7), and 2 equiv. of Ph<sub>2</sub>SiH<sub>2</sub> were required in the presence of 5 mol% of **4** (entry 4). Notably, in the case of **1**-NaHBEt<sub>3</sub>, when the reaction was performed at a lower temperature or with a lower catalyst loading, the conversion significantly decreased (entries 6 and 9).

**Table 7.** Optimization for the reduction of ketimines with **1** and **4**<sup>a</sup>

Entry	Precatalyst (mol%)	Additive (mol%)	Temperature (°C)	Time (h)	Conversion <sup>b</sup> (%)
1	<b>1</b> (5)	—	70	24	10
2	<b>1</b> (5)	KPF <sub>6</sub> (10)	70	24	60
3	<b>4</b> (5)	—	50	17	70
4 <sup>c</sup>	<b>4</b> (5)	—	50	24	> 97
5	<b>1</b> (5)	NaHBEt <sub>3</sub> (10)	50	17	> 97
6	<b>1</b> (5)	NaHBEt <sub>3</sub> (10)	25	17	50
7	<b>1</b> (1)	NaHBEt <sub>3</sub> (2)	50	17	> 97
8	<b>1</b> (1)	NaHBEt <sub>3</sub> (2)	50	3	80
9	<b>1</b> (0.5)	NaHBEt <sub>3</sub> (1)	50	17	65

<sup>a</sup> Typical procedure: activation of **1** with the additive in THF (4 mL) at RT for 5 min or dissolution of **4** in THF (4 mL) at RT was followed by the addition of **7** (1 mmol) and Ph<sub>2</sub>SiH<sub>2</sub> (1 mmol), and the reaction mixture was stirred at 25, 50 or 70°C for 3 to 24 h. <sup>b</sup> Conversions determined by <sup>1</sup>H NMR spectroscopy after methanolysis: 2M NaOH (2 mL), MeOH (2 mL), RT, 2 h. <sup>c</sup> Reaction run with 2 equiv. Ph<sub>2</sub>SiH<sub>2</sub>.

With these optimized conditions in hand (1 equiv. of Ph<sub>2</sub>SiH<sub>2</sub>, 1 mol% of **1**, 2 mol% of NaHBEt<sub>3</sub>, THF, 50°C, 17 h; or 2 equiv. of Ph<sub>2</sub>SiH<sub>2</sub>, 5 mol% of **4**, no additive, THF, 50°C, 24 h), the scope of the hydrosilylation of ketimines was then explored. With several ketimines



Table 8. (continued)<sup>a</sup>

$  \begin{array}{c}  \text{R} \quad \text{N}-\text{Ar} \\  \diagup \quad \diagdown \\  \text{C} \\  \diagdown \quad \diagup \\  \text{C}  \end{array}  + \text{Ph}_2\text{SiH}_2  \xrightarrow[\text{ii) NaOH, MeOH}]{\begin{array}{c} \text{i) } \mathbf{1} \text{ (1 mol\%), NaHBET}_3 \text{ (2 mol\%), THF, 50}^\circ\text{C} \\ \text{or} \\ \mathbf{4} \text{ (5 mol\%), THF, 50}^\circ\text{C} \end{array}}  \begin{array}{c}  \text{HN}-\text{Ar} \\    \\  \text{R} \quad \text{C}  \end{array}  $				
Entry	Substrate	Precatalyst	Conversion <sup>b</sup> (%)	Yield <sup>c</sup> (%)
14		<b>1</b>	90	59
15		<b>1</b>	20	—
16		<b>1</b>	48 <sup>d</sup>	—
17		<b>1</b>	80 <sup>d,e</sup>	66

<sup>a</sup> Typical procedure: activation of **1** (1 mol%) with NaHBET<sub>3</sub> (2 mol%) in THF (4 mL) at RT for 5 min or dissolution of **4** (5 mol%) in THF (4 mL) at RT was followed by the addition of the ketimine (1 mmol) and Ph<sub>2</sub>SiH<sub>2</sub> (1 mmol (**1**) or 2 mmol (**4**)), and the reaction mixture was stirred at 50°C for 17 h (**1**) or 24 h (**4**). <sup>b</sup> Conversions determined by <sup>1</sup>H NMR spectroscopy after methanolysis: 2M NaOH (2 mL), MeOH (2 mL), RT, 2 h. <sup>c</sup> Isolated yields. <sup>d</sup> 70°C. <sup>e</sup> **1** (5 mol%), NaHBET<sub>3</sub> (10 mol%).

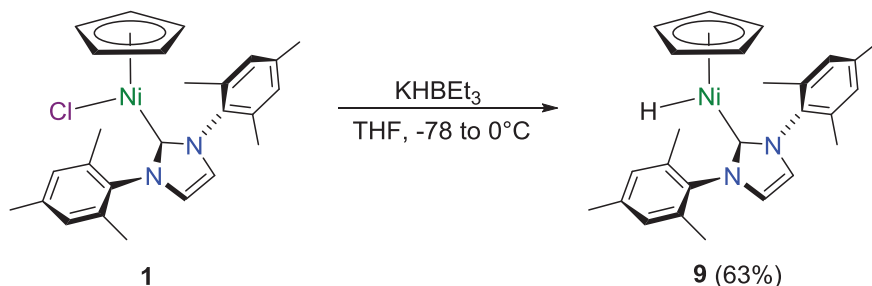
## II.5. Mechanistic studies<sup>[39,45]</sup>

### II.5.1. (1)-NaHBET<sub>3</sub> catalytic system

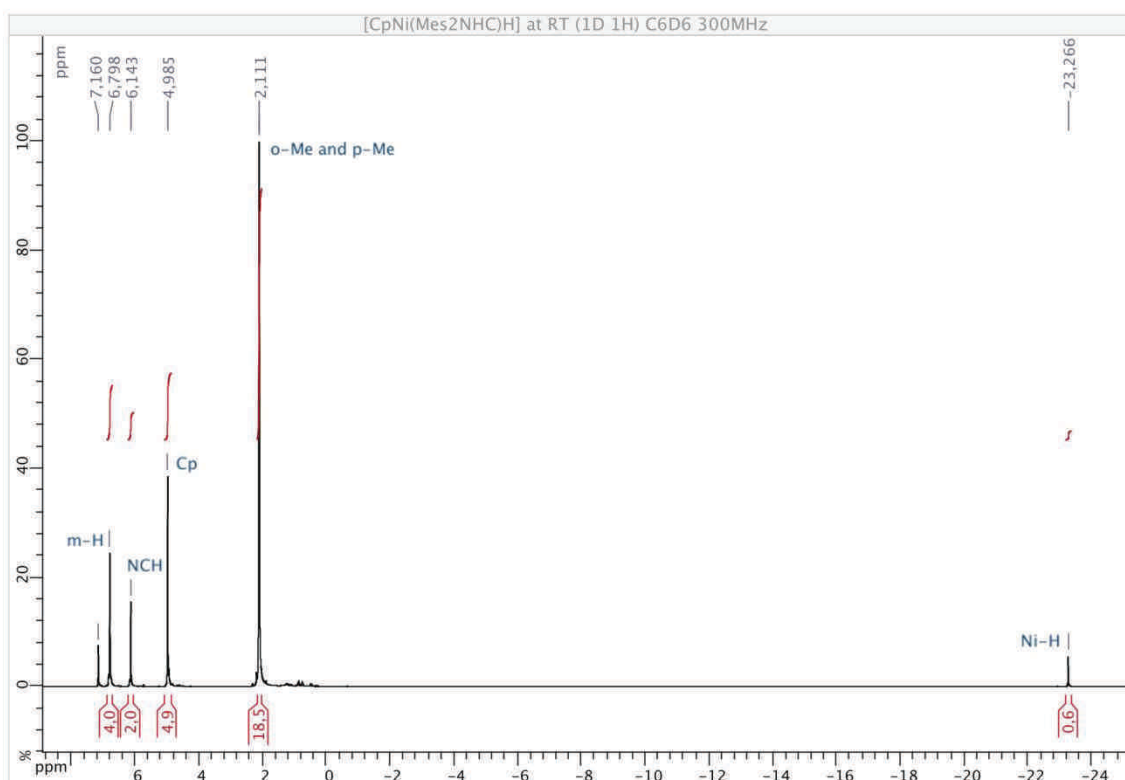
In order to rationalize the role of the triethylborohydride salt, the purple complex **1** was treated with KHBET<sub>3</sub> (1.2 equivalents) in THF at −78°C. The reaction mixture turned to red immediately, and the nickel hydride complex **9** was isolated as thermally sensitive red crystals in 63% yield after work-up (**Scheme 3**). Complex **9** was characterized by <sup>1</sup>H and <sup>13</sup>C{<sup>1</sup>H} NMR spectroscopy and by elemental analysis. Its molecular structure was established by a single-crystal X-ray diffraction study. It is noteworthy that complex **9** had been previously reported to be formed by the reaction of NiCp<sub>2</sub> with [InH<sub>3</sub>(IMes)],<sup>[50]</sup> and had even been characterized by X-ray crystallography, but the hydride ligand was not located. In our case, the quality of the X-ray data allowed us to determine the position of the hydride ligand.

As in the case of **1**,<sup>[51]</sup> the <sup>1</sup>H and <sup>13</sup>C{<sup>1</sup>H} NMR spectra of **9** reveal that an effective plane of symmetry that bisects the molecule exists in solution on the NMR time scale (**Figure 3**). This effective mirror plane contains the hydride ligand, the nickel center and the NHC

carbene carbon atom, as well as the Cp ring centroid. Most informative signals are the hydride resonance, which appears as a singlet at  $-23.27$  ppm in the  $^1\text{H}$  NMR spectrum (**Figure 3**), and the carbene carbon resonance, which appears at  $185.4$  ppm in the  $^{13}\text{C}\{^1\text{H}\}$  NMR spectrum (in  $\text{C}_6\text{D}_6$ ). One can note that the latter resonance is significantly shielded compared to the corresponding resonance of the chloride complex **1**, which appears at  $165.9$  ppm (in  $\text{CDCl}_3$ ).<sup>[51]</sup>

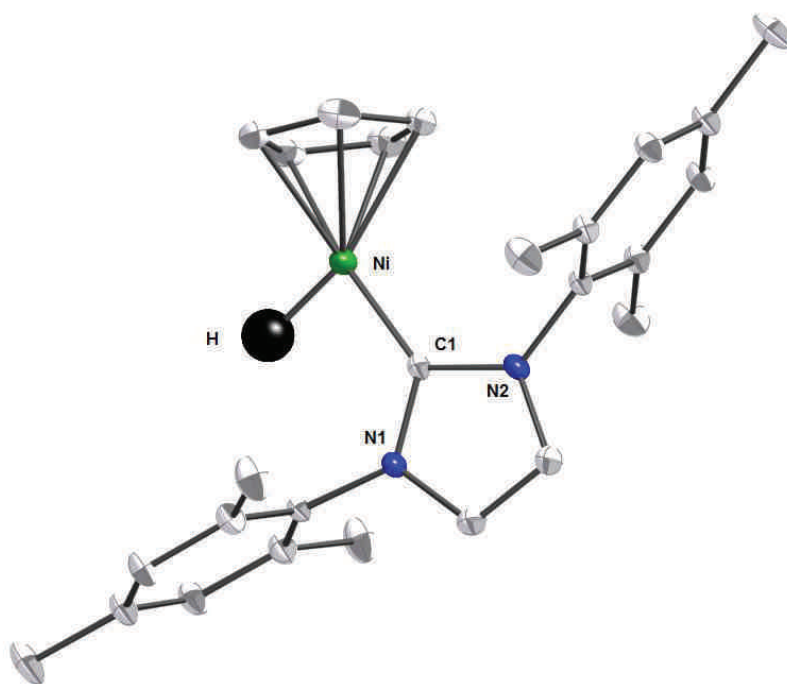


**Scheme 3.** Synthesis of the nickel hydride complex **9**



**Figure 3.**  $^1\text{H}$  NMR spectrum of **9**

Crystals suitable for X-ray structure determination were grown from a concentrated pentane solution of **9** at  $-28^{\circ}\text{C}$ . The molecular structure is shown in **Figure 4**. Crystallographic data and data collection parameters are listed in **Table 10** (see *Experimental section*). A list of selected bond lengths and angles is given in **Table 9**. The structure of **9** features a nickel atom bonded to a  $\eta^5\text{-C}_5\text{H}_5$  group, one IMes ligand and the hydride ligand, as earlier reported by Jones.<sup>[50]</sup> The coordination is globally similar to that of other half-sandwich complexes of the general formula  $[\text{Ni}(\text{NHC})\text{LCp}^{\dagger}]$ , such as its precursor **1**, and features a nickel atom laying at the center of a pseudo-trigonal plan. However, significant variations in the geometry of **9** are observed when compared to **1**, such as the more open C1–Ni–Cp<sub>cent</sub> angle ( $147.0^{\circ}$  vs.  $132.4(2)^{\circ}$  in **1**), which is compensated by the lower C1–Ni–H angle value ( $83.0^{\circ}$  for **9** vs.  $98.4(2)^{\circ}$  for the C1–Ni–Cl of **1**). Moreover, the Ni–C1 distance is shortened in **9** ( $1.858(3)$  Å for **9** vs.  $1.917(9)$  Å for **1**), whereas other bond angles and distances are globally similar to **1**. Finally, the Ni–H distance is comparable to that of the few other mono-nickel hydride species known, such as  $[\text{2,6-}(\text{tBu}_2\text{PO})_2\text{C}_6\text{H}_3]\text{NiH}^{[24]}$  (Ni–H =  $1.37(3)$  Å) or  $[\text{N}(o\text{-NMe}_2\text{C}_6\text{H}_4)_2\text{NiH}]^{[52]}$  (Ni–H =  $1.50(2)$  Å).



**Figure 4.** Molecular structure of **9**. Key atoms are labeled. The only hydrogen atom shown is that bonded to Ni.

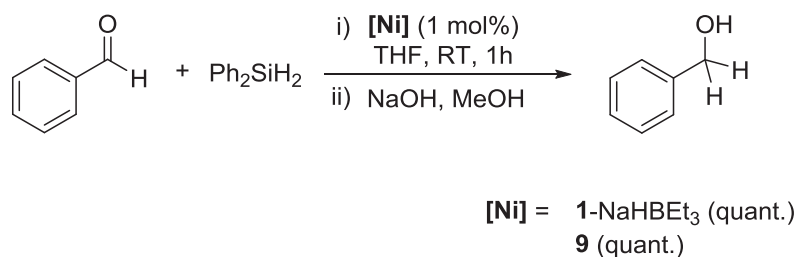


**Table 9.** Selected distances (Å) and angles (°) in complex **9**

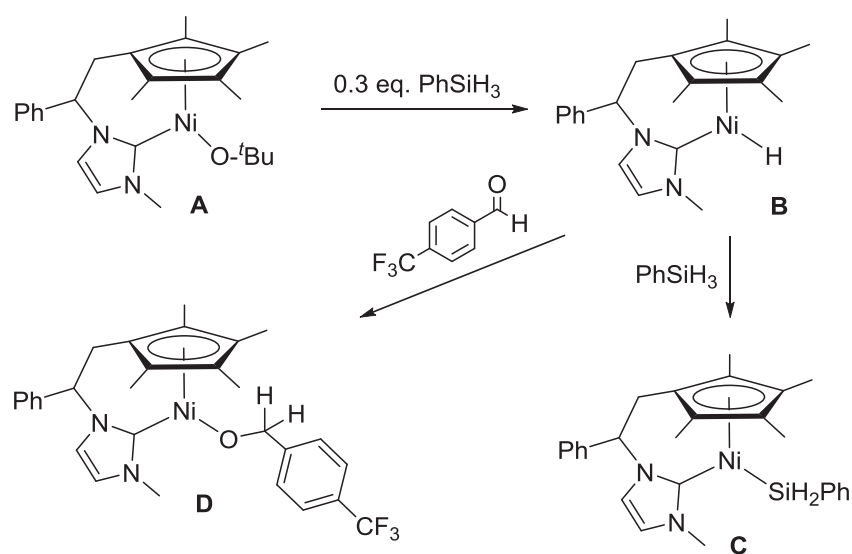
Complex <b>9</b>	
Ni–C1	1.844(3)
Ni–H	1.42(6)
Ni–Cp <sub>cent</sub>	1.771
C1–Ni–H	83(3)
C1–Ni–Cp <sub>cent</sub>	147.0
H–Ni–Cp <sub>cent</sub>	130

The isolated complex **9** was then tested as the catalyst for the reduction of benzaldehyde under the optimized conditions (1 mol% **9**, Ph<sub>2</sub>SiH<sub>2</sub>, THF, room temperature), but without any additive. Full conversion was obtained after 1 h of reaction (**Scheme 4**), which strongly suggests that **9** is the true pre-catalyst in this process.

Similarly, Royo *et al.* simultaneously reported an analogous Cp-NHC tethered nickel-hydride complex **B**, *in situ* generated by reaction of the corresponding alkoxide complex **A** with 0.3 equiv. of PhSiH<sub>3</sub> (**Scheme 5**), that would most probably be the active species in a very similar hydrosilylation process (see also **Chapter I, Scheme 70**).<sup>[53]</sup> The latter complex reacted with excess PhSiH<sub>3</sub> to give the silyl-nickel complex **C**, and with 4-trifluoromethylbenzaldehyde to give the corresponding nickel-alkoxide insertion complex **D**. Nevertheless, a deuterium labeling experiment conducted with a 1:1:1 mixture of benzaldehyde, Ph<sub>2</sub>SiD<sub>2</sub> and **B** in C<sub>6</sub>D<sub>6</sub> instantaneously yielded PhC(O)HD–SiDPh<sub>2</sub>, while the Ni–H complex **B** remained unchanged, which rules out the conventional hydride mechanism, (*i.e.*: *via* carbonyl insertion into the M–H bond) in spite of 4-trifluoromethylbenzaldehyde insertion into the nickel–hydride in the absence of silane.<sup>[54]</sup>



**Scheme 4.** Hydrosilylation of benzaldehyde with diphenylsilane catalyzed by [Ni(IMes)HCp] **9**



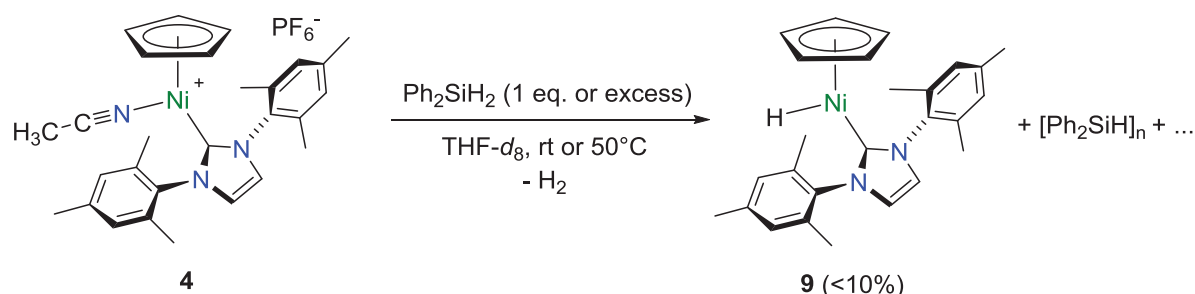
**Scheme 5.** Control experiments performed by Royo *et al.*

To test whether complex **9** catalyzed this hydrosilylation *via* a non-hydride mechanism as suggested by Royo's deuterium labeling experiment,<sup>[53]</sup> or by insertion of the aldehyde into the Ni–H bond,<sup>[52,55]</sup> as reported by Guan with a PCP-pincer nickel hydride complex, and supposed by Mindiola with a dimeric  $[(P,N)\text{Ni}(\mu_2\text{-H})]_2$ ,<sup>[25]</sup> we conducted a series of control experiments. First, **9** was reacted with  $\text{Ph}_2\text{SiH}_2$  in the absence of benzaldehyde. A reaction clearly occurred, but no product could be identified. Then, **9** was reacted with benzaldehyde in the absence of  $\text{Ph}_2\text{SiH}_2$ , and as observed by Jones with another (*P,C,P*)-nickel hydride complex,<sup>[26]</sup> no insertion of benzaldehyde was observed after 3 h at room temperature and the hydride signal remained unchanged in the  $^1\text{H}$  NMR spectrum of the crude reaction mixture. This, of course, contrasts with 4-trifluoromethylbenzaldehyde insertion into the nickel–hydride bond of complex **A**, but goes in the sense of Royo's deuterium labeling experiment. We therefore believe that, although **9** is the true pre-catalyst, the hydride ligand does not directly participate in the reduction reaction, as concluded by Royo *et al.* with the related Cp-NHC tethered nickel-hydride complex **A**.

### II.5.2. (4)-no additive catalytic system

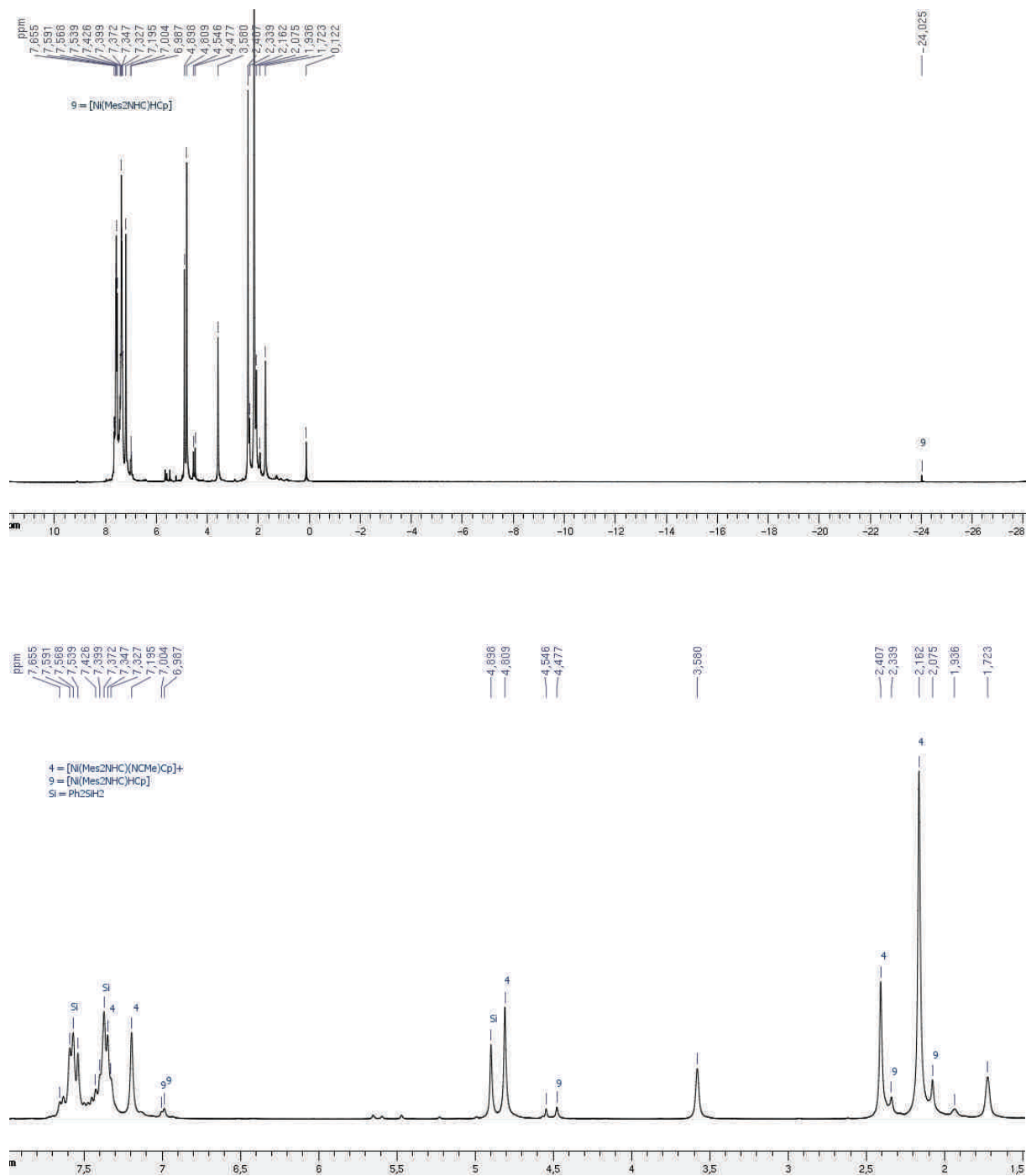
We, of course, wondered if such hydride species was also generated with the catalytic system composed of the sole cationic complex **4** and  $\text{Ph}_2\text{SiH}_2$ .<sup>[52,53,56]</sup>

For that purpose, we reacted **4** with 0.5 or 1 equivalent of  $\text{Ph}_2\text{SiH}_2$  in  $\text{THF-}d_8$  at room temperature and at  $50^\circ\text{C}$ , and monitored the reactions by  $^1\text{H}$  NMR spectroscopy. In all cases, we observed the formation of small amounts (generally less than 10% with respect to the remaining amounts of **4**) of a nickel hydride species, after 5 min of reaction time, which we unambiguously identified as being **9** by comparison with the  $^1\text{H}$  NMR spectrum of a pure sample in  $\text{THF-}d_8$  (**Scheme 6**). Concomitantly, new signals started to appear in the aromatic area (probably resulting from the oligomerization and/or polymerization of  $\text{Ph}_2\text{SiH}_2$ ), as well as a singlet at 1.94 ppm, which we tentatively attribute to free  $\text{CH}_3\text{CN}$ . The rest of the reaction mixture mostly consisted in non-reacted **4** and  $\text{Ph}_2\text{SiH}_2$  (**Figure 4**).

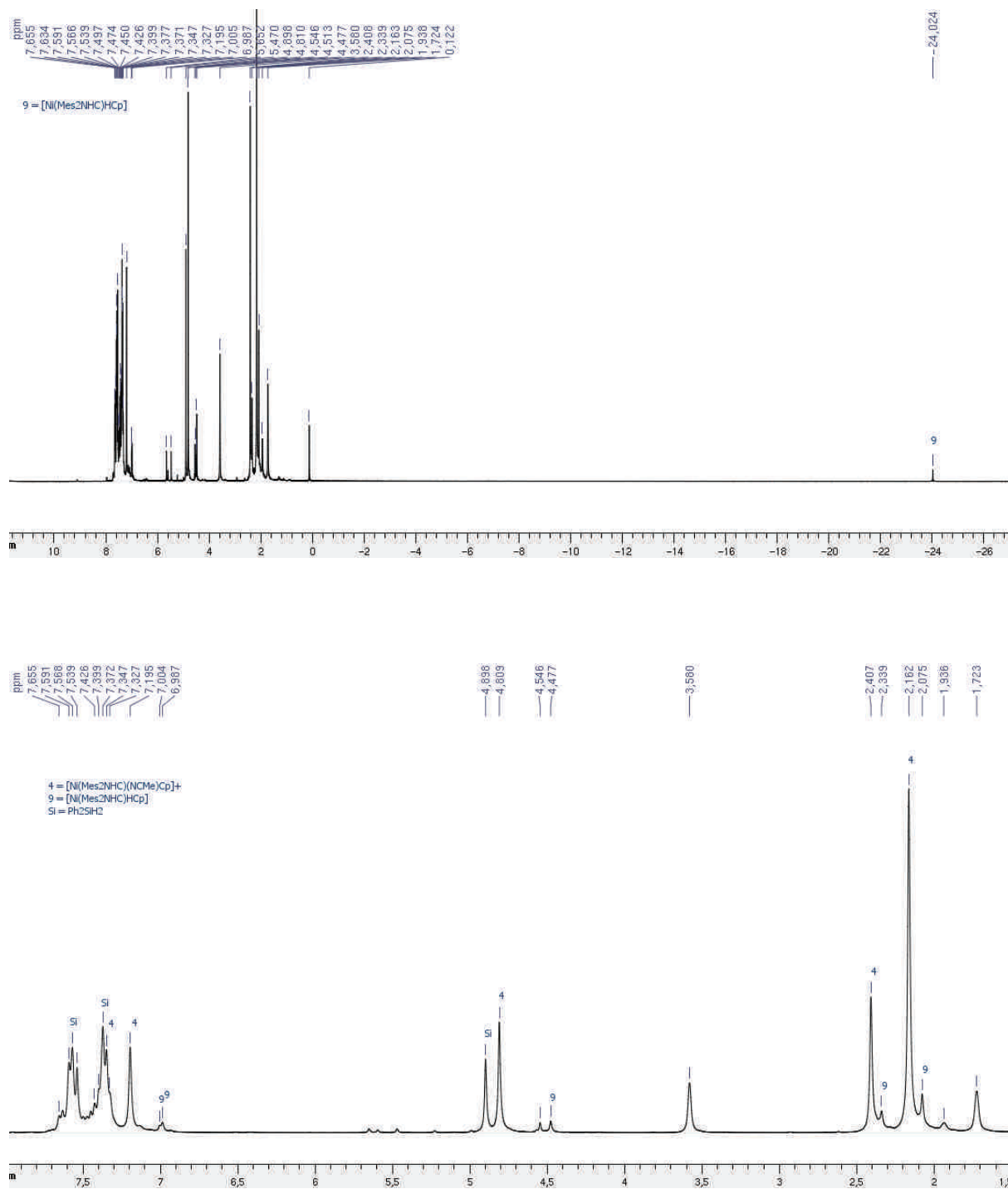


**Scheme 6.** Reaction of  $[\text{Ni}(\text{IMes})(\text{NCMe})\text{Cp}](\text{PF}_6)$  **4** with  $\text{Ph}_2\text{SiH}_2$

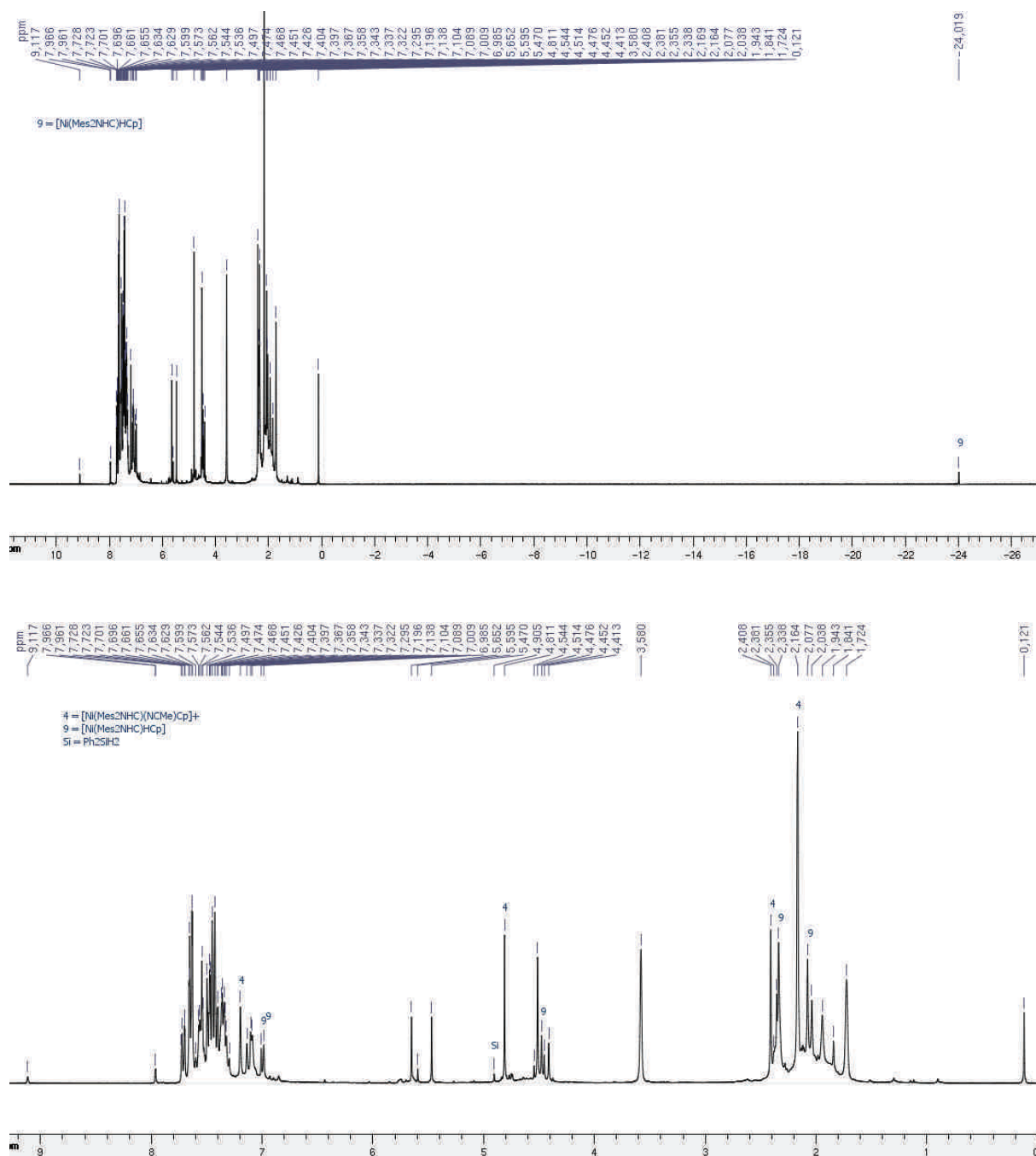
It is noteworthy that in all cases, we also observed the immediate and steady evolution of a gas which we believe is  $\text{H}_2$ , as observed by Zargarian *et al.* in the reaction of analogous nickel complexes of the type  $[\text{Ni}(\text{PR}_3)\text{Me}(1\text{-Me-indenyl})]$  with  $\text{PhSiH}_3$ .<sup>[57]</sup> Finally, after a reaction time varying from 20 min for the reactions conducted at  $50^\circ\text{C}$  to 6 - 22 h for the reactions conducted at RT (with 0.5 or 1 equiv.  $\text{Ph}_2\text{SiH}_2$ ), all  $\text{Ph}_2\text{SiH}_2$  was consumed, and the reaction medium consisted in a complicated mixture of products with small remaining amounts of complexes **4** and **9** (**Figures 5** and **6**). In contrast, the neutral complex **1** strictly gave no reaction with  $\text{Ph}_2\text{SiH}_2$  (0.5 equiv.) in  $\text{THF-}d_8$  at RT, even after 6 h, and required  $70^\circ\text{C}$  to produce trace amount of **9**.



**Figure 4.** Spectrum after 5 min reaction at RT between **4** and  $\text{Ph}_2\text{SiH}_2$  (1.0 equiv.)



**Figure 5.** Spectrum after 25 min reaction at RT between **4** and  $\text{Ph}_2\text{SiH}_2$  (1.0 equiv.)



**Figure 6.** Spectrum after 22 h reaction at RT between **4** and Ph<sub>2</sub>SiH<sub>2</sub> (1.0 equiv.)

These results may explain (i) the total absence of reduction of the aldimine **5** when the reaction was performed in the sole presence of 5 mol% of **1** at RT (**Table 5**, entry 1), as well as the moderate conversion observed in the sole presence of 5 mol% of **1** at 70°C (**Table 5**, entry 2), and (ii) the slightly harsher conditions (50°C) required with **4** (with respect to 1-NaHBET<sub>3</sub>) to observe full reduction (**Table 5**, entries 7 and 8); only small amounts of **1** and **4** are converted to **9** by reaction with Ph<sub>2</sub>SiH<sub>2</sub> (even with a large excess of silane), whereas all **1**

is converted to **9** by reaction with 2 equiv. of NaHBET<sub>3</sub> (**Scheme 2**). Additionally, although (i) another true pre-catalyst (or active species) cannot be ruled out in the absence of NaHBET<sub>3</sub>, and (ii) the hydride ligand of **9** does probably not directly participate in the reduction reaction, these results nevertheless tend to confirm the necessity to generate the nickel hydride complex **9** to observe a catalytic activity.

### III. Conclusion

In summary, we have demonstrated that half-sandwich Ni–NHC complexes can be used as efficient pre-catalysts for the chemoselective reduction of carbonyl (aldehydes and ketones) and imine (aldimines and ketimines) compounds *via* hydrosilylation. In the reduction of carbonyl compounds, the combination of complex **1** and NaHBET<sub>3</sub> proved to efficiently catalyze this transformation at room temperature, for a large array of substrates and with moderate to excellent yields. We have shown that this **1**-NaHBET<sub>3</sub> combination results in the *in situ* formation of the corresponding nickel–hydride complex **9**, which is likely to be the true pre-catalyst of this hydrosilylation, even if the hydride ligand does not seem to be directly implied in the reaction, as shown by control experiments. It is noteworthy that this **1**-NaHBET<sub>3</sub> system also allowed the reduction of aldimines and ketimines, leading to the corresponding amines in moderate to excellent yields. Interestingly, the cationic complex **4** can be used *on its own* instead of **1**-NaHBET<sub>3</sub> for these imine reductions with comparable activity, even if reaction conditions are slightly harsher in this case. Furthermore, the reaction of the cationic complex **4** in the presence of Ph<sub>2</sub>SiH<sub>2</sub> led to the formation of small amounts of the nickel–hydride complex **9**, which reinforces the fact that **9** probably acts as the true pre-catalyst.<sup>[58–60]</sup>

### IV. Experimental section

#### IV.1. General information

All reagents were obtained from commercial sources and used as received, except for the liquid aldehydes, which were distilled prior to use. All reactions were carried out under an

argon atmosphere. Solvents were distilled following conventional methods and stored under an argon atmosphere. Technical grade petroleum ether (40-60°C bp) and diethylether were used for chromatography column.

Solution NMR spectra were recorded at 298 K on FT-Bruker Ultra Shield 300, FT-Bruker Spectrospin 400 (Univ. of Strasbourg), FT-Bruker AVANCE I 300 and Ascend TM 400 (Univ. of Rennes I) spectrometers operating at 300.13 or 400.14 MHz for  $^1\text{H}$ , and at 75.47 or 100.61 MHz for  $^{13}\text{C}\{^1\text{H}\}$ . The chemical shifts are referenced to residual deuterated solvent peaks. Chemical shifts ( $\delta$ ) and coupling constants ( $J$ ) are given in ppm and in Hz, respectively. The peak patterns are indicated as follows: (s, singlet; d, doublet; t, triplet; q, quartet; m, multiplet, and br. for broad).

GC analyses were performed with GC-2014 (Shimadzu) 2010 equipped with a 30-m capillary column (Supelco, SPBTM-20, fused silica capillary column, 30 m $\times$ 0.25 mm $\times$ 0.25 mm film thickness), with  $\text{N}_2$ /air as vector gas. GCMS were measured by GCMS-QP2010S (Shimadzu) with GC-2010 equipped with a 30-m capillary column (Supelco, SLBTM-5ms, fused silica capillary column, 30 M $\times$ 0.25 mm $\times$ 0,25 mm film thickness), with helium as vector gas. The following GC conditions were used: initial temperature 80 °C, for 2 min, then rate 10 °C/min. until 220 °C and 220 °C for 15 min.

HR-MS spectra and elemental analysis were carried out by the corresponding facilities at the CRMPO (Centre Régional de Mesures Physiques de l'Ouest), University of Rennes 1. FTIR spectra were recorded on an IR-ATR Affinity-1 Shimadzu apparatus.

Elemental analyses of complex **9** were performed by the Service d'Analyses, de Mesures Physiques et de Spectroscopie Optique, UMR CNRS 7177, Institut de Chimie, Université de Strasbourg.

$[\text{Ni}(\text{IMes})\text{ClCp}]$  (**1**),<sup>[42,61,62]</sup>  $[\text{Ni}(\text{IPr})\text{ClCp}]$  (**2**),<sup>[42]</sup>  $[\text{Ni}(\text{IMes})\text{ClCp}^*]$  (**3**)<sup>[63]</sup> and  $[\text{Ni}(\text{IMes})(\text{NCMe})\text{Cp}](\text{PF}_6)$  (**4**)<sup>[40]</sup> were prepared according to published methods.

#### IV.2. Synthesis of $[\text{Ni}(\text{IMes})\text{HCp}]$ (**9**)

To a violet solution of  $[\text{Ni}(\text{IMes})\text{ClCp}]$  **1** (500 mg, 1.04 mmol) in THF (10 mL) at  $-78^\circ\text{C}$  was added dropwise a solution of  $\text{KHBET}_3$  (1.25 mmol, 1.0 M in THF). The solution was then allowed to warm to  $0^\circ\text{C}$ , and an immediate color change to red was observed. The solution was rapidly filtered through dry Celite, and the filtrate evaporated under vacuum. The



red residue was then extracted with *n*-pentane (20 mL), and the resulting solution allowed to stand at  $-28\text{ }^{\circ}\text{C}$  for 24 h to afford **9** as red crystals (290 mg, 0.65 mmol, 63 %).

Anal. Calcd for  $\text{C}_{26}\text{H}_{30}\text{N}_2\text{Ni}$ : C, 72.75; H, 7.04; N, 6.53. Found: C, 72.57; H, 7.17; N, 6.43.

$^1\text{H}$  NMR (300.13 MHz, 298 K,  $\text{C}_6\text{D}_6$ ):  $\delta$  6.80 (s, 4H, *m*-H), 6.14 (s, 2H, NCH), 4.99 (s, 5H,  $\text{C}_5\text{H}_5$ ), 2.11 (s, 18H, *o*- and *p*- $\text{CH}_3$ ),  $-23.27$  (s, 1H, Ni-*H*).  $^{13}\text{C}\{^1\text{H}\}$  NMR (100.61 MHz, 298 K,  $\text{C}_6\text{D}_6$ ):  $\delta$  185.4 (NCN), 138.6 and 138.3 (*ipso*-/*p*- $\text{C}_{\text{Ar}}$ ), 135.8 (*o*- $\text{C}_{\text{Ar}}$ ), 129.2 (*m*- $\text{C}_{\text{Ar}}$ ), 121.0 (NCH), 86.8 ( $\text{C}_5\text{H}_5$ ), 21.1 (*p*- $\text{CH}_3$ ), 18.3 (*o*- $\text{CH}_3$ ).

### IV.3. Reactions of $[\text{Ni}(\text{IMes})(\text{NCMe})\text{Cp}](\text{PF}_6)$ (**4**) and $\text{Ph}_2\text{SiH}_2$

To a solution of  $[\text{Ni}(\text{IMes})(\text{NCMe})\text{Cp}](\text{PF}_6)$  **4** (33 mg,  $54.3 \times 10^{-3}$  mmol) in  $\text{THF-}d_8$  (0.5 mL) placed in an NMR tube was added freeze-pump-thaw degassed  $\text{Ph}_2\text{SiH}_2$  (5  $\mu\text{L}$ ,  $27.1 \times 10^{-3}$  mmol for 0.5 equiv.; 10  $\mu\text{L}$ ,  $54.3 \times 10^{-3}$  mmol for 1 equiv.). A slight color change from dark green to dark red immediately occurred, as well as a gas release. The reactions were then either conducted at RT or  $50^{\circ}\text{C}$ , and were monitored by  $^1\text{H}$  NMR spectroscopy. For the reactions run at RT, the first spectra were recorded after *ca.* 5-10 min, and then regularly until all  $\text{Ph}_2\text{SiH}_2$  was consumed, *i.e.* after 6 to 22 h. For the reactions run at  $50^{\circ}\text{C}$ , the first spectra were recorded after *ca.* 5 min at RT, and then every 10 min at  $50^{\circ}\text{C}$  for 40 min. In all cases, all  $\text{Ph}_2\text{SiH}_2$  was consumed after 20 min. The spectra, after 5 min, 25 min and 22 h, of the reaction of **4** with 1.0 equiv. of  $\text{Ph}_2\text{SiH}_2$  at room temperature are shown in the *Mechanistic studies* section (see Figures 3-5). For a comparison purpose, the  $^1\text{H}$  NMR data of **4**, **9** and  $\text{Ph}_2\text{SiH}_2$  in  $\text{THF-}d_8$  are given hereafter.

#### $[\text{Ni}(\text{IMes})(\text{NCMe})\text{Cp}](\text{PF}_6)$ (**4**)

$^1\text{H}$  NMR (400.14 MHz, 298 K,  $\text{THF-}d_8$ ):  $\delta$  7.57 (s, 2H, NCH), 7.20 (s, 4H, *m*-H), 4.81 (s, 5H,  $\text{C}_5\text{H}_5$ ), 2.41 (s, 6H, *p*- $\text{CH}_3$ ), 2.17 (s, 15H, *o*- $\text{CH}_3$  and NCMe).

#### $[\text{Ni}(\text{IMes})\text{HCp}]$ (**9**)

$^1\text{H}$  NMR (300.13 MHz, 298 K,  $\text{THF-}d_8$ ):  $\delta$  7.00 (s, 2H, NCH), 6.98 (s, 4H, *m*-H), 4.46 (s, 5H,  $\text{C}_5\text{H}_5$ ), 2.34 (s, 6H, *p*- $\text{CH}_3$ ), 2.07 (s, 12H, *o*- $\text{CH}_3$ ),  $-24.04$  (s, 1H, Ni-*H*).

#### $\text{Ph}_2\text{SiH}_2$

$^1\text{H}$  NMR (400.14 MHz, 298 K,  $\text{THF-}d_8$ ):  $\delta$  7.58 (dd,  $^3J = 7.8$ ,  $^4J = 1.6$ , 4H, Ph), 7.41-7.32 (m, 6H, Ph), 4.90 (s, 2H,  $\text{SiH}_2$ )

## IV.4. X-ray diffraction study of (9): structure determination and refinement

Single crystals of **9** suitable for X-ray diffraction studies were selected from batches of crystals obtained at  $-28\text{ }^{\circ}\text{C}$  from a pentane solution. Diffraction data were collected at 173(2) K on a Bruker APEX II DUO KappaCCD area detector diffractometer equipped with an Oxford Cryosystem liquid  $\text{N}_2$  device using Mo- $\text{K}\alpha$  radiation ( $\lambda = 0.71073\text{ \AA}$ ). A summary of crystal data, data collection parameters and structure refinements is given in **Table 9**. The crystal-detector distance was 38 mm. The cell parameters were determined (APEX2 software) from reflections taken from three sets of twelve frames, each at 10 s exposure. The structure was solved using direct methods with SHELXS-97 and refined against  $F^2$  for all reflections using the SHELXL-97 software.<sup>[64]</sup> A semi-empirical absorption correction was applied using SADABS in APEX2. All non-hydrogen atoms were refined with anisotropic displacement parameters, using weighted full-matrix least-squares on  $F^2$ . The hydride H1 and, due to the symmetry, the hydrogen atoms H9A, H9B, H15A and H15B were located from Fourier difference maps and refined isotropically. The hydrogen atoms H9A and H9B were refined with restraints. The other H-atoms were included in calculated positions and treated as riding atoms using SHELXL default parameters.

**Table 9.** X-Ray Crystallographic Data and Data Collection Parameters for **9**.

Complex <b>9</b>	
Empirical formula	$\text{C}_{26}\text{H}_{30}\text{N}_2\text{Ni}$
Formula weight	429.23
Crystal system	Orthorhombic
Space group	Pnma
$a$ ( $\text{\AA}$ )	22.906(5)
$b$ ( $\text{\AA}$ )	11.178(3)
$c$ ( $\text{\AA}$ )	8.9631(19)
$V$ ( $\text{\AA}^3$ )	2295.0(9)
$Z$	4
$D_{\text{calcd}}$ ( $\text{Mg}\cdot\text{m}^{-3}$ )	1.242
Absorb coeff ( $\text{mm}^{-1}$ )	0.859
Crystal habit, color	prism, red
Crystal size (mm)	$0.38 \times 0.25 \times 0.20$
$h, k, l_{\text{max}}$	30, 15, 7
$T_{\text{min}}, T_{\text{max}}$	0.736, 0.847
Reflns collected	10258
$R$ [ $I > 2\sigma(I)$ ]	0.0542
$wR^2$ (all data)	0.1594
GOF on $F^2$	1.061

## IV.5. Hydrosilylation of aldehydes and ketones

## IV.5.1. Optimization studies

**Table 10.** Influence of the silane and of the solvent in the hydrosilylation of benzaldehyde with catalyst **1** at 25 °C.<sup>a</sup>

Entry	Catalyst (mol%)	Additive (mol%)	Silane (equiv.)	Solvent	Time (h)	Conversion (%) <sup>b</sup>
1	-	NaHBET <sub>3</sub> (2)	Ph <sub>2</sub> SiH <sub>2</sub> (1)	THF	17	0
2	<b>1</b> (1)	NaHBET <sub>3</sub> (2)	PhSiH <sub>3</sub> (1)	THF	1	15
3	<b>1</b> (1)	NaHBET <sub>3</sub> (2)	Ph <sub>3</sub> SiH (1)	THF	1	0
4	<b>1</b> (1)	NaHBET <sub>3</sub> (2)	Et <sub>3</sub> SiH (1)	THF	1	0
5	<b>1</b> (1)	NaHBET <sub>3</sub> (2)	Me(EtO) <sub>2</sub> SiH (1)	THF	1	14
6	<b>1</b> (1)	NaHBET <sub>3</sub> (2)	Me <sub>2</sub> PhSiH (1)	THF	1	0
7	<b>1</b> (1)	NaHBET <sub>3</sub> (2)	TMDS (1)	THF	1	31
8	<b>1</b> (1)	NaHBET <sub>3</sub> (2)	Ph <sub>2</sub> SiH <sub>2</sub> (1)	Toluene	1	97
9	<b>1</b> (1)	NaHBET <sub>3</sub> (2)	Ph <sub>2</sub> SiH <sub>2</sub> (1)	CPME	1	97
10	<b>1</b> (1)	NaHBET <sub>3</sub> (2)	Ph <sub>2</sub> SiH <sub>2</sub> (1)	DMC	1	76
11	<b>1</b> (1)	NaHBET <sub>3</sub> (2)	Ph <sub>2</sub> SiH <sub>2</sub> (1)	CH <sub>2</sub> Cl <sub>2</sub>	1	0

<sup>a</sup> Typical procedure: activation of **1** with the additive in THF (4 mL) was followed by addition of benzaldehyde (1 mmol) and the silane (1 mmol), and the reaction was stirred at 25 °C. <sup>b</sup> Conversions determined by GC after methanolysis (MeOH, 2M NaOH) and extraction with Et<sub>2</sub>O.

## IV.5.2. General procedure: nickel-catalyzed hydrosilylation of aldehydes

A 10 mL oven dried Schlenk tube containing a stirring bar was loaded with [Ni(IMes)ClCp] **1** (4.6 mg, 1.10<sup>-5</sup> mol) and 4 mL of THF. The resulting purple solution was stirred for 5 min. A solution of NaHBET<sub>3</sub> in THF (20 µl, 1 M in THF, Acros, 2.10<sup>-5</sup> mol) was added dropwise, and the solution was stirred until the color turned to deep red. The aldehyde (1.10<sup>-3</sup> mol) and Ph<sub>2</sub>SiH<sub>2</sub> (186 µL, 1.10<sup>-3</sup> mol) were then added, in this order, and the reaction mixture was stirred in a preheated oil bath at 25 °C for 1 or 17 h. The reaction mixture was

then quenched by the addition of methanol (2 mL) and 2M NaOH (2 mL) and stirred for 2 h. After the addition of water (5 mL), the product was extracted with diethylether (3 x 10 mL). The combined organic layers were dried over anhydrous MgSO<sub>4</sub>, filtered and concentrated under vacuum. The conversion was determined by <sup>1</sup>H NMR. The product was purified by silica gel column chromatography using a petroleum ether/diethyl ether mixture.

#### IV.5.3. General procedure: nickel-catalyzed hydrosilylation of ketones

A 10 mL oven-dried Schlenk tube containing a stirring bar, was loaded with [Ni(IMes)ClCp] **1**, (23 mg, 5.10<sup>-5</sup> mol) and 4 mL of THF. The resulting purple solution was stirred for 5 min. A solution of NaHBET<sub>3</sub> in THF (100 µL, 1 M in THF, Acros, 10.10<sup>-5</sup> mol) was added dropwise, and the solution was stirred until the color turned to deep red. The ketone (1.10<sup>-3</sup> mol) and Ph<sub>2</sub>SiH<sub>2</sub> (186 µL, 1.10<sup>-3</sup> mol) were then added, in this order, and the reaction mixture was stirred in a preheated oil bath at 25°C for 17 h. The reaction mixture was then quenched by the addition of methanol (2 mL) and 2M NaOH (2 mL), and stirred for 2 h. After the addition of water (5 mL), the product was extracted with diethylether (3 x 10 mL). The combined organic layers were dried over anhydrous MgSO<sub>4</sub>, filtered and concentrated under vacuum. The conversion was determined by <sup>1</sup>H NMR. The product was purified by silica gel column chromatography using a petroleum ether - diethyl ether mixture.

### IV.6. Hydrosilylation of aldimines and ketimines

#### IV.6.1. Optimization studies

**Table 11.** Influence of the silane in the hydrosilylation of **5** with catalyst **4**.<sup>a</sup>

Entry	Catalyst (mol%)	Silane (equiv.)	Solvent	Temp	Time (h)	Conversion (%) <sup>b</sup>
1	<b>4</b> (1)	Ph <sub>2</sub> SiH <sub>2</sub> (1 equiv.)	THF	50 °C	24	> 98%
2	<b>4</b> (1)	TMDS (2 equiv.)	THF	70 °C	24	0
3	<b>4</b> (1)	PMHS (4 equiv.)	THF	70 °C	24	30%

<sup>a</sup> Typical procedure: To a solution of **4** (6.1 mg, 1 mol%) in THF (4 mL) at RT was added **5** (1 mmol) and the silane (1-4 equiv.) and the reaction mixture was stirred at 50 or 70 °C for 24 h. <sup>b</sup> Conversions determined by <sup>1</sup>H NMR after methanolysis: MeOH (2 mL), 2M NaOH (2 mL), RT, 2 h. and extraction with Et<sub>2</sub>O.

**Table 12.** Influence of the solvent in the hydrosilylation of **7** with catalysts **1** and **4**.<sup>a</sup>

Entry	Catalyst (mol%)	Silane (equiv.)	Solvent	Temp	Time (h)	Conversion (%) <sup>b</sup>
1	<b>4</b> (5)	Ph <sub>2</sub> SiH <sub>2</sub> (2 equiv.)	THF	70 °C	24	> 98%
2	<b>4</b> (5)	Ph <sub>2</sub> SiH <sub>2</sub> (1 equiv.)	THF	70 °C	24	85%
3	<b>4</b> (5)	Ph <sub>2</sub> SiH <sub>2</sub> (1 equiv.)	2-Me-THF	80 °C	24	60%
4	<b>4</b> (5)	Ph <sub>2</sub> SiH <sub>2</sub> (1 equiv.)	Toluene	100 °C	24	20%
5	<b>4</b> (1)	Ph <sub>2</sub> SiH <sub>2</sub> (1 equiv.)	CH <sub>3</sub> CN	70 °C	24	0%
6	<b>1</b> (1) <sup>c</sup>	Ph <sub>2</sub> SiH <sub>2</sub> (1 equiv.)	CH <sub>3</sub> CN	70 °C	24	0%

<sup>a</sup> *Typical procedure:* To a solution of **4** or **1** in the solvent (4 mL) at RT was added **7** (1 mmol) and the Ph<sub>2</sub>SiH<sub>2</sub> (1 - 2 mmol), and the reaction mixture was stirred at 70, 80 or 100 °C for 24 h. <sup>b</sup> Conversions determined by <sup>1</sup>H NMR after methanolysis: MeOH (2 mL), 2M NaOH (2 mL), RT, 2 h. and extraction with Et<sub>2</sub>O. <sup>c</sup> KPF<sub>6</sub> (2 mol%) was added.

#### IV.6.2. General procedure: nickel-catalyzed hydrosilylation of aldimines with (**1**) and NaHBET<sub>3</sub>

A 10 mL oven dried Schlenk tube containing a stirring bar is loaded with [Ni(IMes)ClCp] **1** (4.6 mg, 1.10<sup>-5</sup> mol) and THF (4 mL). To the resulting purple solution is added dropwise a solution of NaHBET<sub>3</sub> in THF (20 µL, 1 M in THF, Acros, 2.10<sup>-5</sup> mol), and the medium is stirred until the color turns to deep red. The aldimine (1.10<sup>-3</sup> mol) and Ph<sub>2</sub>SiH<sub>2</sub> (186 µL, 1.10<sup>-3</sup> mol) are then added in this order, and the reaction mixture is stirred in a preheated oil bath at 25 °C for 17 h. The reaction is then quenched by adding methanol (2 mL) and 2M NaOH (2 mL), and further stirring the medium for 2 h. After the addition of water (5 mL), the product is extracted with diethylether (3 x 10 mL). The combined organic layers are dried over anhydrous MgSO<sub>4</sub>, filtered and concentrated under vacuum. The conversion is determined by <sup>1</sup>H NMR spectroscopy, and the product purified by silica gel column chromatography using a petroleum ether/diethylether mixture.

#### IV.6.3. General procedure: nickel-catalyzed hydrosilylation of aldimines with (**4**)

A 10 mL oven dried Schlenk tube containing a stirring bar is loaded with [Ni(IMes)(NCMe)Cp](PF<sub>6</sub>) **4** (6.1 mg, 1.10<sup>-5</sup> mol) and THF (4 mL) to give a yellow solution.

The aldimine ( $1.10^{-3}$  mol) and  $\text{Ph}_2\text{SiH}_2$  (186  $\mu\text{L}$ ,  $1.10^{-3}$  mol) are then added in this order, and the reaction mixture is stirred in a preheated oil bath at 50 °C for 24 h. The reaction mixture is then quenched by adding methanol (2 mL) and 2M NaOH (2 mL), and further stirring the medium for 2 h. The work-up is done as described in the typical procedure for the hydrosilylation of aldimines with  $[\text{Ni}(\text{IMes})\text{ClCp}]$  **1** and  $\text{NaHBET}_3$ .

#### IV.7. Characterization of the hydrosilylation products

Characterization of the hydrosilylation products was conducted by Linus P. Bheeter in the group of C. Darcel and J.-B. Sortais at the University of Rennes I (UMR CNRS 6226). Full data can be found in references 39 and 45.

#### V. References

- [1] P. G. Andersson, I. J. Munslow, in *Modern Reduction Methods*, Wiley-VCH, Weinheim, **2008**.
- [2] K. Ziegler, *Angew. Chem.* **1957**, 69, 626–626.
- [3] N. G. Gaylord, *J. Chem. Educ.* **1957**, 34, 367–373.
- [4] I. Ojima, M. Nihonyanagi, Y. Nagai, *J. Chem. Soc., Chem. Commun.* **1972**, 938a–938a.
- [5] I. Ojima, T. Kogure, M. Nihonyanagi, Y. Nagai, *Bull. Chem. Soc. Jpn.* **1972**, 45, 3506–3506.
- [6] K. Riener, M. P. Högerl, P. Gigler, F. E. Kühn, *ACS Catal.* **2012**, 2, 613–621.
- [7] H. Nishiyama, A. Furuta, *Chem. Commun.* **2007**, 760–762.
- [8] N. S. Shaikh, K. Junge, M. Beller, *Org. Lett.* **2007**, 9, 5429–5432.
- [9] A. M. Tondreau, E. Lobkovsky, P. J. Chirik, *Org. Lett.* **2008**, 10, 2789–2792.
- [10] T. Inagaki, L. T. Phong, A. Furuta, J. Ito, H. Nishiyama, *Chem. Eur. J.* **2010**, 16, 3090–3096.
- [11] H. Mimoun, J. Y. de Saint Laumer, L. Giannini, R. Scopelliti, C. Floriani, *J. Am. Chem. Soc.* **1999**, 121, 6158–6166.
- [12] V. Bette, A. Mortreux, C. W. Lehmann, J.-F. Carpentier, *Chem. Commun.* **2003**, 332–333.

- [13] V. Bette, A. Mortreux, D. Savoia, J.-F. Carpentier, *Adv. Synth. Catal.* **2005**, 347, 289–302.
- [14] S. Das, D. Addis, S. Zhou, K. Junge, M. Beller, *J. Am. Chem. Soc.* **2010**, 132, 1770–1771.
- [15] S. Bower, K. A. Kreutzer, S. L. Buchwald, *Angew. Chem. Int. Ed. Engl.* **1996**, 35, 1515–1516.
- [16] K. Selvakumar, J. F. Harrod, *Angew. Chem. Int. Ed.* **2001**, 40, 2129–2131.
- [17] S. Laval, W. Dayoub, L. Pehlivan, E. Métay, A. Favre-Réguillon, D. Delbrayelle, G. Mignani, M. Lemaire, *Tetrahedron Lett.* **2011**, 52, 4072–4075.
- [18] S. Rendler, M. Oestreich, *Angew. Chem. Int. Ed.* **2007**, 46, 498–504.
- [19] C. Deutsch, N. Krause, B. H. Lipshutz, *Chem. Rev.* **2008**, 108, 2916–2927.
- [20] B. Lipshutz, *Synlett* **2009**, 509–524.
- [21] F.-G. Fontaine, R.-V. Nguyen, D. Zargarian, *Can. J. Chem.* **2003**, 81, 1299–1306.
- [22] T. Irrgang, T. Schareina, R. Kempe, *J. Mol. Catal. A* **2006**, 257, 48–52.
- [23] Y. K. Kong, J. Kim, S. Choi, S.-B. Choi, *Tetrahedron Lett.* **2007**, 48, 2033–2036.
- [24] S. Chakraborty, J. A. Krause, H. Guan, *Organometallics* **2009**, 28, 582–586.
- [25] B. L. Tran, M. Pink, D. J. Mindiola, *Organometallics* **2009**, 28, 2234–2243.
- [26] S. Kundu, W. W. Brennessel, W. D. Jones, *Inorg. Chem.* **2011**, 50, 9443–9453.
- [27] F.-F. Wu, J.-N. Zhou, Q. Fang, Y.-H. Hu, S. Li, X.-C. Zhang, A. S. C. Chan, J. Wu, *Chem. Asian J.* **2012**, 7, 2527–2530.
- [28] L. C. Misal Castro, D. Bézier, J.-B. Sortais, C. Darcel, *Adv. Synth. Catal.* **2011**, 353, 1279–1284.
- [29] L. C. Misal Castro, H. Li, J.-B. Sortais, C. Darcel, *Chem. Commun.* **2012**, 48, 10514–10516.
- [30] H. Li, L. C. Misal Castro, J. Zheng, T. Roisnel, V. Dorcet, J.-B. Sortais, C. Darcel, *Angew. Chem. Int. Ed.* **2013**, 52, 8045–8049.
- [31] F. Jiang, D. Bézier, J.-B. Sortais, C. Darcel, *Adv. Synth. Catal.* **2011**, 353, 239–244.
- [32] D. Bézier, G. T. Venkanna, J.-B. Sortais, C. Darcel, *ChemCatChem* **2011**, 3, 1747–1750.
- [33] L. C. M. Castro, J.-B. Sortais, C. Darcel, *Chem. Commun.* **2012**, 48, 151–153.
- [34] J. Zheng, L. C. Misal Castro, T. Roisnel, C. Darcel, J.-B. Sortais, *Inorg. Chim. Acta* **2012**, 380, 301–307.



- [35] D. Bézier, F. Jiang, T. Roisnel, J.-B. Sortais, C. Darcel, *Eur. J. Inorg. Chem.* **2012**, 1333–1337.
- [36] D. Bézier, G. T. Venkanna, L. C. M. Castro, J. Zheng, T. Roisnel, J.-B. Sortais, C. Darcel, *Adv. Synth. Catal.* **2012**, 354, 1879–1884.
- [37] H. Jaafar, H. Li, L. C. Misal Castro, J. Zheng, T. Roisnel, V. Dorcet, J.-B. Sortais, C. Darcel, *Eur. J. Inorg. Chem.* **2012**, 3546–3550.
- [38] V. César, L. C. Misal Castro, T. Dombay, J.-B. Sortais, C. Darcel, S. Labat, K. Miqueu, J.-M. Sotiropoulos, R. Brousses, N. Lugan, G. Lavigne, *Organometallics* **2013**, 32, 4643–4655.
- [39] L. P. Bheeter, M. Henrion, L. Brelot, C. Darcel, M. J. Chetcuti, J.-B. Sortais, V. Ritleng, *Adv. Synth. Catal.* **2012**, 354, 2619–2624.
- [40] V. Ritleng, A. M. Oertel, M. J. Chetcuti, *Dalton Trans.* **2010**, 39, 8153–8160.
- [41] M. Henrion, M. J. Chetcuti, V. Ritleng, *Chem. Commun.* **2014**, 50, 4624–4627.
- [42] R. A. Kelly III, N. M. Scott, S. Díez-González, E. D. Stevens, S. P. Nolan, *Organometallics* **2005**, 24, 3442–3447.
- [43] W. Buchowicz, A. Kozioł, L. B. Jerzykiewicz, T. Lis, S. Pasynkiewicz, A. Pęcherzewska, A. Pietrzykowski, *J. Mol. Catal. A* **2006**, 257, 118–123.
- [44] W. Buchowicz, W. Wojtczak, A. Pietrzykowski, A. Lupa, L. B. Jerzykiewicz, A. Makal, K. Woźniak, *Eur. J. Inorg. Chem.* **2010**, 648–656.
- [45] L. P. Bheeter, M. Henrion, M. J. Chetcuti, C. Darcel, V. Ritleng, J.-B. Sortais, *Catal. Sci. Technol.* **2013**, 3, 3111–3116.
- [46] J. Berding, M. Lutz, A. L. Spek, E. Bouwman, *Appl. Organomet. Chem.* **2011**, 25, 76–81.
- [47] O. Coulembier, A. P. Dove, R. C. Pratt, A. C. Sentman, D. A. Culkin, L. Mespouille, P. Dubois, R. M. Waymouth, J. L. Hedrick, *Angew. Chem. Int. Ed.* **2005**, 44, 4964–4968.
- [48] K. S. Hayes, *Appl. Catal. Gen.* **2001**, 221, 187–195.
- [49] A. H. Vetter, A. Berkessel, *Synthesis* **1995**, 419–422.
- [50] C. D. Abernethy, R. J. Baker, M. L. Cole, A. J. Davies, C. Jones, *Trans. Met. Chem.* **2003**, 28, 296–299.
- [51] C. D. Abernethy, Alan H, Cowley, R. A. Jones, *J. Organomet. Chem.* **2000**, 596, 3–5.
- [52] J. Breitenfeld, R. Scopelliti, X. Hu, *Organometallics* **2012**, 31, 2128–2136.
- [53] L. Postigo, B. Royo, *Adv. Synth. Catal.* **2012**, 354, 2613–2618.



- [54] O. G. Shirobokov, L. G. Kuzmina, G. I. Nikonov, *J. Am. Chem. Soc.* **2011**, *133*, 6487–6489.
- [55] S. Chakraborty, H. Guan, *Dalton Trans.* **2010**, *39*, 7427–7436.
- [56] D. Adhikari, M. Pink, D. J. Mindiola, *Organometallics* **2009**, *28*, 2072–2077.
- [57] F.-G. Fontaine, D. Zargarian, *Organometallics* **2002**, *21*, 401–408.
- [58] J. Zheng, C. Darcel, J.-B. Sortais, *Catal. Sci. Technol.* **2013**, *3*, 81–84.
- [59] J. Zheng, T. Roisnel, C. Darcel, J.-B. Sortais, *ChemCatChem* **2013**, *5*, 2861–2864.
- [60] S. N. MacMillan, W. Hill Harman, J. C. Peters, *Chem. Sci.* **2014**, *5*, 590–597.
- [61] C. D. Abernethy, H. Alan, R. A. Jones, *J. Organomet. Chem.* **2000**, *596*, 3–5.
- [62] V. Ritleng, E. Brenner, M. J. Chetcuti, *J. Chem. Educ.* **2008**, *85*, 1646–1648.
- [63] V. Ritleng, C. Barth, E. Brenner, S. Milosevic, M. J. Chetcuti, *Organometallics* **2008**, *27*, 4223–4228.
- [64] G. M. Sheldrick, *Acta Crystallogr. A* **2008**, *64*, 112–122.

## **Chapter IV.**

### **Synthesis, characterization and catalysis applications of new *N*-heterocyclic carbene–nickel complexes**



# Chapter IV.

## Synthesis, characterization and catalysis applications of new *N*-heterocyclic carbene–nickel complexes

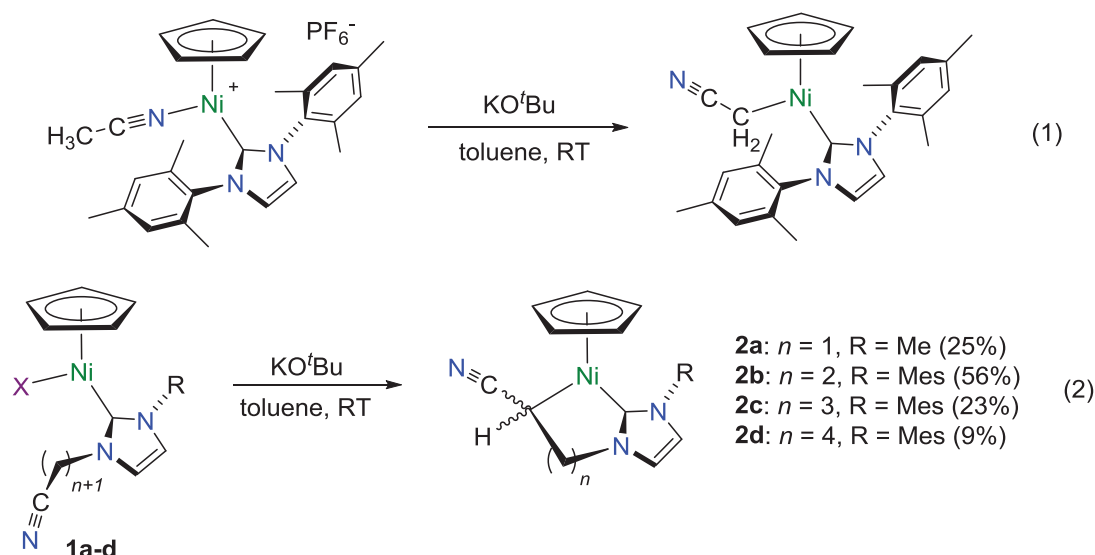
<b>I.</b>	<b>Introduction .....</b>	<b>138</b>
<b>II.</b>	<b>Results and discussion.....</b>	<b>142</b>
II.1.	Facile displacement of $\eta^5$ -cyclopentadienyl ligands from half sandwich alkyl, NHC–nickel complexes.....	142
II.2.	Attempts to synthesize [Ni(IMes)(acac)Cl]: unexpected formation of [IMes.H <sup>+</sup> ] <sub>3</sub> [(NiCl <sub>4</sub> <sup>2-</sup> )(Cl <sup>-</sup> )].....	149
II.3.	Synthesis of <i>malo</i> -NHC–nickel complexes.....	152
II.4.	Synthesis of Ni–CAAC complexes .....	157
II.5.	Catalysis applications of the new nickel carbene complexes .....	161
<b>III.</b>	<b>Conclusion .....</b>	<b>165</b>
<b>IV.</b>	<b>Experimental section .....</b>	<b>166</b>
IV.1.	General information.....	166
IV.2.	Synthesis of [Ni{Mes-NHC-(CH <sub>2</sub> ) <sub>2</sub> CH(CN)}(NCCH <sub>3</sub> ) <sub>2</sub> ] <sup>+</sup> PF <sub>6</sub> <sup>-</sup> (3b) .....	167
IV.3.	Deuterium labeling experiment; reaction of (2b) with DCl .....	167
IV.4.	Synthesis of [Ni{Mes-NHC-(CH <sub>2</sub> ) <sub>2</sub> CH(CN)}(acac)] (4b) .....	168
IV.5.	Synthesis of [Ni{Me-NHC-CH <sub>2</sub> CH(CN)}(acac)] (4a).....	169
IV.6.	Synthesis of [Ni(IMes)(CH <sub>3</sub> )(acac)] (6a) .....	170
IV.7.	Synthesis of [Ni(IMes)(CH <sub>2</sub> CN)(acac)] (6b) .....	170
IV.8.	Synthesis of [IMes.H <sup>+</sup> ] <sub>3</sub> [(NiCl <sub>4</sub> <sup>2-</sup> )(Cl <sup>-</sup> )] (7) .....	171
IV.9.	Synthesis of [Ni(IMes) <sub>2</sub> Cl <sub>2</sub> ] (8).....	171
IV.10.	Synthesis of [Ni(PPh <sub>3</sub> ) <sub>2</sub> (maloNHC)Cl] (10) .....	172
IV.11.	Synthesis of [Ni(IME)(maloNHC)Cp] (12) .....	172
IV.12.	Synthesis of [Ni(IME)(MeO-maloNHC)Cp](OTf) (13) .....	173
IV.13.	Synthesis of [Ni(CAAC)(PPh <sub>3</sub> )Cl <sub>2</sub> ] (15) and of [CAAC.H <sup>+</sup> ][Ni(PPh <sub>3</sub> )Cl <sub>3</sub> ] (16).....	173
IV.14.	X-ray Diffraction Studies. Structure Determination and Refinement .....	174
<b>V.</b>	<b>References .....</b>	<b>175</b>

## I. Introduction

As shown in the first chapter of this manuscript, *N*-heterocyclic carbenes of nickel have become an important class of pre-catalysts, which have been applied to a large array of organic transformations. Moreover, the low cost and high abundance in the Earth's crust of nickel compared to many other of transition metals (84 g/ton of Ni *vs.* 0.015 g/ton of Pd, for instance)<sup>[1]</sup> prompts chemists to pay more and more attention to these systems. However, even if the scope of applicability is impressive, most of the Ni–NHC-catalyzed reactions deserve to be optimized if one considers potential industrialization of these processes. In this regard, main challenges include: (i) the reduction of catalyst loadings, (ii) the use of less demanding reaction conditions, and (iii) the development of user-friendly pre-catalysts. Achieving these goals goes through the development of novel, efficient well-defined Ni(II) pre-catalysts (in contrast to the highly air sensitive and pyrophoric Ni(COD)<sub>2</sub>/NHC systems used in the vast majority of the applications developed up to now). To enhance the activity of well-defined Ni(II)–NHC pre-catalysts, one evident option is to fine tune the steric and electronic properties of the NHC and/or of the other ligands.

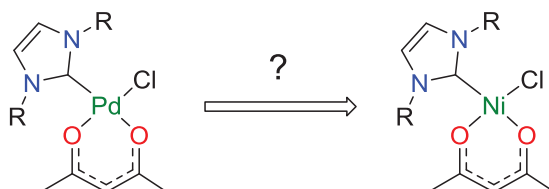
In this context, recent efforts from our group have been directed towards the diversification of well-defined cyclopentadienyl (Cp) Ni–NHC complexes. In particular, the intramolecular version of the base-assisted C–H activation of acetonitrile<sup>[2]</sup> (**Scheme 1**, eqn. (1)) led to a series of half-sandwich (*C,C*)-nickelacycles **2a–d**, starting from complexes **1a–d** (**Scheme 1**, eqn. (2)).<sup>[3]</sup> Regarding the latter work, the introduction of chelating and polyfunctional NHC ligands into the coordination sphere of a metal catalyst generally has interesting consequences, since this can increase the thermal stability<sup>[4]</sup> of the complex and also impose the rigidity required for the preparation of effective asymmetric catalysts in the presence of a chiral center.<sup>[5]</sup> Nevertheless, in the case of "CpM–NHC" complexes, such a chelating ligand may lead to catalyst inhibition since an additional coordination site is now occupied.<sup>[6]</sup> Thus, in the nickelacycles **2a–d**, apart from an eventual Cp ring slippage from the  $\eta^5$ - to an  $\eta^3$ - or  $\eta^1$ -coordination mode, there is no other potentially available coordination site. It was therefore of interest to explore any potential lability of the Cp ligands in these systems,<sup>[7]</sup> and we describe, in this chapter, the facile removal of the Cp ligand of these 18-electron complexes under acidic conditions to afford the corresponding 16-electron *cis*-(*C,C*)-nickel square planar complexes, [Ni{R–NHC–(CH<sub>2</sub>)<sub>2</sub>CH(CN)}(NCMe)<sub>2</sub>](PF<sub>6</sub>), and the

subsequent substitution of the new MeCN ligands by an acetylacetonate ( $\text{acac}^-$ ) anion to give the corresponding neutral complexes  $[\text{Ni}\{\text{R-NHC}-(\text{CH}_2)_2\text{CH}(\text{CN})\}(\text{acac})]$ . Preliminary results regarding their catalytic activities in Suzuki-Miyaura coupling are also given.



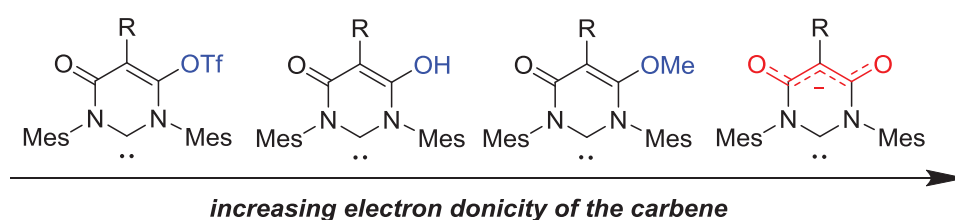
**Scheme 1.** Base-assisted C–H activation of acetonitrile and alkyl nitrile-NHC side arms in  $\text{CpNi-NHC}$  complexes

In the quest of efficient well-defined Ni–NHC catalysts, we were also interested in synthesizing the closely related 16-electron square-planar nickel derivatives of  $[\text{Pd}(\text{NHC})(\text{acac})\text{Cl}]$  complexes (**Scheme 2**), which were shown to be very efficient tools for various applications in Pd-catalyzed C–C and C–N bond formations.<sup>[8–15]</sup> Herein, we present our approach to synthesize such  $[\text{Ni}(\text{NHC})(\text{acac})\text{Cl}]$  complexes, which could be interesting precursors to generate catalytically active mono-ligated Ni–NHC systems.



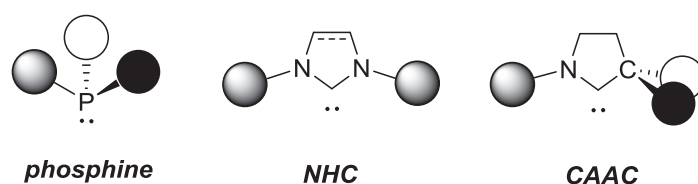
**Scheme 2.**  $[\text{Pd}(\text{NHC})(\text{acac})\text{Cl}]$  complexes and potential  $[\text{Ni}(\text{NHC})(\text{acac})\text{Cl}]$  derivatives

Another approach that can give rise to more active systems, as mentioned above, consists in the modification of the NHC ligand. Classically, imidazolin- and imidazolydene are the most frequently studied ligands. However, replacement of these species by other types of carbenes were recently found to have a positive effect in some metal-catalyzed processes.<sup>[16–19]</sup> Among those new carbene ligands, anionic pyrimidinylidene groups, which possess a malonate backbone (also called *malo*-NHC – **Figure 1**) constitute a promising class of carbenes that give rise to zwitterionic complexes upon complexation to a metal center.<sup>[20–25]</sup> The use of such species in catalysis can indeed be beneficial, as the anionic moiety of the backbone of the *malo*-NHC is pointing toward the outer coordination sphere, and does thus not interfere with the metal's cavity shape.<sup>[20]</sup> Moreover, the electronic properties of *malo*-NHCs can be easily tuned by trapping them with an electrophile, without modification of the steric environment (**Figure 1**). We consequently decided to study the yet unknown coordination chemistry of *malo*-NHCs with nickel, and the activity of the resulting complexes in various organic transformations.



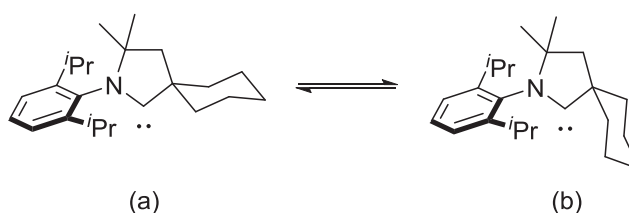
**Figure 1.** Electron-donicity of representative examples of *malo*-NHCs derivatives

Another type of carbenes that attracted our attention are pyrrolidinylidenes, also known as cyclic (alkyl)(amino)carbenes (CAAC), that were first described in 2005 by Bertrand and co-workers.<sup>[26,27]</sup> Indeed, the replacement of one of the electronegative amino substituent of NHCs by a  $\sigma$ -donor alkyl group make CAAC ligands more electron-rich than NHCs, and of course trialkyl phosphines. In addition, the slightly higher energy of the HOMO, and the significantly smaller singlet-triplet gap make CAAC ligands more electrophilic and nucleophilic at the same time, compared to NHCs (see also **Chapter I, Theoretical aspects**). Finally, the different and more encumbered steric environment generated by the quaternary carbon  $\alpha$  to the carbene carbon may also be of interest when compared to phosphines and NHCs (**Figure 2**).<sup>[19]</sup>



**Figure 2.** Representation of the steric environment in phosphines, NHCs, and CAACs

Among the variety of CAAC ligands that have been described, we chose a CAAC ligand bearing a 2,6-diisopropylphenyl (Dipp) group on the nitrogen atom, and a non-substituted cyclohexane ring at the carbon  $\alpha$  to the carbene. This CAAC ligand indeed illustrates the concept of "flexible steric bulk", introduced by Glorius and co-workers,<sup>[28–30]</sup> as it can adopt a conformation that generates a small steric bulk to accept sterically hindered substrates (**Scheme 3**, (a)), and another conformation that generates a more important steric bulk in order to facilitate the reductive elimination process (**Scheme 3**, (b)). We thus thought that the steric and electronic properties of this CAAC ligand could give rise to promising Ni–CAAC catalysts<sup>[31,32]</sup> – as illustrated by the Pd–CAAC-catalyzed  $\alpha$ -arylation of propiophenone and isobutanal with aryl chlorides, which gave the best results observed so far for this reaction, with TON of up to 7200 at room temperature<sup>[26]</sup> – and describe herein the synthesis and catalytic applications of a nickel complex bearing this CAAC ligand.



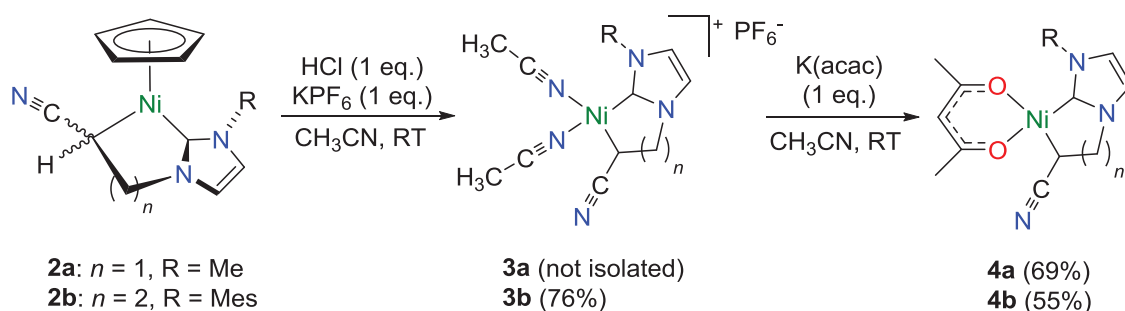
**Scheme 3.** Representation of the "flexible steric bulk" in the C-cyclohexyl functionalized Dipp-CAAC ligand



## II. Results and discussion

### II.1. Facile displacement of $\eta^5$ -cyclopentadienyl ligands from half sandwich alkyl, NHC–nickel complexes

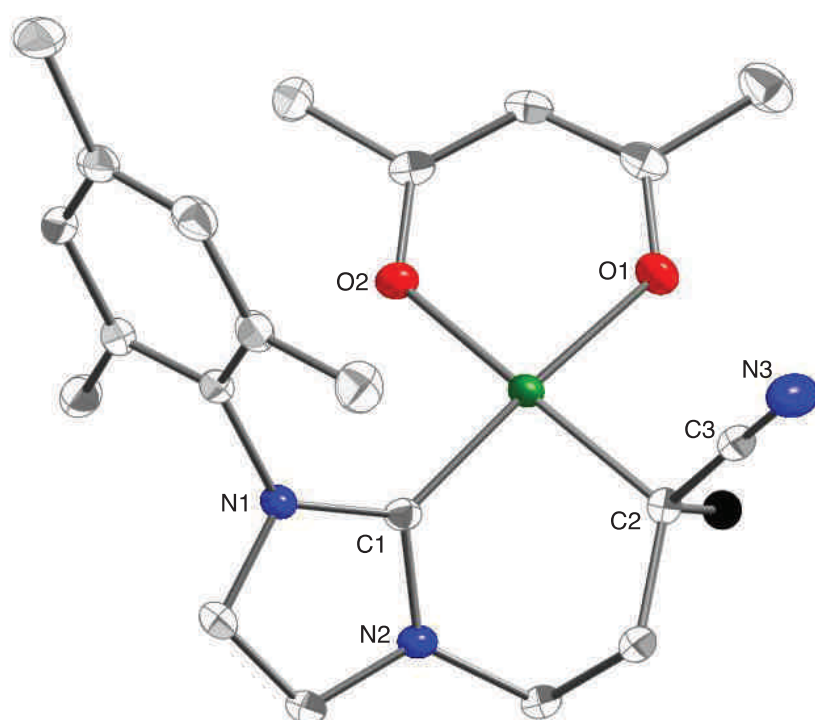
To check the possibility of labilizing the Cp ligand of the half-sandwich alkyl,NHC–nickel complexes **2**, a suspension of **2b** and KPF<sub>6</sub> (1 equiv.) in acetonitrile was treated at room temperature by the drop-wise addition of an equimolar amount of HCl (37%) diluted in acetonitrile to 1.0 M. When the equivalence was reached, an immediate color change from dark green to dark yellow was observed, and <sup>1</sup>H NMR spectra (CD<sub>3</sub>CN) of the reaction medium indicated quantitative loss of the Cp ligand and generation of a cationic square planar complex **3b** (Scheme 3). The latter was isolated as a dark yellow solid in 76% yield after the removal of salts and solvents. However, it proved to be difficult to recrystallize, and this precluded its isolation as an analytically pure solid. Nevertheless, its *in situ* treatment with potassium acetylacetonate (1 equiv.) allowed the substitution of the two labile acetonitrile ligands, and the formation of the more stable neutral chelate derivative **4b**, which was isolated as a light green solid in 55% yield after work up (Scheme 4).



**Scheme 4.**  $\eta^5$ -Cp acidolysis in acetonitrile and subsequent substitution of the resulting acetonitrile ligands by an acetylacetonate chelate

Similarly, the reaction of the five-membered nickelacycle **2a** with equimolar amounts of HCl and KPF<sub>6</sub>, followed by treatment of the resulting solution with potassium acetylacetonate afforded the corresponding neutral square planar complex **4a** in good yield as well (Scheme 4).

An X-ray diffraction study of a single crystal of **4b** (Figure 3), selected from a batch of crystals obtained at  $-28^{\circ}\text{C}$  from a THF/pentane solution, confirmed that the nickel atom is bound in a square-planar geometry (bond angles around  $90 \pm 5^{\circ}$ ; Table 1) to a (C,C)-chelate unit composed of the NHC ligand and its cyanoalkyl side arm, and to an acetylacetonate ligand (that binds in a *cis*-geometry to the nickel atom) through its two oxygen atoms. In addition, it can be noticed that the geometric parameters of the nickelacycle **4b** are almost identical to that of its half-sandwich precursor **2b** (see Table 1).



**Figure 3.** Molecular structure of the (*R*)-enantiomer of **4b**. The only hydrogen atom shown is that of the *CHCN* group (as an isotropic sphere). Ellipsoids are shown at the 50% probability level. Key atoms are labeled.

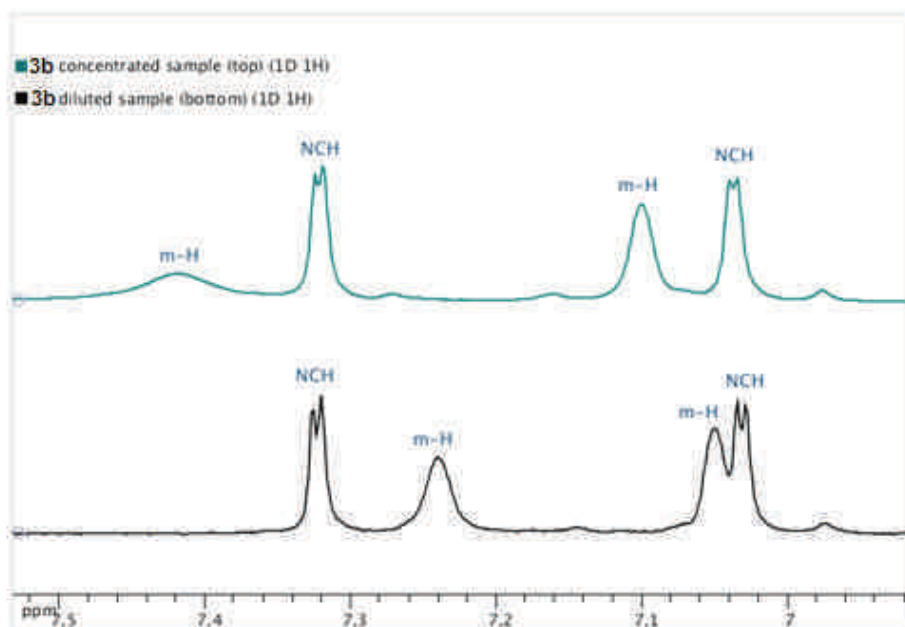
Spectroscopic data of **4a** and **4b** are consistent with the molecular structure of **4b**, and clearly establish the absence of a  $\eta^5\text{-Cp}$  ligand, together with the presence of both a (C,C)-chelate NHC ligand and an acac ligand. The  $^1\text{H}$  NMR ( $\text{CD}_3\text{CN}$ ) spectrum of the cationic complex **3b** shows the presence of the metalacycle, whose signals' chemical shifts and multiplicities are similar to those of **4b**.

**Table 1.** Selected Bond Lengths (Å) and Angles (°) for Complexes **2b** and **4b** with Esd's in parentheses

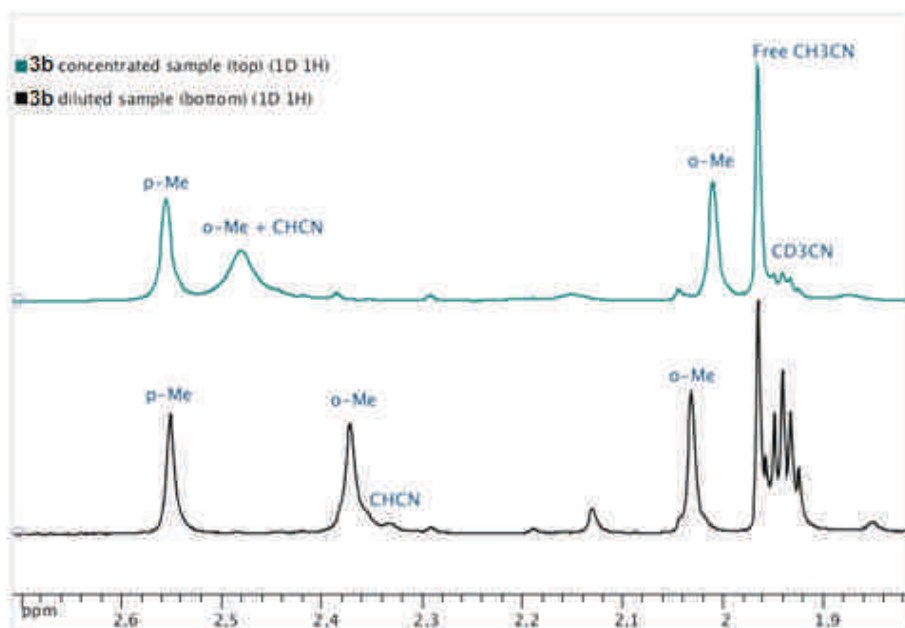
Complex	<b>2b</b>	<b>4b</b>
Ni–C1	1.8560(19)	1.8686(19)
Ni–C2	1.9718(19)	1.961(2)
Ni–O1	–	1.8835(14)
Ni–O2	–	1.8968(14)
C2–C3	1.438(3)	1.447(3)
C3–N3	1.143(3)	1.145(3)
C1–Ni–C2	93.95(8)	91.91(8)
O1–Ni–O2	–	93.29(6)
C1–Ni–O2	–	89.71(7)
C2–Ni–O1	–	84.97(7)
Ni–C2–C3	106.91(15)	107.00(13)
C2–C3–N3	177.7(3)	178.0(2)

However, it should be pointed out that the spectrum of **3b** is concentration dependent (see **Figures 4** and **5**). Thus, while both *meta*-protons of the mesityl ring each appear as two relatively sharp singlets when  $[\mathbf{3b}] \sim 3.10^{-2} \text{ mol.L}^{-1}$ , one signal of the *meta*-protons shifts significantly to lower field when  $[\mathbf{3b}] \sim 0.15 \text{ mol.L}^{-1}$ , and then appears as a very broad singlet (**Figure 4**). Similar behavior is observed for the two *ortho*-methyls of the mesityl ring. Thus, while both appear as two relatively sharp singlets when  $[\mathbf{3b}] \sim 3.10^{-2} \text{ mol.L}^{-1}$ , one significantly shifts to lower field when  $[\mathbf{3b}] \sim 0.15 \text{ mol.L}^{-1}$ , and then appears as a very broad singlet (**Figure 5**). Apart from the *CHCN* proton, whose chemical shift is also concentration dependent, all the other protons give well-resolved sharp signals and hardly change upon concentration variation. The exact reason of this behavior is not well understood, but may well originate from enhanced intermolecular interactions at higher concentrations, and/or from a fluxional process involving mesityl group rotation, that could be linked to the rate of acetonitrile exchange. The presence of free  $\text{CH}_3\text{CN}$  as a singlet on the downfield side of the multiplet due to residual  $\text{CHD}_2\text{CN}$  (**Figure 5**) indicates that  $\text{CH}_3\text{CN}/\text{CD}_3\text{CN}$  exchange is

indeed occurring,<sup>[7]</sup> and a VT NMR experiment run in CD<sub>3</sub>CN from +27°C to +75°C on a diluted solution of **3b** indeed allowed to observe a slight broadening at high temperature (at +70 and +75°C) of the mesityl methyl groups that resonate at 2.6 and 2.1 ppm.

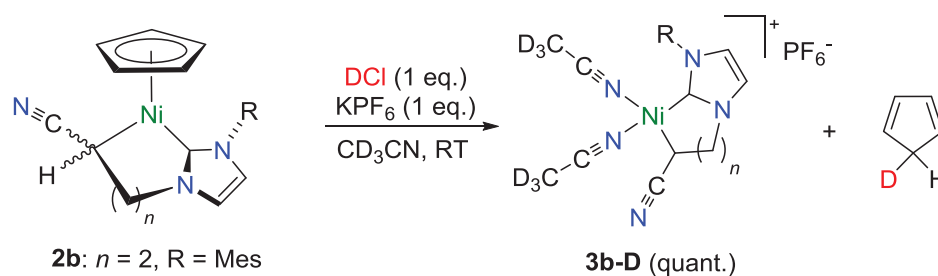


**Figure 4.** Aromatic area of the <sup>1</sup>H NMR spectra (CD<sub>3</sub>CN, 298 K) of **3b** at [**3b**] ~ 3.10<sup>-2</sup> mol.L<sup>-1</sup> (bottom) and 0.15 mol.L<sup>-1</sup> (top)

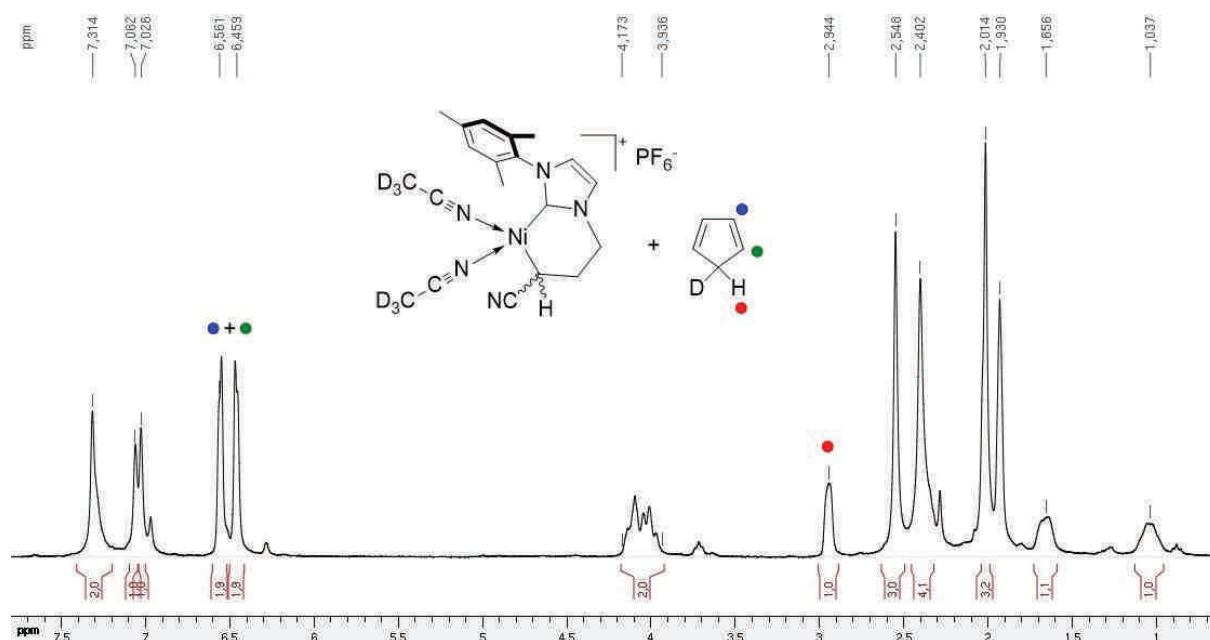


**Figure 5.** Mesityl methyl groups area of the <sup>1</sup>H NMR spectra (CD<sub>3</sub>CN, 298 K) of **3b** at [**3b**] ~ 3.10<sup>-2</sup> mol.L<sup>-1</sup> (bottom) and 0.15 mol.L<sup>-1</sup> (top)

To gain insight into the reaction mechanism and the fate of the Cp ligand, a deuterium labeling experiment with DCl was undertaken. A solution of concentrated DCl in D<sub>2</sub>O (35%), diluted in CD<sub>3</sub>CN to 1.0 M, was added to a suspension of **2b** and KPF<sub>6</sub> in CD<sub>3</sub>CN (**Scheme 5**), and a <sup>1</sup>H NMR spectrum of the reaction medium was immediately recorded. The obtained spectrum (**Figure 6**) clearly showed the clean and quantitative formation of **3b-D** and of free mono-deuterated cyclopentadiene in a 1:1 ratio.



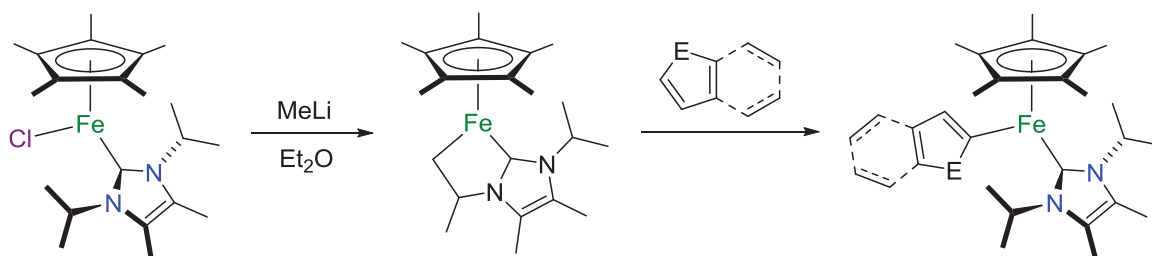
**Scheme 5.**  $\eta^5$ -Cp acidolysis of **2b** with DCl in CD<sub>3</sub>CN



**Figure 6.** <sup>1</sup>H NMR spectra of the  $\eta^5$ -Cp acidolysis reaction of **2b** with DCl in CD<sub>3</sub>CN

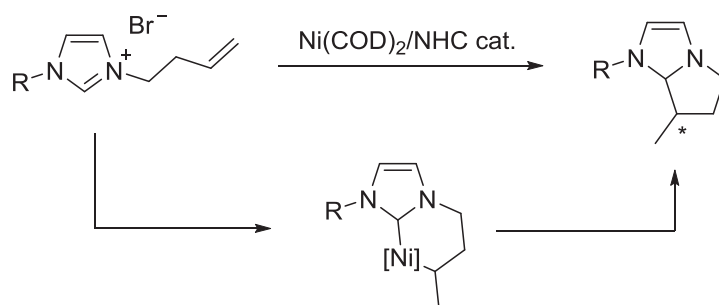
This reaction thus goes through a direct protolysis of the Cp ligand, and is remarkable for a number of reasons: (i) clean Cp ligand demetalation from 18-electron monocyclopentadienyl transition metal complexes in the presence of a proton source is, to our knowledge, unprecedented with non substituted cyclopentadienyl rings,<sup>[33–36]</sup> as these are normally considered to have extremely robust M–C<sub>5</sub>H<sub>5</sub> bonds;<sup>[37]</sup> (ii) it allows the creation of two potentially vacant coordination sites on the nickel, as illustrated by the lability of the two acetonitrile ligands of **3a,b** and their easy substitution by the acetylacetonate chelate to give **4a,b**; and (iii) it demonstrates the robustness of these nickelacycles and, in particular, of the base-generated Ni–alkylnitrile bonds.

The inertness of the Ni–alkylnitrile bonds under acidic conditions is in sharp contrast with the high reactivity of a Fe–alkyl bond found in a closely related alkyl,NHC–iron metalacycle: [Fe(*i*Pr-NHC-CHMeCH<sub>2</sub>)( $\eta^5$ -C<sub>5</sub>Me<sub>5</sub>)], which was also formed by deprotonation (of an NHC-isopropyl arm), and is readily reprotonated by reaction with heteroarenes *via* a proton transfer reaction from the 2-position of the heteroarenes to the methylene group of the cyclometalated NHC ligand (**Scheme 6**).<sup>[38]</sup>



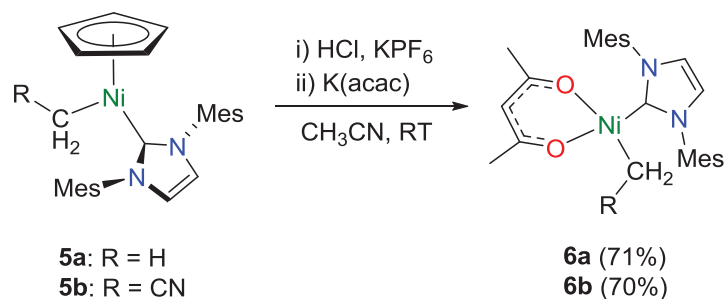
**Scheme 6.** C–H bond activation of heteroarenes mediated by an alkyl,NHC–iron metalacycle

Moreover, the inertness of the Ni–alkylnitrile and Ni–carbene bonds also contrasts with the catalytic annulation of imidazolium salts bearing *N*-alkenyl substituents, reported by Cavell, and which presumably proceeds *via* analogous cyclonickelated NHC/alkyl complexes that would undergo reductive elimination (**Scheme 7**).<sup>[39,40]</sup> We therefore decided to investigate whether the robustness of the alkyl–nickel bonds in **2a,b** was due to a chelate effect or to its electronic nature, and just as importantly, whether the remarkably clean Cp acidolysis could be extended to other systems.



**Scheme 7.** Catalytic annulation of imidazolium salts *via* the formation of NHC/alkyl nickelacycles

For that purpose, we decided to subject the acyclic methyl<sup>[41]</sup> and cyanomethyl complexes  $[\text{Ni}(\text{IMes})(\text{CH}_2\text{R})\text{Cp}]$  ( $\text{R} = \text{H}$ , **5a**;  $\text{R} = \text{CN}$ , **5b**) to similar reaction conditions. They were thus reacted with  $\text{HCl}$  in the presence of 1 equiv. of  $\text{KPF}_6$  in acetonitrile at room temperature, followed by filtration and treatment of the resulting solution with potassium acetylacetonate. The acyclic square planar cyanomethyl complexes  $[\text{Ni}(\text{IMes})(\text{CH}_2\text{R})(\text{acac})]$  **6a,b** were isolated as yellow-green solids in *ca.* 70% yield after work-up (**Scheme 8**).



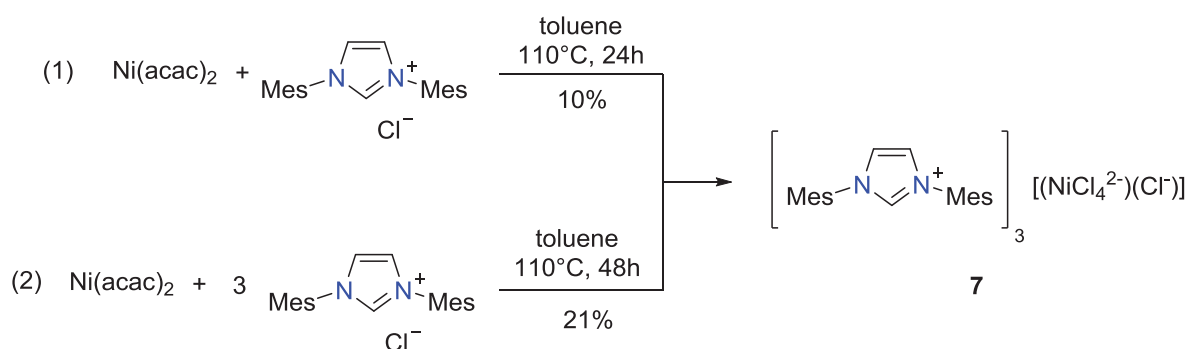
**Scheme 8.**  $\eta^5$ -Cp acidolysis with acyclic alkyl, and cyanoalkyl,NHC–nickel(II) complexes

Spectroscopic data of **6a,b** clearly establish the absence of a  $\eta^5$ -Cp ligand, together with the presence of an IMes ligand, an acetylacetonate chelate and a methyl or cyanomethyl group. In the  $^{13}\text{C}$  NMR spectra, the nickel-bonded carbon atoms are seen at 179.5 (**6a**) and 169.8 ppm (**6b**) for the NHC groups, and at  $-13.7$  (**6a**) and  $-22.5$  ppm (**6b**) for the alkyl groups. The (cyano)alkyl– and carbene–nickel bonds are thus preserved in an acidic medium within acyclic compounds, and Cp ligand displacement also takes place under these conditions. This unequivocally shows that, once formed, the Ni–C bonds in these Ni–NHC complexes are extremely stable whether they are part of a metalacycle or not, and, in the

particular case of the alkyl–nickel bonds, whether they are substituted by a stabilizing electron-withdrawing group or not. Finally, this alkyl–nickel bond inertness towards acid probably allows these Cp ligand removal reactions to take place cleanly, as several attempts to carry out a similar methodology on the neutral chloride complex,  $[\text{Ni}(\text{IMes})\text{ClCp}]$ ,<sup>[41]</sup> and on the cationic complex,  $[\text{Ni}(\text{IMes})(\text{NCCH}_3)\text{Cp}]^+\text{PF}_6^-$ , always led to intractable mixtures.<sup>[42]</sup>

## II.2. Attempts to synthesize $[\text{Ni}(\text{IMes})(\text{acac})\text{Cl}]$ : unexpected formation of $[\text{IMes.H}^+]_3[(\text{NiCl}_4^{2-})(\text{Cl}^-)]$

Our approach to synthesize closely related monodentate  $[\text{Ni}(\text{NHC})(\text{acac})\text{Cl}]$  complexes *via* a direct method (*i.e.* without going through a Cp removal step) was inspired by the work of Nolan and co-workers, who synthesized the Pd derivatives by simple reaction of  $\text{Pd}(\text{acac})_2$  with an imidazolium salt.<sup>[9]</sup> However, when attempting to synthesize  $[\text{Ni}(\text{IMes})(\text{acac})\text{Cl}]$  by reaction of  $\text{Ni}(\text{acac})_2$  with  $\text{IMes.HCl}$  in refluxing toluene for 24 h, the formation of the target complex did not occur. Instead, predominant recovery of the starting material along with formation of small amounts (*ca.* 10%) of a blue solid, which proved to be the nickelate complex  $[\text{IMes.H}^+]_3[(\text{NiCl}_4^{2-})(\text{Cl}^-)]$  **7**, took place (**Scheme 9**, eqn (1)). Further work showed that the yield of this serendipitous synthesis of this blue compound could be slightly improved by increasing the reaction time to 48 h, and the imidazolium salt loading to 3 equiv. relative to  $\text{Ni}(\text{acac})_2$  (**Scheme 9**, eqn (2)).

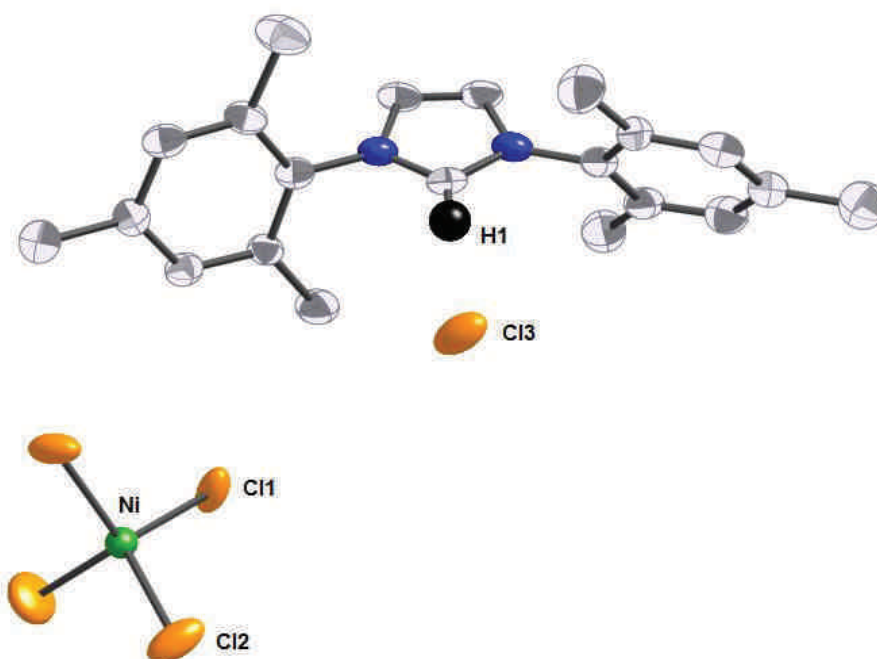


**Scheme 9.** Unexpected synthesis of the tetrachloro nickelate species  $[\text{IMes.H}^+]_3[(\text{NiCl}_4^{2-})(\text{Cl}^-)]$  **7**

An X-ray diffraction study of a single crystal of this blue compound, that was selected from a batch of crystals obtained at room temperature by diffusion in *n*-pentane of a



concentrated solution in acetone, allowed to determine its structure as being that of a tetrachloronickelate anion surrounded by three IMes.H<sup>+</sup> cations and one chloride [IMes.H<sup>+</sup>]<sub>3</sub>[(NiCl<sub>4</sub>)<sup>2-</sup>](Cl<sup>-</sup>) **7** (**Figure 7**). The [NiCl<sub>4</sub>)<sup>2-</sup> has somewhat distorted tetrahedral symmetry (the Cl–Ni–Cl angles are 106.9(1)° and 112.0(1)°) while the two independent Ni–Cl distances are 2.203(1) and 2.246(1) Å (**Table 2**). These values are very close to what has been observed in another single crystal X-ray diffraction studies of this di-anion.<sup>[43,44]</sup>

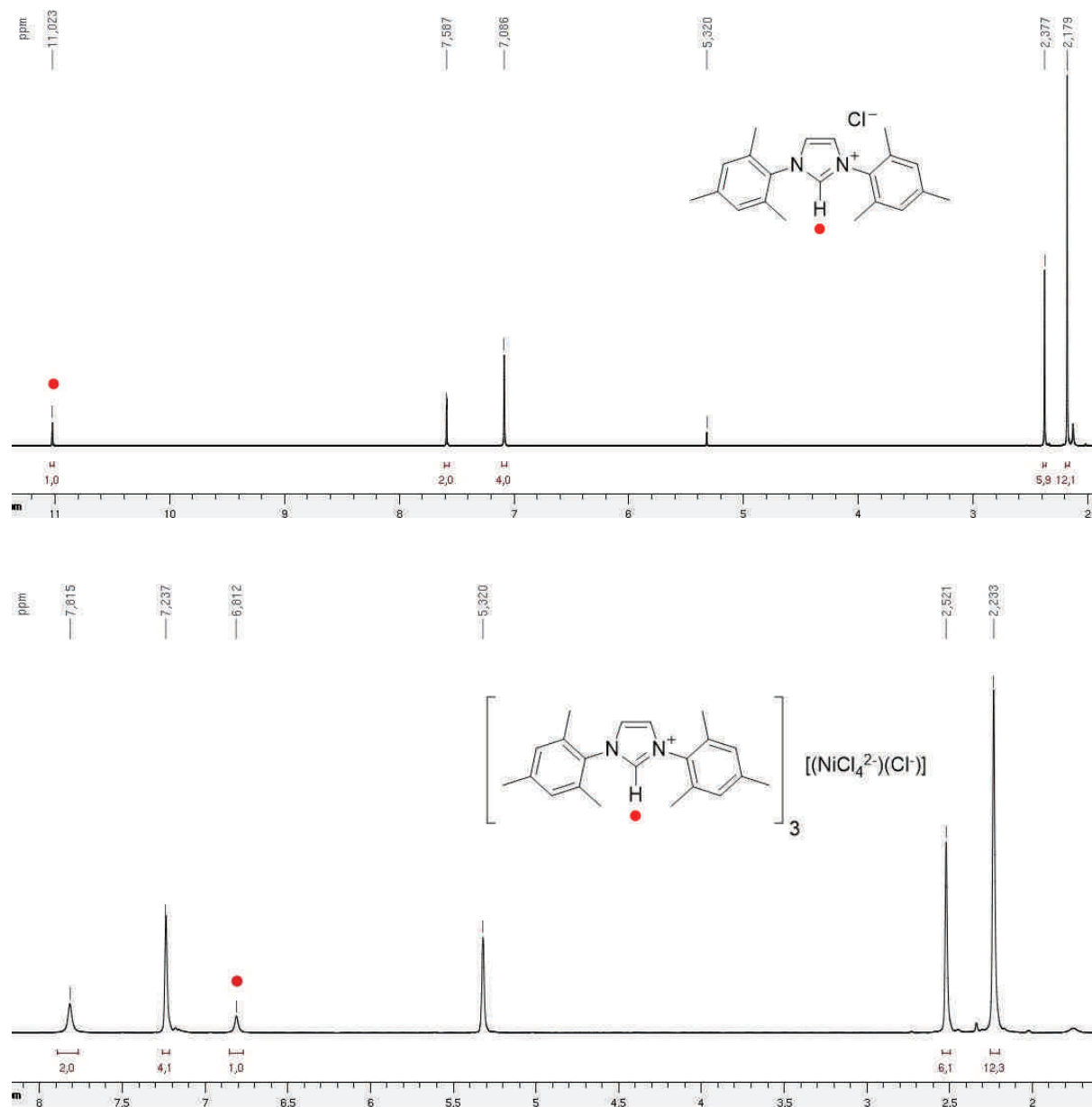


**Figure 7.** Structures of the cation and anions present in crystals of **7**. The only hydrogen atom shown is that of the NCHN group (as an isotropic sphere). Ellipsoids are shown at the 50% probability level. Key atoms are labeled.

**Table 2.** Selected Bond Lengths (Å) and Angles (°) for Complex **7** with Esd's in parentheses

Complex	<b>7</b>
Ni–Cl1	2.203(2)
Ni–Cl2	2.2465(12)
Cl1–Ni–Cl2	106.86(5)
Cl2–Ni–Cl2	111.95(4)
H1⋯Cl3	2.606

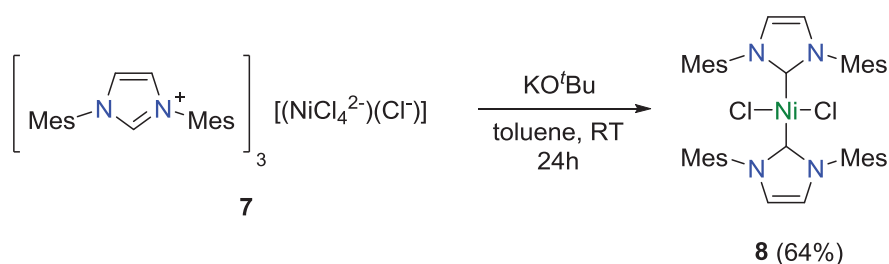
In agreement with the molecular structure determined by X-ray diffraction, the  $^1\text{H}$  NMR spectrum of **7**  $\text{CDCl}_3$  only showed the signals of the imidazolium salt but, surprisingly, the signal of the C2 proton was considerably downfield shifted (**Figure 8**,  $\delta = 6.81$  ppm for **7** vs. 11.02 ppm for  $\text{IMes.HCl}$  in  $\text{CD}_2\text{Cl}_2$ ). A plausible explanation for such observation is that the paramagnetic nature of  $\text{NiCl}_4^{2-}$  could influence the chemical shift value of the C2 proton.



**Figure 8.** Comparison of the  $^1\text{H}$  NMR spectra of  $\text{IMes.HCl}$  and  $[\text{IMes.H}^+]_3[(\text{NiCl}_4^{2-})](\text{Cl}^-)$  in  $\text{CD}_2\text{Cl}_2$

The difficulty encountered in obtaining the target complex [Ni(IMes)(acac)Cl] might arise from (i) the low solubility of Ni(acac)<sub>2</sub>, and (ii) the fact that Ni(acac)<sub>2</sub> exists as a trimer in the solid state,<sup>[45]</sup> where each nickel atom is octahedrally coordinated to six oxygen atoms coming from three acac ligands. The nickel atoms are therefore less accessible than the palladium atoms in Pd(acac)<sub>2</sub>. Remarkably, the formation of such tetrachloro-imidazolium salts nickelate is not unprecedented in the literature, but only halide sources of nickel were used in all previous cases.<sup>[46–51]</sup>

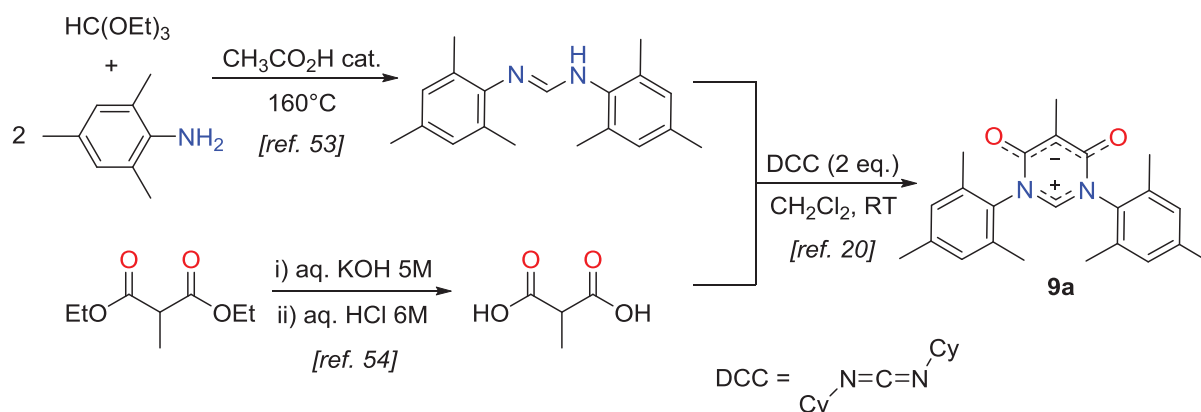
Regarding the reactivity of **7**, it is noteworthy that its treatment with KO<sup>t</sup>Bu in THF at room temperature led to the formation of the *bis*-NHC complex *trans*-[Ni(IMes)<sub>2</sub>Cl<sub>2</sub>] **8** in 64% isolated yield (**Scheme 10**).<sup>[52]</sup>



**Scheme 10.** Reaction of **7** with a strong base

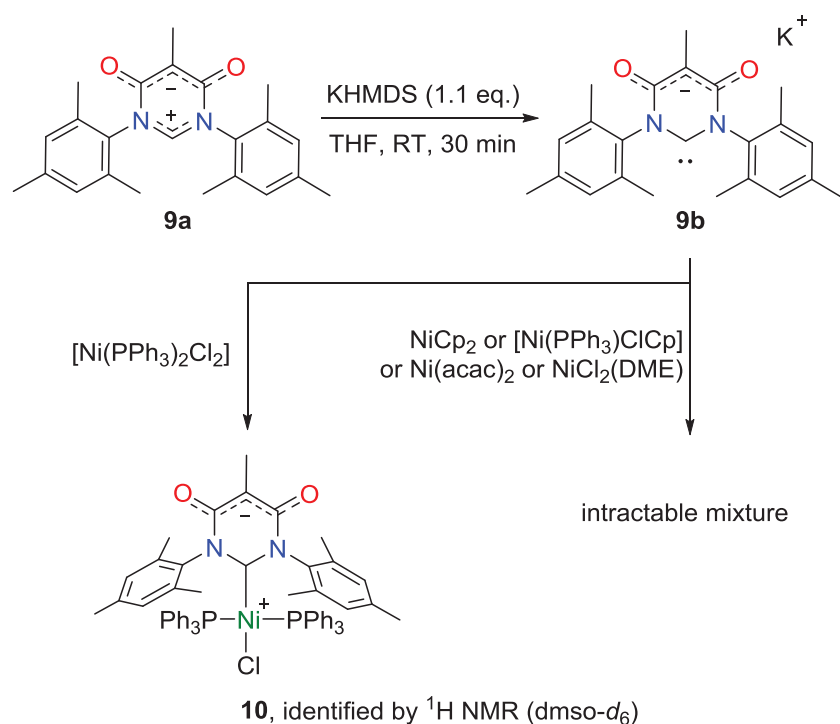
### II.3. Synthesis of *malo*-NHC–nickel complexes

For the synthesis of *malo*-NHC–nickel complexes, we choose the pyrimidinium betaine **9a**, that we synthesized according the literature procedures (**Scheme 11**).<sup>[20,53,54]</sup> The formamidine (Mes)N=CH–NH(Mes) was synthesized in moderate yield (*ca.* 50%) by reaction of 2,6-diisopropylaniline with triethylorthoformate in the presence of sub-stoichiometric amounts of acetic acid.<sup>[53]</sup> In parallel, the synthesis of methylmalonic acid was achieved with an almost quantitative yield by simple hydrolysis of diethyl malonate in basic medium.<sup>[54]</sup> A dicyclohexylcarbodiimide (DCC)-mediated double peptide-type coupling between the formamidine and the methylmalonic acid finally afforded the corresponding pyrimidinium betaine **9a** with *ca.* 90% yield.<sup>[20]</sup>



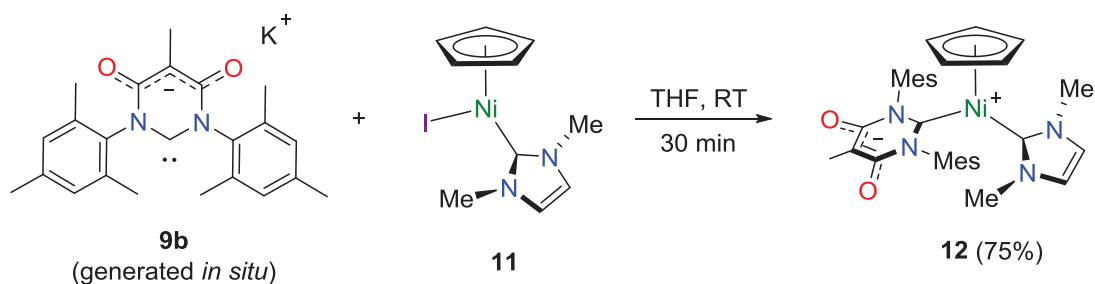
**Scheme 11.** Three-steps synthesis of the pyrimidinium betaine **9a**

By analogy with the known syntheses of half-sandwich nickel complexes bearing a classical imidazolylidene- or imidazolinyldene-NHC ligand,<sup>[41,55]</sup> we investigated the reaction between **9a** and nickelocene in refluxing THF. However, no reaction occurred, and unreacted starting materials were recovered. We then investigated the complexation of the free carbene **9b**, generated by deprotonation of **9a** with KHMDS at room temperature, to different nickel sources (**Scheme 12**). The reaction of **9b** with  $\text{NiCl}_2(\text{DME})$ ,  $\text{Ni}(\text{acac})_2$ , nickelocene and  $[\text{Ni}(\text{PPh}_3)\text{ClCp}]$  led to intractable mixtures in all cases. In contrast, the reaction of **9b** with  $[\text{Ni}(\text{PPh}_3)_2\text{Cl}_2]$  led to the relatively clean formation complex **10**, which we have isolated as a light violet solid, and tentatively identified as  $[\text{Ni}(\text{PPh}_3)_2(\text{malo-NHC})\text{Cl}]$  according to its  $^1\text{H}$  NMR spectrum in  $\text{DMSO-}d_6$ . The presence of the *malo*-NHC was confirmed by its characteristic signals, integrating in a 1:2 ratio relative to the triphenylphosphine signals. However, its very low solubility in organic solvents precluded its recrystallization and thus its isolation as an analytically pure solid.



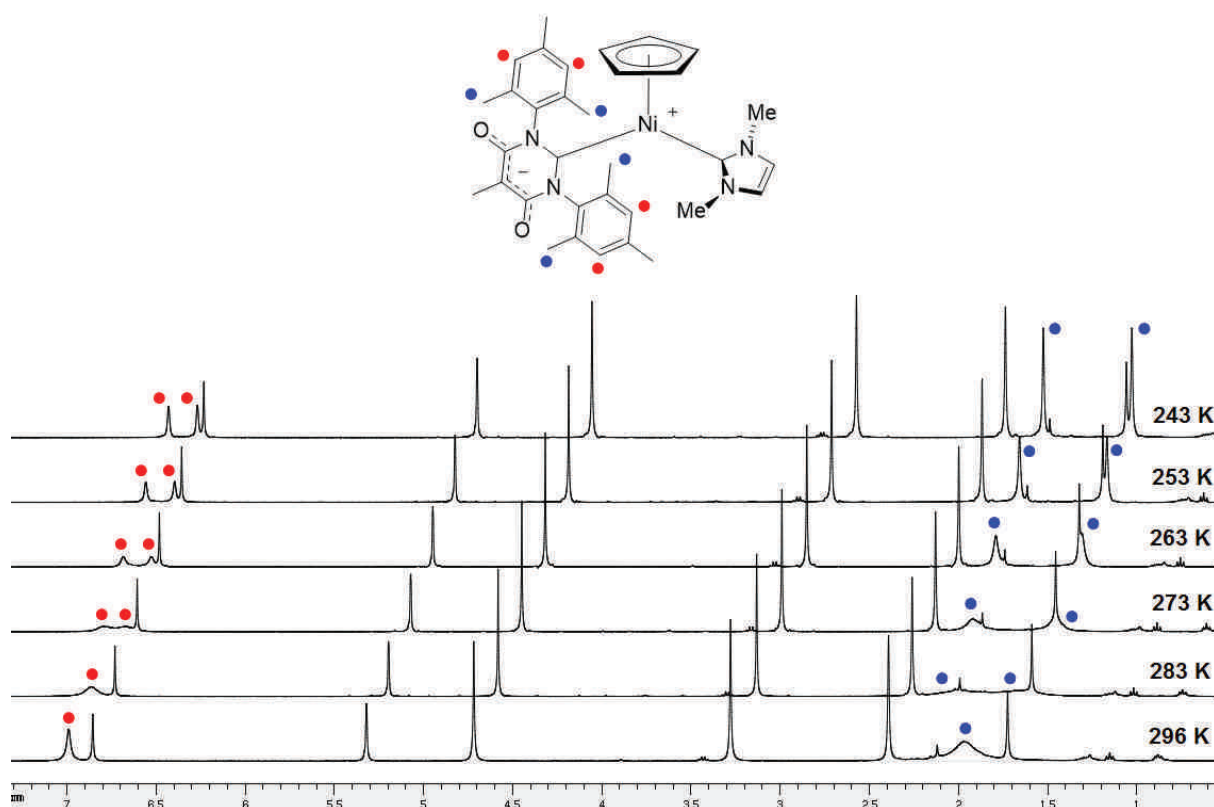
**Scheme 12.** Attempted syntheses of *malo*-NHC-nickel complexes

This result and the preferential substitution of  $\text{Cl}^-$  rather than that of  $\text{PPh}_3$ , tended to confirm César and Lavigne's assumption that *malo*-NHCs behave more like X-type ligands than NHCs.<sup>[20]</sup> We thus decided to react **9b** with  $[\text{Ni}(\text{IMe})\text{ICp}]$  **11** with the hope of substituting the iodide ligand. And indeed, when **9b** (generated *in situ* from **9a**) was reacted with **11** in THF at room temperature, clean formation of the cationic *bis*-carbene complex **12**, which was isolated with a 75% yield after work-up, occurred at room temperature (**Scheme 13**).



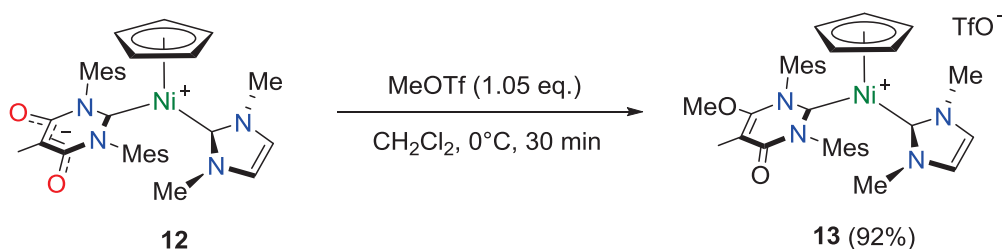
**Scheme 13.** Synthesis of **12** via iodide substitution of  $[\text{Ni}(\text{IMe})\text{ICp}]$  **11**

The  $^1\text{H}$  and  $^{13}\text{C}\{^1\text{H}\}$ NMR spectrum of **12** are straightforward, as they show the presence of one  $\eta^5\text{-Cp}$  ligand, one IMe NHC and one *malo*-NHC. In addition, they reveal that a molecular mirror plane that bisects the molecule is present on the NMR time scale. This effective mirror plane contains the nickel atom, the IMe and *malo*-NHC carbene carbons, and the Cp centroid. The protons of the IMe ring and the NMe groups thus resonate as two singlets in a 1:3 integrated ratio, in the  $^1\text{H}$  NMR spectrum. The protons of the *malo*-NHC ring, the *ortho*-methyl groups, the *meta*-hydrogens, and the *para*-methyl groups of the mesityl groups appear as four singlets in a 3:6:2:3 integrated ratio. Nevertheless, the signals of the two *ortho*-methyls and the two *meta*-hydrogens of the *malo*-NHC are somewhat broad at room temperature. A variable-temperature  $^1\text{H}$  NMR experiment was thus performed on a  $\text{CD}_2\text{Cl}_2$  solution of **10** between 296 and 243 K (**Figure 9**). As the temperature was decreased, the *ortho*-methyl resonances became even broader, and eventually splitted into two signals at a temperature ( $T_C$ ) of *ca.* 283 K. Similar signal splitting was observed for the aromatic *meta*-hydrogen atom signals at *ca.* 273 K. The free energies of activation ( $\Delta G^\ddagger$ ) for this fluxional process (based on the coalescence temperature of the *ortho*-methyl groups and of the *meta*-aromatic protons) are of the order of 55 - 58  $\text{kJ}\cdot\text{mol}^{-1}$ .<sup>[56]</sup> The similar values of the two free energies of activation suggest that the two signal splittings/coalescences are associated to the same dynamic process in compound **12**, which we believe is restricted rotation about the *N*-mesityl bonds at low temperature. This phenomenon was previously observed in a closely related sterically congested *bis*-carbene complex  $[\text{Ni}(\text{IMes})(\text{Me-NHC-}^i\text{Pr})]^+$  (at RT),<sup>[57]</sup> as well as in the  $\text{Cp}^*$  mono-carbene complex  $[\text{Ni}(\text{IMes})\text{ClCp}^*]$ .<sup>[58]</sup>



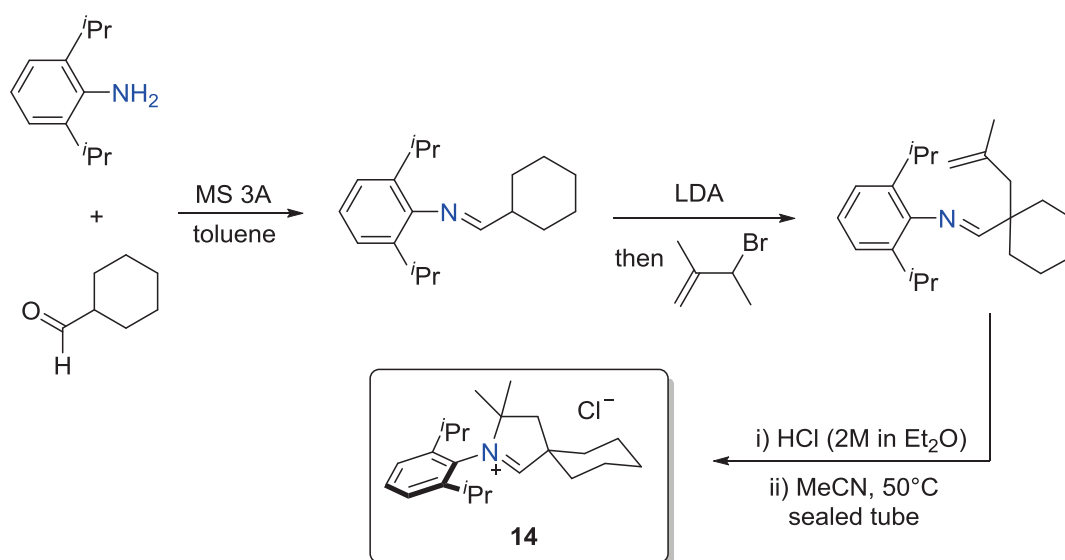
**Figure 9.** VT  $^1\text{H}$  NMR analysis of **12** showing signal splitting/coalescences for the *para*-methyl groups and the *meta*-aromatic protons

The addition of 1.05 equiv. MeOTf on a dichloromethane solution of the zwitterionic complex **12** at 0°C cleanly afforded the corresponding ionic complex **13**, which was isolated as a dark yellow solid in excellent yield (**Scheme 13**). The  $^1\text{H}$  NMR spectrum of **13** clearly indicates the formation of the methoxy moiety of the six-membered NHC backbone by a singlet integrating for 3 protons at 3.50 ppm. In addition, in contrast to what is observed in the  $^1\text{H}$  NMR spectrum of **12**, due to the molecular mirror plane that bisects the molecule, the *para*-methyl groups of the two mesityl *N*-substituents of complex **13** appear as two different signals integrating in a 1:1 ratio, confirming the asymmetry of the MeO-*malo*-NHC. Similarly, the *ortho*-methyl groups appear as two singlets integrating for 6 protons each. Furthermore these signals are broad, which likely indicates a restricted rotation about the *N*-Mesityl bond as observed in **12**. Finally and in contrast, the *meta*-protons coincidentally appear as one singlet integrating for 4 protons. All other signals of **13** are comparable to those of **12**, and deserve no particular comment.

Scheme 13. Post-functionalization of the malonate backbone of **12**

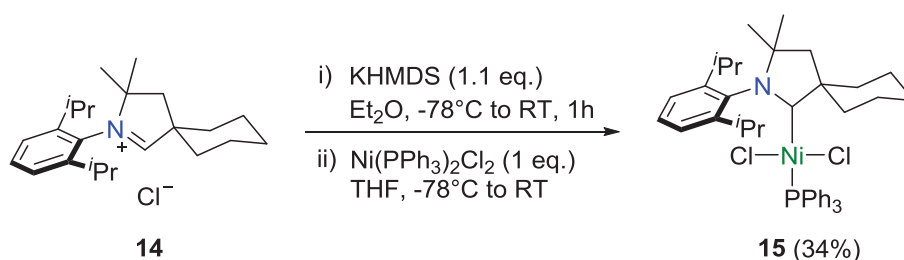
#### II.4. Synthesis of Ni–CAAC complexes

The synthesis of the CAAC precursor **14** has been realized according to the previously reported procedure (Scheme 14).<sup>[59]</sup> Simple condensation of 2,6-diisopropylaniline on cyclohexanecarboxaldehyde allowed us to obtain the corresponding aldimine nearly quantitatively. Subsequent deprotonation of this aldimine, followed by reaction with 3-bromo-2-methylpropene resulted in the formation of the corresponding alkenyl aldimine in *ca.* 90% yield. Addition of a stoichiometric amount of a 2 M solution of HCl in Et<sub>2</sub>O resulted in the formation of a white solid that was isolated, and heated in a sealed tube with acetonitrile at 50°C, this gave the CAAC precursor **14** quantitatively.

Scheme 14. Four-step synthesis of **14**



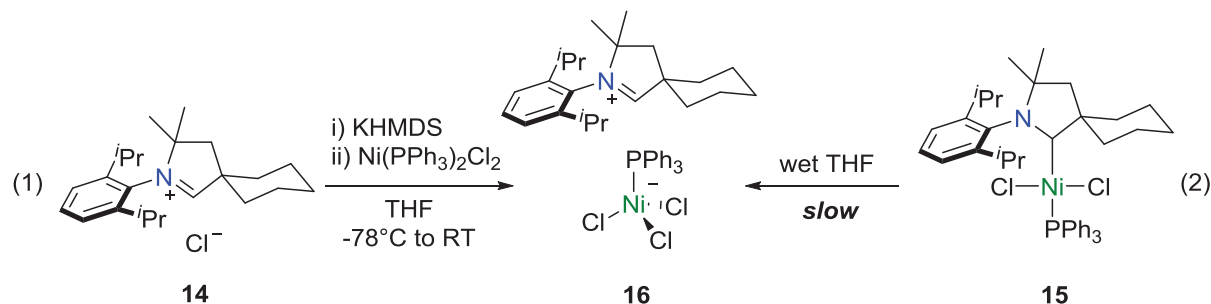
Initial studies then focused on the screening of several nickel sources for complexation. Generation of the free carbene by addition of 1.1 equiv. of KHMDS on **14**, and subsequent reaction with either  $\text{NiCl}_2(\text{DME})$ ,  $\text{Ni}(\text{acac})_2$ ,  $[\text{Ni}(\text{PPh}_3)\text{ClCp}]$  or nickelocene in THF led, however, to intractable mixtures in all cases. In contrast, when a THF solution of the free carbene was added to a suspension of  $[\text{Ni}(\text{PPh}_3)_2\text{Cl}_2]$  in THF at  $-78^\circ\text{C}$  before warming to room temperature, a color change from dark green to reddish took place within minutes, and a violet solid, which we have identified as  $[\text{Ni}(\text{CAAC})(\text{PPh}_3)\text{Cl}_2]$  **15** based on its  $^1\text{H}$  NMR spectrum, was isolated in 34% yield after work-up (**Scheme 15**). The  $^1\text{H}$  NMR spectrum of **15** clearly shows the presence of one  $\text{PPh}_3$  and one CAAC ligand in a 1:1 integrated ratio. Unfortunately, no other spectroscopic data have been obtained yet, and this result still needs to be confirmed by  $^{13}\text{C}$   $\{^1\text{H}\}$  NMR spectroscopy, elemental analysis, and/or X-ray diffraction studies. Nevertheless, in contrast to the reaction of the free *mal*-NHC **9b** with  $[\text{Ni}(\text{PPh}_3)_2\text{Cl}_2]$ , the CAAC ligand would substitute one triphenylphosphine ligand instead of a chloride, and would thus behave as a L-type ligand, like NHCs.



**Scheme 15.** Synthesis of  $[\text{Ni}(\text{CAAC})(\text{PPh}_3)\text{Cl}_2]$  **15**

In the former reaction, however, it is noteworthy that if the deprotonation of **14** is not complete, non negligible amounts (depending on the amount of **14** left) of a blue compound **16** are formed after the addition of the reaction mixture onto  $[\text{Ni}(\text{PPh}_3)_2\text{Cl}_2]$  under otherwise unchanged reaction conditions (**Scheme 16**, eqn. (1)). This blue species could not be identified by  $^1\text{H}$  NMR spectroscopy as its spectrum in  $\text{CD}_2\text{Cl}_2$  showed rather broad signals from 0 to 14 ppm, which suggests that it is paramagnetic. Nevertheless, X-ray quality crystals were obtained by diffusion in *n*-pentane of a concentrated solution in dichloromethane, and the molecular structure of **16** could be determined by a single-crystal X-ray diffraction study. Crystallographic data and data collection parameters are listed in **Table 6** (see *Experimental*

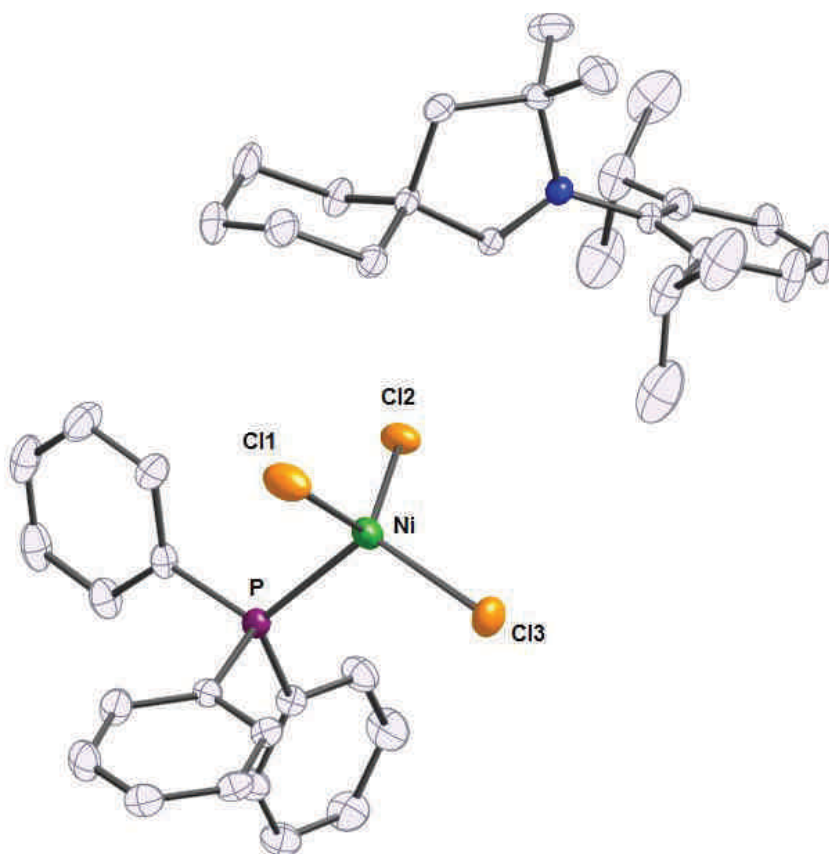
Section). Selected bond lengths and angles are collected in **Table 3**, and the structure is shown in **Figure 10**.



**Scheme 16.** Unexpected synthesis of the nickelate salt **16**

The molecular structure of **16** revealed that it was a nickelate salt akin to **7** with one  $[\text{CAAC}]^+$  cation and one  $[\text{Ni}(\text{PPh}_3)\text{Cl}_3]^-$  anion present in the crystallographic unit. The structure of the  $[\text{CAAC}]^+$  cation does not change significantly compared to the previously reported structure of the triflate salt.<sup>[26]</sup> The phenyl ring of the  $[\text{CAAC}]^+$  cation is oriented perpendicular to the azolium ring with a dihedral angle of  $90.5^\circ$ . In the  $[\text{Ni}(\text{PPh}_3)\text{Cl}_3]^-$  anion, the nickel atom is coordinated by three chlorines atoms and one phosphorus atom in a distorted tetrahedral geometry, with Ni–Cl, and Ni–P bond lengths of 2.2327(5)–2.2573(5) Å, and 2.3121(5) Å, respectively. The angles at nickel are in the ranges  $96.226(19)$ – $118.97(2)^\circ$ . These values lie within the ranges found for other complexes containing a  $[\text{Ni}(\text{PPh}_3)\text{X}_3]^-$  anion.<sup>[60–62]</sup>

The zwitterionic complex **16** was also obtained when attempting to crystallize complex **15** in THF that contained traces of water (**Scheme 16**, eqn. (2)). Slow decomposition of **15** into **16** thus shows a certain sensitivity of the Ni–CAAC bond, which might raise a problem for catalytic applications of **15**.



**Figure 10.** Structure of the cation and anion present in crystals of **16**. Ellipsoids are shown at the 50% probability level. Key atoms are labeled.

**Table 3.** Selected Bond Lengths (Å) and Angles (°) for Complex **16** with Esd's in parentheses

Complex	<b>16</b>
Ni–Cl1	2.2327(5)
Ni–Cl2	2.2428(6)
Ni–Cl3	2.2573(5)
Ni–P	2.3121(5)
Cl1–Ni–Cl2	118.97(2)
Cl1–Ni–Cl3	107.93(2)
Cl2–Ni–Cl3	118.80(2)
Cl1–Ni–P	109.07(2)
Cl2–Ni–P	96.226(19)
Cl3–Ni–P	103.583(18)

## II.5. Catalysis applications of the new nickel carbene complexes

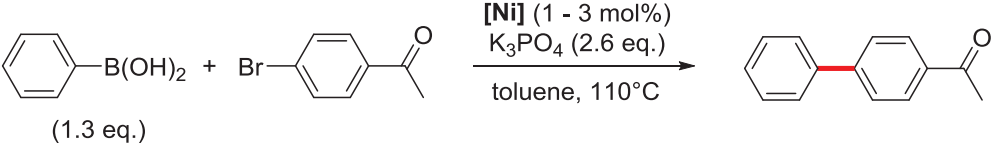
Nickelacycles **2b**, **3b**, and **4b**, as well as the *mal*-NHC–nickel complexes **12** and **13**, and the Ni–CAAC complex **15** have been evaluated as pre-catalysts in different reactions: (i) in the Suzuki-Miyaura coupling of 4-bromoacetophenone with phenylboronic acid in the presence of K<sub>3</sub>PO<sub>4</sub> as the sole additive (**Table 4**), and/or (ii) in the hydrosilylation of benzaldehyde with Ph<sub>2</sub>SiH<sub>2</sub> (**Table 5**), as well as (iii) in the  $\alpha$ -arylation of propiophenone with 4-bromotoluene. These three transformations were chosen for comparison purposes with the previously reported half-sandwich nickel complexes.<sup>[42,57,63–65]</sup>

As we are greatly interested in evaluating our nickel complexes in stoichiometric<sup>[2,3,66]</sup> and catalytic<sup>[65]</sup> C–H bonds transformations (see **Chapter II**), we decided to test some of these complexes in the elegant direct arylation of THF (**Table 6**), which has been very recently described by Lei and co-workers.<sup>[67]</sup> Thus, the use of a Ni(acac)<sub>2</sub>/PPh<sub>3</sub> (1:1 - 10 mol%) catalyst with phenylboronic acids, K<sub>3</sub>PO<sub>4</sub> as a base and di-*tert*-butylperoxide (DTBP) as an additive in THF – which acts as both the solvent and the reactant – at 100°C for 16 h impressively allowed a series of mono-arylation at the  $\alpha$  position of THF in moderate to excellent yields (52 - 93%).<sup>[67]</sup>

In the case of the square planar alkyl,NHC–nickelacycles **3b** and **4b**, we thought that their robustness may open interesting perspectives for their use in catalysis. As expected, the labilization of the Cp ring of the half-sandwich complex **2b**, and its substitution by two labile acetonitrile ligands (complex **3b**) was found to be beneficial in the Suzuki-Miyaura coupling of phenylboronic acid with 4-bromoacetophenone. Thus, only 20% conversion was obtained after 1 h with 3 mol% **2b**, whereas 58% conversion was obtained with **3b** under otherwise unchanged conditions (**Table 4**, entries 1 vs. 2). Although it was less efficient than the cationic complex **3b**, the neutral acac complex **4b** also gave a better activity than **2b**, with a 45% conversion after 1 h (entry 3). Consequently, with nickelacycles **2b**, **3b** and **4b**, the reactivity trend, which is as follows: **3b** > **4b** > **2b**, shows that the more stabilizing the ligands, the less catalytically active the complexes are. Nevertheless, the activity of **3b** does not reach that of the half-sandwich complex [Ni(Mes-NHC-<sup>*n*</sup>Bu)ICp], which was found to be among the most active Ni–NHC catalysts for this reaction, with 88% conversion observed after 15 min with a catalyst loading of 1 mol% only (entries 2 vs. 8).<sup>[63]</sup> The reasons for these moderate activities of the square-planar complexes **3b** and **4b** could arise from: (i) the increased stability of such nickelacycles, compared to acyclic complexes such as [Ni(Mes-

NHC-*n*Bu)ICp], and/or (ii) the inductive electronic effect of the nitrile group, which would inhibit the generation of an active nickel(0) species, and/or (iii) the much less hindered nature of the alkynitrile carbon atom bound to the nickel, compared, for instance, to that of a NHC, which would not favor the reductive elimination step.

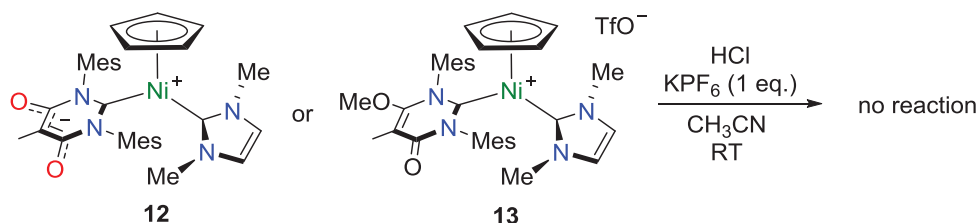
**Table 4.** Suzuki-Miyaura coupling of 4-bromoacetophenone with phenyl boronic acid catalyzed by complexes **2b**, **3b**, **4b**, **12**, **13** and **15**<sup>a</sup>

			
Entry	Catalyst (mol %)	Time (min)	Conversion (%)
1	<b>2b</b> (3)	60	20
2	<b>3b</b> (3)	60	58
3	<b>4b</b> (3)	60	45
4	<b>12</b> (3)	60	21
5	<b>13</b> (3)	60	23
6	<b>15</b> (3)	60	13
7	[Ni(IMes)(IMe)Cp](PF <sub>6</sub> ) (1)	60	20 <sup>[57]</sup>
8	[Ni(Mes-NHC- <i>n</i> Bu)ICp] (1)	15	88 <sup>[63]</sup>

<sup>a</sup> Reaction conditions: phenylboronic acid (1.3 mmol), 4-bromoacetophenone (1 mmol), K<sub>3</sub>PO<sub>4</sub> (2.6 mmol), [Ni] (1 - 3 mol%) in toluene (3 mL) at 110°C. <sup>b</sup> Conversions determined by <sup>1</sup>H NMR; average of two runs.

We also evaluated the half-sandwich *malo*-NHC–nickel complexes **12** and **13** in this transformation. However, the activities of these catalysts proved to be rather low, with only 21 and 23% conversion, obtained with 3 mol% of **12** and **13**, respectively (entries 4 and 5). The *bis*-NHC analogue of **12** and **13**, [Ni(IMes)(IMe)Cp](PF<sub>6</sub>), similarly gave a rather disappointing result in a previous study, with only 20% conversion after 1 h of reaction with a catalyst loading of 1 mol% only (entries 4 and 5 vs. 7).<sup>[57]</sup> As the half-sandwich nickelacycles **2**, complexes **12** and **13** are coordinatively saturated and sterically congested, this probably renders the nickel atom almost inaccessible. Apart from a possible Cp ring slippage from the  $\eta^5$ - to an  $\eta^3$ - or  $\eta^1$ -coordination mode, there thus seems to be no other possibility of accessing the metallic center. Consequently, we studied the potential labilization of the Cp ring in an

acidic medium, as described for complexes **2a,b** and **5a,b** (Schemes 4 and 6).<sup>[65]</sup> However, when treating either complex **12** or **13** with HCl (1 equiv. or large excess) and KPF<sub>6</sub> (1 equiv.) in acetonitrile at room temperature, no reaction occurred, and the starting materials were predominantly recovered (Scheme 17), similar to what was observed with the related *bis*-NHC complexes [Ni(IMes)(IMe)Cp](PF<sub>6</sub>) and [Ni(IMes)(Me–NHC–<sup>*i*</sup>Pr)Cp](PF<sub>6</sub>) in previous work.<sup>[57]</sup>



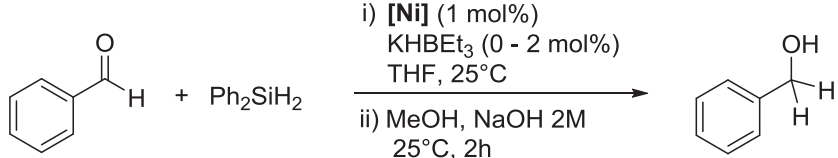
**Scheme 17.** Attempts to labilize the Cp ring of **12** and **13** with HCl

Finally, the Ni–CAAC complex **15** was also tested in the coupling of 4-bromoacetophenone with phenylboronic acid, but proved to be even less active than **12** and **13** (entries 6 vs. 4 and 5).

In the hydrosilylation of benzaldehyde with diphenylsilane (Table 5), complexes **12** and **13** proved to be slightly active at room temperature in the absence of additive (entries 1 and 3), which is in marked contrast to [Ni(IMes)ClCp], which did not show any activity in the absence of an additive after 17 h at room temperature (entry 6, see also Chapter III).<sup>[64]</sup> However, the activities of **12** and **13** were relatively low compared to the [Ni(IMes)ClCp]/NaHBET<sub>3</sub> (1:2) system, for which quantitative conversion was observed within 15 min (entry 7).<sup>[64]</sup> Moreover, in the presence of 2 mol% of KHBET<sub>3</sub>, the activities of **12** and **13**, with only 61% (**12**) and 28% (**13**) conversions after 1 h (entries 2 and 4), proved to be much lower, than that of the [Ni(IMes)ClCp]/NaHBET<sub>3</sub> (1:2) system. Interestingly, in contrast to what was observed in the Suzuki-Miyaura coupling reaction, complex **12** was twice as active as **13**.

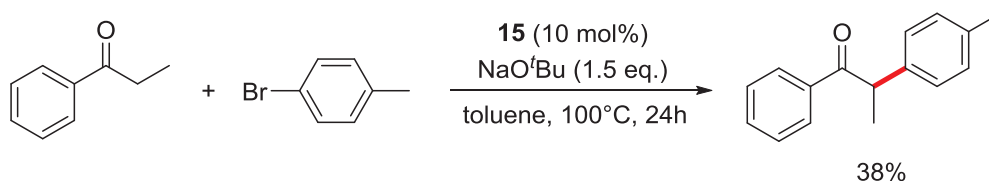
The Ni–CAAC complex **15** was also briefly evaluated in the hydrosilylation of benzaldehyde with diphenylsilane, in the presence of 2 mol% of KHBET<sub>3</sub>, and allowed 31% conversion in 30 min (entry 5). This result, also, does not attain that of the [Ni(IMes)ClCp]/NaHBET<sub>3</sub> (1:2) system.

**Table 5.** Nickel(II)-catalyzed hydrosilylation of benzaldehyde with diphenylsilane<sup>a</sup>

				
Entry	Catalyst	Additive (mol%)	Time (min)	Conversion (%) <sup>b</sup>
1	<b>12</b>	—	60	12
2	<b>12</b>	KHBET <sub>3</sub> (2)	60	61
3	<b>13</b>	—	60	5
4	<b>13</b>	KHBET <sub>3</sub> (2)	60	38
5	<b>15</b>	KHBET <sub>3</sub> (2)	30	31
6	[Ni(IMes)ClCp]	—	17 h	0 <sup>[64]</sup>
7	[Ni(IMes)ClCp]	NaHBET <sub>3</sub> (2)	15	> 97 <sup>[64],c</sup>

<sup>a</sup> Reaction conditions: activation of **1-3** with the additive in THF (4 mL) was followed by addition of benzaldehyde (1 mmol) and Ph<sub>2</sub>SiH<sub>2</sub> (1 mmol), and the reaction mixture was stirred at 25°C. <sup>b</sup> Conversions determined by <sup>1</sup>H NMR after methanolysis (MeOH, 2M NaOH) and extraction with Et<sub>2</sub>O. <sup>c</sup> Conversions determined by GC after methanolysis (MeOH, 2M NaOH) and extraction with Et<sub>2</sub>O.

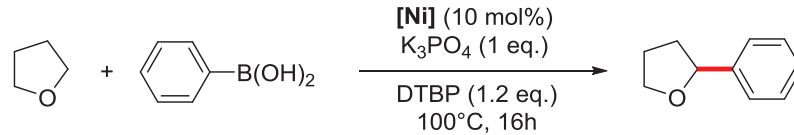
Nevertheless, we were especially interested in evaluating complex **15** as a pre-catalyst in the  $\alpha$ -arylation of propiophenone with 4-bromotoluene to provide a direct comparison with [Ni(IPr)(PPh<sub>3</sub>)Cl<sub>2</sub>] (which only differs in its carbene ligand), and was previously tested in the same reaction.<sup>[68]</sup> Thus, under the exactly same reaction conditions as those employed for [Ni(IPr)(PPh<sub>3</sub>)Cl<sub>2</sub>] (10 mol% of Ni, 1.5 equiv. NaO<sup>t</sup>Bu, toluene, 100°C, 24 h), a 38% yield (determined by GC) was obtained with **15** (Scheme 18) vs. 65% isolated yield for [Ni(IPr)(PPh<sub>3</sub>)Cl<sub>2</sub>].<sup>[68]</sup> This result shows that replacement of an IPr ligand by a CAAC ligand in the complex of type [Ni(carbene)(PPh<sub>3</sub>)Cl<sub>2</sub>] obviously does not have a beneficial impact in this reaction.

**Scheme 18.**  $\alpha$ -Arylation of propiophenone with 4-bromotoluene catalyzed by [Ni(CAAC)(PPh<sub>3</sub>)Cl<sub>2</sub>] **15**

Finally, complexes **12**, **13** and **15** were also evaluated in the direct C–H arylation of THF (**Table 6**). Performing the coupling of THF with phenylboronic acid in the presence of 10 mol% of the well-defined *malo*-NHC complexes **12** or **13**, satisfyingly allowed us to obtain 19% (**12**) and 11% (**13**) isolated yields of 2-phenyl-THF (entries 1 and 2). Nevertheless, these results are far from matching those obtained by Lei and co-workers with Ni(acac)<sub>2</sub>/PPh<sub>3</sub> (entry 4). Besides, they again show that **12** is twice more active than **13**, which illustrates the benefit of the anionic backbone of the *malo*-NHC. The reason is not yet well understood, as these differences in activity may arise from (i) a possible negative interaction of the triflate anion in **13** – as already observed in the nickel-catalyzed Suzuki-Miyaura reaction with cationic half-sandwich Ni–NHC complexes<sup>[69]</sup> – and/or (ii) their difference in donicity, the *malo*-NHC being more donor in **12**.<sup>[22]</sup>

Under otherwise unchanged reaction conditions, a poor yield of 4% was obtained with Ni–CAAC complex **15** (entry 3), which has thus proven to be poorly to moderately active in all tested reactions. The reason is not yet well understood, but further studies on the strength of the Ni–CAAC bond in **15** might allow us to understand this phenomenon.

**Table 6.** Nickel(II)-catalyzed C–H arylation of THF with phenylboronic acid<sup>a</sup>

		
Entry	Catalyst	Yield (%) <sup>b</sup>
1	<b>12</b>	19
2	<b>13</b>	11
3	<b>15</b>	4
4	Ni(acac) <sub>2</sub> + PPh <sub>3</sub>	88 <sup>[67]</sup>

<sup>a</sup> Reaction conditions: phenylboronic acid (0.50 mmol), [Ni] (10 mol%) in THF (3 mL) at 100°C for 16 h. <sup>b</sup> Yields of isolated products.

### III. Conclusion

In summary, an original methodology for the facile and clean removal of the Cp ligand from cyclic and acyclic half-sandwich alkyl,NHC–nickel complexes, which do not present



any readily available coordination sites, has been developed. Of notable interest is the preservation, in the presence of the acid, of the nickel–alkyl and nickel–NHC bonds irrespective of whether they are part of a metalacycle or not. The robustness of these bonds indeed may open up interesting perspectives for the use of this novel class of square planar alkyl,NHC–nickel complexes in coordination chemistry and/or catalysis, even though the first catalytic results obtained in Suzuki–Miyaura coupling were rather disappointing.

Moreover, new nickel–NHC complexes based on *malo*-NHC and CAAC ligands were synthesized, and the coordination chemistry of these ligands with nickel has clearly shown that *malo*-NHCs behave as anionic X-type ligands, whereas CAACs behave as neutral L-type ligands. The catalytic activity of these complexes has been briefly evaluated in several reactions, and although they were generally moderately active, these results are encouraging. This study is only at its infancy, and we have no doubt that further work on ligand design, on the complexation of these carbenes to other nickel sources, and on their potential in catalytic applications, will give rise to interesting nickel–carbene catalysts in a near future.

## IV. Experimental section

### IV.1. General information

All reactions were carried out using standard Schlenk or glove-box techniques under an atmosphere of dry argon. Solvents were distilled from appropriate drying agents under argon. Solution NMR spectra were recorded at 298 K on FT-Bruker Ultra Shield 300 and FT Bruker Spectrospin 400 spectrometers operating at 300.13 or 400.14 MHz for  $^1\text{H}$  and at 75.47 or 100.61 MHz for  $^{13}\text{C}\{^1\text{H}\}$ . The  $^1\text{H}$  NMR variable-temperature experiments were recorded at 400 MHz in  $\text{CD}_2\text{Cl}_2$ , from 243 K to 296 K for complex **12**.  $^1\text{H}$  2D COSY spectra were obtained for complexes **3b** and **4a,b** to help in the  $^1\text{H}$  signal assignments. The chemical shifts are referenced to the residual deuterated or  $^{13}\text{C}$  solvent peaks. Chemical shifts ( $\delta$ ) and coupling constants ( $J$ ) are expressed in ppm and Hz respectively. Chemical shifts and full NMR data of **3b** are given for  $[\textbf{3b}] \sim 3 \cdot 10^{-2} \text{ mol.L}^{-1}$  in  $\text{CD}_3\text{CN}$ . IR spectra of solid samples of **3b**, **4a,b** and **6a,b** were recorded on a FT-IR Nicolet 380 spectrometer equipped with a diamond SMART-iTR ATR. Vibrational frequencies are expressed in  $\text{cm}^{-1}$ . Elemental

analyses were performed by the Service d'Analyses, de Mesures Physiques et de Spectroscopie Optique, UMR CNRS 7177, Institut de Chimie, Université de Strasbourg. Commercial compounds were used as received. [Ni{Me-NHC-CH<sub>2</sub>CH(CN)}Cp] **2a**,<sup>[3]</sup> [Ni{Mes-NHC-(CH<sub>2</sub>)<sub>2</sub>CH(CN)}Cp] **2b**,<sup>[3]</sup> [Ni(IMes)(CH<sub>3</sub>)Cp] **5a**,<sup>[41]</sup> [Ni(IMes)(CH<sub>2</sub>CN)Cp] **5b**,<sup>[2]</sup> the pyridinium salt **9a**,<sup>[20,53,54]</sup> [Ni(IMe)ICp]<sup>[58]</sup> and the CAAC precursor **14**,<sup>[59]</sup> were prepared according to the published methods.

## IV.2. Synthesis of [Ni{Mes-NHC-(CH<sub>2</sub>)<sub>2</sub>CH(CN)}(NCCH<sub>3</sub>)<sub>2</sub>]<sup>+</sup>PF<sub>6</sub><sup>−</sup> (**3b**)

To a dark green suspension of **2b** (300 mg, 0.798 mmol) and KPF<sub>6</sub> (147 mg, 0.799 mmol) in acetonitrile (5 mL) at room temperature was added drop-wise an equimolar amount of aqueous HCl (37%) diluted in acetonitrile to 1.0 M (0.80 mL, 0.800 mmol). The reaction mixture readily turned ochre yellow and was stirred for 10 min before filtration on a Celite pad, which was subsequently rinsed with acetonitrile until the washings were colorless. Volatiles were evaporated under vacuum, and the resulting solid was washed with pentane (3 x 10 mL), diethyl ether (3 x 10 mL) and dried under vacuum at 50°C to afford **3b** as a dark yellow solid (325 mg, 0.604 mmol, 76%).

<sup>1</sup>H NMR (CD<sub>3</sub>CN, 300.13 MHz):  $\delta$  7.32 (d, <sup>3</sup>*J* = 1.8 Hz, 1H, NCH), 7.24 (s, 1H, *m*-H), 7.05 (s, 1H, *m*-H), 7.03 (d, <sup>3</sup>*J* = 1.8 Hz, 1H, NCH), 4.13 and 4.03 (2m, 2 x 1H, NCH<sub>2</sub>), 2.56 (s, 3H, *p*-Me), 2.38 (s, 3H, *o*-Me), 2.33 (m, 1H, CHCN), 2.03 (s, 3H, *o*-Me), 1.69 (m, 1H, NCH<sub>2</sub>CH<sub>2</sub>), 1.08 (m, 1H, NCH<sub>2</sub>CH<sub>2</sub>). Free CH<sub>3</sub>CN that results from exchange with CD<sub>3</sub>CN is seen as a singlet (at 1.96 ppm) on the downfield side of the multiplet due to residual CHD<sub>2</sub>CN observed at 1.94 ppm. <sup>13</sup>C{<sup>1</sup>H} NMR (CD<sub>3</sub>CN, 100.61 MHz):  $\delta$  156.1 (br., NCN), 140.3 (*p*- or *ipso*-C<sub>Ar</sub>), 136.5, 136.2, 135.7 (*ipso*- or *p*-C<sub>Ar</sub>, *o*-C<sub>Ar</sub> and CHCN), 130.4 and 130.0 (*m*-C<sub>Ar</sub>), 125.4 and 123.6 (NCH), 50.6 (NCH<sub>2</sub>), 29.2 (NCH<sub>2</sub>CH<sub>2</sub>), 21.1 (*p*-Me), 19.2 and 18.3 (*o*-Me), −2.0 (br., CHCN). IR [ATR]:  $\nu$ (C<sub>sp2</sub>–H) 3176 (w), 3145 (w);  $\nu$ (C<sub>sp3</sub>–H) 2923 (w), 2861 (w);  $\nu$ (CH<sub>3</sub>CN) 2352(w), 2322 (w), 2293 (w);  $\nu$ (C≡N) 2234 (m);  $\nu$ (P–F) 826 (s).

## IV.3. Deuterium labeling experiment; reaction of (2b) with DCI

To a dark green suspension of **2b** (50 mg, 0.133 mmol) and KPF<sub>6</sub> (25 mg, 0.133 mmol) in CD<sub>3</sub>CN (2 mL) (C ~ 7.10<sup>−2</sup> mol.L<sup>−1</sup>) at room temperature was added drop-wise a

solution of DCl (35 wt.% in D<sub>2</sub>O) diluted in CD<sub>3</sub>CN to 1.0 M. The addition was stopped as soon as a color change from dark green to ochre yellow was observed. The reaction mixture was then stirred for 5 min, before it was allowed to settle and a sample was removed with a syringe and directly analyzed by <sup>1</sup>H NMR. The obtained spectrum shows the presence of [Ni{Mes-NHC-(CH<sub>2</sub>)<sub>2</sub>CH(CN)}(NCCD<sub>3</sub>)<sub>2</sub>]<sup>+</sup>PF<sub>6</sub><sup>-</sup> **3b-D** and mono-deuterated cyclopentadiene C<sub>4</sub>H<sub>4</sub>CHD in a 1:1 ratio.

<sup>1</sup>H NMR (CD<sub>3</sub>CN, 300.13 MHz):  $\delta$  7.33 (s, 2H, NCH and *m*-H), 7.07 (s, 1H, *m*-H), 7.04 (s, 1H, NCH), 6.56 and 6.48 (2d, <sup>3</sup>*J* n.r., 2 x 2H, C<sub>4</sub>H<sub>4</sub>CHD), 4.11 and 4.02 (2m, 2 x 1H, NCH<sub>2</sub>), 2.95 (br. s, 1H, C<sub>4</sub>H<sub>4</sub>CHD), 2.56 (s, 3H, *p*-Me), 2.41 (br. s, 4H, *o*-Me and CHCN), 2.03 (s, 3H, *o*-Me), 1.66 (br. s, 1H, NCH<sub>2</sub>CH<sub>2</sub>), 1.05 (br. s, 1H, NCH<sub>2</sub>CH<sub>2</sub>).

#### IV.4. Synthesis of [Ni{Mes-NHC-(CH<sub>2</sub>)<sub>2</sub>CH(CN)}(acac)] (**4b**)

To a dark green suspension of **2b** (1.00 g, 2.66 mmol) and KPF<sub>6</sub> (490 mg, 2.66 mmol) in acetonitrile (20 mL) at room temperature was added drop-wise an equimolar amount of aqueous HCl (37%) diluted in acetonitrile to 1.0 M (2.66 mL, 2.66 mmol). The reaction mixture turned yellow and was stirred for 10 min before filtration on a Celite pad, which was subsequently rinsed with acetonitrile until the washings were colorless. Potassium acetylacetonate (368 mg, 2.66 mmol) was then added to the filtrate and the reaction mixture was stirred for 30 min. The resulting light green suspension was filtered through Celite and the solvent evaporated under vacuum. Recrystallization from a thf/pentane mixture then afforded **4b** as light green microcrystals (650 mg, 1.46 mmol, 55%) that were washed with pentane (3 x 10 mL) and dried under vacuum.

Anal. Calcd for C<sub>21</sub>H<sub>25</sub>N<sub>3</sub>NiO<sub>2</sub>•<sup>1</sup>/<sub>2</sub>C<sub>4</sub>H<sub>8</sub>O: C, 61.91; H, 6.55; N, 9.42. Found: C, 61.99; H, 6.60; N, 9.30. [The crystals contain half a molecule of thf per formula unit, as shown by the NMR data and the X-ray diffraction study]. <sup>1</sup>H NMR (CD<sub>2</sub>Cl<sub>2</sub>, 400.14 MHz):  $\delta$  7.04 (d, <sup>3</sup>*J* = 1.8 Hz, 1H, NCH), 7.04 (s, 1H, *m*-H), 6.88 (s, 1H, *m*-H), 6.70 (d, <sup>3</sup>*J* = 1.8 Hz, 1H, NCH), 5.11 (s, 1H, CH[C(O)Me]<sub>2</sub>), 4.13 (m, 1H, NCH<sub>2</sub>), 4.01 (m, 1H, NCH<sub>2</sub>), 3.68 (m, 2H, 0.5 thf), 2.59 (s, 3H, *o*-Me), 2.31 (s, 3H, *p*-Me), 2.10 (s, 3H, *o*-Me), 1.82 (m, 2H, 0.5 thf), 1.78-1.71 (m, 2H, CHCN and NCH<sub>2</sub>CH<sub>2</sub>), 1.74 (s, 3H, C(O)Me), 1.27 (s, 3H, C(O)Me), 1.15 (m, 1H, NCH<sub>2</sub>CH<sub>2</sub>). <sup>1</sup>H NMR (CD<sub>3</sub>CN, 400.14 MHz):  $\delta$  7.22 (d, <sup>3</sup>*J* = 1.8 Hz, 1H, NCH), 7.07 (s, 1H, *m*-H), 6.94 (s, 1H, *m*-H), 6.83 (d, <sup>3</sup>*J* = 1.8 Hz, 1H, NCH), 5.15 (s, 1H, CH[C(O)Me]<sub>2</sub>), 4.07

(2m, 2 x 1H, NCH<sub>2</sub>), 3.65 (m, 2H, 0.5 thf), 2.51 (s, 3H, *o*-Me), 2.31 (s, 3H, *p*-Me), 2.08 (s, 3H, *o*-Me), 1.80 (m, 2H, 0.5 thf), 1.75 (dd, <sup>3</sup>*J* = 8.8 Hz, <sup>3</sup>*J* = 7.6 Hz, 1H, CHCN), 1.70 (s, 3H, C(O)Me), 1.65 (m, 1H, NCH<sub>2</sub>CH<sub>2</sub>), 1.31 (s, 3H, C(O)Me), 1.01 (m, 1H, NCH<sub>2</sub>CH<sub>2</sub>). <sup>13</sup>C{<sup>1</sup>H} NMR (CD<sub>3</sub>CN, 75.47 MHz): δ 187.8 and 186.8 (CO), 163.1 (NCN), 138.9 (*p*- or *ipso*-C<sub>Ar</sub>), 138.1 (*ipso*- or *p*-C<sub>Ar</sub>), 136.3 (*o*-C<sub>Ar</sub>), 135.7 (CHCN), 129.6 (*m*-C<sub>Ar</sub>), 124.4 and 122.5 (NCH), 100.7 (CH[C(O)Me]<sub>2</sub>), 68.3 (thf), 50.9 (NCH<sub>2</sub>), 30.8 (NCH<sub>2</sub>CH<sub>2</sub>), 27.0 and 25.2 (C(O)Me), 26.3 (thf), 21.1 (*p*-Me), 18.9 (*o*-Me), -2.2 (CHCN). IR [ATR]: ν(C<sub>sp2</sub>-H) 3152 (w), 3121 (w), 3093 (w); ν(C<sub>sp3</sub>-H) 2966 (w), 2916 (w), 2858 (w); ν(C≡N) 2187 (m); ν(C=O) + ν(C=C) 1581 (m), 1520 (s).

#### IV.5. Synthesis of [Ni{Me-NHC-CH<sub>2</sub>CH(CN)}(acac)] (4a)

To a dark green suspension of **2a** (300 mg, 1.16 mmol) and KPF<sub>6</sub> (214 mg, 1.16 mmol) in acetonitrile (5 mL) at room temperature was added drop-wise an equimolar amount of aqueous HCl (37%) diluted in acetonitrile to 1.0 M (1.16 mL, 1.16 mmol). The reaction mixture turned yellow and was stirred for 10 min before filtration on a Celite pad, which was subsequently rinsed with acetonitrile until the washings were colorless. Potassium acetylacetonate (160 mg, 1.16 mmol) was then added to the filtrate and the reaction mixture was stirred for 30 min. The resulting light brown-green suspension was filtered through Celite and the solvent evaporated under vacuum. The residue was then redissolved in THF (5 mL), filtered through Celite again, and precipitated from a thf/pentane (1:4) mixture to afford **4a** as a yellow powder (235 mg, 0.805 mmol, 69%) that was washed with pentane (3 x 10 mL) and dried under vacuum.

Anal. Calcd for C<sub>12</sub>H<sub>15</sub>N<sub>3</sub>NiO<sub>2</sub>: C, 49.37; H, 5.18; N, 14.39. Found: C, 49.47; H, 5.37; N, 14.10. <sup>1</sup>H NMR (CDCl<sub>3</sub>, 300.13 MHz): δ 6.78 (d, <sup>3</sup>*J* = 1.8 Hz, 1H, NCH), 6.58 (d, <sup>3</sup>*J* = 1.8 Hz, 1H, NCH), 5.38 (s, 1H, CH[C(O)Me]<sub>2</sub>), 3.79 (dd, <sup>2</sup>*J* = 12.2 Hz, <sup>3</sup>*J* = 8.1 Hz, 1H, NCH<sub>2</sub>), 3.72 (s, 3H, NCH<sub>3</sub>), 3.51 (dd, <sup>2</sup>*J* = 12.2 Hz, <sup>3</sup>*J* = 3.3 Hz, 1H, NCH<sub>2</sub>), 2.20 (dd, <sup>3</sup>*J* = 8.1 Hz, <sup>3</sup>*J* = 3.3 Hz, 1H, CHCN), 1.88 (s, 3H, C(O)Me), 1.84 (s, 3H, C(O)Me). <sup>13</sup>C{<sup>1</sup>H} NMR (CDCl<sub>3</sub>, 75.47 MHz): δ 187.5 and 185.9 (CO), 160.8 (NCN), 136.3 (CHCN), 123.8 and 117.3 (NCH), 100.5 (CH[C(O)Me]<sub>2</sub>), 52.4 (NCH<sub>2</sub>), 35.5 (NCH<sub>3</sub>), 27.2 and 26.5 (C(O)Me), 4.0 (CHCN). IR [ATR]: ν(C<sub>sp2</sub>-H) 3147 (w), 3116 (w); ν(C<sub>sp3</sub>-H) 2940 (w); ν(C≡N) 2185 (m); ν(C=O) + ν(C=C) 1575 (m), 1518 (s).

#### IV.6. Synthesis of [Ni(IMes)(CH<sub>3</sub>)(acac)] (**6a**)

To a brownish suspension of **5a** (300 mg, 0.677 mmol) and KPF<sub>6</sub> (125 mg, 0.679 mmol) in acetonitrile (5 mL) at room temperature was added drop-wise an equimolar amount of aqueous HCl (37%) diluted in acetonitrile to 1.0 M (0.68 mL, 0.680 mmol). The reaction mixture turned yellow and was stirred for 10 min before filtration on a Celite pad, which was subsequently rinsed with acetonitrile until the washings were colorless. Potassium acetylacetonate (94 mg, 0.680 mmol) was then added to the filtrate and the reaction mixture was stirred for 30 min at room temperature. The resulting light brown suspension was filtered through Celite and the solvent evaporated under vacuum. The residue was then extracted in toluene (5 mL) and filtered through Celite again. Solvent evaporation afforded **6a** as a yellow solid (228 mg, 0.478 mmol, 71%) that was washed with pentane (3 x 10 mL) and dried under vacuum.

Anal. Calcd for C<sub>27</sub>H<sub>34</sub>N<sub>2</sub>NiO<sub>2</sub>: C, 67.95; H, 7.18; N, 5.87. Found: C, 67.98; H, 7.35; N, 5.65. <sup>1</sup>H NMR (CD<sub>3</sub>CN, 300.13 MHz): δ 7.12 (s, 4H, *m*-H), 7.10 (s, 2H, NCH), 5.06 (s, 1H, CH[C(O)Me]<sub>2</sub>), 2.40 (s, 6H, *p*-Me), 2.17 (s, 12H, *o*-Me), 1.54 (s, 3H, C(O)Me), 1.51 (s, 3H, C(O)Me), -1.13 (s, 3H, CH<sub>3</sub>). <sup>13</sup>C{<sup>1</sup>H} NMR (CD<sub>3</sub>CN, 75.47 MHz): δ 186.6 and 186.1 (CO), 179.5 (NCN), 139.6 (*p*- or *ipso*-C<sub>Ar</sub>), 137.9 and 136.4 (br. *o*-C<sub>Ar</sub>), 137.7 (*ipso*- or *p*-C<sub>Ar</sub>), 129.9 (*m*-C<sub>Ar</sub>), 124.3 (NCH), 100.0 (CH[C(O)Me]<sub>2</sub>), 27.2 and 26.5 (C(O)Me), 21.2 (*p*-Me), 18.6 (br. *o*-Me), -13.7 (CH<sub>3</sub>). IR [ATR]: ν(C<sub>sp2</sub>-H) 3164 (w), 3134 (w), 3079 (w); ν(C<sub>sp3</sub>-H) 2951 (m), 2917 (m), 2854 (m); ν(C=O) + ν(C=C) 1578 (s), 1515 (s).

#### IV.7. Synthesis of [Ni(IMes)(CH<sub>2</sub>CN)(acac)] (**6b**)

To a dark green suspension of **5b** (500 mg, 1.07 mmol) and KPF<sub>6</sub> (197 mg, 1.07 mmol) in acetonitrile (10 mL) at room temperature was added drop-wise an equimolar amount of aqueous HCl (37%) diluted in acetonitrile to 1.0 M (1.07 mL, 1.07 mmol). The reaction mixture turned yellow and was stirred for 10 min before filtration on a Celite pad, which was subsequently rinsed with acetonitrile until the washings were colorless. Potassium acetylacetonate (148 mg, 1.07 mmol) was then added to the filtrate and the reaction mixture was stirred for 30 min. The resulting greenish suspension was filtered through Celite and the solvent evaporated under vacuum. The residue was then redissolved in THF (5 mL), filtered through Celite again, and recrystallized from a thf/pentane (1:4) mixture at 4°C to afford **6b**

as a yellow-green solid (378 mg, 0.753 mmol, 70%) that was washed with pentane (3 x 10 mL) and dried under vacuum.

Anal. Calcd for  $C_{28}H_{33}N_3NiO_2$ : C, 66.96; H, 6.62; N, 8.37. Found: C, 67.12; H, 6.64; N, 8.26.  $^1H$  NMR ( $CD_3CN$ , 300.13 MHz):  $\delta$  7.17 (s, 6H, *m*-H and NCH), 5.18 (s, 1H,  $CH[C(O)Me]_2$ ), 2.41 (s, 6H, *p*-Me), 2.16 (br. s, 12H, *o*-Me), 1.60 (s, 3H,  $C(O)Me$ ), 1.59 (s, 3H,  $C(O)Me$ ), -0.13 (s, 2H,  $CH_2CN$ ).  $^1H$  NMR ( $CDCl_3$ , 300.13 MHz):  $\delta$  7.10 (s, 4H, *m*-H), 6.95 (s, 2H, NCH), 5.06 (s, 1H,  $CH[C(O)Me]_2$ ), 2.41 (s, 6H, *p*-Me), 2.23 (s, 12H, *o*-Me), 1.66 (s, 3H,  $C(O)Me$ ), 1.53 (s, 3H,  $C(O)Me$ ), -0.02 (s, 2H,  $CH_2CN$ ).  $^{13}C\{^1H\}$  NMR ( $CD_3CN$ , 75.47 MHz):  $\delta$  187.0 and 186.9 (CO), 169.8 (NCN), 140.1 (*p*- or *ipso*- $C_{Ar}$ ), 137.6 and 136.0 (br. *o*- $C_{Ar}$ ), 136.7 (*ipso*- or *p*- $C_{Ar}$ ), 130.1 (*m*- $C_{Ar}$ ), 125.2 (NCH), 100.6 ( $CH[C(O)Me]_2$ ), 26.9 and 26.1 ( $C(O)Me$ ), 21.3 (*p*-Me), 18.4 (br. *o*-Me), -22.4 ( $CH_2CN$ ). IR [ATR]:  $\nu(C_{sp^2}-H)$  3171 (w), 3128 (w), 3079 (w);  $\nu(C_{sp^3}-H)$  2957 (m), 2918 (m), 2859 (w);  $\nu(C\equiv N)$  2193 (m);  $\nu(C=O)$  +  $\nu(C=C)$  1578 (s), 1519 (s).

#### IV.8. Synthesis of $[IMes.H^+]_3[(NiCl_4^{2-})(Cl^-)]$ (7)

A light-green suspension of anhydrous  $Ni(acac)_2$  (154 mg, 0.599 mmol) and the imidazolium salt  $IMes.HCl$  (613 mg, 1.797 mmol) in toluene (20 mL) was stirred at 110°C for 48 h. A blue solid slowly formed, which was directly filtered on a sintered glass frit and washed with toluene (3 x 5 mL) and *n*-pentane (3 x 5 mL). Removal of the volatiles *in vacuo* afforded **2** as a blue solid (145 mg, 0.126 mmol, 21 %).

$^1H$  NMR ( $CD_2Cl_2$ , 300.13 MHz):  $\delta$  7.82 (s, 2H, NCH), 5.18 (s, 1H,  $CH[C(O)Me]_2$ ), 7.24 (s, 4H, *m*-H), 6.81 (s, 1H, NCHN), 2.52 (s, 6H, *p*-Me), 2.23 (s, 12H, *o*-Me).  $^{13}C\{^1H\}$  NMR ( $CD_2Cl_2$ , 75.47 MHz):  $\delta$  141.7 ( $C_{Ar}$ ), 139.0 (NCN), 134.7 ( $C_{Ar}$ ), 131.1 ( $C_{Ar}$ ), 130.6 ( $C_{Ar}$ ), 123.9 (NCH), 23.6 (*o*-Me), 21.5 (*p*-Me).

#### IV.9. Synthesis of $[Ni(IMes)_2Cl_2]$ (8)

A suspension of **7** (50 mg, 0.043 mmol) and  $KO^tBu$  (11 mg, 0.095 mmol) in toluene (10 mL) was stirred at room temperature for 24 h, during which the color slowly changed from blue to pale-orange. The reaction mixture was then filtered over Celite, and washed with

toluene until the washings were colorless. Evaporation of the solvents afforded **8** as an orange solid (20 mg, 0.028 mmol, 64 %).

$^1\text{H}$  NMR ( $\text{CDCl}_3$ , 300.13 MHz):  $\delta$  7.01 (s, 8H, *m*-H), 6.62 (s, 4H, NCH), 2.54 (s, 12H, *p*-Me), 1.95 (s, 24H, *o*-Me).  $^{13}\text{C}\{^1\text{H}\}$  NMR ( $\text{CDCl}_3$ , 75.47 MHz):  $\delta$  167.5 (NCN), 137.4 ( $\text{C}_{\text{Ar}}$ ), 136.2 ( $\text{C}_{\text{Ar}}$ ), 129.0 ( $\text{C}_{\text{Ar}}$ ), 122.4 (NCH), 21.3 (*o*-Me), 19.1 (*p*-Me).

#### IV.10. Synthesis of $[\text{Ni}(\text{PPh}_3)_2(\text{maloNHC})\text{Cl}]$ (**10**)

A solution of the pyridinium salt **9a** (mg, mmol) in THF (mL) was treated at room temperature by drop-wise addition of a 0.5M solution of KHMDS in toluene (mL, mmol). The reaction mixture was stirred for 30 min before addition of  $[\text{Ni}(\text{PPh}_3)_2\text{Cl}_2]$  ( mg, mmol) to the solution containing the free carbene, and the resulting dark green suspension was stirred for a further 10 min to give a violet suspension. The reaction media was filtered, and **10** was predominantly recovered as a light violet solid that was washed with *n*-pentane before drying under vacuum.

$^1\text{H}$  NMR ( $\text{DMSO}-d_6$ , 300.13 MHz):  $\delta$  7.38 (m, 18H, *m*- and *p*-H( $\text{PPh}_3$ )), 7.22 (m, 12H, *o*-H( $\text{PPh}_3$ )), 7.03 (s, 4H, *m*-H(*malo*-NHC)), 2.27 (s, 6H, *p*-Me), 2.05 (s, 12H, *o*-Me), 1.80 (s, 3H,  $\text{CH}_3$  apical).

#### IV.11. Synthesis of $[\text{Ni}(\text{IMe})(\text{maloNHC})\text{Cp}]$ (**12**)

A solution of the pyridinium salt **9a** (210 mg, 0.579 mmol) in THF (3 mL) was treated at room temperature by drop-wise addition of a 0.5M solution of KHMDS in toluene (1.27 mL, 0.636 mmol). The reaction mixture was stirred for 30 min before addition of  $[\text{Ni}(\text{IMe})\text{ICp}]$  **11** (200 mg, 0.579 mmol) to the solution containing the free carbene. The resulting red-brown solution quickly gave a brown suspension. After 30 min at room temperature, the reaction medium was evaporated to dryness before extraction of the brownish residue with  $\text{CH}_2\text{Cl}_2$  ( $3 \times 10$  mL), and filtration over Celite. The filtrate was then concentrated to *ca.* 5 mL before addition of  $\text{Et}_2\text{O}$  (20 mL) to afford **12** as a light brown solid that was subsequently washed with  $\text{Et}_2\text{O}$  until the washings were colorless, and dried under (252 mg, 0.433 mmol, 75%).



$^1\text{H}$  NMR ( $\text{CDCl}_3$ , 300.13 MHz):  $\delta$  6.96 (s, 4H, *m*-H), 6.84 (s, 2H, NCH), 4.72 (s, 5H,  $\eta^5\text{-C}_5\text{H}_5$ ), 3.32 (s, 6H,  $\text{NCH}_3$ ), 2.36 (s, 6H, *p*-Me), 2.00 (br. s, 12H, *o*-Me), 1.86 (s, 3H,  $\text{CH}_3$  apical).  $^{13}\text{C}\{^1\text{H}\}$  NMR ( $\text{CDCl}_3$ , 75.47 MHz):  $\delta$  189.8 (CO), 162.6 and 162.0 (NCN), 141.7 and 137.9 (*ipso*-/*p*- $\text{C}_{\text{Ar}}$ ), 137.4 (*o*- $\text{C}_{\text{Ar}}$ ), 129.3 (*m*- $\text{C}_{\text{Ar}}$ ), 124.2 (NCH), 93.3 ( $\text{C}_5\text{H}_5$ ), 90.5 ( $\text{C}$  apical), 39.2 ( $\text{NCH}_3$ ), 21.2 (*p*-Me), 18.8 (*o*-Me), 9.0 ( $\text{CH}_3$  apical).

#### IV.12. Synthesis of $[\text{Ni}(\text{IMe})(\text{MeO-maloNHC})\text{Cp}](\text{OTf})$ (**13**)

A solution of **12** (200 mg, 0.344 mmol) in  $\text{CH}_2\text{Cl}_2$  (10 mL) was placed at  $0^\circ\text{C}$  before drop-wise addition of MeOTf (40  $\mu\text{L}$ , 0.361 mmol). The reaction mixture was then stirred for 30 min at  $0^\circ\text{C}$  before the volatiles were removed *in vacuo* to afford **13** (235 mg, 0.315 mmol, 92%) as a brown solid that washed with  $\text{Et}_2\text{O}$  ( $4 \times 10$  mL), and dried under vacuum.

$^1\text{H}$  NMR ( $\text{CDCl}_3$ , 400.13 MHz):  $\delta$  7.13 (s, 4H, *m*-H), 7.07 (s, 2H, NCH), 4.77 (s, 5H,  $\eta^5\text{-C}_5\text{H}_5$ ), 3.50 (s, 3H,  $\text{OCH}_3$ ), 3.28 (s, 6H,  $\text{NCH}_3$ ), 2.46 (s, 3H, *p*-Me), 2.42 (s, 3H, *p*-Me), 2.01 (br. s, 9H, *o*-Me +  $\text{CH}_3$  apical), 1.93 (br. s, 6H, *o*-Me).

#### IV.13. Synthesis of $[\text{Ni}(\text{CAAC})(\text{PPh}_3)\text{Cl}_2]$ (**15**) and of $[\text{CAAC.H}^+][\text{Ni}(\text{PPh}_3)\text{Cl}_3^-]$ (**16**)

To a suspension of the CAAC precursor **14** (500 mg, 1.38 mmol) in  $\text{Et}_2\text{O}$  (10 mL) at  $-78^\circ\text{C}$  was added drop-wise a 0.5 M solution of KHMDS in toluene (3.04 mL, 1.52 mmol). The reaction mixture then was allowed to warm to room temperature, and stirred for 1 h before the volatiles were removed *in vacuo*. The free carbene was extracted with THF ( $2 \times 10$  mL), and added to a suspension of  $[\text{Ni}(\text{PPh}_3)_2\text{Cl}_2]$  (903 mg, 1.38 mmol) in THF (20 mL) at  $-78^\circ\text{C}$ . The reaction medium was then allowed to warm to room temperature during which a color change from dark green to reddish was observed. The suspension was immediately filtered over Celite, and the filtrate was concentrated to *ca.* 10 mL before addition of *n*-pentane (30 mL). The precipitation of a white solid (triphenylphosphine) was observed. The suspension was again filtered on Celite, and the filtrate concentrated to *ca.* 5 mL. Depending on the quantity of **14** still present in the reaction medium, a notable amount of blue crystals were formed, and subsequently filtered before washing with *n*-pentane ( $3 \times 10$  mL) and drying under vacuum to afford **16**. The reddish filtrate was placed at  $-28^\circ\text{C}$  overnight to yield



**15** (335 mg, 0.467 mmol, 34%) as a violet solid that was washed with *n*-pentane (3 × 20 mL) and dried under vacuum.

**15**:  $^1\text{H}$  NMR ( $\text{C}_6\text{D}_6$ , 300.13 MHz):  $\delta$  7.84 (d,  $^3J = 6.6$  Hz, 6H, *o*-H( $\text{PPh}_3$ )), 7.37 (s, 3H,  $\text{H}_{\text{Ar}}(\text{CAAC})$ ), 7.10-6.94 (m, 9H, *m*- and *p*-H( $\text{PPh}_3$ )), 3.77 (t,  $^2J = 13.4$  Hz, 2H), 3.23 (sept,  $^3J = 6.2$  Hz, 2H,  $\text{CH}(\text{CH}_3)_2$ ), 2.02 (d,  $^2J = 13.4$  Hz, 2H), 1.79 (d,  $^2J = 13.4$  Hz, 2H), 1.72-1.53 (m, 4H), 1.46 (d,  $^3J = 6.1$  Hz, 6H,  $\text{CH}(\text{CH}_3)_2$ ), 1.41-1.32 (m, 2H), 1.20 d,  $^3J = 6.1$  Hz, 6H,  $\text{CH}(\text{CH}_3)_2$ ), 0.98 (s, 6H,  $\text{C}(\text{CH}_3)_2$ ).

#### IV.14. X-ray Diffraction Studies. Structure Determination and Refinement

Single crystals of **4b**, **7** and **16** suitable for X-ray diffraction studies was selected from batches of crystals obtained at  $-28$  °C from a THF/pentane solution, at RT from an acetone/pentane solution, and at RT from a dichloromethane/pentane solution respectively. Diffraction data were collected at 173(2) K on a Bruker APEX II DUO KappaCCD area detector diffractometer equipped with an Oxford Cryosystem liquid  $\text{N}_2$  device using Mo- $\text{K}\alpha$  radiation ( $\lambda = 0.71073$  Å). A summary of crystal data, data collection parameters and structure refinements is given in **Table 6**. The crystal-detector distance was 38 mm. The cell parameters were determined (APEX2 software) from reflections taken from three sets of twelve frames, each at ten s exposure. The structure was solved using direct methods with SHELXS-97 and refined against  $F^2$  for all reflections using the SHELXL-97 software.<sup>[70]</sup> A semi-empirical absorption correction was applied using SADABS in APEX2. All non-hydrogen atoms were refined with anisotropic displacement parameters, using weighted full-matrix least-squares on  $F^2$ . Hydrogen atoms were included in calculated positions and treated as riding atoms using SHELXL default parameters.

**Table 6.** X-Ray Crystallographic Data and Data Collection Parameters for **4b**, **7** and **16**

Complex	<b>4b</b>	<b>7</b>	<b>16</b>
Empirical formula	2(C <sub>21</sub> H <sub>25</sub> N <sub>3</sub> NiO <sub>2</sub> )•C <sub>4</sub> H <sub>8</sub> O	3(C <sub>21</sub> H <sub>25</sub> N <sub>2</sub> )•Cl <sub>4</sub> Ni•Cl	C <sub>23</sub> H <sub>36</sub> N•C <sub>18</sub> H <sub>15</sub> Cl <sub>3</sub> NiP
Formula weight	892.40	1152.25	753.85
Crystal system	Tetragonal	Hexagonal	Triclinic
Space group	I -4	<i>P</i> 6 <sub>3</sub>	P1
<i>a</i> (Å)	18.4575(4)	15.975(1)	11.7585(10)
<i>c</i> (Å)	13.1542(4)	15.450(1)	15.0414(12)
<i>V</i> (Å <sup>3</sup> )	4481.36(19)	3414.6(4)	2080.8(3)
<i>Z</i>	4	2	2
<i>D</i> <sub>calcd</sub> (Mg.m <sup>-3</sup> )	1.323	1.121	1.203
Absorp coeff (mm <sup>-1</sup> )	0.891	0.52	0.72
Crystal habit, color	block, yellow	prism, blue	prism, blue
Crystal size (mm)	0.20 × 0.15 × 0.10	0.55 × 0.15 × 0.15	0.30 × 0.28 × 0.20
<i>h</i> , <i>k</i> , <i>l</i> <sub>max</sub>	24, 23, 17	17, 18, 18	16, 17, 21
<i>T</i> <sub>min</sub> , <i>T</i> <sub>max</sub>	0.842, 0.916	0.764, 0.926	0.634, 0.746
Reflns collected	29009	17385	34754
<i>R</i> [ <i>I</i> > 2σ( <i>I</i> )]	0.0259	0.066	0.030
<i>wR</i> <sup>2</sup> (all data)	0.0677	0.125	0.119
GOF on <i>F</i> <sup>2</sup>	1.048	0.91	1.08

## V. References

- [1] P. Enghag, *Encyclopedia of the Elements: Technical Data - History - Processing - Applications*, Wiley-VCH, Weinheim, **2004**.
- [2] A. M. Oertel, V. Ritleng, M. J. Chetcuti, L. F. Veiros, *J. Am. Chem. Soc.* **2010**, *132*, 13588–13589.

- [3] A. M. Oertel, J. Freudenreich, J. Gein, V. Ritleng, L. F. Veiros, M. J. Chetcuti, *Organometallics* **2011**, *30*, 3400–3411.
- [4] M. Poyatos, J. A. Mata, E. Peris, *Chem. Rev.* **2009**, *109*, 3677–3707.
- [5] L. H. Gade, S. Bellemin-Laponnaz, *Coord. Chem. Rev.* **2007**, *251*, 718–725.
- [6] B. Royo, E. Peris, *Eur. J. Inorg. Chem.* **2012**, 1309–1318.
- [7] S. Milosevic, E. Brenner, V. Ritleng, M. J. Chetcuti, *Dalton Trans.* **2008**, 1973–1975.
- [8] O. Navarro, N. Marion, N. M. Scott, J. González, D. Amoroso, A. Bell, S. P. Nolan, *Tetrahedron* **2005**, *61*, 9716–9722.
- [9] N. Marion, E. C. Ecarnot, O. Navarro, D. Amoroso, A. Bell, S. P. Nolan, *J. Org. Chem.* **2006**, *71*, 3816–3821.
- [10] O. H. Winkelmann, A. Riekstins, S. P. Nolan, O. Navarro, *Organometallics* **2009**, *28*, 5809–5813.
- [11] N. Marion, O. Navarro, J. Mei, E. D. Stevens, N. M. Scott, S. P. Nolan, *J. Am. Chem. Soc.* **2006**, *128*, 4101–4111.
- [12] N. Marion, O. Navarro, E. D. Stevens, E. C. Ecarnot, A. Bell, D. Amoroso, S. P. Nolan, *Chem. Asian J.* **2010**, *5*, 841–846.
- [13] S. Meiries, A. Chartoire, A. M. Z. Slawin, S. P. Nolan, *Organometallics* **2012**, *31*, 3402–3409.
- [14] S. Meiries, K. Speck, D. B. Cordes, A. M. Z. Slawin, S. P. Nolan, *Organometallics* **2013**, *32*, 330–339.
- [15] N. Marion, S. P. Nolan, *Acc. Chem. Res.* **2008**, *41*, 1440–1449.
- [16] D. Bourissou, O. Guerret, F. P. Gabbaï, G. Bertrand, *Chem. Rev.* **2000**, *100*, 39–92.
- [17] P. L. Arnold, S. Pearson, *Coord. Chem. Rev.* **2007**, *251*, 596–609.
- [18] O. Schuster, L. Yang, H. G. Raubenheimer, M. Albrecht, *Chem. Rev.* **2009**, *109*, 3445–3478.
- [19] M. Melaimi, M. Soleilhavoup, G. Bertrand, *Angew. Chem. Int. Ed.* **2010**, *49*, 8810–8849.
- [20] V. César, N. Lugan, G. Lavigne, *J. Am. Chem. Soc.* **2008**, *130*, 11286–11287.
- [21] V. César, N. Lugan, G. Lavigne, *Eur. J. Inorg. Chem.* **2010**, *2010*, 361–365.
- [22] V. César, N. Lugan, G. Lavigne, *Chem. Eur. J.* **2010**, *16*, 11432–11442.
- [23] M. G. Hobbs, C. J. Knapp, P. T. Welsh, J. Borau-Garcia, T. Ziegler, R. Roesler, *Chem. Eur. J.* **2010**, *16*, 14520–14533.

- [24] V. César, C. Barthes, Y. C. Farré, S. V. Cuisiat, B. Y. Vacher, R. Brousses, N. Lugan, G. Lavigne, *Dalton Trans.* **2013**, 42, 7373–7385.
- [25] V. César, L. C. Misal Castro, T. Dombray, J.-B. Sortais, C. Darcel, S. Labat, K. Miqueu, J.-M. Sotiropoulos, R. Brousses, N. Lugan, G. Lavigne, *Organometallics* **2013**, 32, 4643–4655.
- [26] V. Lavallo, Y. Canac, C. Präsang, B. Donnadieu, G. Bertrand, *Angew. Chem. Int. Ed.* **2005**, 44, 5705–5709.
- [27] V. Lavallo, Y. Canac, A. DeHope, B. Donnadieu, G. Bertrand, *Angew. Chem.* **2005**, 117, 7402–7405.
- [28] G. Altenhoff, R. Goddard, C. W. Lehmann, F. Glorius, *Angew. Chem. Int. Ed.* **2003**, 42, 3690–3693.
- [29] G. Altenhoff, R. Goddard, C. W. Lehmann, F. Glorius, *J. Am. Chem. Soc.* **2004**, 126, 15195–15201.
- [30] S. Würtz, F. Glorius, *Acc. Chem. Res.* **2008**, 41, 1523–1533.
- [31] S. Pelties, R. Wolf, *Z. Anorg. Allg. Chem.* **2013**, 639, 2581–2585.
- [32] K. C. Mondal, P. P. Samuel, Y. Li, H. W. Roesky, S. Roy, L. Ackermann, N. S. Sidhu, G. M. Sheldrick, E. Carl, S. Demeshko, S. De, P. Parameswaran, L. Ungur, L. F. Chibotaru, D. M. Andrada, *Eur. J. Inorg. Chem.* **2014**, 818–823.
- [33] J. Honzíček, P. Kratochvíl, J. Vinklárík, A. Eisner, Z. Padělková, *Organometallics* **2012**, 31, 2193–2202.
- [34] S. Top, E. B. Kaloun, S. Toppi, A. Herrbach, M. J. McGlinchey, G. Jaouen, *Organometallics* **2001**, 20, 4554–4561.
- [35] C. L. B. Macdonald, J. D. Gorden, A. Voigt, S. Filipponi, A. H. Cowley, *Dalton Trans.* **2008**, 1161–1176.
- [36] G. M. de Lima, D. J. Duncalf, S. P. Constantine, *Main Group Met. Chem.* **2001**, 24, 675–680.
- [37] R. H. Crabtree, *The Organometallic Chemistry of the Transition Metals*, John Wiley, **2001**.
- [38] Y. Ohki, T. Hatanaka, K. Tatsumi, *J. Am. Chem. Soc.* **2008**, 130, 17174–17186.
- [39] A. T. Normand, S. K. Yen, H. V. Huynh, T. S. A. Hor, K. J. Cavell, *Organometallics* **2008**, 27, 3153–3160.
- [40] A. T. Normand, K. J. Hawkes, N. D. Clement, K. J. Cavell, B. F. Yates, *Organometallics* **2007**, 26, 5352–5363.

- [41] C. D. Abernethy, Alan H, Cowley, R. A. Jones, *J. Organomet. Chem.* **2000**, 596, 3–5.
- [42] V. Ritleng, A. M. Oertel, M. J. Chetcuti, *Dalton Trans.* **2010**, 39, 8153–8160.
- [43] P. Pauling, *Inorg. Chem.* **1966**, 5, 1498–1505.
- [44] S. Hameury, P. de Frémont, P.-A. R. Breuil, H. Olivier-Bourbigou, P. Braunstein, *Inorg. Chem.* **2014**, DOI: 10.1021/ic500349t.
- [45] G. J. Bullen, R. Mason, P. Pauling, *Inorg. Chem.* **1965**, 4, 456–462.
- [46] K. Bica, P. Gaertner, *Eur. J. Org. Chem.* **2008**, 3453–3456.
- [47] X. Wei, L. Yu, D. Wang, X. Jin, G. Z. Chen, *Green Chem.* **2008**, 10, 296–305.
- [48] T. Sasaki, M. Tada, C. Zhong, T. Kume, Y. Iwasawa, *J. Mol. Catal. A* **2008**, 279, 200–209.
- [49] M. B. Meredith, C. H. McMillen, J. T. Goodman, T. P. Hanusa, *Polyhedron* **2009**, 28, 2355–2358.
- [50] G. Liu, M. Hou, J. Song, Z. Zhang, T. Wu, B. Han, *J. Mol. Catal. A* **2010**, 316, 90–94.
- [51] C. Zhong, T. Sasaki, M. Tada, Y. Iwasawa, *J. Catal.* **2006**, 242, 357–364.
- [52] K. Matsubara, K. Ueno, Y. Shibata, *Organometallics* **2006**, 25, 3422–3427.
- [53] K. E. Krahulic, G. D. Enright, M. Parvez, R. Roesler, *J. Am. Chem. Soc.* **2005**, 127, 4142–4143.
- [54] Y. Pan, C. W. Kee, Z. Jiang, T. Ma, Y. Zhao, Y. Yang, H. Xue, C.-H. Tan, *Chem. Eur. J.* **2011**, 17, 8363–8370.
- [55] R. A. Kelly III, N. M. Scott, S. Díez-González, E. D. Stevens, S. P. Nolan, *Organometallics* **2005**, 24, 3442–3447.
- [56] H. S. Gutowsky, C. H. Holm, *J. Chem. Phys.* **2004**, 25, 1228–1234.
- [57] A. M. Oertel, V. Ritleng, L. Burr, M. J. Chetcuti, *Organometallics* **2011**, 30, 6685–6691.
- [58] V. Ritleng, C. Barth, E. Brenner, S. Milosevic, M. J. Chetcuti, *Organometallics* **2008**, 27, 4223–4228.
- [59] R. Jazzar, R. D. Dewhurst, J.-B. Bourg, B. Donnadieu, Y. Canac, G. Bertrand, *Angew. Chem. Int. Ed.* **2007**, 46, 2899–2902.
- [60] J. Wolf, A. Labande, M. Natella, J.-C. Daran, R. Poli, *J. Mol. Catal. Chem.* **2006**, 259, 205–212.
- [61] J. Wolf, A. Labande, J.-C. Daran, R. Poli, *J. Organomet. Chem.* **2006**, 691, 433–443.

- [62] G. D. Stucky, J. B. Folkers, T. J. Kistenmacher, *Acta Crystallogr.* **1967**, 23, 1064–1070.
- [63] A. M. Oertel, V. Ritleng, M. J. Chetcuti, *Organometallics* **2012**, 31, 2829–2840.
- [64] L. P. Bheeter, M. Henrion, L. BreLOT, C. Darcel, M. J. Chetcuti, J.-B. Sortais, V. Ritleng, *Adv. Synth. Catal.* **2012**, 354, 2619–2624.
- [65] M. Henrion, M. J. Chetcuti, V. Ritleng, *Chem. Commun.* **2014**, 50, 4624–4627.
- [66] A. M. Oertel, V. Ritleng, A. Busiah, L. F. Veiros, M. J. Chetcuti, *Organometallics* **2011**, 30, 6495–6498.
- [67] D. Liu, C. Liu, H. Li, A. Lei, *Angew. Chem. Int. Ed.* **2013**, 52, 4453–4456.
- [68] K. Matsubara, K. Ueno, Y. Koga, K. Hara, *J. Org. Chem.* **2007**, 72, 5069–5076.
- [69] W. Buchowicz, Ł. Banach, J. Conder, P. A. Guńka, D. Kubicki, P. Buchalski, *Dalton Trans.* **2014**, 43, 5847–5857.
- [70] G. M. Sheldrick, *Acta Crystallogr. A* **2008**, 64, 112–122.

## **General conclusion**





The manuscript of this thesis deals with the syntheses, coordination chemistry and catalysis applications of *N*-heterocyclic carbenes (NHCs) coordinated to a nickel atom. The choice of such compounds was motivated by the use of nickel, which is an abundant and cheap metal that exhibits interesting activities in a large array of catalytic organic transformations. Furthermore, the use of NHCs, which are easily accessible and tunable ligands, can provide a wide choice of electronically and sterically different Ni–NHC complexes.

**Chapter I** briefly summarizes the historical and theoretical aspects of carbenes as transition-metals ligands. A detailed presentation of catalysis applications of these Ni–NHC systems is also given, especially in cross-coupling reactions involving the formation of Carbon–Carbon and Carbon–Heteroatom bonds, as well as in reduction and oxidation reactions.

In **Chapter II**, we present an efficient methodology for the Ni–NHC-catalyzed  $\alpha$ -arylation of acyclic ketones with the inexpensive and easy-to-handle half-sandwich complex [Ni(IPr)ClCp]. The latter complex is the most productive nickel-based catalyst to date, as loadings as low as 1 mol% could be used with aromatic and aliphatic enolizable acyclic ketones, as well as aryl iodides and bromides, to give the coupling products in moderate to excellent yields. This methodology is complementary to the few others Ni-catalyzed  $\alpha$ -arylation processes, where only cyclic enolizable ketones were used with high loadings of air-sensitive and pyrophoric Ni(COD)<sub>2</sub>. Our methodology is thus superior in terms of cost and practicability. We also synthesized a Ni–Ph complex [Ni(IMes)(Ph)Cp] and a Ni–propiophenone complex [Ni(IMes){CH(CH<sub>3</sub>)C(O)Ph}Cp], that were then evaluated as potential active intermediates. Nevertheless, control experiments suggest that [Ni(IMes)(Ph)Cp] is not an intermediate, whereas [Ni(IMes){CH(CH<sub>3</sub>)C(O)Ph}Cp] could partly act as an active intermediate. However, experiments in the presence of radical inhibitors and initiators strongly suggest that a radical mechanism is more likely.

Half-sandwich Ni–NHC complexes also proved to be very active pre-catalysts in the hydrosilylation of (pseudo)carbonyl derivatives, which is presented in **Chapter III**. The use of [Ni(IMes)ClCp]/NaHBET<sub>3</sub> (1:2) was found to efficiently catalyze the reduction of

aldehydes, ketones, aldimines and ketimines *via* hydrosilylation. Interestingly, the cationic complex  $[\text{Ni}(\text{IMes})(\text{NCMe})\text{Cp}](\text{PF}_6)$  can be alternatively used without additive for the reduction of aldimines and ketimines, even if slightly harsher reaction conditions are necessary, compared to the  $[\text{Ni}(\text{IMes})\text{ClCp}]/\text{NaHBEt}_3$  (1:2) catalyst. Mechanistic studies demonstrated that the Ni–hydride complex  $[\text{Ni}(\text{IMes})\text{HCp}]$  is predominantly formed *in situ* starting from the  $[\text{Ni}(\text{IMes})\text{ClCp}]/\text{NaHBEt}_3$  (1:2) combination. The same hydride complex was obtained in small amounts by reaction of the cationic complex  $[\text{Ni}(\text{IMes})(\text{NCMe})\text{Cp}](\text{PF}_6)$  with diphenylsilane. This hydride species was evaluated in the hydrosilylation process, and the results show that it is thought to be the true pre-catalyst. Furthermore, control experiments tend to show that these hydrosilylation processes proceed *via* a non-hydride mechanism.

Finally, in **Chapter IV**, we present the syntheses, characterizations and catalysis applications of new Ni–NHC complexes. During this study, we developed an original methodology for the facile and clean removal of the Cp ligand from cyclic and acyclic half-sandwich alkyl,NHC–nickel complexes, which do not present any readily available coordination sites. Remarkably, the nickel–alkyl and nickel–NHC bonds of these species, irrespective of whether they are part of a metalacycle or not, are preserved in the presence of acid. Furthermore, new Ni–NHC complexes based on *malo*-NHC and CAAC ligands were synthesized, and the coordination chemistry of these ligands with nickel has clearly shown that *malo*-NHC behave as anionic X-type ligands, whereas CAACs behave as neutral L-type ligands. Preliminary results in homogeneous catalysis – and more precisely in the Suzuki–Miyaura reaction, the hydrosilylation of benzaldehyde, the  $\alpha$ -arylation of propiophenone and the direct C–H arylation of THF – showed a moderate activity of the above mentioned complexes. Nevertheless, further work on ligand design and on their potential catalytic applications will undoubtedly give rise to interesting nickel–carbene catalysts in a near future.

## **Publications**



**E. Brenner, D. Matt, M. Henrion, M. Teci and L. Toupet**

*Calix[4]arenes with one and two N-linked imidazolium units as precursors of N-heterocyclic carbene complexes. Coordination chemistry and use in Suzuki-Miyaura cross-coupling. Dalton Trans. 2011, 40, 9889–9898.*

**L. P. Beether, M. Henrion, L. Brelot, C. Darcel, M. J. Chetcuti, J.-B. Sortais and V. Ritleng**

*Hydrosilylation of aldehydes and ketones catalyzed by an N-heterocyclic carbene–nickel hydride complex under mild conditions. Adv. Synth. Catal. 2012, 354, 2619–2624.*

**M. Henrion, A. M. Oertel, V. Ritleng and M. J. Chetcuti**

*Facile displacement of  $\eta^5$ -cyclopentadienyl ligands from half-sandwich alkyl,NHC–nickel complexes: an original route to robust cis-C,C-square planar complexes. Chem. Commun. 2013, 49, 6424–6426.*

**L. P. Beether, M. Henrion, M. J. Chetcuti, C. Darcel, V. Ritleng and J.-B. Sortais**

*Cyclopentadienyl N-heterocyclic carbene–nickel complexes as efficient pre-catalysts for the hydrosilylation of imines. Catal. Sci. Technol. 2013, 3, 3111–3116.*

**M. Rocquin, M. Henrion, M.-G. Willinger, P. Bertani, M. J. Chetcuti and V. Ritleng**

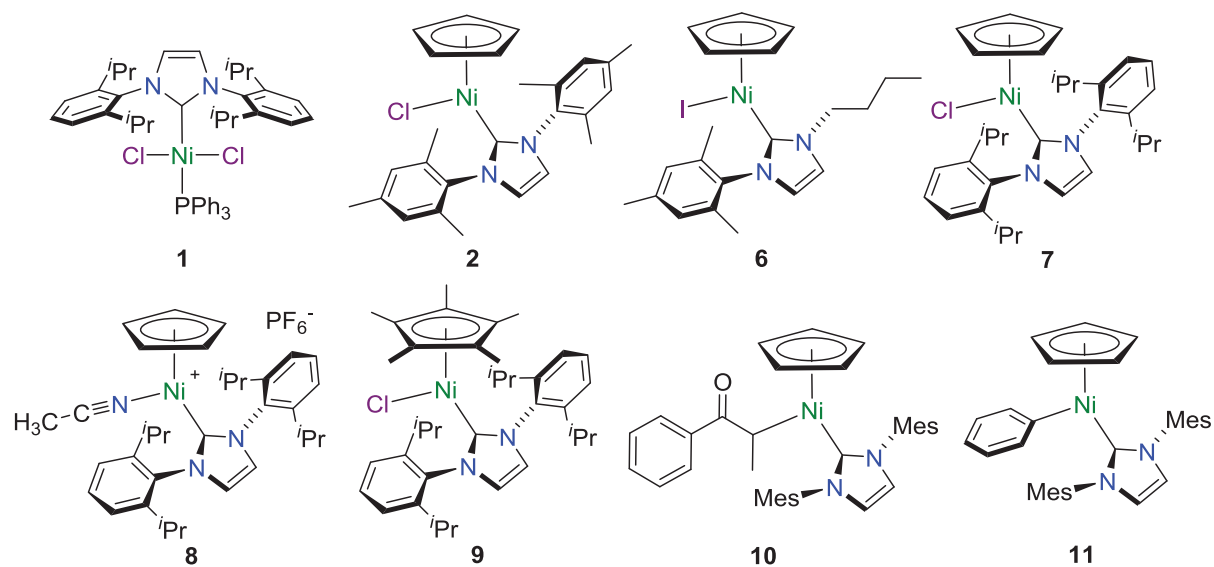
*One-step synthesis of a highly homogeneous SBA-NHC hybrid material: en route to single-site NHC–metal heterogeneous catalysts with high loadings. Dalton Trans. 2014, 43, 3722–3729.*

**M. Henrion, M. J. Chetcuti and V. Ritleng**

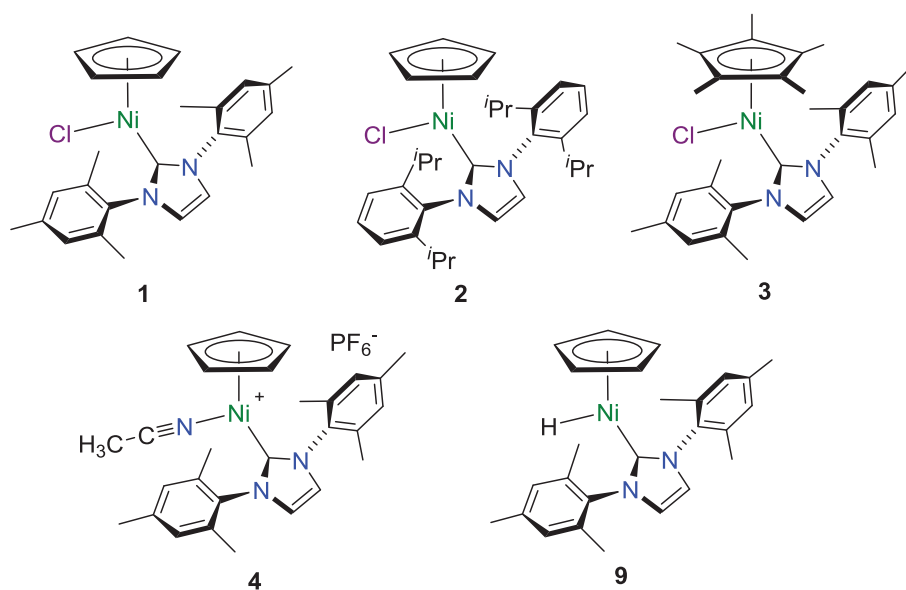
*From the metalation of acetone to the catalytic  $\alpha$ -arylation of acyclic ketones with inexpensive and easy-to-handle half-sandwich NHC–nickel(II) complexes. Chem. Commun. 2014, 50, 4624–4627.*



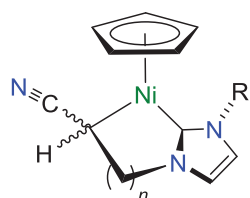
**Chapter II. From acetone metalation to the catalytic  $\alpha$ -arylation of acyclic ketones with *N*-heterocyclic carbene–nickel(II) complexes**



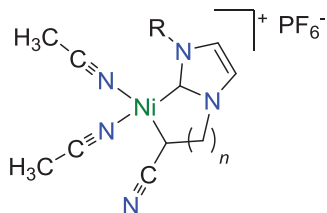
**Chapter III. Ni–NHC-catalyzed hydrosilylation of Carbon–Heteroatom double bonds**



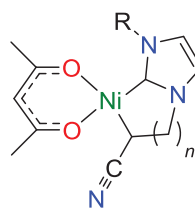
Chapter IV. Synthesis, characterization and catalysis applications of new *N*-heterocyclic carbene–nickel complexes



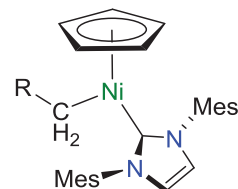
**2a:**  $n = 1$ ,  $R = \text{Me}$   
**2b:**  $n = 2$ ,  $R = \text{Mes}$



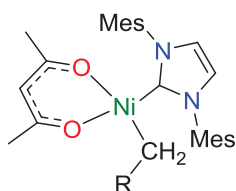
**3b:**  $n = 2$ ,  $R = \text{Mes}$



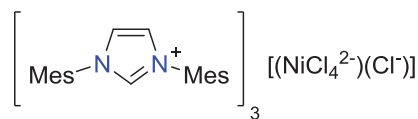
**4a:**  $n = 1$ ,  $R = \text{Me}$   
**4b:**  $n = 2$ ,  $R = \text{Mes}$



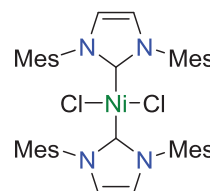
**5a:**  $R = \text{H}$   
**5b:**  $R = \text{CN}$



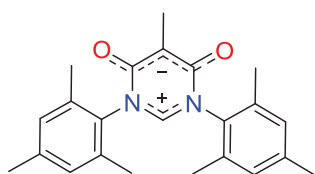
**6a:**  $R = \text{H}$   
**6b:**  $R = \text{CN}$



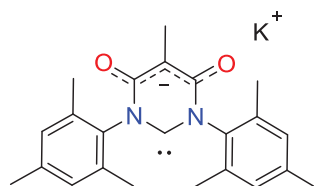
**7**



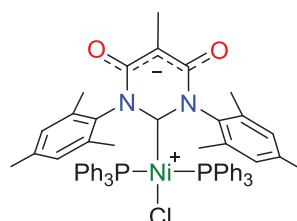
**8**



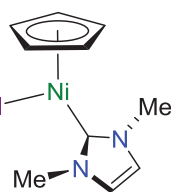
**9a**



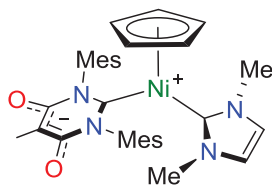
**9b**



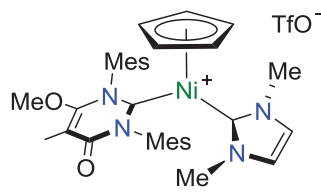
**10**



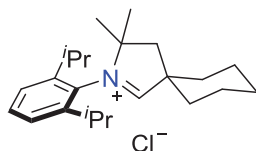
**11**



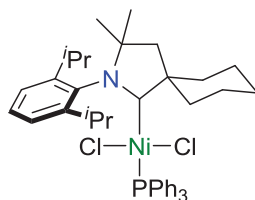
**12**



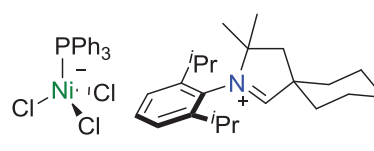
**13**



**14**



**15**



**16**



# Synthèse et applications en catalyse homogène de complexes nickel(II)–carbène *N*-hétérocyclique

## Résumé

Une étude détaillée a été effectuée sur des composés organométalliques de carbènes *N*-hétérocycliques (NHC) de nickel(II), et plus particulièrement sur des complexes demi-sandwich nickel(II)–NHC. Ces complexes ont montré des activités sans précédent en catalyse homogène, notamment en  $\alpha$ -arylation de cétones acycliques, où des charges en pré-catalyseur de seulement 1 mol% ont pu être utilisées. L'étude mécanistique de cette réaction tend à montrer l'implication d'intermédiaires radicalaires. De plus, ces complexes demi-sandwich se sont révélés être des pré-catalyseurs performants en hydrosilylation de dérivés carbonylés et d'imines. Les méthodologies qui en découlent fournissent de façon efficace et sélective les produits de réduction correspondants, dans des conditions réactionnelles douces. Un intermédiaire réactionnel demi-sandwich de type nickel–hydrure, agissant probablement comme le véritable précurseur catalytique, a en outre pu être isolé. D'autre part, la synthèse de nouveaux complexes Ni–NHC a remarquablement mené à une nouvelle méthodologie de substitution du ligand cyclopentadienyl dans des dérivés demi-sandwich alkyl,NHC–Ni. Enfin, l'utilisation de NHCs moins classiques, comme les NHCs possédant un squelette malonate, ou encore les carbènes (alkyl)(amine) cycliques, a mené à l'isolement de nouveaux complexes carbéniques de nickel(II), dont les premiers résultats catalytiques sont encourageants.

**Mots-clés :** nickel – carbène *N*-hétérocyclique – complexes demi-sandwich –  $\alpha$ -arylation de cétones – hydrosilylation

## Abstract

A detailed study has been conducted on organometallic compounds of *N*-heterocyclic carbenes (NHC) of nickel(II), in particular on half-sandwich nickel(II)–NHC complexes. These complexes showed unprecedented catalytic activity in homogeneous catalysis, especially in the  $\alpha$ -arylation of acyclic ketones, where catalyst loadings as low as 1 mol% could be used. Mechanistic experiments suggest that radicals are implied. Furthermore, these half-sandwich complexes proved to be efficient pre-catalysts in the hydrosilylation of carbonyl compounds and imines, allowing the reduction processes to proceed under mild reaction conditions. During the course of these studies, a half-sandwich nickel–hydride intermediate that probably acts as the true pre-catalyst was isolated. Remarkably, the synthesis of new Ni–NHC complexes led to a methodology for cyclopentadienyl ligand substitution in stable 18-electron alkyl,NHC–Ni derivatives. Finally, the use of less common NHC ligands, such as NHCs possessing a malonate backbone, or else, the use of cyclic (alkyl)(amino) carbenes, led to the isolation of new nickel–carbene complexes, which gave encouraging preliminary catalytic results.

**Key words:** nickel – *N*-heterocyclic carbene – half-sandwich complexes – ketone  $\alpha$ -arylation – hydrosilylation